STATUS OF THESIS

Title of thesis | A Novel Construction of Vector Combinatorial (VC) Code Families and Detection Scheme for SAC OCDMA Systems

I HASSAN YOUSIF AHMED MOHMED

Hereby allow my thesis to be placed at the Information Resources Center (IRC) of Universiti Teknologi PETRONAS (UTP) with the following conditions:

1. The thesis becomes the property of UTP.
2. The IRC of UTP may make copies of the thesis for academic purposes only.
3. This thesis is classified as

☐ Confidential

☑ Non-confidential

If this thesis is confidential, please state the reason:

_____

The contents of the thesis will remain confidential for _____ years.

Remarks on disclosure:

_____

Endorsed by

Signature of Author	Signature of Supervisor
Hassan Yousif Ahmed Mohmed	Dr. Mohamad Naufal Mohamad Saad
Wad Madni- Sudan	Electrical and Electronic Department
	Univeristi Teknologi PETRONAS
	Tronoh, Bandar Seri Iskandar
	Perak-Malaysia
Date: _____	Date: _____

UNIVERSITI TEKNOLOGI PETRONAS

A NOVEL CONSTRUCTION OF VECTOR COMBINATORIAL (VC) CODE FAMILIES AND DETECTION SCHEME FOR SAC OCDMA SYSTEMS

.

by

HASSAN YOUSIF AHMED MOHMED

The undersigned certify that they have read, and recommend to the Postgraduate Studies Programme for acceptance this thesis for the fulfillment of the requirements for the degree stated.

Signature _____

Main Supervisor Dr. Mohamad Naufal Mohamad Saad

Signature _____

Co- Supervisor Dr. Ibrahima Faye

Signature _____

Head of Department Dr. Nor Hisham Hamid

Date _____

UNIVERSITI TEKNOLOGI PETRONAS

A NOVEL CONSTRUCTION OF VECTOR COMBINATORIAL (VC) CODE FAMILIES AND DETECTION SCHEME FOR SAC OCDMA SYSTEMS

By

HASSAN YOUSIF AHMED MOHMED

A Thesis

Submitted to the Postgraduate Studies Programme as a Requirement for the

Degree of

DOCTOR OF PHILOSOPHY

DEPARTMENT OF ELECTRICAL AND ELECTRONICS ENGINEERING

UNIVERSITI TEKNOLOGI PETRONAS

BANDAR SERI ISKANDAR,

PERAK

MAY 2010

DECLARATION OF THESIS

Title of thesis	A Novel Construction of Vector Combinatorial (VC) Code Families and Detection Scheme for SAC OCDMA Systems

I _____HASSAN YOUSIF AHMED MOHMED_____

hereby declare that the thesis is based on my original work except for quotations and citations which have been duly acknowledged. I also declare that it has not been previously or concurrently submitted for any other degree at UTP or other institutions.

Witnessed by

_____ _____

Signature of Author Signature of Supervisor

Permanent address: Wad Madni- Sudan Name of Supervisor

Dr. Mohamad Naufal Mohamad Saad

_____

Date : _____ Date : _____

DEDICATION

To My Family...

ACKNOWLEDGMENT

First and foremost, my utmost thanks and gratitude to ALLAH SOBHANAHU WA TAALA, for bestowing the great needed strength, audacity and knowledge in completing this work. I would like to express my gratitude to my family for their endless support, without their love and sacrifice, I never could have come this far.

I would like to express my grateful thanks and appreciations to my main supervisor, Dr Mohammed Naufal Mohammed Saad whom through him, ALLAH Almighty has made it possible for this research to complete. His support, guidance and encouragement through out the duration of this study are sincerely acknowledged.

Many thanks and special appreciations are forward to my co-supervisor Dr Ibrahima Faye, for his continuous cooperation, encouragement and assistance. His advices throughout the duration of my study are highly appreciated.

I'm grateful to all the members of the Electrical and Electronic Engineering Department who assisted me through my thesis.

Especial thanks to my friends in UTP, my stay at UTP would not been as enjoyable and rewarding without them.

ABSTRACT

There has been growing interests in using optical code division multiple access (OCDMA) systems for the next generation high-speed optical fiber networks. The advantage of spectral amplitude coding (SAC-OCDMA) over conventional OCDMA systems is that, when using appropriate detection technique, the multiple access interference (MAI) can totally be canceled. The motivation of this research is to develop new code families to enhance the overall performance of optical OCDMA systems. Four aspects are tackled in this research. Firstly, a comprehensive discussion takes place on all important aspects of existing codes from advantages and disadvantages point of view. Two algorithms are proposed to construct several code families namely Vector Combinatorial (VC). Secondly, a new detection technique based on exclusive-OR (XOR) logic is developed and compared to the reported detection techniques. Thirdly, a software simulation for SAC OCDMA system with the VC families using a commercial optical system, Virtual Photonic Instrument, "VPI^{TM} TransmissionMaker 7.1" is conducted. Finally, an extensive investigation to study and characterize the VC-OCDMA in local area network (LAN) is conducted. For the performance analysis, the effects of phase-induced intensity noise (PIIN), shot noise, and thermal noise are considered simultaneously. The performances of the system compared to reported systems were characterized by referring to the signal to noise ratio (SNR), the bit error rate (BER) and the effective power (P_{sr}). Numerical results show that, an acceptable BER of 10^{-9} was achieved by the VC codes with 120 active users while a much better performance can be achieved when the effective received power P_{sr} > -26 dBm. In particular, the BER can be significantly improved when the VC optimal channel spacing width is carefully selected; best performance occurs at a spacing bandwidth between 0.8 and 1 nm. The simulation results indicate that VC code has a superior performance compared to other reported codes for the same transmission quality. It is also found that for a transmitted power at 0 dBm, the BER specified by eye diagrams patterns are 10^{-14} and 10^{-5} for VC and Modified Quadratic Congruence (MQC) codes respectively.

ABSTRAK

Ada telah berkembang kepentingan dalam menggunakan kode divisi optik multiple access (OCDMA) sistem bagi generasi selanjutnya berkecepatan tinggi jaringan serat optik. Keuntungan dari spektrum amplitudo pengkodean (SAC-OCDMA) atas sistem OCDMA konvensional adalah bahwa, bila menggunakan teknik deteksi yang tepat, campur tangan multiple access (MAI) benar-benar dapat dibatalkan. Motivasi dari penelitian ini adalah untuk mengembangkan keluarga kode baru untuk meningkatkan kinerja keseluruhan sistem OCDMA optical. Dua algoritma yang diusulkan untuk membangun keluarga beberapa kode yaitu Vector Kombinatorial (VC). Kedua, teknik deteksi baru berdasarkan eksklusif-OR (XOR) logika dikembangkan dan dibandingkan dengan teknik deteksi dilaporkan. Ketiga, sebuah simulasi perangkat lunak untuk sistem OCDMA SAC dengan keluarga VC menggunakan sistem optik komersial, Virtual Foton Instrumen, "VPI^{TM} TransmissionMaker 7,1" dilakukan. Akhirnya, sebuah penyelidikan yang ekstensif untuk mempelajari dan mencirikan VC-OCDMA dalam jaringan area lokal (LAN) dilakukan. Untuk analisis performa, efek dari fase-akibat intensitas kebisingan (PIIN), suara tembakan, dan kebisingan dianggap termal secara simultan. Kinerja sistem dibandingkan dengan sistem dilaporkan adalah ditandai dengan mengacu pada sinyal ke rasio noise (SNR), tingkat kesalahan bit (BER) dan kekuasaan efektif (P_{sr}). Hasil numerik menunjukkan bahwa, sebuah BER 10^{-9} diterima dicapai oleh kode VC dengan 120 pengguna aktif sedangkan kinerja yang lebih baik dapat dicapai jika daya efektif yang diterima Psr> -26 dBm. Secara khusus, BER dapat ditingkatkan jika saluran VC jarak optimal lebar dipilih dengan cermat; kinerja terbaik terjadi pada bandwidth jarak antara 0,8 dan 1 nm. Hasil simulasi menunjukkan bahwa kode VC memiliki kinerja yang unggul dibandingkan dengan yang lain melaporkan kode untuk kualitas transmisi yang sama. Hal ini juga menemukan bahwa untuk daya yang ditransmisikan pada 0 dBm, BER yang ditentukan oleh pola mata diagram adalah 10^{-14} dan 10^{-5} untuk VC dan Dimodifikasi Kuadratik kongruensi (MQC) kode masing masing.

TABLE OF CONTENTS

LIST OF TABLES

LIST OF FIGURES

LIST OF ABBREVIATIONS

BER	Bit Error Rate
CDMA	Code Division Multiple Access
CW	Continuous Wave
FDMA	Frequency Division Multiple Access
LAN	Local Area Network
MAI	Multiple Access Interference
MAN	Metropolitan Access Network
NRZ	Non Return to Zero
OCDMA	Optical Code Division Multiple Access
PRBS	Pseudo Random Binary Sequence
RF	Radio Frequency
TDMA	Time Division Multiple Access
WAN	Wide Area Network
WDAM	Wavelength Division Multiple Access
B	Noise Equivalent Electrical Bandwidth
e	Electronic Charge
$G(v)$	Single Sideband Power Spectral Density
h	Planck's Constant
K_B	Boltzmann's constant
P_{sr}	Effective Power of a Broad-band Source
R_L	Receiver Load Resistance
T	Absolute Temperature
Tn	Absolute Receiver Noise Temperature
$u(v)$	Unit Step Function
v_c	Central Frequency of the Original Broadband Optical Pulse

v_0 Central Optical Frequency

Δv Optical Source Bandwidth

τ_c Coherence Time of the Source

η Quantum Efficiency

$\Re$ Responsivity of the Photodetectors

λ_a Autocorrelation

λ_c Cross Correlation

CHAPTER 1
INTRODUCTION

1.1 Background

In recent years, the demand on optical communication systems has been rapidly increasing due to the large bandwidth offered by the optical fibers. This demand is fueled by many different factors. Multimedia services promise to integrate moving images, statistic images, text, and sound in an interactive environment. At the same time, businesses are relying increasingly on internet for day to day operations. This is because the internet provides an immediate and accessible set of information, resources and services. The tremendous growth of the Internet has brought enormous number of users consuming large amount of bandwidth since data transfers involve videos, database queries, updates and images [1-7]. These demands have driven the need to replace conventional low-capacity copper access links to higher-capacity connections. To realize the demands for bandwidth and new services, a new technology must be deployed and fiber optic is one such key technology [8]. Optical fiber offers many advantages over conventional media (e.g. coaxial cable and twisted pair). It offers unlimited bandwidth and is considered as the ultimate solution to deliver broadband access to the last mile. It also offers a much lower attenuation factor where optical signals can be transmitted over very long distances without signal regeneration or amplification [8-11]. In addition, many channels can be multiplexed to share the same fiber optic medium and thus reducing the number of links required and the cost to end users [12].

A single mode optical fiber can support transmission capacity in the range of Terabits per second [6]. Optical multiplexing techniques have to be employed to exploit full system transmission capacity [8-11]. In optical communication network, due to the usage of light as a carrier, several wavelengths can be multiplexed on the same fiber

in order to increase the overall bandwidth. Therefore, fiber optic systems could be the answer to many urgent needs of the telecommunication systems, as they could provide the necessary bandwidth for the transmission of broadband data to the end users.

1.2 Telecommunication Networks

In general, telecommunications networks can be divided into four classes [13]. Figure 1.1 shows four generic categories of telecommunication networks.

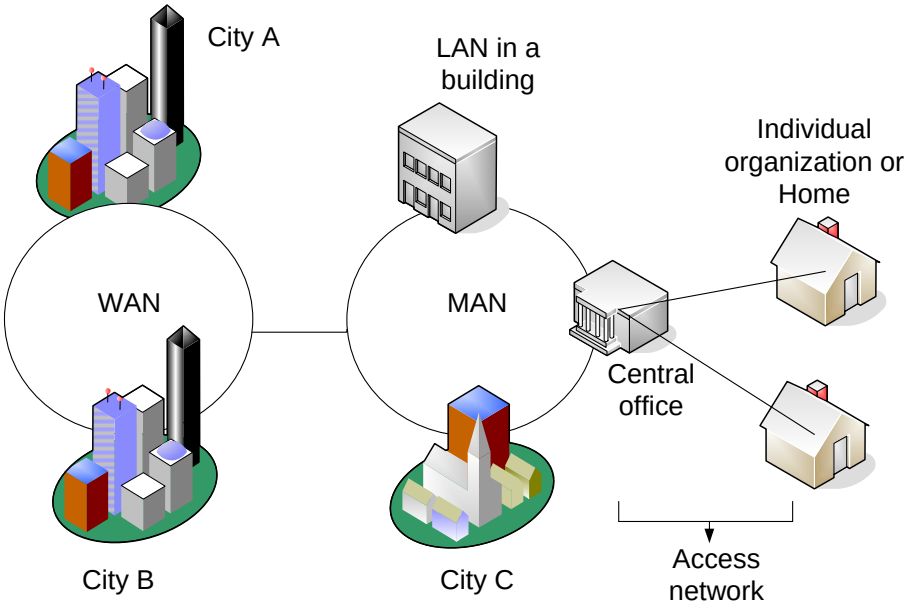

Figure 1.1 Broad categories of network ranging from LANs to WANs.

1. A *wide area network* (WAN) spans a large geographical area. The links can range from connections between switching facilities in neighboring cities to long-haul terrestrial or undersea transmission lines running across a country or between countries. WANs are usually owned and operated by either private enterprises or telecommunication service providers.

2. A *metropolitan area network* (MAN) spans a smaller area than that spanned by a WAN. This could range from interconnection between buildings converting several

blocks within a city or could encompass an entire city and the metropolitan area surrounding it. MANs are owned and operated by many organizations.

3. A *local area network* (LAN) interconnects users in a localized area such as a room, a department, a building, an office or factory complex, or a campus. LANs usually are owned, used, and operated privately by a single organization.

4. An *access network* encompasses connections that extend from a central communication switching facility to individual businesses, organizations, and homes. One of its functions is to collect and concentrate the information flows from customer locations and then send this aggregated traffic to the central office. In the other transmission direction, access networks allow carriers to provide voice, data, video and other services to subscribers. Such access networks typically are owned by service providers.

1.3 Multiple Access Techniques

A multiple access communication system is a communication system where a number of users share a common transmission medium to transmit messages to a number of destinations. Optical fibers provide vast bandwidth for multiple access operations which allows multi users to simultaneously access the shared medium. Therefore, we need to find a way to share the vast bandwidth of the optical medium in a manner which is fair and fast. A multiple access is required for combining and separating traffics on a shared physical medium when the users are not at the same place. A more detailed discussion on the differences between multiplexing and multiple access techniques will be provided in Chapter 2.

There are three major multiple access schemes available; Time Division Multiple Access (TDMA), Wavelength Division Multiple Access (WDMA) and Code Division Multiple Access (CDMA). TDMA and WDMA are traditionally used in fiber optic communication systems to allocate the available bandwidth among the different users. In a TDMA system, each channel occupies a time slot, which interleaves with time slots of other channels. In a WDMA system, each channel occupies a narrow bandwidth around a center wavelength or frequency. However, both of them present

significant drawbacks in local area systems requiring large number of users [12]. In optical CDMA systems, a data bit is typically encoded by sub-dividing it into many smaller chips. Each user is assigned a unique signature code that specifies the chips that must contain optical power. In a particular technique, a CDMA user inserts its code or address in each data bit and asynchronously initiates transmission. In optical CDMA, the field of the optical signal carrying the data exhibits a set of signal processing operation. Hence this modifies it's time and/or frequency appearance, in a way distinguishable only by the intended receiver. At the receiver, the complement decoder is used to correlate the incoming chip stream, thus reproducing the desired signal. The signature codes have good auto-correlation and cross-correlation properties that enable each user to differentiate its own data. Other users in the network will produce multiple-access interference (MAI), but as long as the MAI is less than the autocorrelation peak, the desired data is detected correctly [21]. CDMA offers unique features such as flexibility, high security, enhanced privacy, asynchronous nature, plug and play functionality, and provides differentiated service at the physical layer. The advantages and disadvantages of these three schemes are discussed in more details in Chapter 2.

1.4 Problem Statement

CDMA was invented and used as the first technique for wireless communication. It gives the best results compared to other wireless multiple access techniques. This fact has led many researchers to study if the advantages of CDMA could also be utilized in optical communication systems for the sake of accommodating a large number of users simultaneously.

Optical CDMA started almost around two decades ago [11]. In the beginning, communication community tried to apply the same CDMA techniques already established in wireless communication. The results they achieved were far from comparable to the success of that in wireless [22-23]. This is mainly due to the fundamental difference between the radio frequency (RF) and optical fiber communication environments. For instance, the output characteristics of an optical source, such as phase and polarization are not controllable as of a microwave source.

The optical fiber exhibits phenomena that are either not present or insignificant in RF channel. Also the photo-detector senses incident power only, the phase and polarization cannot be easily detected. A complex architecture is required, in order to control and detect such parameters and this becomes inappropriate for an access communication system. To overcome the stated problems, researchers have been trying to establish newer encoding and decoding techniques in order to achieve the CDMA objectives. Another limitation is optics to electronics and electronics to optics conversion which limits the transmission speed and increased the overall system cost. A modern approach is to use an all optics processing scheme (Optical signal processing) [24-25]. The encoding and decoding operations that occur in the optical domain are desirable which leads to avoidance of an ultra-fast electronics.

Interest in optical CDMA is always high due to increasing demand for networks with higher capabilities at low cost. This demand is fueled by many different factors. Business and government applications are relying increasingly on the Internet. Multimedia services promise to integrate moving images, statistic images, text, and sound in an interactive environment. The tremendous growth of internet has brought huge number of users consuming large amount of bandwidth since data transfers involve videos, database queries, updates and images [9-11]. The conventional bandwidth, such as twisted wire pairs and coaxial cables is limited and for this reason it will not be able to integrate these broadband services sufficiently.

In a TDMA system, users are assigned time slots during which they can transmit their data. Since only one user can transmit at a time, the receiver must operate at the aggregate of the system which is roughly equal to the number of nodes connected product the data rate per node. TDMA systems also introduce significant latency penalties because of the coordination required to coordinate and grant requests for time slots from users by the central node [13-14].

WDMA systems allocate the available optical bandwidth into distinct wavelength channels that are sent simultaneously by different users to permit multiple access. It is difficult to construct a WDMA system for a dynamic set of multiple users because of the significant amount of coordination among the nodes required for successful operation. To build a WDMA network with a dynamic user base, control channels

and collision detection schemes would need to be implemented that would waste significant bandwidth [15].

Optical CDMA communication systems require neither the time nor the frequency management systems of the previous techniques. The three major factors that affect the performance of optical CDMA are code design, detection technique and transmitter-receiver structure.

Many code families have been proposed for various OCDMA technologies. Different families can be categorized based on the coding scheme [7-9, 26-37]. For example, for time-spread systems [7-9, 26], Optical Orthogonal Code (OCC) [8-9] and Prime Codes [7] have been proposed. For the wavelength-hopping time-spreading OCDMA system, fast-frequency hopping [27], Carrier hopping [7], and Extended Carrier Hopping prime codes [28]. For the spectral-amplitude coding (SAC) OCDMA systems [29-37], Hadamard [29], Integer Lattice code [30-31], Balance Incomplete Block Design (BIBD) code, Modified Quadratic Congruence (MQC), Modified Frequency Hopping (MFH) code [32-33], Double Weight (DW) code [35, 60], Enhance Double Weight (EDW) code [36] and most recently the Random Diagonal (RD) [37]. However, some of these codes have much poorer cross-correlation (e.g. Hadamard code [29], RD code [37]), or the number of available codes is quite restricted (e.g. integer lattice exists for m and k where m and k need to be a co-prime (it is enough if one is an even and the other is odd) [30], a prime number for modified quadratic congruence (MQC) [32-33], a prime power for Modified Frequency Hopping (MFH) [32-33], an even natural numbers for Modified Double Weight (MDW) [35], and an odd natural numbers for Enhanced Double Weight (EDW) [36]). Also it is not very clear if any of the codes has been tested on the actual fiber or even on the software-simulated environments. In this thesis, we propose new codes for Optical CDMA namely Vector Combinatorial (VC) Code families. It will be shown principally by extensive theoretical studies and comprehensive simulations that the transmission performance of VC code families is significantly better than that of existing codes such as Modified Quadratic Congruence, (MQC), Modified Frequency Hopping code (MFH) and Hadamard code. The detailed review of the OCDMA and their implementation in local area networks is given in Chapter 6.

1.5 Objectives

The main goal of this research is to develop a new code family for the spectral-amplitude coding (SAC) optical CDMA. The objectives of this research can be summarized as follows:

- To develop new optical CDMA codes known as VC code families.
- To develop a new detection scheme based on XOR subtract technique.
- To develop transmitter and receiver structure for proposed system.
- To apply and study the performance of a new CDMA code families in local Area Networks (LAN) environment.

1.6 Scope of Works

In this thesis, multiple access and multiplexing issues are focused on through studies performed at the physical layer. At the physical layer, the standard parameters usually involved are the bit-error rate (BER), signal-to-noise ratio (SNR), transmitted power, received power and loss. Figure 1.2 illustrates the study structure of this research and also the scope of work. Optical spectrum CDMA is a new technique of multiplexing and multiple access in optical communications. For code development, the study focuses on theoretical modeling and code structure construction. It is important to note that, almost all current research works in OCDMA focus on these two activities. Nevertheless, in this thesis we also include the applications to make the study more complete. The scope of focus in code application is on local networks as these are the areas that are predictable to be better ready for the implementation of OCDMA technology.

Besides theoretical model development, extensive studies are also conducted through software simulation, an approach that is generally lacking in other recent works in this field. Even so, as far as the scope of work of this study is concerned, the experimental results are expected to be adequate to prove the feasibility and viability of the new codes (as theoretically expected) and their outperformance compared to other existing codes.

As shown in Figure 1.2, there are three main subjects that will be considered in this thesis; which are the code development, transmitter-receiver structure with respect to detection technique and OSCDMA code applications with more emphasis given to the former. The more detail structure of study is provided in the respective chapter according to specific issues under study. The issues in devices will be addressed only as they are required, especially when discussing the encoders and decoders structure.

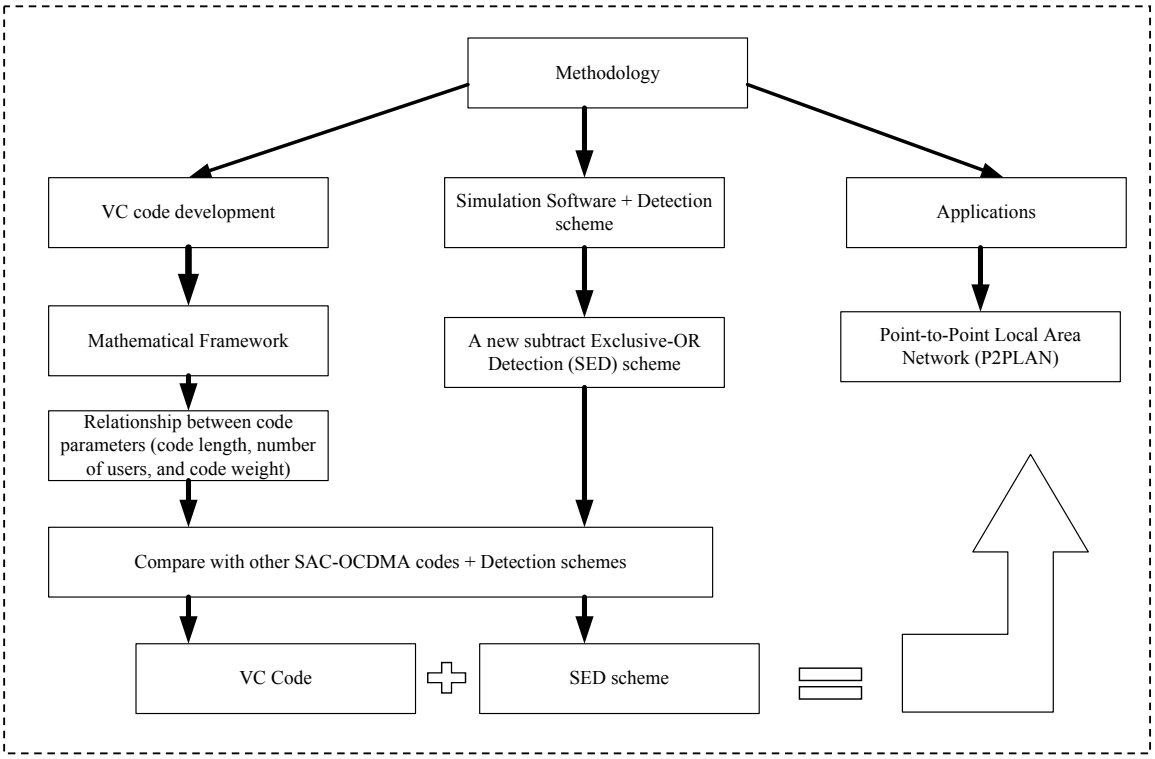

Figure 1.2: A general study model of this research work.

1.7 Methodology

A general methodology is adopted in this research. As mentioned in Figure 1.2, one of the main challenges and potential advantages of the proposed system is to develop and implement new code families that are well beyond the capability of current codes. Therefore, extensive studies from literature review point of view for reported optical CDMA systems will be addressed in Chapter 2. A comprehensive treatment of the theoretical and simulation studies will be detailed in Chapters 3, 4 and 5. In the form of anticipation, we would expect the new optical CDMA codes would lead to many design configurations such as new encoder, decoder and new detection scheme. Four stages are covered in this research.

In the first stage, a comprehensive theoretical analysis for the VC code families and the existing optical codes such as Modified Quadratic Congruence (MQC), Hadamard code, Modified Frequency Hopping (MFH) code and Double Weight (DW) code has taken a place. The choices of these codes are made because Hadamard is originally the basic and widely familiar code; MQC and MFH are the famous codes reported in spectral amplitude coding whose performance have been shown to outperform that of others while RD code is the latest code mentioned in the literature. At this stage, all the mathematical relations between the number of users, code length, weight and their performances are developed and discussed comparatively. Moreover, an algorithm to generate the code patterns has been developed using C++ tools.

In the second stage, after the completion of all the mathematical models, an optical system simulator is used to study the performance of the code in CDMA systems. Simulation tools can offer a powerful method to assist in analyzing the design of an optical component, circuit, or network before costly prototypes are built. VPItransmissionMaker^{TM} WDM, version 7.1 has been used to accomplish this work. Optimization and characterization are needed at this stage to get the best combination of codes that are suitable for the applications in LAN and MAN. This simulation software considers all possible practical effects during implementation, such as dispersion, non-linear effect of the fiber, and attenuation of the fiber. The bit error rate, chip spacing, signal received power, and eye opening, are simulated with

different values of input optical power of the light source and bit rate of the system for various fiber links.

In the third stage, although the main focus of this thesis is the feasibility of VC code families for communication systems, it is to be appreciated to study and characterize the input and output powers for the LEDs and Laser Ring as optical sources for OCDMA systems. Therefore, an experiment test for a laser ring for the proposed code is conducted.

In the final stage of this research, the experimental setup for the implementation of the new optical code is proposed. In addition, an experimental test for the input and output powers is conducted. Comparisons are then made between simulation and theoretical results. Moreover, the implementation of VC code in a local access network (LAN) is addressed in this stage as well.

1.8 Contributions of this research

In this thesis, new code families for spectral-amplitude coding OCDMA systems to enhance the performance of optical CDMA systems have been proposed. We can summarize the added values to the spectral-amplitude coding field of optical code-division multiple access (OCDMA) systems by this work as follows:

- New code families with no restriction of choosing the code weight and number of users (free cardinality).
- A new balance detection technique based on exclusive OR logic.
- A new transmitter-receiver structure for spectral-amplitude coding.

1.9 Thesis Overview

This thesis is organized into 7 Chapters. Chapter 1, an introduction chapter, discusses the need for high speed networks and the main reasons for using fiber optic in these networks.

The main problems faced in the implementation of the spectral-amplitude coding system, the objectives and scope of study are also outlined. The background information required here are important in following through the presentation, result and discussion in the subsequent chapters.

Chapter 2 introduces time-spread, frequency-hopping and spectral-amplitude coded OCDMA, providing a comprehensive literature review of the historical development of these techniques. More details about the multiplexing and multiple access technologies, as these are the main focus in this study, also will be addressed in this chapter. This starts with discussion on various existing multiplexing and multiple access techniques, advantages of OCDMA against other techniques, various Optical CDMA codes properties and strengths and weaknesses.

Chapter 3 concentrates on the core works of this thesis whereby a detailed discussion on the proposed families of VC codes is provided. The code structure and theory are constructed here. The existing technique is studied as well.

Recent studies show that, an OCDMA system cannot be designed by considering the properties of the code only, the detection technique also plays an important role and should be addressed as well. Therefore, this issue is highlighted in a chapter by itself, Chapter 4. This chapter also highlights a newly proposed detection scheme based on XOR subtraction. The influence of noise is also detailed in this chapter.

Chapter 5 concentrates on the performance of the proposed optical CDMA code based on the theoretical development. The basic design issues such as types of modulation and types of optical source are first verified and optimized in this chapter. Thus Chapter 5 functions as an initial verification stage before further simulation and experimentation are performed.

Chapter 6 then focuses on the implementation of the new codes (beside other codes for comparative analyses purposes) in local network. Then, finally Chapter 7 discuses

the whole study and summarizes the important findings and contributions. Suggestions on the future works are also provided in this chapter.

CHAPTER 2
OPTICAL CODE DIVISION MULTIPLE ACCESS SYSTEMS

2.1 Introduction

Fiber communication systems are gaining attention as a solution of providing high-bandwidth connection in the local area network (LAN) and metropolitan area network (MAN), where a large number of subscribers within a relatively small area require, from time to time, to communicate with others in the network at the rates of Gbit/s. Unlike the situation in the wide area network (WAN), the data flow in LANs could be more bursty and the control of the network more complex. One important requirement of the potential LAN technologies is to allow the users to have easy access to the network and effectively share the bandwidth with others in a fast and fair manner. In this chapter, we first address the operating principles of multiplexing, multiple access and their applications in details. The next topic includes the use of CDMA in optical domain and the operational concepts. It starts with a discussion on various existing multiplexing and multiple-access techniques, followed by the classification of the OCDMA systems, the most studied codes for Optical CDMA codes and their properties, and concluded through highlight the advantages of OCDMA in LANs and MANs networks.

2.2 Multiplexing and Multiple Access Techniques

There is no big difference between multiplexing and multiple access techniques. Multiple access techniques are often used to allow a transmission medium to be shared between different users (all users have equal access). The basic multiple access techniques mainly used in communication systems are: Frequency Division Multiple

Access (FDMA), Time Division Multiple Access (TDMA) and Code Division Multiple Access (CDMA).

Multiplexing is the combination of multiple signals into a single signal transmission. Multiplexing technique which makes possible to pad a number of logical channels (each capable of supporting an independent connection) into the same physical channel or line. The advantage of multiplexing is to reduce costs by better utilizing the capacity of the line. There are three main types of multiplexing techniques in communication systems namely Time Division Multiplexing (TDM), Frequency Division Multiplexing (FDM) and Wavelength Division Multiplexing (WDM).

According to the definition of the multiple access and multiplexing, multiplexing is more suitable for metro and long distance networks, while access is more suitable for shorter distance access networks. Due to this, our study will deal substantially with multiple access since the focus application is on local area networks.

2.3 Fiber Optic Multiple access Techniques

If there is more than one independent user trying to share some resources, the need for a multiple access techniques arises. In the absence of such techniques, conflicts can occur if more than one user tries to access the resources at the same time. Therefore, the multiple access schemes should avoid or at least resolve these collisions. Optical fiber offers vast amount of bandwidth for multiple access operations, permitting many users to simultaneously communicate on the same transmission medium. Three multiple access approaches are often considered to make the system bandwidth available to the individual user as illustrated in Figure 2.1. Traditional fiber optic communication systems use either TDMA or WDMA schemes to allocate bandwidth among multiple users. Unfortunately, both present significant drawbacks in local area systems requiring large number of users.

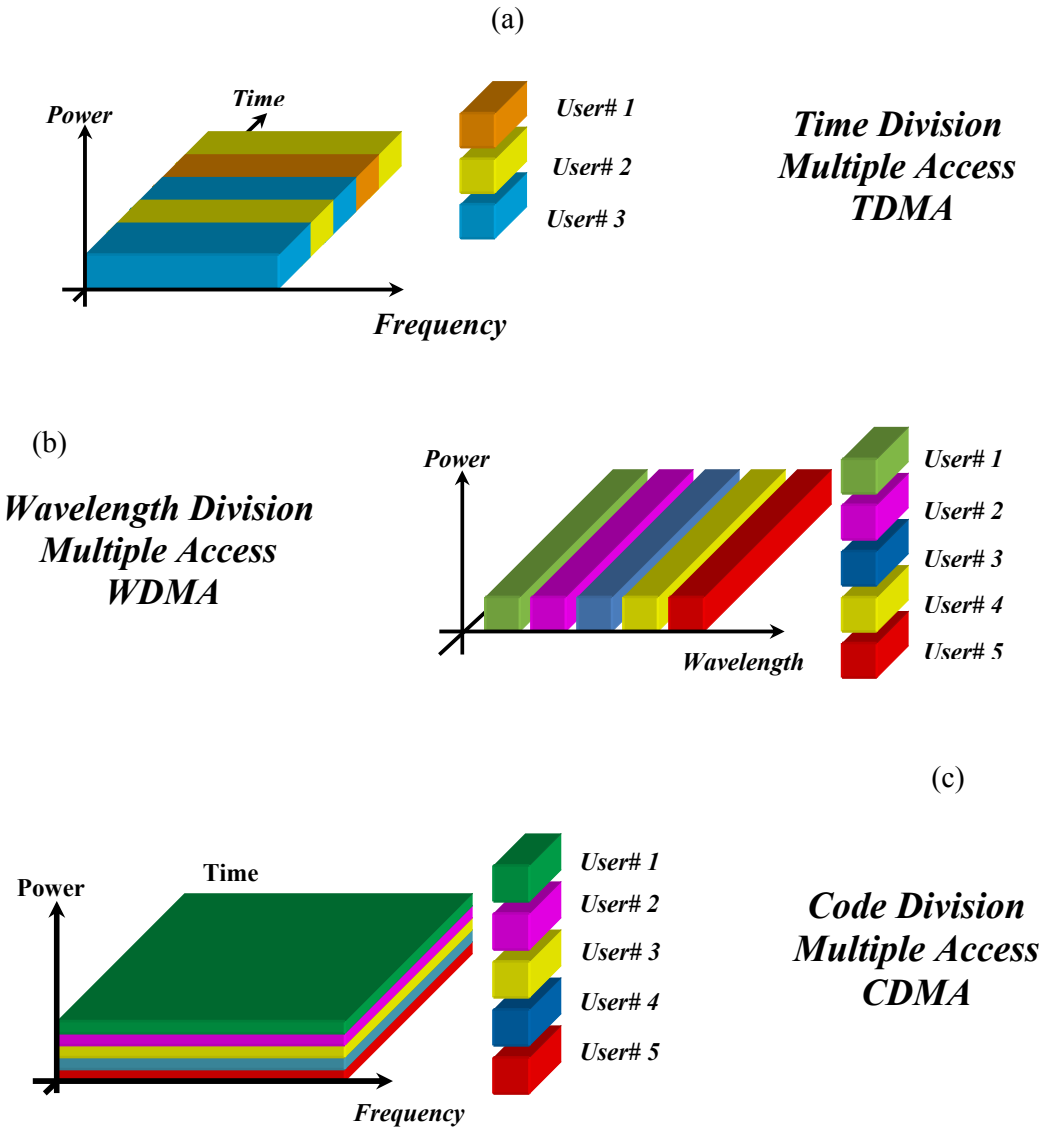

Figure 2.1: Multiple access schemes.

2.3.1 Time Division Multiple Access (TDMA)

In TDMA scheme [13-14], the bandwidth is divided into frames of equal duration, and each frame is divided into the same number of time slots. All time slots have equal duration. Each slot position within a frame is allocated to a different user. This means a particular user transmits in specific time slot in each transmitting frame. The length of the transmission frame is determined by the data bit period and is subdivided into a number of time slots according to the width of optical pulse.

In TDMA, the total system throughput is limited by the product of the number of users and their respective transmission rates since only one user can transmit at a time. For instance, if 100 users wish to transmit at 1Gbit/s, at a minimum the communication hardware would need to be capable of sustaining a throughput of 100Gbit/s, which is very hard to achieve this requirement at the present time. In addition, TDMA systems require strong centralized control to allocate time slots and maintain synchronous operation [13].

2.3.2 Wavelength Division Multiple Access (WDMA)

Unlike TDMA, a WDMA system allows each user to transmit at the peak speed of the network hardware since each channel is transmitted on a single wavelength of light [15-18]. WDMA systems allocate the available optical bandwidth into unique wavelength channels that are sent simultaneously by different users to permit multiple accesses. A WDMA system could easily support a bandwidth of 1 Terabit/s, ideal for the needs of a local area network. The problem with using WDMA in LANs is the need for a significant amount of dynamic coordination between nodes [13]. A dedicated control channel can be used for pre-transmission coordination. However, this wastes bandwidth that could otherwise be used for data transmission and introduces latency as nodes attempt to negotiate a connection [13].

2.3.3 Code Division Multiple Access (CDMA)

A CDMA is a spread-spectrum multiplexing technique by which the users access a common channel simultaneously and asynchronously [11, 19-20]. CDMA schemes do not achieve their multiple access property by division of the transmission of different

users in either time or frequency, but instead make a division by assigning each user a different code. Before a transmission is carried out, a CDMA user needs to insert its code or address in each data bit and asynchronously initiates transmission. As such, the system only allows those who hold the code used in the transmission to decode the message. Those users without the specific code will not be allowed to collect the desired data. Thus, this modifies its spectrum appearance in a way recognizable only by intended receiver. Otherwise, only noise-like bursts are observed.

A comparison between the advantages and disadvantages of these three schemes are given in Table 2.1.

Table 2.1: Comparison of Common Optical Multiple Access Schemes.

Multiple Access Schemes	Advantages	Disadvantages
1. TDMA	1. Dedicated channels provided. 2. High throughput. 3. Deterministic access.	1. Accurate synchronization needed. 2. Not efficient in bursty traffic. 3. Bandwidth wasted. 4. Channel not efficiently used. 5. Performance degrades with the number of simultaneous users.
2. WDMA	1.Dedicated channels provided.	1. Channel crosstalk. 2. Channel idle most of the time. 3. Low bandwidth efficiency. 4. Non-linear effects.
3. CDMA	1. Simultaneous users allowed. 2. Asynchronous access. 3. No delay or scheduling. 4. High bandwidth efficiency. 5. Efficient for bursty traffic. 6. Dedicated channels provided.	1. Performance degrades with the number of simultaneous users.

2.4 Optical Code Division Multiple Access Systems

Recently there has been growing interest in applying CDMA technique in optical domain [19-20] to support the increasing bandwidth demands of multimedia applications such as video conferencing and internet browsing. By utilizing CDMA in optical networks, we can achieve link capacities on the order of multi THz ideal for the local communication channels because CDMA offers the flexibility needed in the burst LAN environment. Therefore, the additional bandwidth required by spread spectrum can be accommodated by using a fiber-optic and incoherent optical signal processing [11]. In addition, OCDMA allows many users to access the same optical fiber channel asynchronously through the assignment of unique signature sequence.

OCDMA has many attractive characteristics when compared to its wireless counterpart, such as nearly perfect power control, fixed user positions and high signal to noise ratios [9, 11]. Moreover, it connects large number of asynchronous users with low latency and jitter, permits quality of service guarantees to be managed at the physical layer, offers strong security and has simplified network topologies. The key advantage of using CDMA is that, CDMA can be encoded and decoded in optical domain without converting the signal to electronic unless required. This is extremely important because the electronic processing is much slower than the optical transmission rate. Due to these, OCDMA has been recognized as one of the most important technologies for supporting many users in shared simultaneous media, and in some cases can increase the transmission capacity of an optical fiber [8-9].

OCDMA is an exciting development in short hauls optical networking because it can support both wide and narrow bandwidths applications on the same network. The code design plays an important role due to its ability to reduce the total received noise powers to total received powers. However, for improperly designed codes, the performance of OCDMA is known to be limited by the Multiple Access Interference (MAI) originating from other users trying to use the medium simultaneously [9] or crosstalk from other users. Many Optical Code Division Multiple Access codes have been proposed, which can also be implemented as multiplexing systems in point to point links.

Figure 2.2 illustrates how this system works. As stated in [8-9, 38], an encoder structure in the optical CDMA network is employed in every transmitter to encode

every modulated data bit with the specific code to each intended user. A broadcast architecture, using a passive star coupler, is used to connect all users to all the receivers. Then, the star coupler combines the signals from all users and these are sent to all of the matched filter receivers in the network (From Figure 2.2, we assume all components such as star coupler, multiplexer, etc, exist in OCDMA domain) . When a particular signal reaches the receiver, a decoder will match the code used in individual data bit with the receiver code. The fundamental task of the decoder is to retrieve the data bits encoded with the local code and discard the rest of the signals.

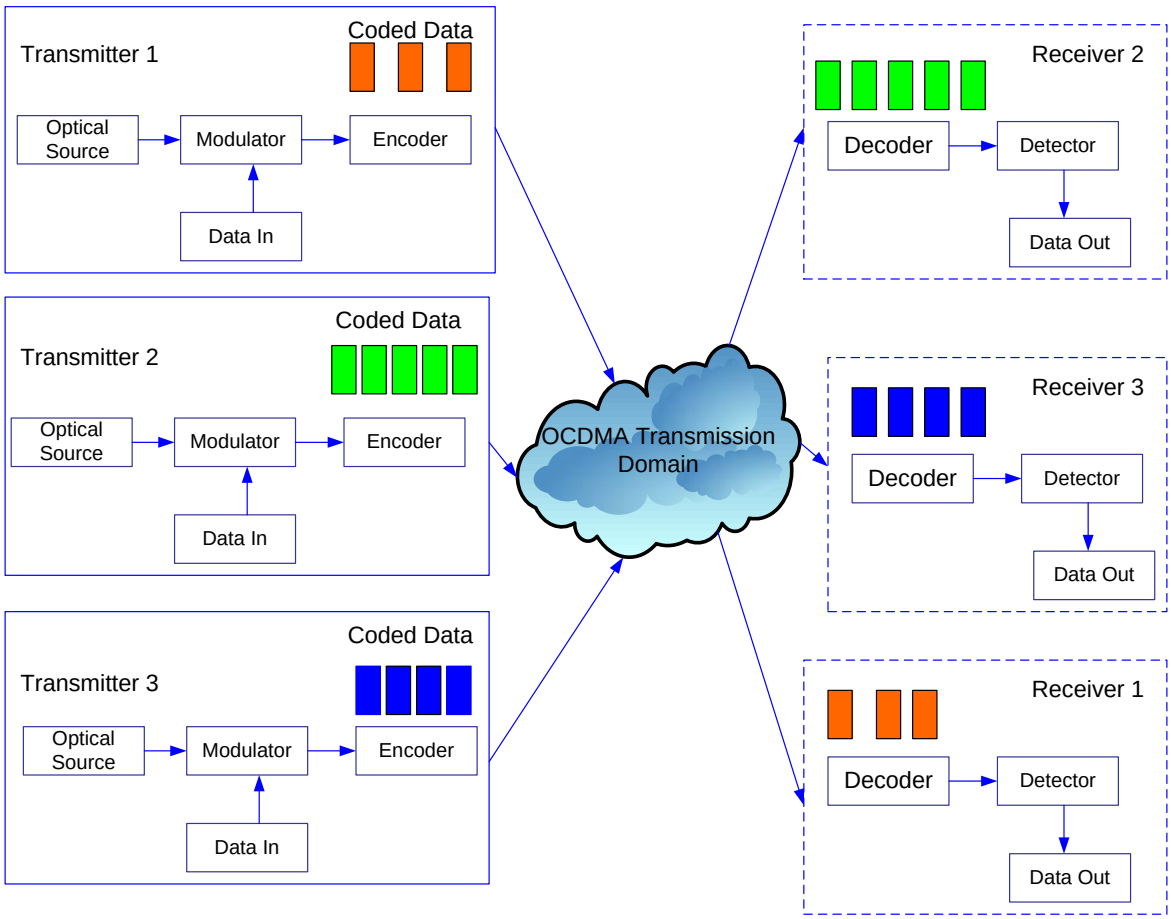

Figure 2.2: Optical CDMA networks.

In fact, these encoded bits which do not match the codes are not totally rejected by the encoder and some noises or also known as interference may also pass through the

decoder. However, for large number of users, the performance of OCDMA is known to be limited by the Multiple Access Interference (MAI) originating from other users trying to use the medium simultaneously.

2.5 Classification of Optical Code Division Multiple Access Systems

There have been growing interests in the coding schemes and enabling technologies in the area of optical code-division multiple-access (OCDMA) [39]. Three different categories can be used to specify optical CDMA systems as shown in Figure 2.3. Based on different choices of optical sources (e.g., coherent vs. incoherent, narrowband vs. broadband), detection schemes (e.g., coherent vs. incoherent), and coding techniques (e.g., time vs. wavelength, amplitude vs. phase), coding schemes can be classified into six main categories: (1) pulse-amplitude coding, (2) pulse-phase coding, (3) spectral-amplitude coding, (4) spectral-phase coding, (5) spatial coding, and (6) wavelength-hopping time-spreading (or simply wavelength-time) coding.
The first two techniques involved coding in the time domain.

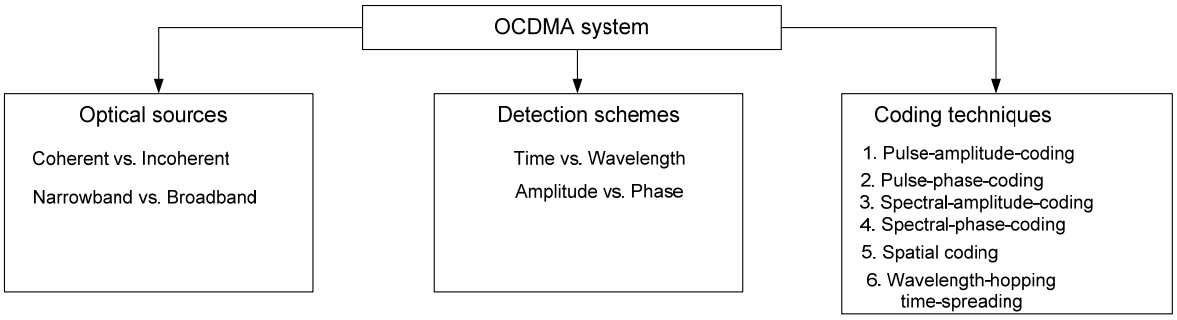

Figure 2.3: Classification of Optical CDMA systems.

Nevertheless, these two time-domain techniques are not inherently suitable for dense, high-speed, long-span optical networks because ultra short pulses are required, making the systems susceptible to fiber dispersion and nonlinearities.

In spectral-amplitude coding and spectral-phase coding, coding is performed in the wavelength domain [39]. The spectral nature of the codes is decoupled from the temporal nature of the data so that code length is now independent of data rate. Spectral OCDMA systems are code synchronous, on the condition that coded spectra must be linked to a common wavelength reference plane. An ultra short pulse is first dispersed in multiple wavelengths by a grating in free space, spectral coding is performed by passing spectral components of the pulse through a phase or amplitude mask, and the coded spectral components are finally recombined by another grating to form a code sequence.

The scheme in spatial coding requires the use of multiple fibers or multi-core fibers with two dimensional (2D) optical codes in the time and space domains simultaneously [39]. Similarly, the wavelength-hopping time-spreading scheme requires 2D coding in the time and wavelength domains [39]. The wavelength-time schemes provide lower probability of interception and offer scalability and flexibility. Probability of interception is enhanced because the pulses of each code sequence are transmitted in different wavelengths, making eavesdropping more difficult. This feature in the physical layer can be useful for time-sensitive secure transmissions, such as in strategic or military systems, where encryption delay is critical [39].

The optical CDMA (OCDMA) system consists of two basic categories, namely coherent and non-coherent, which is also known as positive OCDMA, while the all-optical CDMA system is referred to as an incoherent system.

2.5.1 Coherent OCDMA Systems

Coherent OCDMA [40-44] requires the exact knowledge of the carrier phase. This means the phase plays an important role in coding design for such systems. Since coherent system is phase sensitive, the use of such techniques will of course be more complex than that of incoherent ones, because of the need to provide adequate optical phase control. On the other hand, if the phase can be controlled adequately, then it should add new dimensions to the design of OCDMA networks, potentially bringing very useful results. The coherent OCDMA system may be partly optical or all-optical. In the partly optical system the chip sequence is generated electronically. The optical receiver gives out the electrical chip sequence which is recognized electronically.

Example of coherent OCDMA systems are the delayed line based coherent direct sequence OCDMA and time spread OCDMA.

2.5.1.1 Delay Line Based Coherent Direct Sequence OCDMA

In Coherent Direct Sequence Optical CDMA as shown in Figure 2.4 [45], each pulse is modulated by the value of the on-off keyed data, and then split into sub-pulses along different optical paths [45]. All pulses are gathered through combiner or passive coupler then coupled into the same fiber. The received signals will be decoded to distinguish the desired signal from others. Detection and decision circuits are used to compare the decoded signals with the threshold value. The main disadvantages of this technique are that it needs synchronization and is costly because of the laser source.

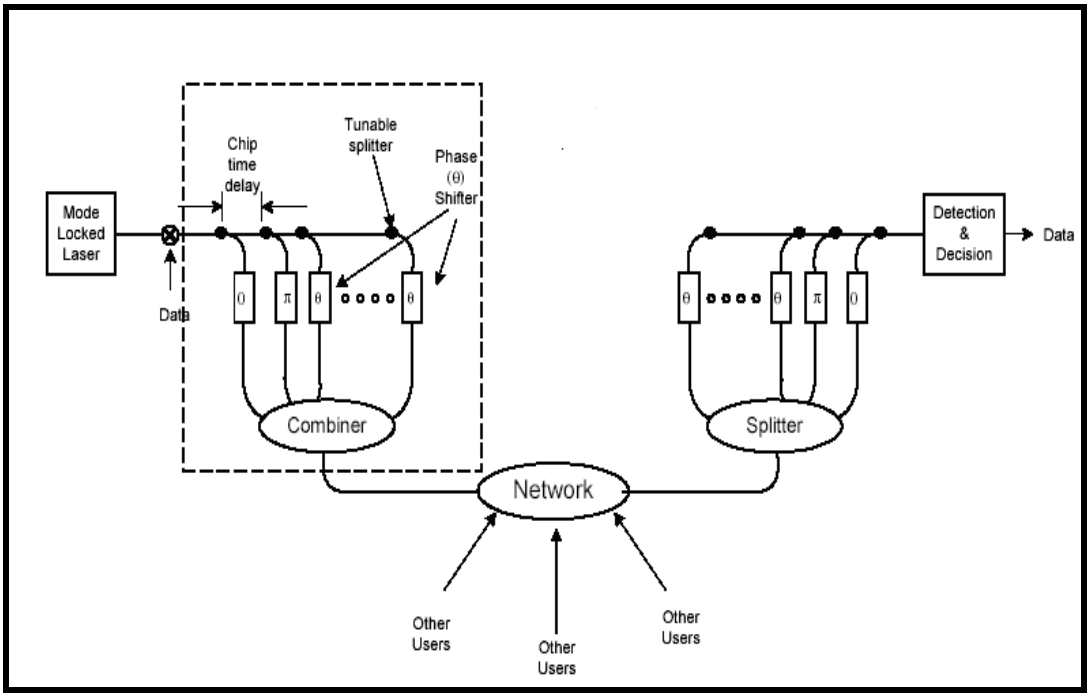

Figure 2.4: Delayed Lines Based Coherent Direct Sequence Optical CDMA.

2.5.1.2 Time Spread Optical CDMA

The idea of using the frequency axis as an encoding resource for time spreading optical CDMA is promising; first it was proposed by Winer *et al* [46-48]. Figure 2.5 shows an example for time spread Optical CDMA. This system requires a Mode

locked Loop Laser with a broad coherent bandwidth. The output of the laser is modulated with On-Off keyed (OOK) modulation by the binary data. Laser light is focused on a Brag grating that separates the frequency or wavelength components of the light. A Programmable Liquid Crystal (PLC) phase mask then shifts the phase of each of the spectral components according to the assigned bipolar code. Finally, the other Brag grating recombines the separated spectral components and gathered light is rejected into the fiber. Unfortunately, this system is too complicated to implement. In addition, the use of lenses suffers from high splitting or insertion losses.

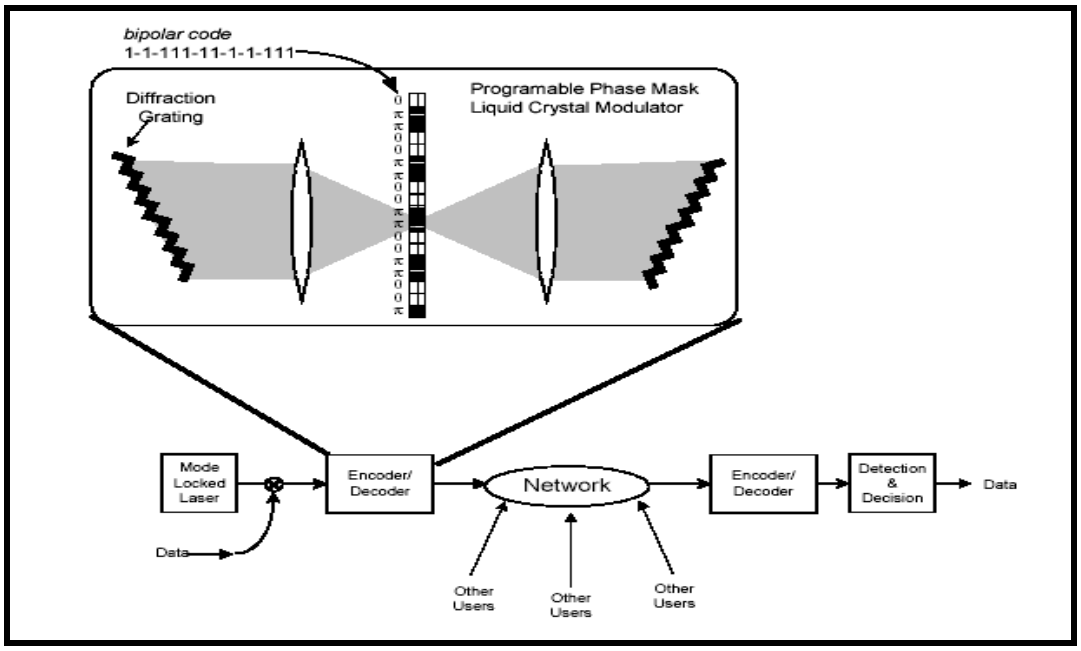

Figure 2.5: Time Spread Optical CDMA.

2.5.2 Incoherent OCDMA system

While coherent detection refers to the detection signals with knowledge of the phase information of the carriers, incoherent detection [49-52] refers to the case without such knowledge. In other words, a system consisting of unipolar sequences in the signature code is called incoherent system. Incoherent detection has gained more attention by optical communication community around the globe because such system does not require phase synchronization. As a result, the hardware complexity of the system is extremely reduced. Many versions of incoherent systems have been

proposed and the main effort has been targeted on the codes and its encoder/decoder structure. There are three main systems that have been proposed which are: Direct Spreading, Spectral Amplitude Coding and Frequency Hopping systems.

2.5.2.1 Incoherent Direct Spreading optical CDMA system

This system depends on direct spreading with unipolar codes [8-9]. Figure 2.6 illustrates an incoherent direct spreading optical CDMA system. Previous systems have used tap delay lines for the encoder/decoder structure. However, programmable ladder are more attractive today. As shown in Figure 2.6, the receiver decoder is identical to encoder except that it performs the inverse function. Chip-pulses that arrive in advance are delayed; this means all the chip-components of the signal pass through an equivalent path. The pulses arriving from the desired transmitter will hold up in the same chip duration, thus requiring a fast time-gate.

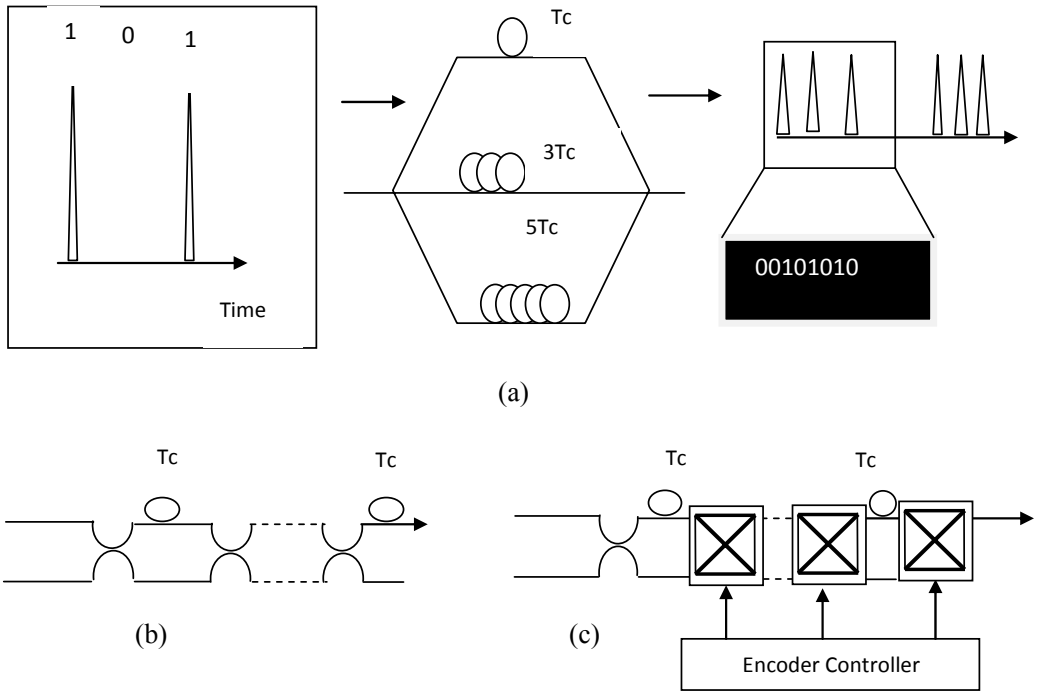

Figure 2.6: Incoherent DS-OCDMA Encoding/Decoding (a) Tapped Delay lines, (b) Ladder network, (c) Programmable Ladder network**.**

2.5.2.2 Incoherent spectral intensity optical CDMA System

In this type [29, 53-58], each code channel uses a spectral amplitude encoder either to selectively block or transmit certain frequency components as in Figure 2.7 below. Also, there is a balanced receiver which contains two photo detectors. This balanced receiver is used as a part of the receiver, which filters the incoming signal with the same spectral amplitude filter also called the direct filter, being used at the transmitter as well as its complementary filter [59]. Then the two photo detectors detect the output from the complementary filter. These two photo detectors are connected in a balanced fashion. For unmatched transmitters, half of transmitter spectral components will match the direct filter and the other half will match the complementary filter. The output of the balance receiver represents the difference between the two photo detectors, with unmatched channels being cancelled, while the matched channel is demodulated. It is possible to design codes with the full orthogonality in the incoherent spectral intensity OCDMA system, since there is a subtraction between two photo detectors.

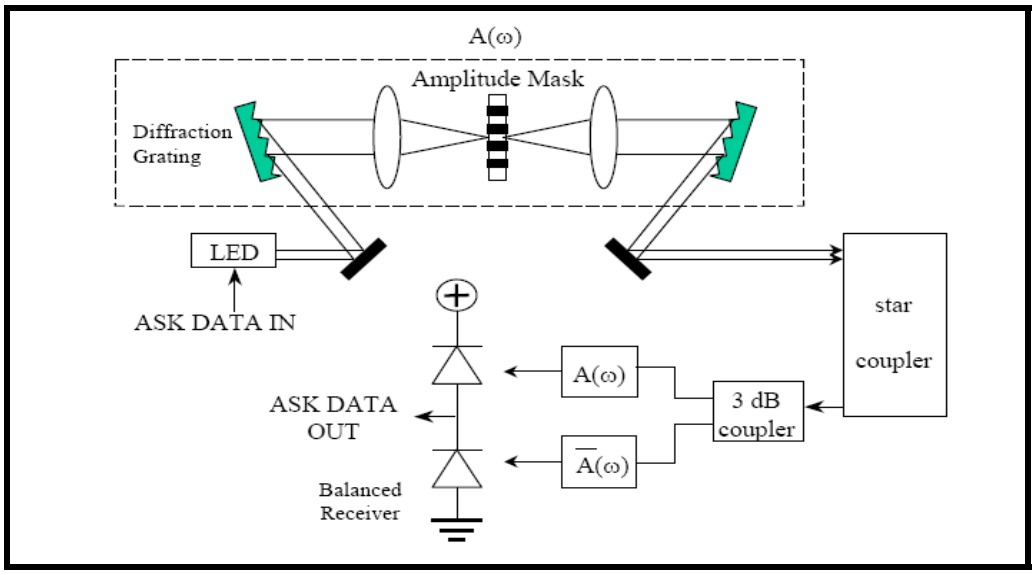

Figure 2.7: Incoherent Spectral Intensity Encoded Optical CDMA System.

The advantages of this technique are, it does not require system clock, uses LED and with no tapped delay lines. And the disadvantages of these techniques are, loss of

perfect orthogonality between the users due to Gaussian shape of LED spectrum and it needs tunable filters to reshape the spectrum. Bipolar technique is also achieved through phase shifting which is optically complex.

2.5.2.3 Optical Spectral CDMA (OSCDMA) System

In OSCDMA, there are *N* users with optical transmitters and receivers [35, 60]. The system uses incoherent broadband light source to derive its channel by selectively blocking out part of the light, giving it the appearance of a bar code as shown in Figure 2.8. The architecture of the OSCDMA can be seen in Figure 2.9. The encoder and decoder of OSCDMA are implemented using any type of optical filtering technology, including thin-film filters, fiber Bragg gratings, or free space diffraction gratings.

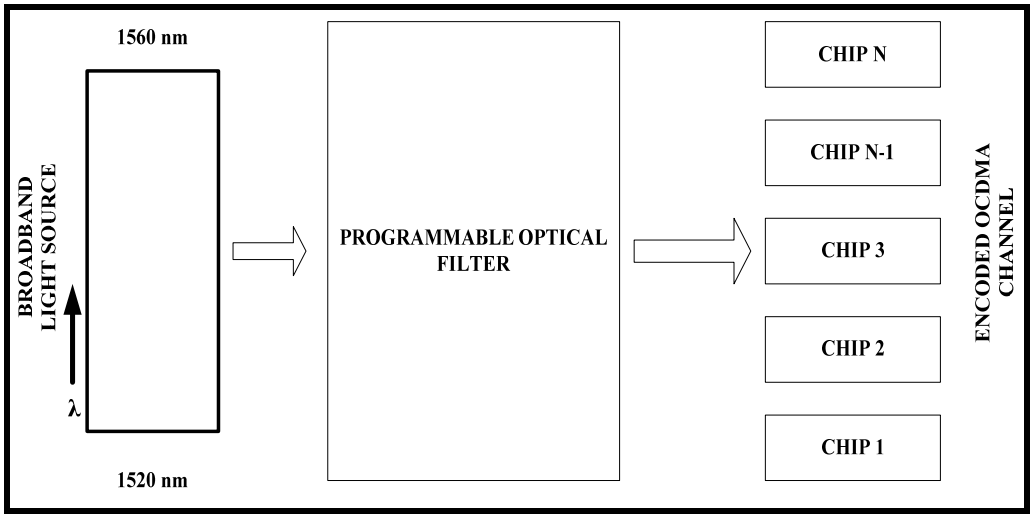

Figure 2.8: OSCDMA Transmitter Encoding.

The Optical Spectral (OSCDMA) system has many advantages compared to other techniques such as using an LED as an optical source which makes the system cheaper, no requirement for synchronization and simplicity of encoder/decoder structure design.

As shown in Figure 2.8, OSCDMA system consists of a common optical source (LED, Laser, etc) connected to a fiber strand that provides energy spanning all points on the network. Individual transceivers tap into this energy at any point, allowing information to be transmitted and received from anywhere on the network. At the receiving end, the receiver with the matching bar code connects to the transmitter and takes the signal destined for it to recover the transmitted messages.

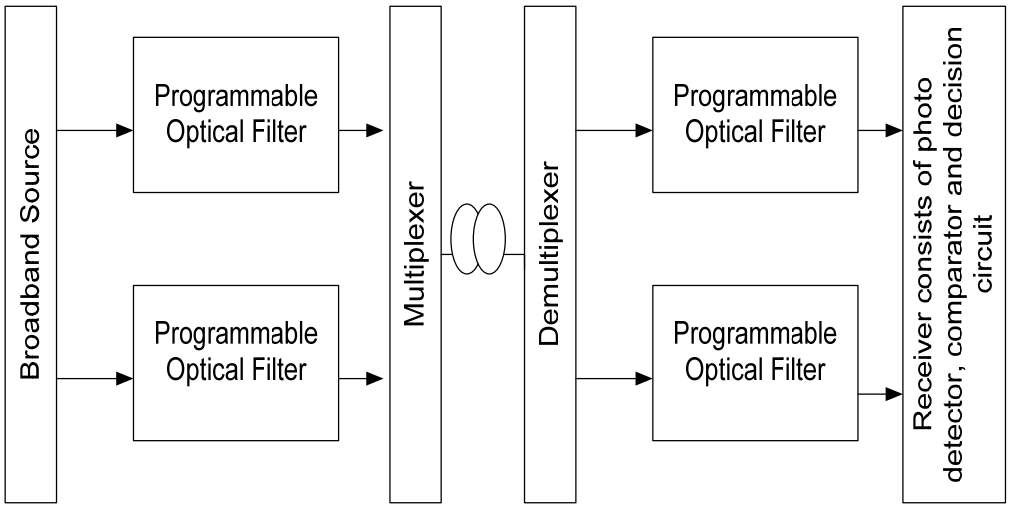

Figure 2.9: The system architecture of OSCDMA.

2.6 Construction of coherent OCDMA Codes

In this section to simplify the concepts of OCDMA system, some comparisons need to be made. Several examples of coherent codes will be given in this section, while incoherent codes will be addressed in the following section. The bipolar [+1, -1] codes for coherent OCDMA originated from radio spread-spectrum technology in the 1940s [39]. The technology was aimed at avoidance of jamming and eavesdropping in military communication systems. The bipolar codes used in wireless CDMA are designed to have close-to-zero cross correlation functions to minimize MAI. The most popular codes are the Walsh (Hadamard) code, maximal length sequence and Gold sequence.

2.6.1 Walsh (Hadamard) code

Walsh codes are employed to improve the bandwidth efficiency of wireless CDMA since they have zero cross correlation functions when they are all synchronized in time [39]. Hadamard codes have length of $N = 2^n$, denoted by H^j_N where n is a positive integer, $j \in [0, N-1]$ is the jth row extracted bipolar sequence of H_N.

$$H_1 = [1], H_2 = \begin{bmatrix} 1 & 1 \\ 1 & -1 \end{bmatrix}, H_3 = \begin{bmatrix} H_2 & H_2 \\ H_2 & \overline{H_2} \end{bmatrix} = \begin{bmatrix} 1 & 1 & 1 & 1 \\ 1 & -1 & 1 & -1 \\ 1 & 1 & -1 & -1 \\ 1 & -1 & -1 & 1 \end{bmatrix} \tag{2.1}$$

$$H_{2^{n+1}} = \begin{bmatrix} H_2 & H_2 \\ H_2 & \overline{H_2} \end{bmatrix} \tag{2.2}$$

where $\overline{H}$ represents the complement of H_{2^n}. The cross correlation of any two code sequences is zero i.e. $\left(H_N^{(j)} \left(H_N^{(k)} \right)^T = 0 \right)$ and autocorrelation for the same code sequence is $N\left(H_N^{(k)} \left(H_N^{(k)} \right)^T = N \right)$.

2.6.2 Maximal-Length Sequence

The maximal-length sequences are of great interest in cellular spread spectrum networks because the correlation functions between different shifts of the sequences are always equal to –1 and, thus, they can be used as different code sequences with an excellent correlation property. The code sequences can be expressed as:

$$S_m = \left[cc^{(-1)} \; c^{(-2)} \; \ldots c^{(-i)} \; \ldots c^{(-2^m+2)} \right]^T$$

For a length $2m$-1 where $c^{(-i)}$ represents the ith cyclic left-shift of c, and T the vector transpose. For a code sequence c= [+1+1-1+1-1-1-1], $c^{(-1)}$ = [+1-1+1-1-1-1+1] ... etc [39].

2.6.3 Gold sequences

Gold Sequences belong to an important family of bipolar codes that can be used in asynchronous wireless CDMA. Gold sequences not only provide a large cardinality but also have a good periodic cross correlation property for asynchronous operations [39]. The set of gold sequences is then given by

$$S_{gold} = \left[xyx \oplus y^{(-1)} \quad x \oplus y^{(-2)} \quad ...x \oplus y^{(i)} \quad ...x \oplus y^{(-(N-1))} \right]^T$$

where $y^{(i)} = \left[y_i y_{i+1} ... y_{N-1}, y_0 y_1 ... y_{i+1} \right]$ is the ith cyclic left-shift of $\left[y_0 y_1 ... y_i, y_{1-N} \right]$, $y_i = \{+1, -1\}$ and "$\oplus$" denotes an exclusive OR operation. These gold sequences have a three-valued cross correlation function given by $-t_m$, -1, and t_m^{-2} where $tm=1+2^{(m+1)/2}$ for odd m, $t_m=1+2^{(m+2)/2}$ for even m.

Take N=7 as an example, the preferred pair of gold sequences of length 7 are represented by x, y, x $\oplus$ y= {+1+1+1+1-1+1-1} etc [39].

2.7 Construction of incoherent OCDMA Codes

In OCDMA with incoherent optical signal processing, the signature code is a family of unipolar (0, 1) sequences. This type of system mainly depends on the amplitude in code design. Optical Orthogonal Code (OOC) and Prime codes are two well-known families suitable for time-spreading system [7-9]. Many codes have been proposed for the wavelength-hopping time-spreading OCDMA system such as, fast-frequency hopping [27], Carrier hopping [7], and Extended Carrier hopping prime codes [28]. While for the spectral-amplitude coding (SAC) OCDMA systems [29-37], Hadamard [29], Integer Lattice code [30-31], Balance Incomplete Block Design (BIBD) code, Modified Quadratic Congruence (MQC), Modified Frequency Hopping (MFH) code [32-33], Double Weight (DW) code [35, 60], Enhance Double Weight (EDW) code [36] and most recently the Random Diagonal (RD) [37].

2.7.1 Time-spreading systems codes

There have been many codes proposed for time-spreading systems. The most popular of them are OOCs and Prime codes which will be discussed in detail in the following section.

2.7.1.1 Primes Codes

The number of code sequences in the prime code over Galois field *GF* (*p*) of a prime number *p*. The minimum Hamming distance of the prime code is *p*-1 and the code is a kind of maximum distance separable cyclic code [39]. The Prime codes are of length $N = p^2$ and are derived from prime sequences of length p obtained from a Galois field GF(*p*), where *p* is a prime number. The code size and weight is equal to *p*. The number of users and weight of the code can be any prime number *p* [7, 39, 61].

The codes can be constructed as follows.

1. Starting with GF(*P*) = (0, 1,2, …., *p*-1), a Prime sequence $S_X = (S_{X0}, S_{X1}, ..., S_{X(P-1)})$ is constructed by multiplying every element j of GF(*p*) by an element *X* of GF(*p*) modulo *p*. Therefore,

$$S_{Xj} = (X.j) \bmod P \text{ for } X.j = 0,1,2,..., p-1 \tag{2.3}$$

   p distinct prime sequences can be obtained.

2. The obtained prime sequences are mapped into a binary code sequence $C_X = (c_X[0], c_X[1], ..., c_X[n-1])$ by assigning ones in positions $i = S_{Xj} + jP$ for, j = 0, 1, 2,…,*p*-1 and zeros in all other positions. Therefore**,**

$$C_x[i] = \begin{cases} 1 \ for \ \ i = S_{Xj} + jP, \ \ j = 0,1,....,P-1 \\ 0 \qquad\qquad\qquad Otherwise \end{cases} \tag{2.4}$$

   For *X* = 0, 1, …., *P*-1.

Since the number of coincidences of one's is at the most two, the maximum cross correlation of the prime code is bordered to two. However, the function of autocorrelation side lobes do not go beyond one, but the autocorrelation function peak

is equal to the prime number p (examples of the prime sequences for $p = 5$ are given in Appendix A.1).

2.7.1.2 Optical Orthogonal Codes (OOC)

An optical orthogonal code (OOC) [8-9, 39, 62-63] which is characterized by (L, w, λa, λc) is a family of [0, 1] with length L and weight w (number of ones) and good properties of autocorrelation and cross correlation (high autocorrelation and low cross correlation). The good autocorrelation facilitates the detection of the desired signal and low cross correlation minimizes MAI influence in the network. From mathematical point of view, the correlation properties can be expressed as follows.

a. Autocorrelation property: for any $X \in C$ and any integer τ, $0 \le \tau \le N$

$$\sum_{t=0}^{N-1} X_t X_{t \otimes \tau} \le \lambda_a \tag{2.5}$$

b. Cross correlation property for any $X \ne Y \in C$ and any integer τ

$$\sum_{i=0}^{N-1} X_t Y_{t \otimes \tau} \le \lambda_c \tag{2.6}$$

The relations between number of user |C|, code length N and code weight W is given:

$$|C| = \frac{N\text{-}1}{W(W\text{-}1)} \tag{2.7}$$

The size of an optical orthogonal code C is the total number of code word. The sequences of OOC are designed to satisfy two conditions:

(i) Each sequence can be easily distinguished from a shifted version of itself.

(ii) Each sequence can be easily distinguished from every other sequence in the set.

The codeword length N increases with increasing number of user and weight. The OOC code sequence for 7 users is listed in Appendix A.2.

There are many techniques to construct optical orthogonal code (OOC) which are:

1. The Iterative Construction Technique.
2. The Greedy Algorithms and general lower bounds.
3. The Projective Geometry Technique.

The projective geometry technique is the most popular construction method. The disadvantages of the OOCs are that they have very large code sequence to support even a moderate number of clients. Moreover, all mentioned methods used in code construction are complex and require extra system memory to store constructed codes beforehand. In addition, all OOC families are designed following the requirement for $\lambda_a = \lambda_c \leq 1$.

2.7.2 Wavelength Hopping/Time Spreading Codes

To provide large cardinality in DS-OCDMA systems, codes with very long code length are needed to give good correlation properties. In other word, a very large bandwidth is required, creating a stringent requirement for encoding and decoding hardware speed. Two dimension codes have been proposed for frequency hopping systems. The most popular codes are the Carrier Hopping Prime code, the Multilength Carrier Hopping and Extended Hopping Prime code. The development of Carrier Hopping Prime Code will be discussed in detail in the following section. Figure 2.10 shows Incoherent Frequency Hopping/Time spreading OCDMA system.

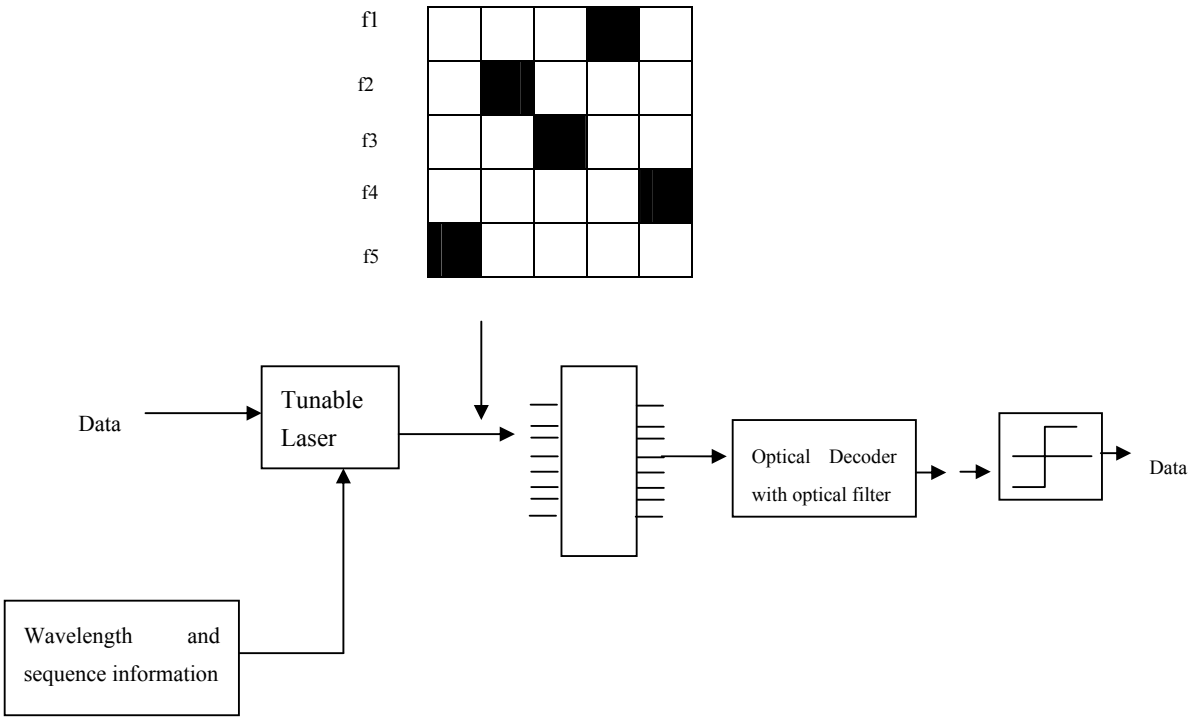

Figure 2.10: Incoherent Frequency Hopping/Time spreading OCDMA system.

2.7.2.1 Carrier Hopping Prime Code (CHPC)

The carrier hopping prime code (CHPC) uses a two-dimensional approach. In which the code sequences are represented both in time and wavelength. The CHPC has a general representation of $w \times p_1 p_2 ... p_k$ binary matrices of length $p_1 p_2 ... p_k$, weight w and a cardinality of $p_1 p_2 ... p_k$, where $p_k \geq p_k\text{-}1 \geq ... \geq p_2 \geq p_1 \geq w$. The weight w is the number of rows, and it is related to the length of the carrier hopping matrices. Because each matrix has a single pulse '1' per row and each pulse is assigned to a different carrier, the CHPC has autocorrelation side lobes of zeros and a maximum cross correlation of one.

2.7.3 Spectral Amplitude Coding Codes

This approach was first proposed by Zacarrin and Kavehrad [29, 52, 54]. Spectral-amplitude-coding systems have been proposed to minimize the multi access interference in DS-OCDMA system. The most popular of them are Integer Lattice code [30-31], Balance Incomplete Block Design (BIBD) code, Modified Quadratic Congruence (MQC) code, Modified Frequency Hopping (MFH) code [32-33], Double Weight (DW) code [35, 60], Enhance Double Weight (EDW) code [36] and most recently the Random Diagonal (RD) code [37]. The development of Hadamard, MQC, MFH, DW, MDW, and RD codes will be discussed in detailed in the following sections.

2.7.3.1 Hadamard code

Hadamard code is constructed based on a matrix. Hadamard matrix is an orthogonal $n \times n$ matrix of the entries +1 and -1 with the property that any row differs from any other row in exactly $n/2$ position. One row of the matrix contains all +1s, while the other rows contain evenly the +1s and -1s of n/2 each. Furthermore, all the entries in the first row and the first column of H_n have all +1s. The $n \times n$ Hadamard matrixes can exist only if n is a power of 2 meaning that $n = 2^m$.

The $n \times n$ is Hadamard matrix H_n, where $n = 2^m$ is generated by the cone matrix.

$$\mathrm{H}_{M=1} = \begin{bmatrix} 1 & 1 \\ 1 & -1 \end{bmatrix}. \tag{2.8}$$

For M=2 the Hadamard matrix will be

$$H_2 = \begin{bmatrix} H_1 & H_1 \\ H_1 & \overline{H_1} \end{bmatrix} = \begin{bmatrix} 1 & 1 & 1 & 1 \\ 1 & -1 & 1 & -1 \\ 1 & 1 & -1 & -1 \\ 1 & -1 & -1 & 1 \end{bmatrix} \tag{2.9}$$

The Unipolar Hadamard matrix H_M has the following properties;

1. M should be greater than 2.
2. Code length $N = 2^M$.
3. Code Weight $W = 2^{M-1}$.
4. User K= $2^M - 1$. (The case K= 1 has been excluded since the row of the unipolar Hadamard matrix is all ones).
5. The ratio of $\frac{W}{\lambda} = 2$ (i.e λ is cross correlation properties).

Example of Hadamard code sequence for 6 users is listed in Appendix A.3.

2.7.3.2 Modified Quadratic Congruence Code (MQC)

The MQC is defined as $(p^2 + p,\ p+1,\ 1)$, and the followings are the steps of its construction:

Step 1: A sequence of integer numbers, which are the elements of the Galois field $GF(p)$ over an odd prime number p, is constructed using the expression given by,

$$y_{\alpha,\beta}(k) = \begin{cases} \left[d(k+\alpha)^2 + \beta\right] \bmod(p) & k = 0,1,\ldots,p-1 \\ \left[\alpha + b\right] \bmod(p) & k = p \end{cases} \tag{2.10}$$

Where, $d \in \{1,2,\ldots,p-1\}$ and $b, \alpha, \beta \in \{0,1,2,\ldots,p-1\}$. Every constructed sequence has (p+1) elements, and thus the p^2 different sequences can be generated for each pair of the fixed parameters of d and b by changing the parameters α and β. These distinguished sequences are from a code family; therefore, there is a p (p-1) code

family when *d* and *b* change.

Step2: The following mapping expression is used to generate a binary sequence from the created sequence of numbers,

$$C_{\alpha,\beta}(i) = \begin{cases} 1, & if\ i = kp + y_{\alpha,\beta}(k) \\ 0, & otherwise \end{cases} \tag{2.11}$$

Where $i = 0,1,2,....,p^2\text{-}1$, and k is the largest integer less than or equal to i/p.

p^2 is the size of the MQC code and each code consists of $p^2 + p$ elements, with each p+1 group consists of one "1" and p-1 "0s". Always the in-phase cross correlation between any two codes is equal to one.

2.7.3.3 Modified Frequency Hopping Code (MFH)

The MFH is defined as $(q^2 + q, q + 1, 1)$, and the followings are the steps of its construction.

Step1: Let *GF(q)* be a finite field of element and β a primitive element of *GF(q).*

We can construct a number sequence $Y_{\alpha,b}(k)$ with the elements of *GF (q)* using the following formula:

$$y_{a,b}(K) = \begin{cases} \beta^{(\alpha+K)} + b, & K = 0,1,2,.....,q-2 \\ b, & K = q-1 \\ \alpha, & K = q \end{cases} \tag{2.12}$$

where α and b are elements of *GF(q)* expressed by $\alpha \in \{0,1,2,....,q-2\}$ and $b \in \{0,1,2,....,q-1\}$.

The parameters α and b are fixed for each specified number sequence. This number of sequences can be constructed as follows:

$$y'(K) = \begin{cases} b, & K = 0,1,2,.....,q-1 \\ q-1, & K = q. \end{cases} \tag{2.13}$$

Step 2: Based on generated number sequence $y(k)$, a sequence of binary number S (i) can be constructed by using the mapping method as follows:

$$s(i)=\begin{cases}1, & \text{if } i=Kp+y(K)\\ 0, & \text{else}\end{cases} \tag{2.14}$$

The MFH code consists of the properties as listed below:

1. Every code sequence q^2+q possesses the elements that can be separated into $(q+1)$ groups, with each group containing one "1" and $(q-1)$ "0s".
2. Between any two sequences, the in-phase cross correlation is always equal to 1. In addition, the first one can be easily obtained from the mapping method in the two properties, as explained in Step 2.

Appendix A lists out several code examples for the different values of parameters α and b when q is equal to 2^2 (i.e. $q=4$).

2.7.3.4 The Double Weight (DW) Code

The DW code is proposed by *Aljunid et al*. [35, 60], for SAC system, constructed using a basic matrix and a mapping technique. The DW code can be represented by $K\times N$ matrix where K rows and N columns represent the number of users and code length respectively. A basic DW code is given by a 2×3 matrix as shown below:

$$\mathbf{H}_{\mathrm{M=1}}=\begin{bmatrix}\mathbf{1}\downarrow & \mathbf{2}\downarrow & \mathbf{1}\downarrow\\ 0 & 1 & 1\\ 1 & 1 & 0\end{bmatrix} \tag{2.15}$$

It should be pointed out that $H_{M=1}$ has a chip combination sequence of 1, 2, 1 for three columns. The purpose of the 1, 2, 1 combination is to maintain the cross correlation value of one. Only one overlap will occur between two chips [35, 60]. To increase the number of users a mapping technique is introduced:

$$H_{M=2}=\left|\begin{array}{ccc:ccc} 0 & 0 & 0 & 0 & 1 & 1 \\ 0 & 0 & 0 & 1 & 1 & 0 \\ \hdashline 0 & 1 & 1 & 0 & 0 & 0 \\ 1 & 1 & 0 & 0 & 0 & 0 \end{array}\right| = \left|\begin{array}{cc} 0 & H_1 \\ H_1 & 0 \end{array}\right| \tag{2.16}$$

In (2.17) notice that the number of rows and columns should be doubled. The relation between mapping process (M) and K and N is given by

$$K = 2^{M} \tag{2.17}$$

$$N = 2^{M} + 2^{M-1} \tag{2.18}$$

From equations (2.18) and (2.19), the length of the code can be derived as equation (2.19) below.

$$N = \begin{cases} \frac{3}{2}K, & \text{when } K \text{ is even} \\ \frac{3K}{2}+\frac{1}{2}, & \text{when } K \text{ is odd} \end{cases} \tag{2.19}$$

For both even and odd, equation (2.19) can be rewritten as:

$$N = \frac{3K}{2} + \frac{1}{2}\left[\sin\left(\frac{K\pi}{2}\right)\right]^2 \tag{2.20}$$

The DW code properties can be summarized as follows:

a. Each code sequence has a fixed weight of 2**.**
b. Cross correlation λ_c is always equal to 1.
c. The weighted chips are always in pairs.
d. The chips combination is maintained 1, 2, 1 for every three columns for consecutive pairs of codes.
e. The relation between the number of users (K) and code length (N) is given by:

$$N = \frac{3K}{2} + \frac{1}{2}\left[\sin\left(\frac{K\pi}{2}\right)\right]^2 \tag{2.21}$$

2.7.3.5 Modified Double Weight Code (MDW)

The MDW code is a modified version of the DW code family and has the same properties as DW code. Equation 2.23 shows the basic matrix construction of MDW. This basic matrix consists of a minimum number of *K* and *N* for a specific number of code weights. The construction of all matrixes A, B, C and D depends on the weight *W*.

$$\left[\begin{array}{c|c} [A] & [B] \\ \hline [C] & [D] \end{array}\right] \tag{2.22}$$

[A] Consists of a $1 \times 3\sum_{j=1}^{\frac{W}{2}-1} j$ matrix of zeros.

[B] Consists of a 1 x 3***n*** matrix of [X_2] for every 3 columns. (i.e. a 1 x 3***n*** matrix with ***n*** times repetition of [X_2]), where $n = \frac{W}{2}$.

[C] Is the basic code matrix for the next smaller weight, $W = 2(\boldsymbol{n}\text{-}1)$.

[D] Is an ***n*** x ***n*** matrix of [X_3] as shown in equation (2.23)

$$[D] = [X_3] = \begin{bmatrix} 000 & 000 & [X_3] \\ 000 & [X_3] & 000 \\ [X_3] & 000 & 000 \end{bmatrix} \tag{2.23}$$

Where:

$$X_1 = [0 \;\; 0 \;\; 0] \tag{2.24}$$

$$X_2 = [0 \;\; 1 \;\; 1] \tag{2.25}$$

$$X_3 = [1 \;\; 1 \;\; 0] \tag{2.26}$$

The two basic components in the basic matrix of MDW code are:

Basic Code Length:

$$N_B = 3\sum_{m=1}^{\frac{w}{2}} m \tag{2.27}$$

Basic number of users:

$$K_B = \frac{w}{2} + 1 \tag{2.28}$$

Example of MDW code sequence for 6 users is listed in Appendix A.4.

2.7.3.6 Random Diagonal (RD) Code

The RD is proposed by Hilal *et al*. [37], for SAC system. The RD code is constructed using a basic matrix and a mapping technique. The design of this new code can be performed by dividing the code sequence into two groups, which are code segment and data segment.

Step1, data segment: Let the elements in this group contain only one "1" to keep cross correlation zero at data level (λ=0). This property is represented by the matrix ($K\times K$) where K will represent number of users.

$$[Y_1] = \begin{bmatrix} 001 \\ 010 \\ 100 \end{bmatrix} \tag{2.29}$$

Step2, code segment: The representation of this matrix can be expressed as follows for *W=4:*

$$[Y_2] = \begin{bmatrix} 01110 \\ 11001 \\ 10110 \end{bmatrix} \tag{2.30}$$

where $[Y_2]$ consists of two parts - weight matrix part [W],and basic matrix part [B]. Basic part [B] can be expressed as:

$$[B] = \begin{bmatrix} 011 \\ 110 \\ 101 \end{bmatrix} \tag{2.31}$$

The weight part called [*M*] matrix $\begin{bmatrix} 10 \\ 01 \\ 10 \end{bmatrix}$ is responsible for increasing the number of weights.

For *K-th* user matrix [*M*] and [*B*] can be expressed as:

$$[B](j) = \begin{bmatrix} 0 & 1 & 1 \\ 1 & 1 & 0 \\ 1 & 0 & 1 \\ 1 & 1 & 0 \\ \vdots & \vdots & \vdots \\ a_{j1} a_{j2} a_{j3} \end{bmatrix} \text{ and } [M](j) = \begin{bmatrix} 0 & 1 \\ 1 & 0 \\ 0 & 1 \\ 1 & 0 \\ \vdots & \vdots \\ a_{j1} a_{j2} \end{bmatrix}$$

After combining all of these matrices, the whole code can be expressed as:

$$Z_1 = \begin{bmatrix} 00101110 \\ 01011001 \\ 10010110 \end{bmatrix} \tag{2.32}$$

The general equation describing number of users *K*, code length *N* and code weight *W* is given as:

$$N = K + 2W - 3 \tag{2.33}$$

2.8 OCDMA Applications

The scalability and reliability of optical CDMA techniques are reflected in the variety of applications. For optical CDMA networking, its potential for enhanced security, decentralized control, and flexibility in bandwidth granularity provides interesting possibilities to overcome TDMA and WDMA drawbacks. These applications depend on many factors including network scalability, device integration, system cost, and environmental robustness [39]. An example of the OCDMA system application is in

Local Area Network (LAN) environment. This will be addressed in the following section.

2.8.1 Local Area Network (LAN)

While Ethernet and Gigabit Ethernet continue to play a dominant role in LAN environments, the scalability of these networks is presently limited by the electronic technology in the hubs and switching nodes used to actively resolve contention on the LAN. Ultimately, the electronic bottleneck at switching nodes currently limits the scalability, flexibility, and cost of the overall LAN network [39]. These limitations have motivated the communication community to study the potential of OCDMA in local area networks where the traffic is typically bursty. Optical CDMA has the potential to provide large cardinality and adapt gracefully to dynamic service needs and unpredictable network loading conditions. While optical CDMA has the potential to provide scalability beyond the limits of today's LAN environments that are still dominated by electronic switching technologies, it is also an efficient approach when compared to other multiple access optical networking technologies that have been reported over the last two decades.

2.8.1.1 Passive Star Network

In this section, star network is used to describe the OCDMA networks. A star network is a general class of interconnectivity among many nodes with a centralized node that broadcasts all network transmissions to all receivers (Figure 2.11). Each user is assigned a unique address on the network that enables it to distinguish traffic destined for its receiver from the traffic on the rest of the network. The implementation of star networks in the optical domain is promising for LAN environments and short distance interconnection networks. This is because star networks can provide bidirectional, transparent, full-duplex communications among many optical nodes [39]. To enable optical traffic from individual input optical fibers to be optically combined and broadcast to many output optical fibers, star couples are used. To support new services or higher data rates, individual nodes can be upgraded effectively without replacing the fiber interconnection network. The star network is especially important

for applications that require high bandwidth communications among many users, such as a distributed computer interconnect, where each destination node has approximately the same expected network demand.

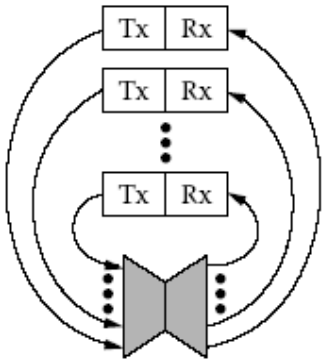

Figure 2.11: Star fiber network topology.

2.8.1.2 OCDMA for Local Area Networks

Optical Code Division Multiple Access (OCDMA) [8-11] offers an attractive alternative for local area networks where the traffic tends to be bursty. OCDMA offers several advantages in local area networks. First of all, OCDMA allows simultaneous users to send their data asynchronously and with no waiting time [10] through the assignment of unique signature sequence. It also offers strong security in the physical layer. As a result, OCDMA receives substantial attention for the use in LAN. However, the performance of OCDMA is known to be limited by the Multiple Access Interference (MAI) originating from other users trying to use the medium simultaneously.

As it is important to have reliable and flexible networks for the future, it will be attractive for networks to change their quality of service (QoS), classes of service and data rate provided to the individual users on the fly according to their current application requirements. Optical CDMA provides a more flexible and robust bandwidth sharing technique for adaptable network interfaces. The cost and complexity of each optical CDMA node can be designed for the data rate and service

desired at a given node. Additionally, when users do not require the maximum data rate or the highest QoS, these codes can be assigned to other users to free available bandwidth for high priority applications. The optical network interfaces can also be simplified and potentially lowering the cost than equivalent implementations of optical LANs using OTDMA and WDMA.

For nodes that are assigned to lower QoS levels, it is not necessary to access all wavelengths available on the optical CDMA LAN since encoding and decoding the full weight of the code is not required. This is extremely important in the bandwidth utilization. In optical CDMA trade-offs in system performance, cost, network size, and QoS, provides an inherently flexible optical multiple access environment that retains many of the same benefits of traditional electronic LANs but with the scalability of optics.

2.9 Summary

Optical code division multiple access (OCDMA) is one of the multiple access techniques used in the field of optical communication. In this technique, a data bit is naturally encoded by sub-dividing it into many smaller chips. Each user is assigned a unique signature code that specifies the chips that must contain optical power. At the receiver, the complement decoder is used to correlate the incoming chip stream, thus reproducing the autocorrelation peak. The advantages of OCDMA technique against other multiple techniques such as time division multiple access (TDMA) and wavelength division multiple access (WDMA) are numerous.

The OCDMA system consists of two basic categories, namely coherent and incoherent, which is also known as positive OCDMA. Example of coherent OCDMA systems are the delayed line-based coherent direct sequence OCDMA and time spread optical CDMA. Examples of incoherent OCDMA systems are Direct Spreading, Spectral Amplitude Coding systems and Frequency Hopping systems. The use of these systems has been elaborated with more emphasis on spectral amplitude coding.

Many codes have been proposed for OCDMA such as Prime codes, Optical Orthogonal codes (OOC), Hadamard codes, Modified Quadratic Congruence codes

(MQC), and Modified Frequency Hopping codes (MFH). Hadamard is originally the basic and popular code. MQC and MFH have the ideal cross correlation properties and shorter code length for the price of strict number of users and code construction complexity; while the code length of Prime codes and OOC codes are too long. RD codes have the cross correlation of more than one.

A local area network (LAN) environment is selected to implement the code. Several classes of star networks relevant for optical CDMA implementations have been reported and demonstrated, each having their own particular advantages. Passive star network has been addressed in this chapter.

In this thesis, the scope of focus in code application is on local area network (LAN) as these are the areas that are expected to be better ready for the implementation of OCDMA multiple access technology. The setup is based on a point-to-point transmission which represents a segment of a typical star LAN and will be discussed in Chapter 6.

CHAPTER 3
DEVELOPMENT OF VECTOR COMBINATORIAL CODE FAMILIES

3.1 Introduction

In this chapter, we have proposed a series of new code families for the spectral-amplitude coding optical code-division multiple-access (CDMA) system namely Vector Combinatorial (VC). We have constructed these code families by using an algebraic way based on Euclidian vectors for any positive integer number. One of the important properties of these codes is that the maximum cross-correlation is always one which means that multiple access interference (MAI) and phase induced intensity noise (PIIN) are reduced. Two algorithms are developed to construct several code families for different applications. In Section 3.2 we address the key issues and consideration of optical codes design. Next, in Sections 3.3 and 3.4, the construction algorithms, correlation properties, and cardinality of various VC code families which are zero cross correlation vector combinatorial (ZVC), ideal vector combinatorial (IVC) code, non-ideal vector combinatorial (NVC) and vector combinatorial (VC) code are studied. A set of C++ programming tools for codes patterns generation is developed. Simplicity of construction, larger code sequence families, good property in cross correlation, and easy to implement using fiber Bragg gratings (FBGs) are the properties that make the proposed VC families interesting candidates for future optical communication systems.

Figure 3.1 shows the study structure of OCDMA code development activities. The theoretical analyses have been conducted on the ZVC and VC codes, and the existing optical codes such as Hadamard code, Modified Frequency Hopping code and Random Diagonal code. All the mathematical relations between the code length and weight are developed and discussed comparatively, referring also to the development

of the reported codes which use similar techniques such as Hadamard, MQC, MFH and RD code, and their properties as discussed in Chapter 2.

As shown in Figure 3.1, Hadamard, Modified Frequency Hopping (MFH) and Random Diagonal codes are chosen for comparison with our proposed codes. The choices are made because Hadamard is originally the basic and widely familiar code, MFH is the famous code reported in spectral amplitude coding whose performance has been shown to outperform that of others while RD code is the latest code mentioned in the literature.

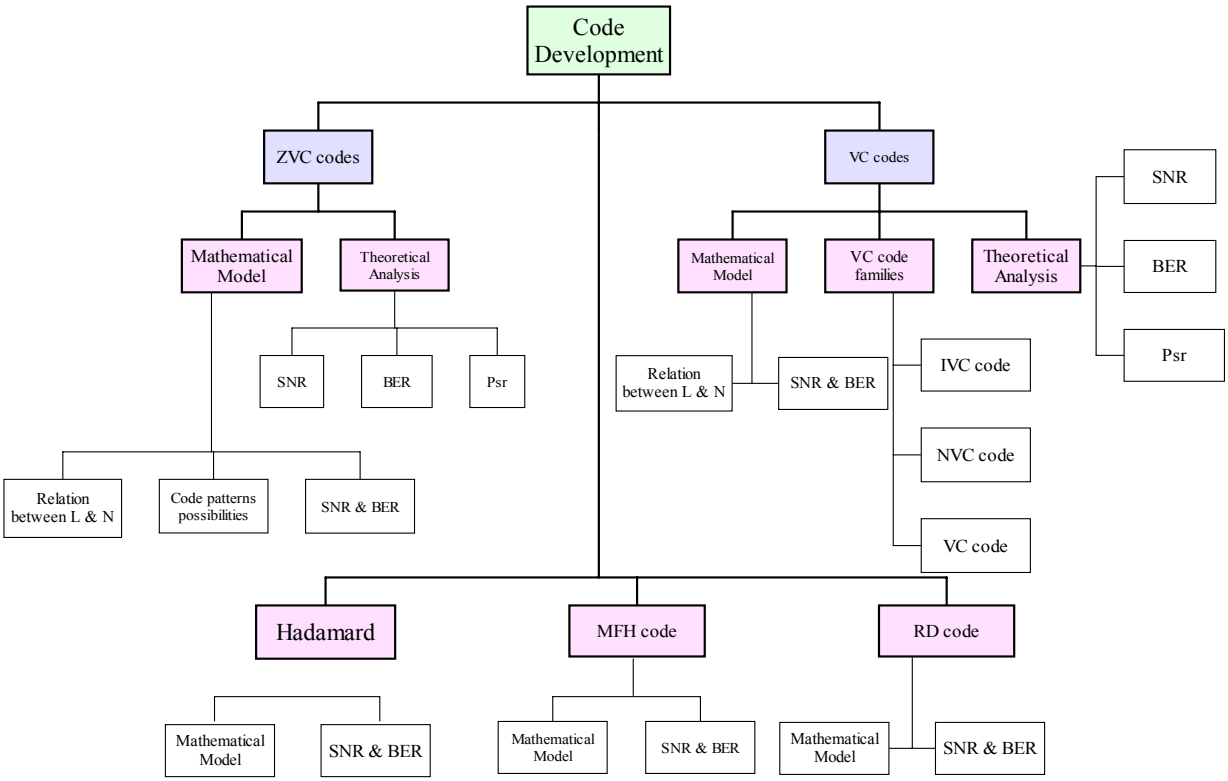

Figure 3.1: Scope of Study in OCDMA Code Development.

3.2 Optical Codes Design Consideration

In spectral-amplitude coding OCDMA, the proposed code must be capable to: effectively suppress the intensity noise, increase the number of active users and improve the bit error rate (BER) performance.

Generally, any code for an OCDMA system can be characterized by the parameters (L, W, λc) where L is the code length, W is the code weight (number of marks) and λc is the cross correlation or the number of overlapping sequences. Correlation functions are important parameters in understanding the properties of OCDMA codes. There are two types of correlation, autocorrelation and cross correlation functions. The cross correlation represents the degree of mutual interference between two code sequences. Autocorrelation function determines how well a code sequence is detected at an intended receiver in the presence of mutual interference.

The essential goal of OCDMA system design is to extract data with the desired code word in the presence of all other users or code words. Two conditions must be satisfied in code sequences design [8-9, 26, 60]

1. The autocorrelation (λ_a) property should be made as high as possible to differentiate the received signal in the presence of background noise in the system. For a code sequence $X = (x_1, x_2, \cdots, x_N)$, the autocorrelation function can be represented as:

$$\lambda_a = \sum_{i=1}^{N} x_i x_i \tag{3.1}$$

2. The cross correlation (λ_c) property between any pair of code sequences should be kept as low as possible to reduce the contribution of multiple access interference (MAI) to total received signal. For the code sequences $X = (x_1, x_2, \cdots, x_N)$ and $Y = (y_1, y_2, \cdots, y_N)$, the cross correlation function can be represented by:

$$\lambda_c = \sum_{i=1}^{N} x_i y_i \tag{3.2}$$

Design codes with ideal in-phase cross correlation $(\lambda_c \leq 1)$, are required in the OCDMA systems since these codes eliminate multi-user interference and also suppress the effect of phase-induced intensity noise or PIIN [29-35].

3.3 ZVC Code Construction

Definition: In mathematics, the standard basis (also called natural basis or canonical basis) of the *n*-dimensional Euclidean space $\boldsymbol{R}^n$ is the basis obtained by taking the *n* basis vectors [64]:

$$\{e_i : 1 \le i \le n\}$$

where e_i is the vector with a 1 in the *i*th coordinate and 0 elsewhere. For example, the standard basis for $\boldsymbol{R}^3$ is given by the three vectors;

$$e_1 = (1,0,0)$$
$$e_2 = (0,1,0)$$
$$e_3 = (0,0,1)$$

Let $\boldsymbol{R}$ denotes the field of real numbers. The space of all $\boldsymbol{n}$-tuples of real numbers forms an $\boldsymbol{n}$-dimensional vector space over $\boldsymbol{R}$ denoted by $\boldsymbol{R^n}$. An element $\boldsymbol{x}$ of $\boldsymbol{R^n}$ can be written as a column vector:

$$\boldsymbol{x} = \begin{pmatrix} x_1 \\ x_2 \\ \vdots \\ x_n \end{pmatrix}$$

Based on the above definitions, the ZVC code can be constructed using the following steps.

Step1:

Considering the parameter code weight *W*, and number of users *N*; let v_i be a column vector where *i* is a positive integer in a set R^W having "0s" at all rows (users) except row *i* whose magnitude is "1". The sequence $v_1, v_2, ..., v_w$ is a basis of R^W, called the standard basis. For R^3 (i.e., *W*=3), the column vectors can be constructed as in (3.3), (3.4), and (3.5) according to *i* position.

$$\boldsymbol{v}_1 = \begin{pmatrix} 1 \\ 0 \\ 0 \end{pmatrix} \tag{3.3}$$

$$\boldsymbol{v}_2 = \begin{pmatrix} 0 \\ 1 \\ 0 \end{pmatrix} \tag{3.4}$$

$$\boldsymbol{v}_3 = \begin{pmatrix} 0 \\ 0 \\ 1 \end{pmatrix} \tag{3.5}$$

*Step2:*Let N be the number of users and L the code length. We can write the code in a matrix form corresponding to the code word of the i^{th} user. We obtain $N \times L$ matrix with two dimension N line and L column as shown in Figure 3.2.

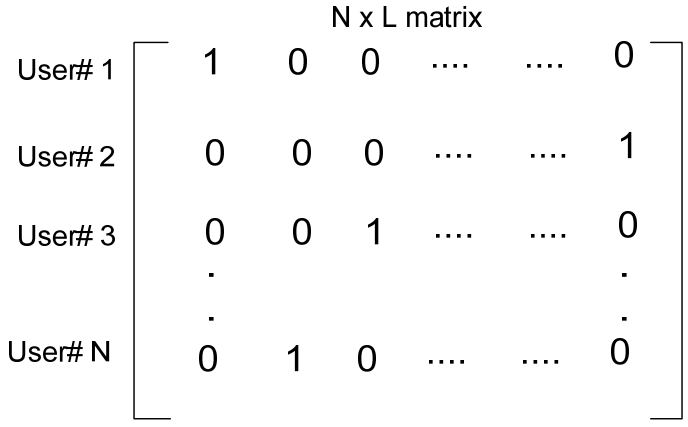

Figure 3.2: A general matrix of ZVC code.

In order to have a zero cross correlation, we must have only ‘’1’’ in each column. This means for ZVC any column is an element of the standard basis of R^W. Given the number of users N and the weight W, we can generate all possibilities of ZVC having length $L=N\times W$ by getting all permutations of the vectors $v_1, v_2, ..., v_w$ with repetition of each vector W-times. The permutation has been done for all vectors to generate the code patterns for certain values of N and W. From Permutation process, symmetric patterns appeared for the same weight and number of users i.e., swapping between the users’ locations, the first user becomes second user or the last user and so forth, so we have to find way to remove the symmetric patterns. Figure 3.3 shows the flowchart step of ZVC codes.

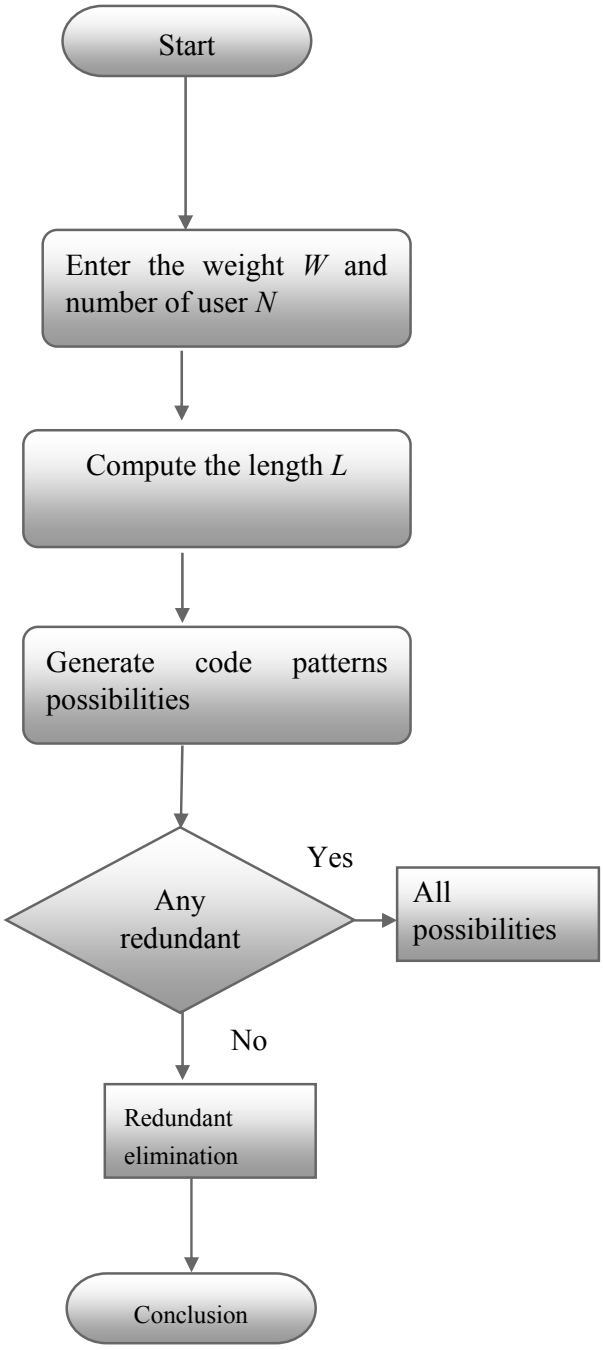

Figure 3.3: Flow chart of ZVC code construction.

3.3.1 Redundant patterns

As mentioned above there is a redundant code that must be removed from the permutation process. The code length L is given by:

$$L = N \times W \tag{3.6}$$

Using Eq. (3.6), the code possibilities (C-poss) for given N and W can be calculated as follows:

$$C\text{ - poss } = \frac{(W \times N)!}{(W! \times \overline{W}!)} \tag{3.7}$$

Where $\overline{W}$ represent the invert of W (i.e., the number of zero). From equation (3.7) it can be seen that several identical patterns can be obtained for the same values of W and N. Let us investigate the following example.

N=2

W=2

L= $N \times W$= 2×2= 4.

$\overline{W}$ = L-W= 4-2= 2

Therefore, substituting the above values in (3.7) yields:

$$C\text{ - poss} = \frac{(W \times N)!}{(W! \times \overline{W}!)} = \frac{(2x2)!}{(2!x2)} = 6$$

We obtain the codes patterns possibilities as shown in (3.8), (3.9), (3.10), (3.11), (3.12) and (3.13) as shown in Figure 3.4.

$$H_{z1} = \begin{pmatrix} 1100 \\ 0011 \end{pmatrix} \tag{3.8}$$

$$H_{z2} = \begin{pmatrix} 0110 \\ 1001 \end{pmatrix} \tag{3.9}$$

$$H_{z3} = \begin{pmatrix} 1010 \\ 0101 \end{pmatrix} \tag{3.10}$$

$$H_{z4} = \begin{pmatrix} 0011 \\ 1100 \end{pmatrix} \tag{3.11}$$

$$H_{z5} = \begin{pmatrix} 0101 \\ 1010 \end{pmatrix} \tag{3.12}$$

$$H_{z6} = \begin{pmatrix} 1001 \\ 0110 \end{pmatrix} \tag{3.13}$$

3.3.2 Elimination of redundant patterns

From the above code pattern possibilities (3.8-3.13), we can observe that there is symmetry between (3.8) and (3.1), (3.9) and (3.13), (3.10) and (3.12). In order to remove symmetric patterns, equation (3.7) can be rewritten as follows:

$$N_c = \frac{(W \times N)!}{N!(W!)^N} \tag{3.14}$$

Where N_c is the number of code pattern possibility after modification. Using equation (3.14), consider the same example (N=2, W=2), then C-poss becomes:

$$N_c = \frac{(W \times N)!}{N!(W!)^N} = \frac{(2 \times 2)!}{2!(2!)^2} = 3$$

Using equation (3.14), C-poss becomes 3 instead of 6 which mean we can rewrite the code patterns as Hz_1, Hz_2, and Hz_3.

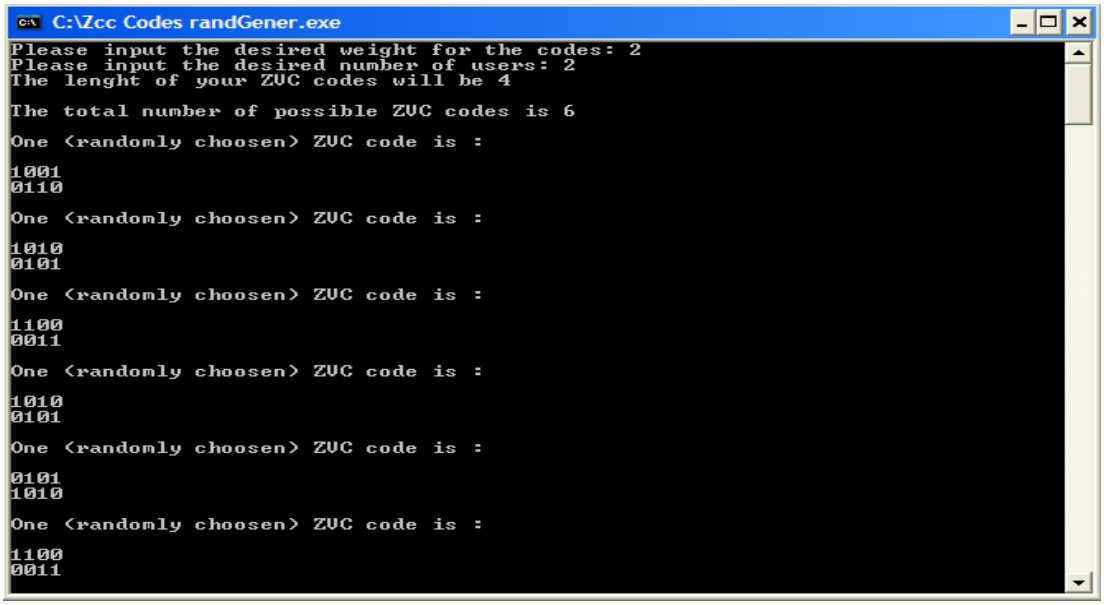

Figure 3.4: Snapshot of ZVC code patterns.

3.4 VC Code Families Construction

Based on the column vector definition mentioned above, the design of new proposed code family which is referred to as vector combinatorial (VC) code, can be

constructed by dividing the code construction into three steps; vector construction, vector combination and mapping technique.

Step 1:

Vector construction: based on the standard basis, we first construct a column vector having only two "1" which will make the cross correlation exactly equal to 1. Let $V_{(i, i+1)}$ be a column vector whose *ith* element is one and others are zeros and its length equals *N* as follows.

$$V_{(i,\,i+1)} = \begin{pmatrix} 1 \\ 0 \\ . \\ . \\ 1 \end{pmatrix} \tag{3.15}$$

Step 2:

Vectors combination: in order to make the in-phase CC exactly equal to 1 in each column while maintaining the weight value in the row (code word for each user), every vector in the matrix (see Figure 3.5) is indexed as $V_{(i,\ i+1)}$ for *i* fixed to user arrangement and *i*+1 shifts down by one up to *N* to make the CC with *N*-1 exactly equal to 1 (i.e., for *N*=5 (vector length), the maximum value of i= *N*-1 =4. Therefore for *N*=4, the corresponding *i* values for the column vectors will be calculated as: *i*=1; $V_{(i,\ i+1)} = V_{12}, V_{13}, V_{14}$; for *i*=2, $V_{(i,\ i+1)} = V_{23}, V_{34}$; for *i*=3, $V_{(i,\ i+1)} = V_{34}$), which means *i* represents the number of row (user).

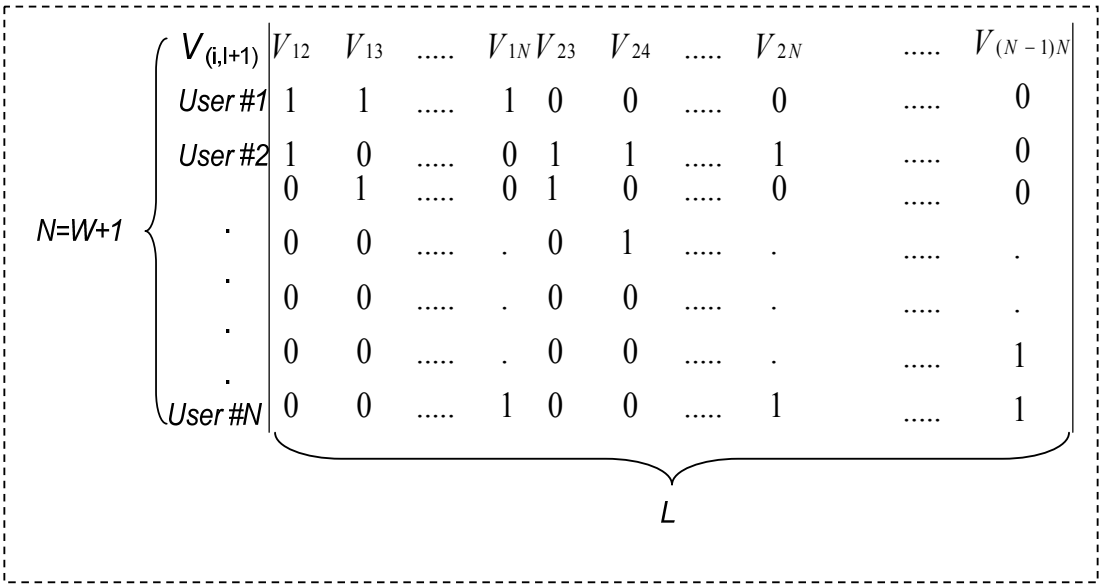

Figure 3.5: An IC basic matrix structure.

In Figure 3.5, we have shown the procedure of generating (0, 1) sequence after combining all column vectors. To be more precise from the figure, we can observe that each column vector contains two "1"s; W represents number of "1"s per row; N are number of rows (number of users). Thus, the sequence $(V_{12},V_{13},...,V_{1N})(V_{23},V_{24},...,V_{2N})\ldots\ldots,V_{(N-1)N})$ gives a code pattern having ideal in-phase CC (λ=1) called ideal case (IC).

By using an IC, the new code families can be constructed based on the conditions N-1=W, N-1<W and N-1>W for IVC, NVC and VC, respectively. Figure 3.6 shows the flowchart step of VC code families' construction.

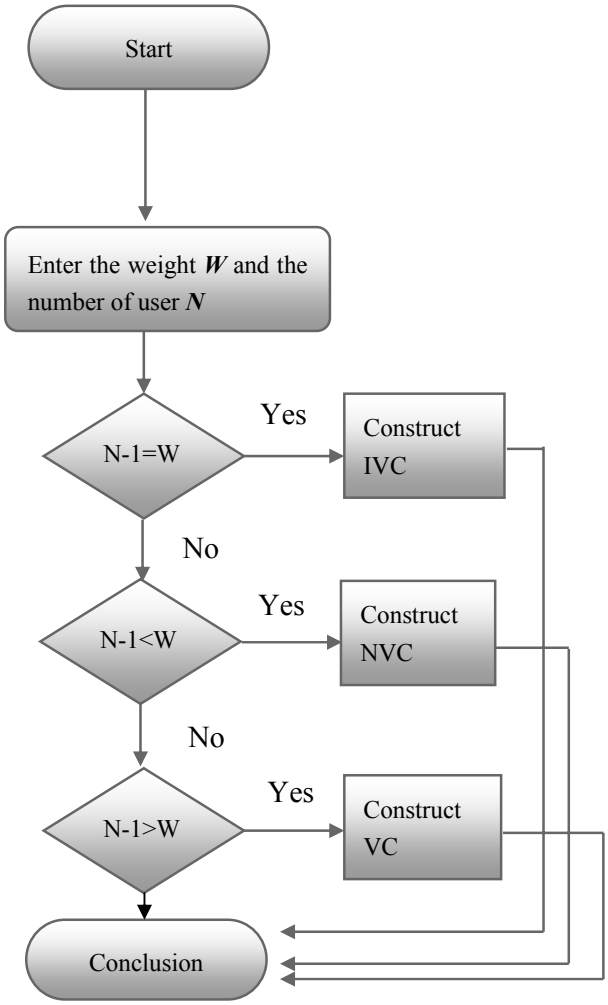

Figure 3.6: Flow chart of VC codes families' construction.

3.4.1 IVC Code Construction

The IVC construction based on the condition *N-1=W,* for example for *W*=4 and *N*=3 the column vector can be constructed as follows.

$$v_{12}=\begin{pmatrix}1\\1\\0\\0\end{pmatrix},\ v_{13}=\begin{pmatrix}1\\0\\1\\0\end{pmatrix}\ v_{14}=\begin{pmatrix}1\\0\\0\\1\end{pmatrix}\ v_{23}=\begin{pmatrix}0\\1\\1\\0\end{pmatrix}\ v_{24}=\begin{pmatrix}0\\1\\0\\1\end{pmatrix}\ v_{45}=\begin{pmatrix}0\\0\\1\\1\end{pmatrix}$$

The code length for the entire sequence is given by:

$$L = \frac{N \times W}{2} \tag{3.16}$$

Figure 3.7 and Table 3.1 show IVC code sequences when W=3 and N=4.

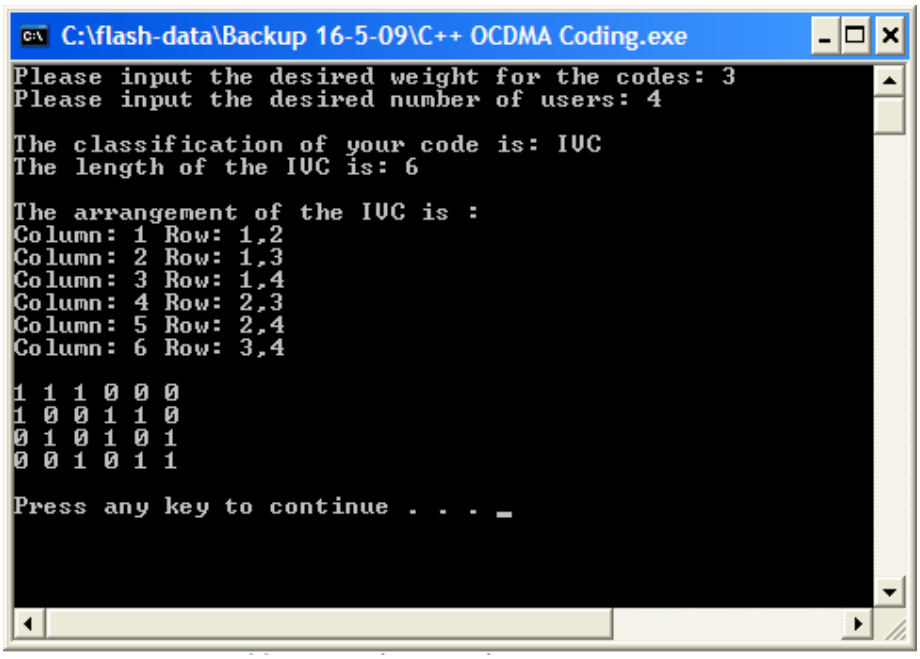

Figure 3.7: Snapshot of IVC code sequences.

Table 3.1: Code Sequences for IVC when W=3 and N=4.

1	1	1	0	0	0
1	0	0	1	1	0
0	1	0	1	0	1
0	0	1	0	1	1

The IVC code has the following properties:

1. The cross correlation is always fixed to one.
2. The number of users is always equal to W+1.
3. The code weight can be any number.

3.4.2 NVC Code Construction

The NVC construction based on the condition *N-1<W,* for example for *W*=3 and *N*=3 the column vector can be constructed as follows.

$$v_{12}=\begin{pmatrix}1\\1\\0\end{pmatrix}, v_{13}=\begin{pmatrix}1\\0\\1\end{pmatrix}, v_{23}=\begin{pmatrix}0\\1\\1\end{pmatrix}, v_1=\begin{pmatrix}1\\0\\0\end{pmatrix}, v_2=\begin{pmatrix}0\\1\\0\end{pmatrix}, v_3=\begin{pmatrix}0\\0\\1\end{pmatrix},$$

As shown in Figure 3.8, we need to increase the weight from *N*-1 to *W* without increasing the CC to satisfy the condition *N-1=W* (*i.e., v_{12}, v_{13}* and v_{23}). Therefore, a zero-CC with the parameters (*W-N*+1, *N*) must be added (i.e., v_1, v_2 and v_3 repeated *W-N*+1 times). The length for this zero-CC is *N*(*W-N*+1). The code length for the whole sequence is given by:

$$L=\frac{N(2W-N+1)}{2} \tag{3.17}$$

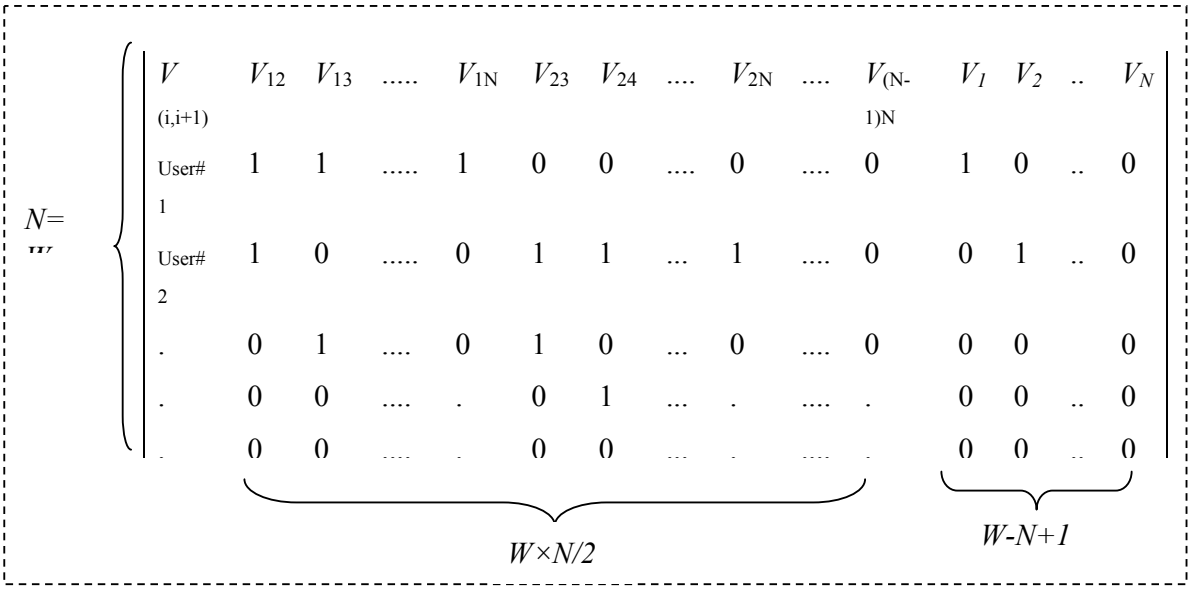

Figure 3.8: A basic matrix of NVC code structure.

Figure 3.9 and Table 3.2 show NVC code sequences when *W*=3 and *N*=3.

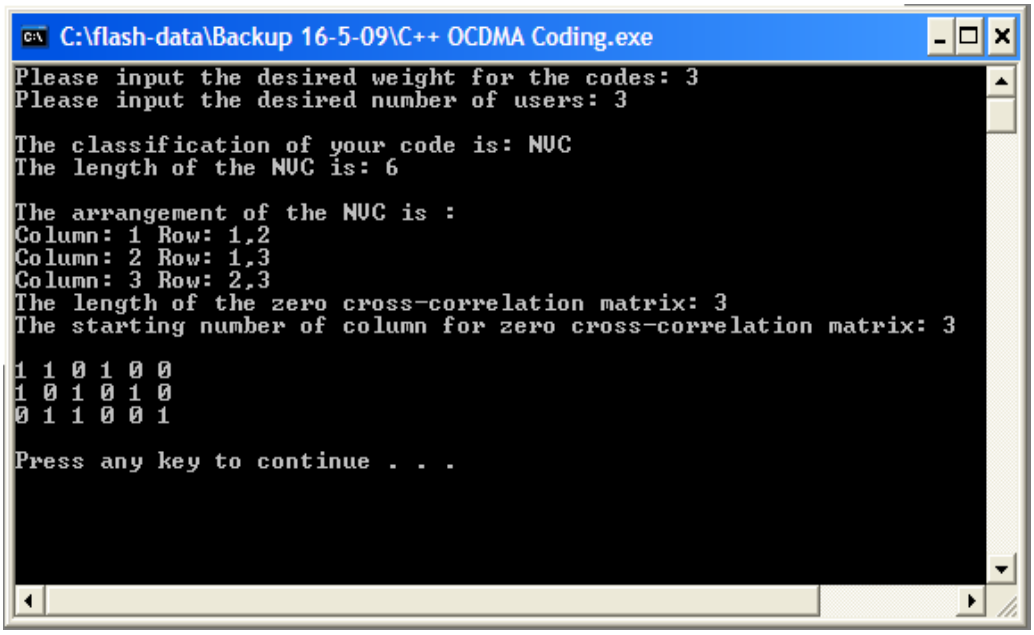

Figure 3.9: Snapshot of NVC code sequences.

Table 3.2: Code Sequences for NVC when W=3 and N=3.

1	1	0	1	0	0
1	0	1	0	1	0
0	1	1	0	0	1

The NVC code has the following properties:

1. The cross correlation is always fixed to one.
2. The number of users is always equal to W.
3. The code weight can be any number.

3.4.3 VC Code Construction

Although the IC can be constructed easily using a column vector (see Figure 3.5), the requirement that $N\text{-}1=W$ must be satisfied inherently limits the number of users. Therefore, to overcome this problem, a mapping technique must be applied based on the condition $N\text{-}1>W$. For W=3 and N=5, the column vectors can be constructed as follows:

$$v_{12}=\begin{pmatrix}1\\1\\0\\0\end{pmatrix}, v_{13}=\begin{pmatrix}1\\0\\1\\0\end{pmatrix}, v_{14}=\begin{pmatrix}1\\0\\0\\1\end{pmatrix}, v_{23}=\begin{pmatrix}0\\1\\1\\0\end{pmatrix}, v_{24}=\begin{pmatrix}0\\1\\0\\1\end{pmatrix}, v_{34}=\begin{pmatrix}0\\0\\1\\1\end{pmatrix},$$

From these column vectors N can be written as follows:

$$N = P(W+1) + R \tag{3.18}$$

Where P and R are positive integer numbers representing number of $(W+1)$ repeating in diagonal fashion, and the remaining users after module division for N respectively, and R can be expressed as:

$$R = N \bmod (W+1) \tag{3.19}$$

To clarify equations (3.18) and (3.19), where *mod* represents modulo division, example calculations are given. For N=18, W=5; substituting these values in equations (3.18) and (3.19), gives 18=3× (5+1) +0, which means P=3 and R=0. For N=17, W=4, gives 17=3× (4+1) +2, which means P=3 and R=2.

3.4.3.1 Mapping technique

The mapping technique is a mechanism used in [60, 65] in order to increase the number of users beyond the basic number of users offered by the basic matrix for a specific weight. Figure 3.10 shows a graphic representation of mapping techniques for VC code family.

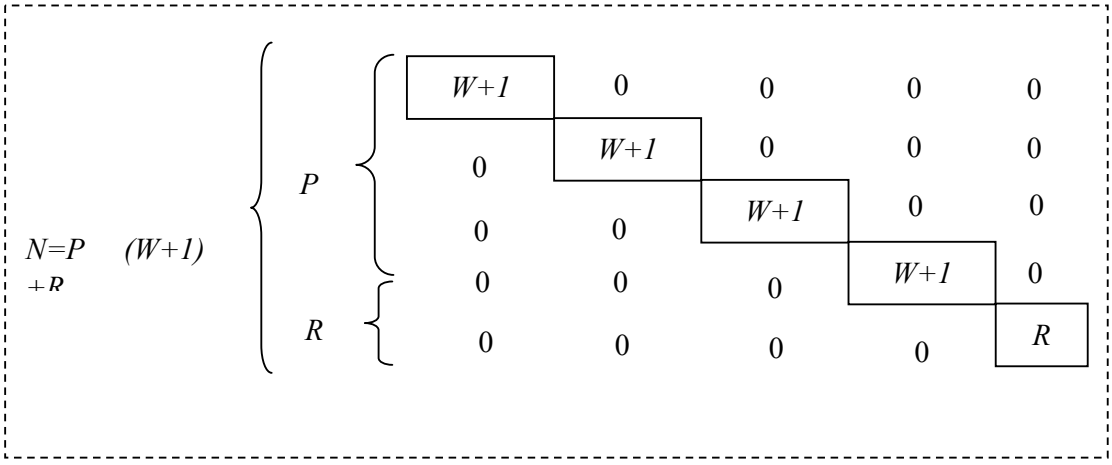

Figure 3.10: A graphic representation of mapping techniques for $N= P (W+1) + R$.

In order to increase the number of users in the VC code family, a mapping technique must be applied. The mapping technique (see Figure 3.9) operates by repeating the IC in diagonal fashion for the *(W+1)* users *P*-times and filling the empty spaces with zeros, maintaining the combination *W*+1 to ensure a maximum cross correlation of one. The length of that part is $P.\frac{W(W+1)}{2}$. Consequently, an IC with the parameters (*W*, *R*) must be added if *R*<*W+1* is to be satisfied (i.e., *R*=*N mod (W+1)* ≠0) (see Figure 3.9). The length of that second part of the code is $\frac{R\times(2W-R+1)}{2}$. Finally, the whole length *L* is given by

$$L=\frac{PW(W+1)}{2}+\frac{R(2W-R+1)}{2}=\frac{WN+R(W+1-R)}{2}. \tag{3.20}$$

Figure 3.11 and Table 3.3 show some VC code sequences when *W*=3 and *N*=5. In this figure, a snapshot of VC code sequences when *W*=3 and *N*=5 is illustrated.

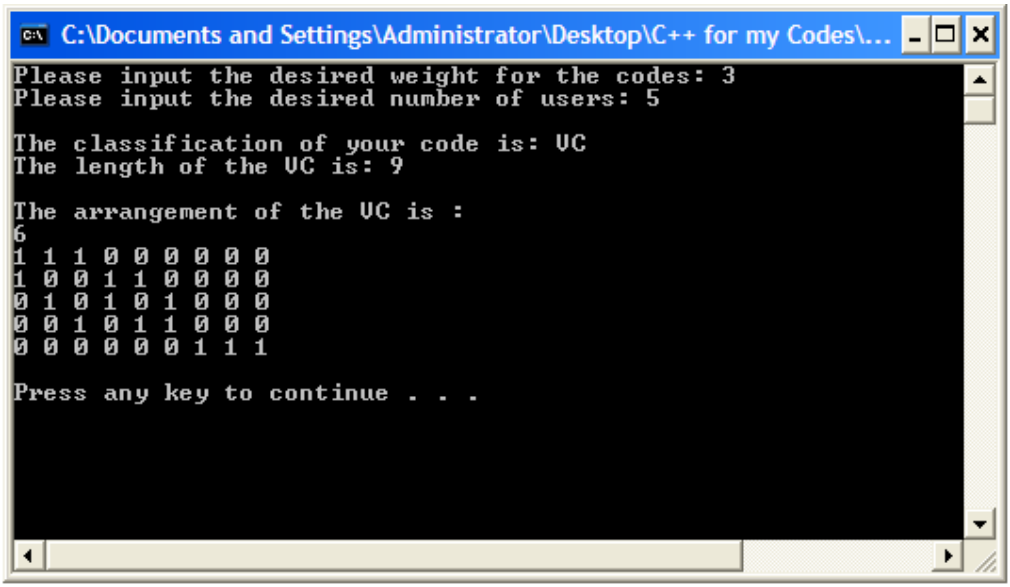

Figure 3.11: Snapshot of VC code sequences.

Table 3.3: Code Sequences for NVC when W=3 and N=5.

1	1	1	0	0	0	0	0	0
1	0	0	1	1	0	0	0	0
0	1	0	1	0	1	0	0	0
0	0	1	0	1	1	1	1	1

The VC code has the following properties:

1. The maximum cross correlation is one.
2. The number of users is always equal to $P(W+1)+R$.
3. The code weight can be any number.

3.5 Code Evaluation and Comparison

Recent studies have shown that, the code construction not only depends on the cross correlation properties, the code length plays an important role and should be addressed as well. Long code is a disadvantage since the code is either subjected to very wide band source or requires narrow filter bandwidths, while short code limits the freedom of code selection. Therefore, a tradeoff between the number of code words and code lengths must be made. Four code families have been developed which are ZVC, IVC, NVC and VC. In the following sections, evaluations and comparisons among the VC families themselves and reported codes are demonstrated.

3.5.1 ZVC Code

In OCDMA system to suppress the cross correlation, the value of λ should be kept as small as possible. Design codes with zero cross correlation mean less noise to a system which results in reducing the hardware complexity. The ZVC code is long and this is considered as a disadvantage, therefore, we have to make a tradeoff between the code length and multiple access interference (MAI), because a MAI is a dominant source of the noises.

Table 3.4: SAC-OCDMA Code Comparison.

Code	Existence	Weight	λ	Code length
MFH	$K= q^2$	q+1	1	$N= q^2 +q$ [32-33]
MDW	$K= n$	Even	1	N=3n+8/3[sin(Nii/3)]^2 [60]
ZCC	$K=2^m$	2^m -1	0	$C=2^m$ [65]
Hadamard $M \geq 2$	$K=2^M$ -1	2^{M-1}	2^{M-2}	$N= 2^M$ [29]
ZVC	Any number	Positive integer	0	$L=W\times N$

For example in MFH code, although the code length is shorter compared to ZVC, the cross correlation is always equal to unity, and this contributes to phase induced intensity noise (PIIN); while in ZVC the cross correlation is always equal to zero which eliminates the effect of PIIN. In Table 3.4, ZVC shows flexibility in terms of choosing the number of users and the weight due to the use of a novel method in code construction which generates many possibilities from a given number of users and weights. The table also shows that, the ZVC codes have a zero cross correlation while Hadamard codes have increasing value of cross correlation as the number of users increased.

3.5.2 VC Code Families

The three VC code families have been compared with reported codes. The proposed IVC code always has the number of users equal to W+1, which makes shorter length easily obtainable. For the NVC code, it is important for the number of users to always equal W due to the fact that big weight provides a strong signal as required by the users. For the VC, the number of users is always equal to P $(W+1)$ $+R$. For comparison, the properties of Hadamard, MDW, MQC, MFH and VC families are listed in Table 3.5.

Table 3.5: SAC-OCDMA Code Comparison.

Code family	Existence	Weight	Size	λ	Code length
MQC	Primes $p>2$	p+1	p^2	1	p^2+p [32-33]
MFH	All GF	q+1	q^2	1	q^2+q [32-33]
MDW	Even integer n	$n>2$	$\frac{w}{2}+1$	1	3n+8/3[sin(Nπ/3)]^2 [60]
Hadamard	$m \geq 2$	2^{m-1}	2^m-1	2^{m-2}	2^m [29]
RD	Positive integer $n>3$	$n>3$	$N+3-2W$	2	$N = K + 2W - 3$ [37]
IVC	$N=W+1$	Positive integer	Any number of users	1	$L = \frac{WN}{2}$
NVC	$N<W+1$	Positive integer	Any number of users	1	$L = \frac{N(2W - N + 1)}{2}$
VC	$N>W+1$	Positive integer	Any number of users	1	$L = \frac{(WN + R(W + 1 - R))}{2}$

It shows that the VC code exists for any number of users and weight, while the IVC and NVC exist for a restricted number of users. In addition, the VC code exists for any positive integer (regardless whether it is even, odd, prime, etc), while MDW exists for even n weight, Hadamard codes exists only when the weight is 2^{m-1} where $m\geq 2$, MQC and MFH exist for a prime number p and a prime power Q given by $Q= p^n$, where n is a positive integer respectively. The table also shows that, the VC codes have an ideal cross correlation while Hadamard codes have increasing value of cross correlation as the number of users increased. The value of cross correlation is 2 for the recently proposed code RD [37]. In particular, the sequence of the number of users for Hadamard and MFH codes are 3,7,15,31,63,127 and 1,4,9,25,49,121 respectively. This is not efficient because there will be some excess code sequences that are unused. For example in Hadamard code, if only 20 users are required, M will have to be at least 5, which supports up 31 users, thus rendering 11 codes unused and this makes the code less efficient. However, it is clear that VC code families are more efficient because the sequence can be constructed exactly according to the number of users.

Table 3.6: Comparison of VC, MDW, MQC and MFH for the same number of users, N=49.

Code	Number of users	Weight	λ	Code length
MQC	49	7	1	56
MFH	49	7	1	56
MDW	49	4	1	127
VC	49	2	1	50

We have also compared the performance of the VC in terms of code length with that of reported codes. For comparison, the properties of VC, MQC, and MFH are listed in Table 3.6. Table 3.6 shows the code lengths required by MQC (p=7), MFH (q=7, n=1) and VC (W=2, P=16, R=1) to support 49 users. From the table we can observe that, VC provides better performance than other codes for the same number of users in terms of code length. The VC exists for practical code length that is neither too long nor too short.

3.6 The Advantages of the VC Code Families

The advantages of the VC code families are listed below:

1. Simplicity of code construction.
2. Large number of conditions and, consequently more code families.
3. Good property in cross correlation.
4. Exist for every positive integer.
5. Free cardinality (number of users).
6. Ideal maximum cross correlation λ=1.
7. Easy to implement using fiber Bragg gratings (FBGs).

3.7 SUMMARY

The performance of OCDMA is limited by strong noise originating from other users attempting to use the medium simultaneously, referred to as Multiple Access Interference (MAI). MAI increases with the number of simultaneous users and severely limits the capacity of the system. A code with small cross correlation value is desirable. This chapter focuses on the properties of the VC code families and the inherent advantages of the proposed code against other codes such as Hadamard, MFH, MQC, MDW, and RD code.

In this chapter, the VC code families' construction is studied in detail. Euclidean vectors, combinatorial theory and algebraic methods are applied to develop these code families. The code constructions include vector construction, vectors combination and mapping technique. Many identical zero cross correlation code families have been developed. Three kinds of codes possessing ideal in-phase cross correlation have been introduced. The IVC code has been constructed based on the condition N-1=W which means the number of users is always equal to W+1. The NVC code has been constructed based on the condition N-1<W which means the number of users always equals to W. For the VC the number of users always equals to P (W+1) +R and this code was constructed based the condition N-1>W using a mapping technique.

Recent studies have shown that, the code construction not only depends on the cross correlation properties but the code length plays an important role and should be addressed as well. Long code length is a disadvantage since the code is either subject to very wide band source or requires narrow filter bandwidths, while short length limits the freedom of code selection. Therefore, a tradeoff between the number of code words and code lengths must be made. VC code families exist for practical code lengths that are neither too long nor too short. The major advantages of developed VC code families are simplicity of code construction, large number of conditions and, consequently more code families, good property in cross correlation, existence for every positive integer, free cardinality (number of users), ideal in-phase cross correlation and easy to implement using fiber Bragg gratings (FBGs).

CHAPTER 4
PERFORMANCE ANALYSIS OF NOISE EFFECT AND DETECTION SCHEMES

4.1 Introduction

This chapter discusses the detection schemes for the ZVC and VC code families. It begins with an extensive overview of multiple access interference (MAI) effects, noise definitions and comprehensive analysis of OCDMA detection schemes. The performance of the ZVC code family is evaluated using a newly proposed detection scheme namely direct recovery scheme (DRS). The IVC and NVC code families have a cross correlation that is always equal to one, and thus the Complementary detection scheme can be used to give accurate results. For the VC code the mapping technique is applied to increase the number of users, but at a cost of an unfixed cross correlation property. A subtract exclusive OR detection (XOR) scheme that allows MAI cancellation in the case where code sequences have in-phase cross correlation of 0 or 1 is proposed and presented in this chapter. The theoretical and simulated results of the new scheme are compared against the complementary and AND subtraction schemes. Among the VC families, VC code family will be used in detail in both the detection schemes, although other codes can also be applied.

4.2 Multiple Access Interference (MAI)

The essential goal of the design of OCDMA systems is to extract the desired user data in the presence of other users or code words [8-9]. The performance of OCDMA is limited by strong noise originating from other users attempting to use the medium simultaneously for transmitting concurrent data streams using the same time and

frequency, referred to as Multiple Access Interference (MAI). MAI severely increases with the number of simultaneous users resulting in performance deterioration, increase in bit error rate (BER) and eventually limits the capacity of the system. Therefore, MAI is considered the dominant source of noise in an OCDMA system. Due to this problem, it is important that an intelligent design of the code sequence considers reducing the contribution of MAI to the total received signal [10]. A good detection scheme design is needed to reduce the effect of MAI. One system that has been proposed to cancel the MAI by using appropriate detection schemes is spectral-amplitude coding (SAC) system [29-33].

It is found that MAI can affect the performance of a system in the following ways:

1. The overlapping chips used by the intended user and other users (using the same spectra) can cause disturbance, which will lead to the corruption of the user's data. This means that if all unwanted signals (other channels) are regarded as noise, the interference will lower the intended user's SNR; the problem which can be solved using good detection schemes.

2. Even when the mentioned problem in (1) can be overcome using the subtraction technique, this method will only be effective if the amplitude of the spectral is flat throughout the entire spectrum. In practice, this will not happen as the imbalance spectral amplitude will still cause MAI to occur. However, MAI can be minimized by controlling the power level (using optical attenuator) of the signals that are received.

3. The presence of overlapping spectra causes another type of noise which is referred to as the Phase Induced Intensity Noise (PIIN). The phase incoherence of the overlapping signals on the same spectra leads to fluctuations of the total signal intensity, and hence causes PIIN. It should be pointed out that, although the PIIN is caused by MAI, the reduction of MAI at the electrical layer will not eliminate the PIIN. This is due to the fact that the subtraction can only eliminate the undesired data, not the intensity noise which already exists at the photo-detector. To effectively suppress the PIIN, the interference at the optical layer itself needs to be eliminated first. The proposed technique of XOR detection can achieve this goal, as explained in the next section [see sections 4.5.1, 4.5.2].

4.3 Noise Estimation

Errors in the detection mechanism can arise from various noises and disturbances associated with the signal detection system. The term noise is used to describe any unwanted signal that tends to disturb the transmission and processing of the signal in a physical system [1]. In other words, any signal that masks, reduces the information content, interferes with the desired signal in any way is regarded as noise. The noise sources can be either external to the system or internal to the system. This chapter addresses mainly internal noise, which is present in every communication system and represents a basic limitation on the transmission or detection of signals. The first is Intrinsic Noise that arise due to the physical aspects of the system design, particularly in the optoelectronic and electronic devices used to construct the receiver. Examples of intrinsic noise are PIIN, thermal noise and shot noise. Thermal noise arises from the random motion of electronics in a conductor. Shot noise arises from electronic devices due to the discrete nature of current flow in the devices. The second is Coupled Noise arising from interactions between the receiver circuitry and the surrounding environment. Atmospheric noise, nearby power suppliers, and fast switching logic circuitry, are some examples of couple's noise.

4.3.1 Phase Induced Intensity Noise (PIIN)

The mix of an incoherent light source upon the input of the photodetector causes an intensity noise in the output current called PIIN. For the mixing of two uncorrelated identically polarized light fields, assuming that they have negligible self intensity noise, having the same spectrum and intensity, and that the spectra width is very much larger than the maximum electrical bandwidth, the photocurrent variance due to PIIN is given by [67-68]:

$$\left\langle i^2 \right\rangle = I^2 \tau_c B \tag{4.1}$$

where, τ_c is coherence time of the source, I is the average photocurrent and B is noise equivalent electrical bandwidth of the receiver.

Phase induced intensity noise is strongly related to multiple access interference (MAI) because both are generated from the overlapping of light spectra from different users.

Although MAI can be solved by electrical balance detection scheme as in the spectral amplitude coding, PIIN cannot be cancelled by any detection scheme because it is not an additive noise. Thus, in the OCDMA systems, phase induced intensity noise can severely affect the performance of the overall system [38, 68]. Since PIIN cannot be canceled at the electrical detection level, the only way to reduce the PIIN is to keep the values of the cross correlation that represent the overlapping of signals as low as possible (λ=1).

4.3.2 Shot Noise

Shot noise arises from the statistical nature of the production and collection of photoelectronics when an optical signal is incident on a photodetector. Shot noise in electronic circuits is strongly related to the random nature of charges that pass a certain point in a circuit. The statistics that describe the charge crossing determines the noise characteristics. If the charges cross the barrier in a periodic, predictable fashion, the current flow is consistent and the noise is not generated. If the number of carriers that cross the barrier is random and independent of the number of carriers preceding or following, the current can be represented by a Poisson distribution [69]. When the number of events that occur per unit observation time is large, a Gaussian distribution may replace the Poisson distribution. A Gaussian distribution with a white power spectral density (PSD) accurately describes electronic shot noise. The noise associated with the passage of carriers across a potential barrier is known as 'shot noise'. The non-Gaussian nature of the photodetection process makes the evaluation of the shot noise more difficult, more than that of thermal noise [1].

The total electronic shot noise associated with a current I_{DC} flowing through a potential barrier is given by,

$$I_{shot} = \sqrt{2qI_{DC}B} \quad \text{(Amps)} \tag{4.2}$$

where q = electronic charge, 1.602×10^{-19} coulombs, and B = observation bandwidth.

4.3.3 Thermal Noise

Thermal noise is due to induced random fluctuations in the charge carriers in a resistance [69]. Since thermal noise is present in all electronic elements that contain dissipative resistance, there will be thermal noise present in the resistance of a photodetector. The thermal noise is associated with parallel resistance R_p and a series resistance R_s which can be accounted for with a current-noise generator in parallel with R_p and a voltage-noise generator in series with R_s , as illustrated in Figure 4.1. The impact of the photodetector thermal noise will be influenced by how the photodetector is terminated. In most cases, the effect of the photodetector thermal noise is best accounted for by incorporating the noise sources into the calculations for the equivalent input current noise due to the electronics' current i_{elec}.

Thermal noise is given by [69-70]

$$\langle i^2 \rangle = \frac{4K_b TB}{R_L} \tag{4.3}$$

Where T is the absolute temperature, K_b is Boltzmann's constant, B is the electrical bandwidth and R is the receiver local resistance.

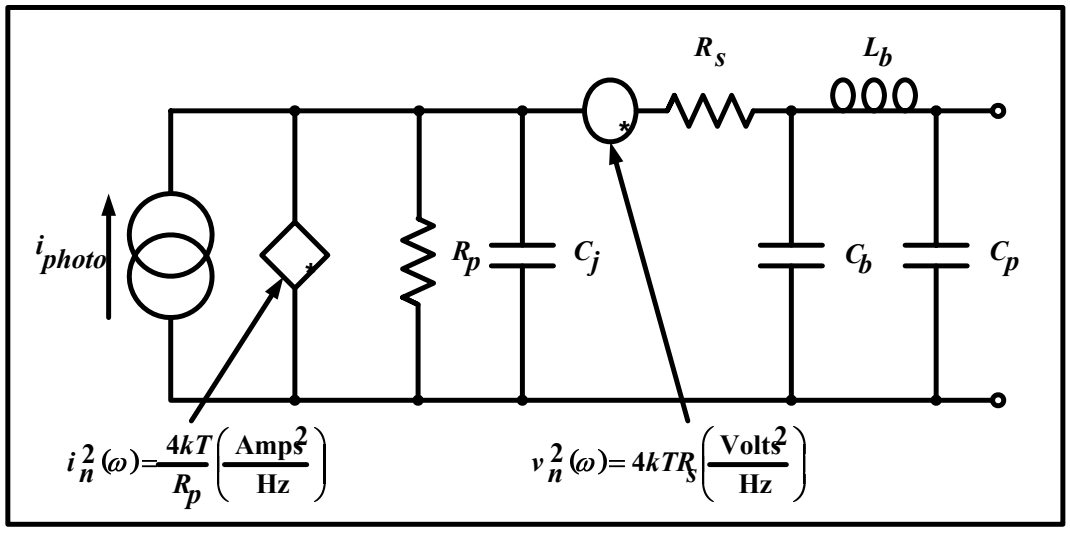

Figure 4.1: Thermal-noise sources in a photodetector

4.4 Categorization of Optical CDMA Systems

Optical CDMA systems can be divided into two major categories. The first is coherent system; in this type of system in order to achieve successful detection, knowledge of the phase and amplitude is needed. Bipolar [-1, +1] codes are used in coherent systems [71-72]. The second is incoherent systems, where the performance of the system depends mainly on the amplitude. Unipolar [0, 1] codes are used mainly in incoherent systems [60, 73-75], although bipolar codes can also be obtained by sending complementary spectrally encoded signals in SAC systems [51, 68]. For the sake of phase synchronization, coherent systems need more expensive and complex hardware than incoherent systems. Coherent systems have been excluded due to their complexity and high cost of hardware. Therefore, this research is focused on incoherent SAC OCDMA systems as they show better results compared to other incoherent systems [54].

In an incoherent OCDMA system, each user is assigned a unique code sequence as its address signature based on the spectral amplitude only. When a user wants to transmit one data bit, it sends out a code sequence matching to the address signature of the intended receiver. At the receiver, all the code sequences from different users are correlated. If correct code sequences are received, then the results will be an autocorrelation function with a high peak. For incorrect code sequences, cross correlation functions and cross talk are generated, and they create multiple access interference (MAI) [54]. MAI can be reduced by using subtraction technique. The most common subtraction technique is the Complementary subtraction technique, which is also known as balanced detection technique [54].

4.5 Spectral Amplitude Coding Detection Schemes

Many detection techniques for SAC-OCDMA systems have been proposed aiming to reduce MAI [54, 76-80]. In most research, Complementary and AND techniques have been used at the receiver side to recover the original signal. In this thesis, two new approaches are introduced called direct recovery scheme (DRS) and exclusive OR subtraction technique (XOR) for ZVC and VC code families respectively. The purpose of these new subtractions is to overcome the limitations that have been

addressed in reported techniques such as hardware cost and at the same time to improve the system performance.

4.5.1 Complementary Subtraction Technique

Figure 4.2 shows a block diagram for unipolar codes where a pulse with a spectral distribution of A (v) is sent to represent data '1' and nothing is sent to represent data '0' [8-9, 28-29]. At the receiver, the signal is split into two by 1: α splitter.

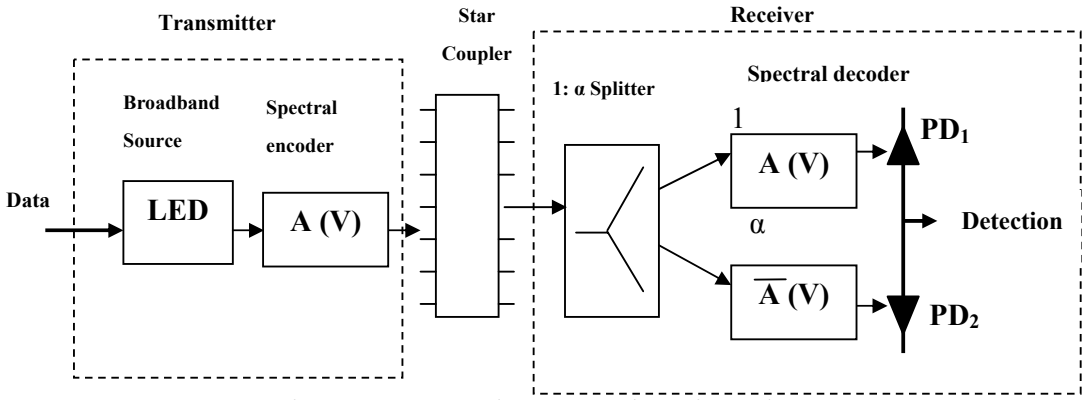

Figure 4.2: Complementary detection scheme.

If the code is a (L, w, λ), then the MAI for (k-1) user at the first photodetector is λ (k-1), and the MAI at the second photodetector is α(w- λ)(k-1). When α=(w- λ)/ λ, the MAI on both receivers is equal and can canceled by balance detection.

In complementary subtraction technique, first proposed by M. Kavehrad [29], the cross correlation is defined as:

$$\theta_{AB}(k) = \sum_{i=0}^{N-1} a_i b_{i+k} \tag{4.4}$$

where A and B are the two OCMA code sequences. The complementary of sequence (A) is given by $(\overline{A})$ whose elements are obtained from (A) by $\overline{a}_{i=}1 - a_i$. Let A = 0011 and B = 0110 and therefore $\overline{A}$ = 1100. The periodic cross correlation sequence between $\overline{A}$ and (B) is similar to Equation (4.4) and is expressed as:

$$\theta_{\overline{AB}}(N) = \sum_{i=0}^{L-1} \overline{a}_i b_{i+k} \tag{4.5}$$

The sequences that are sought for are

$$\theta_{AB}(N) = \theta_{\bar{A}B}(N) \tag{4.6}$$

At the receiver, the photodetectors will detect the two complementary inputs which will be fed to the subtractor whose cross correlation output, Z can be expressed as:

$$Z_{Complementary} = \theta_{AB}(N) - \theta_{\bar{A}B}(N) = 0 \tag{4.7}$$

Finally the answer is 0, which means that at the output of the subtractor there will be no more cross correlation terms, indicating that there is no more signal from other users in the intended channel.

4.5.2 AND Subtraction Technique

The AND subtraction is a technique proposed by Aljunid *et al.* [60], for cross correlation cancellation for SAC OCDMA systems. In AND subtraction technique, the cross correlation $\theta_{\bar{A}B}(N)$ is substituted by $\theta_{(A\delta B)B}$, where $\theta_{(A\delta B)}$ represents the AND operation between sequences *A* and *B*. For example, let *A* = 0011 and *B* = 0110, and therefore (*A* AND *B*) = 0010. Example of an AND receiver is shown in Figure 4.3.

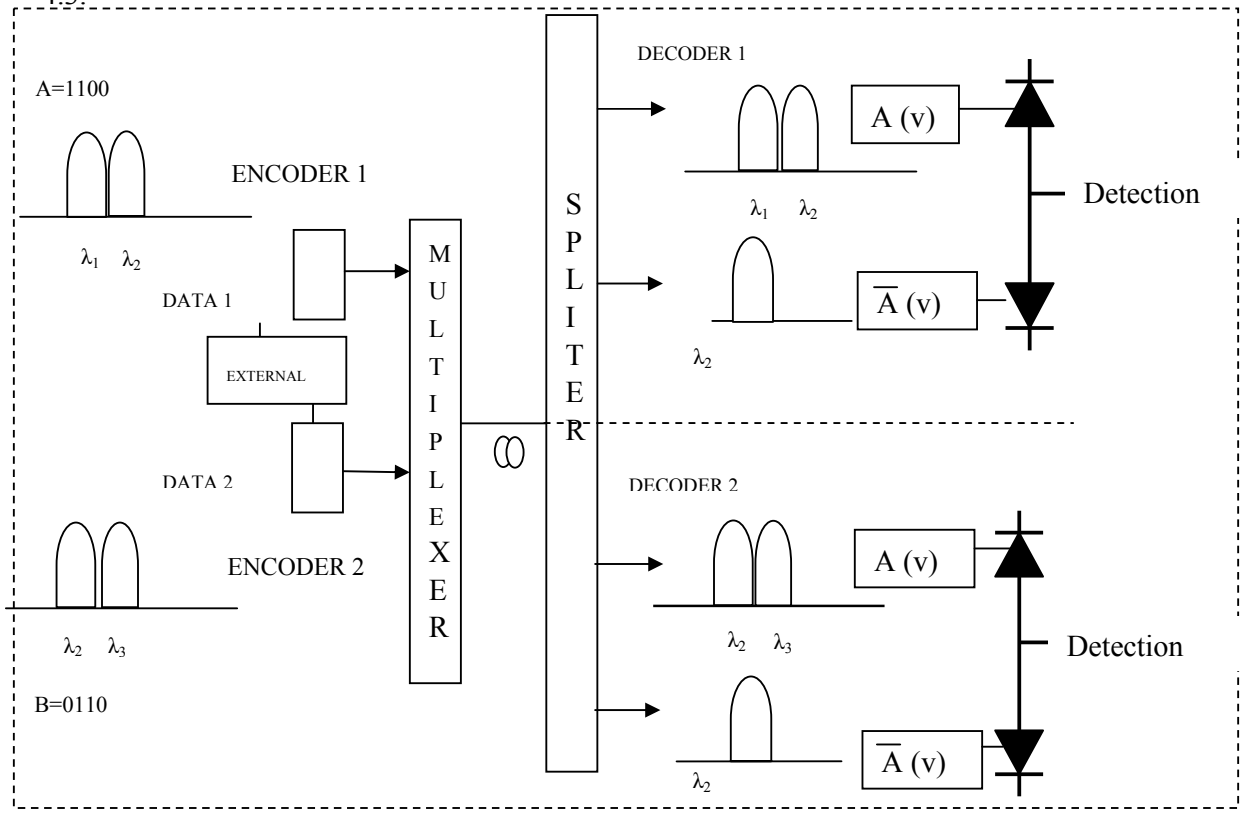

Figure 4.3: Implementation of the AND Subtraction Technique.

At the receiver side,

$$Z_{AND} = \theta_{AB}(N) - \theta_{(A\&B)B}(N) = 0 \tag{4.8}$$

Equation (4.8) shows that, with AND subtraction technique, the multiple access interference or the interference from other channels can also be cancelled out. The advantage of AND subtraction detection technique is that it requires less number of filters compared to the complementary subtraction technique.

4.5.2 Direct Recovery Scheme

This section discusses in detail the direct recovery scheme (DRS), which is used as the detection technique in the ZVC OSCDMA code. In the direct detection scheme, illustrated in Figure 4.4, there is only a single decoder and thus a single detector is required.

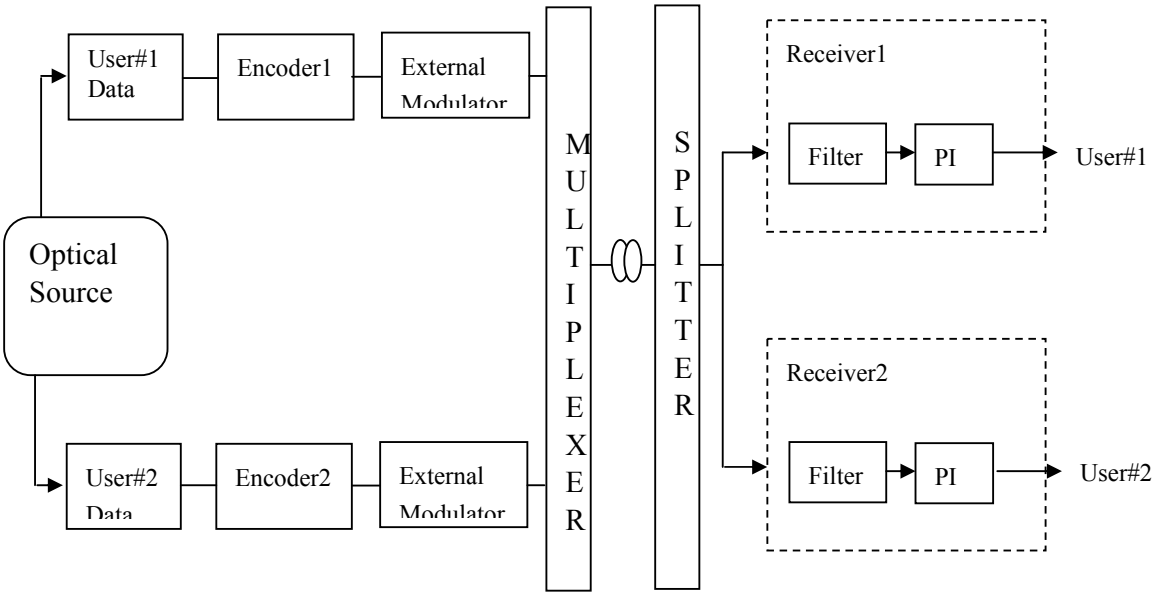

Figure 4.4: Implementation of the direct recovery scheme (DRS).

The difference between this technique and the conventional Complementary [29, 54] subtraction and AND subtraction [35, 60] is in the decoder. With AND and Complementary subtraction techniques, the number of photodiodes is two because these detections are used for optical spectrum CDMA codes which have ideal in-phase cross correlation (λ=l) such as the MQC code and the DW code. The direct

recovery scheme is used in this thesis as a proposed detection for the ZVC code because the value of cross correlation is always equal to zero (λ=0), thus the detection of this code can be done directly without the complicated detection as in previous techniques. Since the cross correlation is always equal to zero, the phase induced intensity noise (PIIN) is suppressed at the receiver. Consequently, this will improve the performance of the system in terms of MAI reduction, hardware complexity and cost.

4.5.3 XOR Detection Scheme

In XOR subtraction technique, the cross correlation $\theta_{\overline{AB}}(N)$ is substituted by $\Theta(XOR(A,B))(A\_bar)$, where $\Theta(XOR(A,B))$ represents the XOR operation between sequences *A* and *B*. For example, let *A* = 11100 and *B* = 10011, and therefore (*A* XOR *B*) = 01111. Example of an XOR receiver is shown in Figure 4.5.

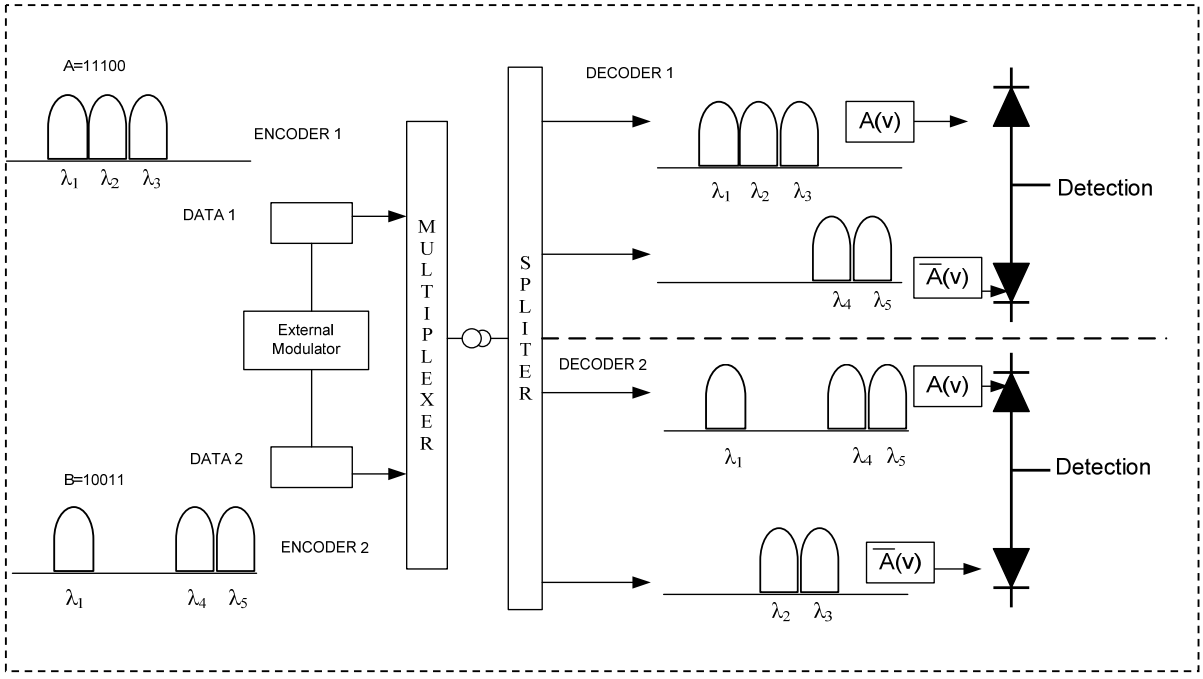

Figure 4.5: Implementation of the XOR detection scheme.

At the receiver side

$$Z_{SED} = \Theta(A,B) - \frac{\Theta(XOR(A,B),(A\_bar))}{W-1} \tag{4.9}$$

where Θ represents an AND operation. Equation (4.9) shows that, with XOR subtraction technique, the multiple access interference or the interference from other channels can also be cancelled out. This subtraction technique can be implemented with any OCDMA codes, but for comparison purposes, the VC code is used as an example. The operations of Complementary, AND, and XOR detection schemes are listed in Table 4.1 for the sequences *A*=110 and *B*=101, for comparison. From the Table, it can be observed that the whole subtraction result is zero; which means that the MAI can be cancelled out by using the three detection techniques. In terms of cross correlation, the Complementary and AND subtraction can successfully recover desired signal only for codes having fixed cross correlation, besides AND filters out the half of the signal. In the proposed XOR detection scheme in this work, the balance detection can be achieved even if the cross correlation is not fixed while still maintaining a strong signal.

The overall system cost and complexity can be reduced by using less number of filters in XOR subtraction since the chips are always in adjacent fashion. At the same time, the performance of the OCDMA system is improved significantly because with less number of filters in the decoder, the total power loss can be reduced and this can be clearly seen in the simulation result.

As mentioned earlier, the three subtraction techniques can be implemented with any OCDMA codes. In the next section, for the purpose of comparing theoretical performances, VC code families are used as an example.

Table 4.1: Comparison between XOR, Complementary and AND Subtraction Techniques

Code sequence	XOR technique			AND technique			Complementary technique		
	λ_1	λ_2	λ_3	λ_1	λ_2	λ_3	λ_1	λ_2	λ_3
A	1	1	0	1	1	0	1	1	0
B	1	0	1	1	0	1	1	0	1
	$\Theta((a,b)=1$			$\Theta(a,b)=1$			$\Theta(a,b)=1$		
	$\Theta(xor(a,b))=011$			$\Theta(a(a,b))=100$			a= 110		
	$\Theta((a\_bar)b)=001$			b=101			a b= 001		
	$\Theta(xor(a,b))(a\_bar)=1$			$\Theta(and(a,b)b)=1$			$\Theta(\bar{a}b)=1$		
Z	$\Theta(a,b)-\frac{\Theta(xor(a,b),(a\_bar))}{W-1}=0$			$Z_{AND}=\Theta(and(a,b))-\Theta(and(a,b)b)=0$			$Z_{complementary}=\Theta(and(a,b))-\Theta((a\_bar)b)=0$		

4.6 Optical CDMA Systems Using VC Code Families

The performance of VC code families in the presence of the phase induced intensity noise (PIIN), the photodiode shot noise and the thermal noise by using the two subtraction techniques is elaborated on this section. Only the Complementary and XOR techniques are being considered because AND technique performs similar to Complementary technique with fewer filters.

4.6.1 Complementary Subtraction System

The setup of the proposed IVC system using complementary subtraction technique is shown in Figure 4.6 where the output from the top of first FBG group is used directly as decoded output. In the performance analysis, incoherent intensity noise, as well as shot and thermal noise in both photodetectors have been considered. The effect of the receiver dark current is neglected because its value is small compared with the shot

and thermal noise [30-33, 35-38]. Gaussian approximation is used for the calculation of the BER (Bit Error Rate) as in [30-33, 73-76].

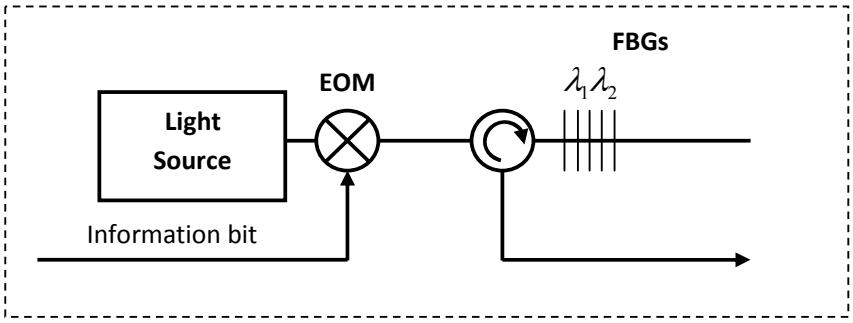

(a)

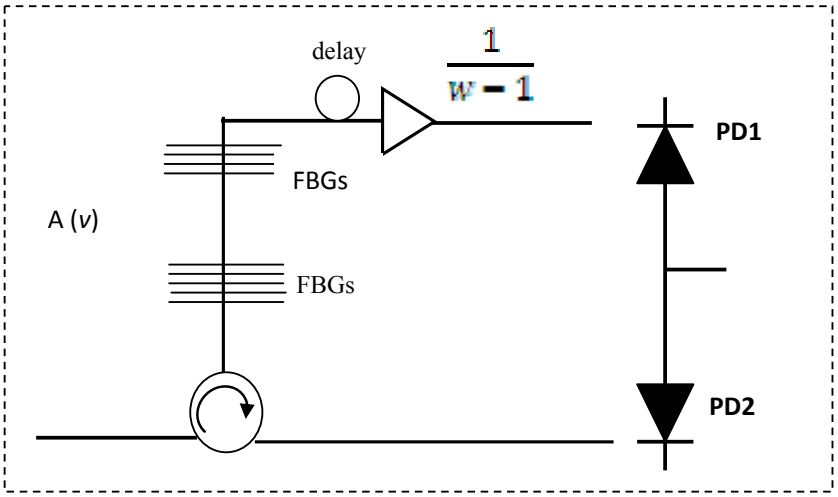

(b)

Figure 4.6: Optical CDMA System Architecture using Complementary Subtraction Technique (a) Transmitter, (b) Receiver.

The variance of the photocurrent due to the detection of an ideally unpolarized thermal light, which can be generated by spontaneous emission [30-33, 35-38] can be expressed as:

$$\langle i^2 \rangle = 2eIB + I^2 B\tau_c + \frac{4K_b T_n B}{R_L} \tag{4.10}$$

The parameters used in Equation (4.10) are as shown in Table 4.2. In Equation (4.10), the first term results from the shot noise, the second term denotes the effect of Phase Induced Intensity Noise (PIIN) and the third term represents the effect of thermal noise.

When incoherent light fields are mixed and incident upon a photodetector, the phase noise of the fields causes an intensity noise term in the photodetector output. The coherent time of a thermal source τ_c is given by [38]:

$$\tau_c = \frac{\int_0^\infty G^2(v)dv}{\left[\int_0^\infty G(v)dv\right]^2} \tag{4.11}$$

Where, G(v) is the power spectral density (PSD) of the thermal noise source. In equation (4.11), the total effect of PIIN has a negative binomial distribution [76], while thermal noise has a Gaussian distribution; in general Gaussian approximation is used for entire noise.

Table 4.2: Symbols and Parameters for the Setup in Figure 4.5

No	Symbols	Parameters
1	e	Electron charge
2	I	Average photocurrent
3	B	Noise–equivalent electrical bandwidth of the receiver
4	τ_c	Coherence time of the source
5	K_b	Boltzmann constant
6	T_n	Absolute receiver noise temperature
7	R_L	Receive load resistor

The total effect of PIIN and shot noise obeys negative binomial distribution [76]. In order to analyze the system with a transmitter and a receiver as shown in Figure 4.5, the same assumptions used in [30-33, 35-38] are used here. The assumptions are as follows:

1. Each light source is ideally unpolarized and its spectrum is flat over the bandwidth [$\boldsymbol{\nu}_o$-$\Delta\boldsymbol{\nu}$/2, $\boldsymbol{\nu}_o$+$\Delta\boldsymbol{\nu}$/2], where ν_o is the central optical frequency and $\Delta\boldsymbol{\nu}$ is the optical source bandwidth in Hertz.
2. Each power spectral component has identical spectral width.
3. Each user has equal power at the receiver.
4. Each bit stream from each user is synchronized.

The above assumptions are important for mathematical simplicity. Based on the above assumptions, we can easily analyze the system performance using Gaussian approximation. The power spectral density of the received optical signals can be written as [38]:

$$r(v) = \frac{P_{sr}}{\Delta V}\sum_{N=1}^{N} d_N \sum_{i=1}^{L} c_N(i)\left\{u\left[v - v_o - \frac{\Delta v}{2L}(-L+2i-2)\right] - u\left[v - v_o - \frac{\Delta v}{2L}(-L+2i)\right]\right\} \qquad (4.12)$$

Where P_{sr} is the effective power of a broadband source at the receiver, N is the active users and L is the VC code length, d_N is the data bit of the Nth user that is "1" or "0", and $u(v)$ is the unit step function expressed as:

$$u(v) = \begin{cases} 1, & v \geq 0 \\ 0, & v < 0 \end{cases} \qquad (4.13)$$

In the following analysis the effects of both shot and thermal noises as well as the effect of PIIN are considered.

Let $C_N(i)$ denote the *ith* element of Nth IVC code sequence, the code properties can be written as:

$$\sum_{i=1}^{L} C_N(i)C_m(i) = \begin{cases} W, & For \quad N = m \\ 1, & For \quad N \neq m \end{cases} \qquad (4.14)$$

and

$$\sum_{i=1}^{L} C_N(i)\overline{C}_m(i) = \begin{cases} 0, & For \quad N = m \\ W-1, & For \quad N \neq m \end{cases} \tag{4.15}$$

From Equation (4.12), the power spectral density at photodetector 1 and photodectotor 2 as in Figure 4.5 of the *m*th receiver during one bit period can be written as:

$$G_1(V) = \frac{P_{sr}}{\Delta V}\sum_{N=1}^{N} d_N \sum_{i=1}^{L} C_N(i)\overline{C}m(i)\{\ u\left[V - V_0 - \frac{\Delta V}{2L}(-L+2i-2)\right] - u\left[V - V_0 - \frac{\Delta V}{2L}(-L+2i)\right]\ \} \tag{4.16}$$

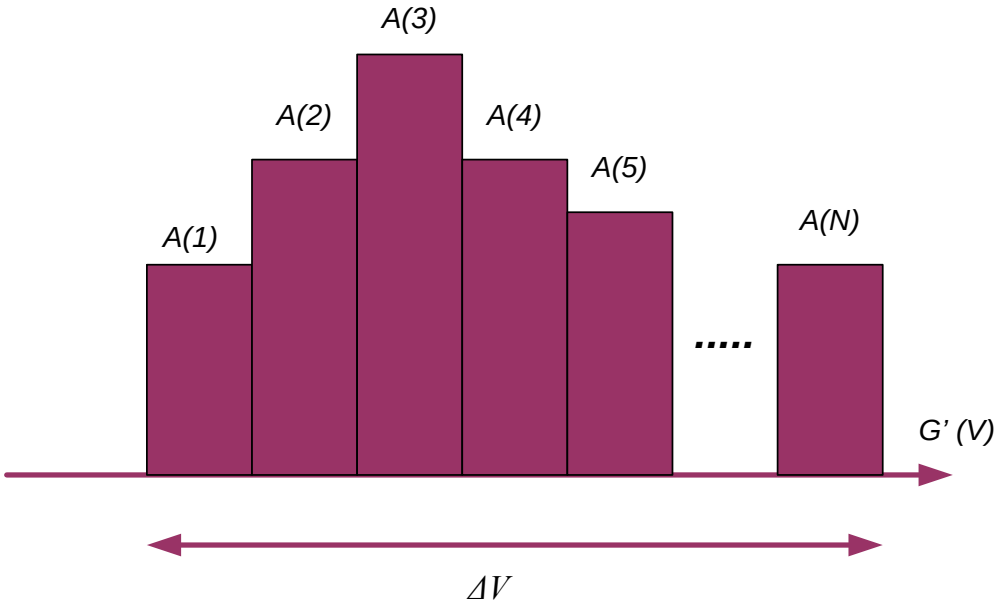

Figure 4.6: The PSD of the Received Signal $r(v)$.

$$G2(V) = \frac{P_{sr}}{\Delta V}\sum_{N=1}^{N} d_N \sum_{i=1}^{L} C_N(i)Cm(i)\{\ u\left[V - V_0 - \frac{\Delta V}{2L}(-L+2i-2)\right] - u\left[V - V_0 - \frac{\Delta V}{2L}(-L+2i)\right]\ \} \tag{4.17}$$

Then

$$\int_0^{\infty} G_1(V)dV \quad = \quad \frac{P_{sr}}{L} \sum_{N=1}^{N} \sum_{N \neq m} d_N \tag{4.18}$$

$$\int_0^{\infty} G_2(V)dV \quad = \frac{P_{sr}W}{\Delta V} + \sum_{N=1}^{N} \sum_{N \neq m} d_N \tag{4.19}$$

To calculate the integral of $G_1^2(V)$ and $G_2^2(V)$, first let us consider an example of the PSD (denoted by $G'(V)$) of the received superimposed signal, which is shown, in Figure 4.6, where $A(i)$ is the amplitude of the signal of the ***i***th spectral slot with width of $\frac{\Delta V}{N}$.

The integral of $G'^2(V)$ can be expressed as:

$$\int_0^{\infty} G'^2(V)dv \; = \; \frac{\Delta V}{N} \sum_{i=1}^{N} A^2(i) \tag{4.20}$$

Therefore, using (4.18), (4.19) and (4.20) the following is obtained.

$$\int_0^{\infty} G_1^2(V)dV = \frac{P_{sr}^2}{L\Delta V} \sum_{i=1}^{L} \left\{ \overline{C}m(i) \cdot \left[\sum_{N=1}^{N} d_N C_N(i) \right] \cdot \left[\sum_{q=1}^{N} d_q C_q(i) \right] \right\} \tag{4.21}$$

And

$$\int_0^{\infty} G_2^2(V)dV = \frac{P_{sr}^2}{L\Delta V} \sum_{i=1}^{L} \left\{ C_m(i) \cdot \left[\sum_{N=1}^{N} d_N C_N(i) \right] \cdot \left[\sum_{q=1}^{N} d_q C_q(i) \right] \right\} \tag{4.22}$$

Based on equations (4.21) and (4.22), d_N is the data bit of the *N*th user that carries the value of either "1" or "0". Consequently, the photocurrent ***I*** can be expressed as:

$$I = I_2 - I_1 = \Re \int_0^{\infty} G_2(V)dv - \Re \int_0^{\infty} G_1(V)dv \tag{4.23}$$

Then

$$\mathrm{I} = \Re\left[\frac{P_{sr}}{L}\right] \cdot \left[W + \sum_{N=1}^{N} \sum_{N \neq m} d_N - \sum_{N=1}^{N} \sum_{N \neq l} d_N \right]$$

After the integration and subtraction processes, the photocurrent can be expressed as:

$$\mathrm{I} = \Re \frac{P_{sr}}{L} W \tag{4.24}$$

$$\Re = \frac{\eta e}{h V_c} \tag{4.25}$$

Here, η is the quantum efficiency, e is the electron charge, h is the Planck's constant, and V_c is the central frequency of the original broad band optical pulse. Since the noise in photodetector 1 and 2 are independent, the power of the noise sources that exist in the photocurrent can be written as [38]:

$$\langle I^2 \rangle = \langle I_1^2 \rangle + \langle I_2^2 \rangle + \langle I_{th}^2 \rangle \tag{4.26}$$

Where,

I^2 = Total noise power;

I_1^2 = Shot noise;

I_2^2 = Phase Induced Intensity Noise (PIIN);

I_{th}^2 = Thermal noise.

From equation (4.26)

$$\langle I^2 \rangle = 2eB(I_1 + I_2) + BI_1^2\tau_{c1} + BI_2^2\tau_{c2} + \frac{4K_bT_nB}{R_L} \tag{4.27}$$

Therefore

$$\langle I^2 \rangle = 2eB\Re\left[\int_0^\infty G_1(v)dv + \int_0^\infty G_2(v)dv\right] + B\Re^2 \int_0^\infty G_1^2(v)dv + B\Re^2 \int_0^\infty G_2^2(v)dv + \frac{4K_bT_nB}{R_L} \tag{4.28}$$

From equation (4.13), when all the users are transmitting bit '1' using the average value as $\sum_{N=1}^{N} c_N \approx \frac{NW}{L}$ and the noise power can be written as:

$$\langle I^2 \rangle = 2eB\Re \left[\frac{P_{sr}}{L}((N-1)+W+(N-1)\right] + B\Re^2\left[\frac{P_{sr}^2}{\Delta V L}\cdot\left[\frac{NW}{L}\right].[(N-1)+W+(N-1)]\right]+ \frac{4K_bT_nB}{R_L} \quad (4.29)$$

Noting that the probability of sending bit '1' at any time for each user is $\frac{1}{2}$ [38], then the above equation becomes

$$\langle I^2 \rangle = \frac{P_{sr}\, e\, B\, \Re}{L}\left[(2N-2)+W\right] + \frac{P_{sr}^2\, B\Re^2\, N\, W}{2\,\Delta V\, L^2}\left[(2N-2)+W\right]+ \frac{4K_bT_nB}{R_L} \quad (4.30)$$

From (4.24) and (4.30), the average of SNR can be expressed as in (4.31) and (4.32) below.

$$SNR = \frac{(I_2-I_1)^2}{\langle I^2 \rangle} \quad (4.31)$$

$$SNR = \frac{\frac{\Re^2 P_{sr}^2 W^2}{L^2}}{\frac{P_{sr}\, e\, B\, \Re}{L}\left[(2N-2)+W\right] + \frac{P_{sr}^2\, B\Re^2\, N\, W}{2\,\Delta V\, L^2}\left[(2N-2)+W\right]+ \frac{4K_bT_nB}{R_L}} \quad (4.32)$$

where $\Re$ is the photodiode responsivity, P_{sr} is the effective power of a broad band source at the receiver, e is the electronic charge, B is the electrical equivalent noise bandwidth of the receiver, K_B is the Boltzmann's constant, Tn the absolute receiver noise temperature, R_L is the receiver load resistor, ΔV is the optical source bandwidth, W, N, L are the code weight, the number of users, and the code length, respectively. There are the parameters of IVC code. The Bit Error Rate (BER) is computed from the SNR using Gaussian approximation as follows [38],

$$\text{BER} = P_e = \frac{1}{2}\, erfc\left(\sqrt{\frac{SNR}{8}}\right) \quad (4.33)$$

4.6.2 XOR Subtraction System

An optical CDMA system using XOR subtraction is shown in Figure 4.7.

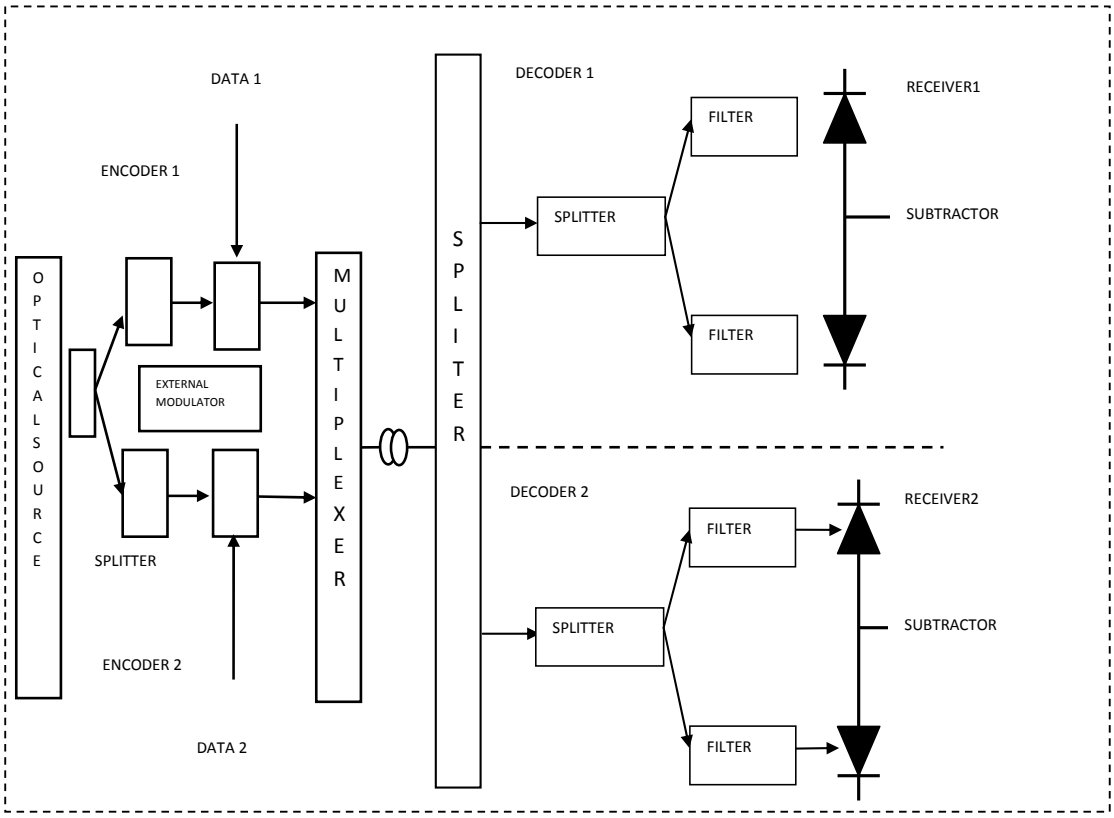

Figure 4.7: Optical CDMA System Architecture Using XOR Subtraction Technique.

As mentioned earlier, the differences of this technique compared to the conventional complementary, and AND subtraction techniques are at the cross correlation and the signal status. The complementary and AND subtraction can successfully recover desired signal only for codes having fixed cross correlation. With AND subtraction technique, only the chips that do not overlap with each other only will be filtered out, which means weak signal. In the proposed XOR detection technique, the balanced detection can be achieved even if the cross correlation is not fixed while it is still possible to maintain a strong signal.

Therefore, the code properties for VC code families using XOR subtraction technique also differ from the complementary and AND techniques, as explained below. This results in different performance such as in the signal to noise ratio and bit error rate.

The balanced detection using XOR outperforms Complementary and AND even if the cross correlation is not fixed. The properties of the IVC and NVC are given in this section although they have been mentioned in previous section.

If $C_N(i)$ denotes the ***i***th element of the ***N***th IVC code sequence, the code properties for XOR can be written as:

$$V_{a,b} = \sum_{i=1}^{L} a_x(i) b_y(i)$$

$$PD1_{(0)}(x,y) = \begin{cases} W, & x = y \\ \\ 1, & x \neq y \ for \ N = W+1 \end{cases} \tag{4.34}$$

And

$$V_{a,b} = \sum_{i=0}^{L} a_x(i) b_y(i) \oplus . \bar{a}_x(i) b_y(i)$$

$$PD2_{(1)}(x,y) = \begin{cases} 0, & x = y \\ \\ W-1, & x \neq y \ for \ N = W+1 \end{cases} \tag{4.35}$$

Then the balanced photodiode for the desire user# (x,y) executes the correlation function H as:

$$\text{H} = \sum_{i=1}^{L} a_x(i) b_y(i) \ - \ \sum_{i=1}^{L} a_x(i) b_y(i) \oplus . \bar{a}_x(i) b_y(i)$$

Thus

$$PD1_{(0)}(x,y) - \frac{PD2_{(1)}(x,y)}{W-1} = \begin{cases} W, & x = y \\ \\ 0, & else \end{cases} \tag{4.36}$$

By using the value of the properties in (4.23) and (4.24), the signal to noise ratio of the XOR subtraction technique can be determined using the same mathematical operations as in Equations 4.16 to 4.32, where it can be expressed as:

$$SNR = \frac{\frac{\Re^2 P_{sr}^2 W^2}{L^2}}{\frac{P_{sr}\, e\, B\, \Re}{L}\left[(2N-2)+W\right] + \frac{P_{sr}^2 B \Re^2 N W}{2\Delta V L^2}\left[(2N-2)+W\right] + \frac{4K_b T_n B}{R_L}} \tag{4.37}$$

If $C_N(i)$ denotes the ***i***th element of the ***N***th NVC code sequence, the code properties for XOR can be written as:

$$V_{a,b} = \sum_{i=0}^{L} a_c(i) b_d(i)$$

$$PD1_{(0)}(c,d) = \begin{cases} W, & c = d \\ 1, & c \neq d \ \ for\ N = W \end{cases} \tag{4.38}$$

And

$$V_{a,b} = \sum_{i=1}^{L} a_c(i) b_d(i) \oplus . \overline{a}_c(i) b_d(i)$$

$$PD2_{(1)}(c,d) = \begin{cases} 0, & c = d \\ W-1, & c \neq d \ \ for\ N = W \end{cases} \tag{4.39}$$

The balanced photodiode for the desired user #(c,d) that executes the correlation function K rejects the MAI coming from the interfering users and obtains the desired information bit.

$$\text{K}= \sum_{i=1}^{L} a_c(i) b_d(i) - \sum_{i=1}^{L} a_c(i) b_d(i) \oplus . \overline{a}_c(i) b_d(i)$$

Thus

$$PD1_{(0)}(c,d) - \frac{PD2_{(1)}(c,d)}{W-1} = \begin{cases} W, & c = d \\ 0, & else \end{cases} \quad (4.40)$$

By using the value of the properties in (4.38) and (4.39), the Signal to Noise ratio of the XOR subtraction technique can be determined using the same mathematical operations as in Equations 4.16 to 4.32, where it can be expressed as:

$$SNR = \frac{\frac{\Re^2 P_{sr}^2 W^2}{L^2}}{\frac{P_{sr} e B \Re}{L}\left[(2N-2)+W\right] + \frac{P_{sr}^2 B^2 \Re^2 N W}{2\Delta V L^2}\left[(2N-2)+W\right] + \frac{4K_b T_n B}{R_L}} \quad (4.41)$$

As mentioned earlier, the differences of the XOR detection as compared to the Complementary and AND subtraction are the cross correlation and signal properties. With the XOR technique, balanced detection can be achieved even if the cross correlation is not fixed; thus, large number of code sequences can be generated. This technique will improve the performance of the system in terms of the scalability and signal-to-noise ratio.

Now, let $C_K(i)$ denotes the ith element of the N^{th} VC code sequence. The code properties for the XOR technique can therefore be written as:

$$PD1_{(0)}(f,g,z,t) = \begin{cases} W, & f = z, g = t \\ 1, & f \neq z, g = t \quad For \quad N = (W+1) \\ 0, & g \neq t \quad For \quad N = P(W+1) + R \end{cases} \quad (4.42)$$

$$PD2_{(1)}(f,g,z,t) = \begin{cases} 0, & f = z, g = t \\ W-1 & f \neq z, g = t \quad For \quad N = (W+1) \\ 0, & g \neq t \quad For \quad N = P(W+1) + R \end{cases} \quad (4.43)$$

The balanced photodiode for the desired user #(f,g) that executes the correlation function Q rejects the MAI coming from the interfering users and obtains the desired information bit.

$$Q = \sum_{i=1}^{L} a_{(f,g)}(i) b_{(z,t)}(i) - \sum_{i=0}^{L} a_{(f,g)}(i) \oplus b_{(z,t)}(i) . \overline{a}_{(f,g)}$$

where $\oplus$ represents XOR operation.

Thus,

$$PD1_{(0)}(f,g,z,t) - \frac{PD2_{(1)}(f,g,z,t)}{W-1} = \begin{cases} W, & f = z, g = t \\ 0, & else \end{cases} \quad (4.45)$$

Equations (4.16), (4.17) can be simplified further as follows,

$$G_1(V) = \frac{P_{sr}}{\Delta V} \sum_{n=1}^{N} d_n . \sum_{i=0}^{L-1} \sum_{j=0}^{L_1-1} C_{ij\,(f,g)}(i) \overline{C}_{ij(z,t)} \left\{ u\left[\frac{\Delta V}{2L}\right] \right\} \quad (4.46)$$

$$G_2(V) = \frac{P_{sr}}{\Delta V} \sum_{n=1}^{N} d_n . \sum_{i=0}^{L-1} \sum_{j=0}^{L_1-1} C_{ij\,(f,g)} C_{ij(z,t)} \left\{ u\left[\frac{\Delta V}{2L}\right] \right\} \quad (4.47)$$

In Equations (4.46) and (4.47), d_N is the data bit of the *N*th user that carries the value of either '1' or '0'. Therefore the photodetector current can be calculated by integration as follows.

$$I_1 = \int_0^{\infty} G_1(v) dv \quad (4.48)$$

And

$$I_2 = \int_0^{\infty} G_2(v) dv \quad (4.49)$$

where I_1 and I_2 are the power spectral density at photodetectors 1and 2. By using the properties of VC code to obtain pure photocurrent after the subtraction process on the photo-detectors, Eq. (4.48) and Eq. (4.49) become:

$$I = I_2 - I_1 = \int_0^{\infty} G_1(v) dv - \int_0^{\infty} G_2(v) dv \quad (4.50)$$

After the integration and subtraction processes the photocurrent I can be expressed as:

$$I = \Re \frac{P_{sr}}{L} W \tag{4.51}$$

$$\Re = \frac{\eta e}{h V_c} \tag{4.52}$$

Now using (4.20),

$$\langle I^2 \rangle = 2eB(I_1 + I_2) + BI_1^2 \tau_{c1} + BI_2^2 \tau_{c2} + \frac{4K_b T_n B}{R_L} \tag{4.53}$$

Therefore,

$$\langle I^2 \rangle = 2eB\Re\left[\int_0^\infty G_1(v)dv + \int_0^\infty G_2(v)dv \right] + B\Re^2 \int_0^\infty G_1^2(v)dv + B\Re^2 \int_0^\infty G_2^2(v)dv + \frac{4K_b T_n B}{R_L} \tag{4.54}$$

From equation (4.13), when all the users are transmitting bit '1' using the average value as $\sum_{N=1}^{N} c_N \approx \frac{NW}{L}$, the noise power can be written as:

$$\langle I_{Tot}^2 \rangle = 2eB \left[\frac{P_{sr}}{L}((N-1) + W + (N-1)\right] + B\Re^2 \left[\frac{P_{sr}^2}{\Delta V L} \cdot \left[\frac{NW}{L}\right] \cdot \left[\begin{matrix}(N-1) + W \\ + (N-1)\end{matrix}\right]\right] + \frac{4K_b T_n B}{R_L} \tag{4.55}$$

Noting that the probability of sending bit '1' at any time for each user is a $\frac{1}{2}$ [38], then Equation (4.53) becomes

$$\langle I_{Tot}^2 \rangle = \frac{P_{sr} eB\Re}{L}\left[(2N-2) + W\right] + \frac{P_{sr}^2 B\Re^2 NW}{2\Delta V L^2}\left[(2N-2)/(P+R) + W\right] + \frac{4K_b T_n B}{R_L} \tag{4.56}$$

From (4.52) and (4.56), the average of SNR can be obtained as in (4.57) and (4.58) below.

$$SNR = \frac{(I_2 - I_1)^2}{\langle I_{Tot}^2 \rangle} \tag{4.57}$$

$$SNR = \frac{\frac{\Re^2 P_{Sr}^2 W^2}{L^2}}{\frac{P_{Sr} e B \Re}{L}\left[(2N-2)+W\right] + \frac{P_{Sr}^2 B \Re^2 N}{2\Delta V L^2}\left[W + \frac{2(N-1)}{P+R}\right] + \frac{4K_b T_n B}{R_L}} \tag{4.58}$$

where, P and R represent the number of mapping and the remaining of N after *modulo* operation. The Bit Error Rate (BER) is computed from the SNR using Gaussian approximation as in Eq. (4.59) below [38].

$$BER = P_e = \tfrac{1}{2}\, erfc\left(\sqrt{\tfrac{SNR}{8}}\right) \tag{4.59}$$

4.7 Performance Comparison Between Complementary, AND and XOR Subtraction Techniques

Recent studies have shown that an optical CDMA system cannot be designed only by considering the properties of the code. The detection technique also plays an important role and should be addressed as well. The advantage of SAC over frequency and temporal OCDMA systems is its ability to reduce the contribution of total noise to total received powers successfully. In order to study the performance, comparisons among the XOR, complementary and AND subtraction techniques are made by using the calculated results. The performance is characterized by BER and SNR, looking at the effects of the number of users and received power. The performance of the system is characterized by the effect of the various noises, which is analyzed accordingly. The relationship between the number of simultaneous user and BER in OCDMA system using XOR, Complementary and AND subtraction techniques are shown in section 4.7.1. The parameters used in the analysis are listed in Table 4.3.

4.7.1 Effect of Number of Users on the System Performance

Table 4.3: Typical Parameters Used in the Calculation

Photodetector Quantum efficiency	$\eta = 0.6$
Line-width Broad band Source	$\Delta V = 3.75$ THz
Operating Wavelength	$\lambda_o = 1550$ nm
Electrical Bandwidth	$B =$ 311 MHz
Data Bit Rate	$R_b =$ 622 Mbps
Receiver Noise Temperature	$T_n = 300$ K
Receiver Load Resister	$R_L = 1030\,\Omega$

Figure 4.8 shows the calculated results using equation 4.58 for the variations of signal-to-noise ratio (SNR) with the number of active users. The figure clearly shows that the XOR technique supports more users as compared to the complementary and AND techniques.

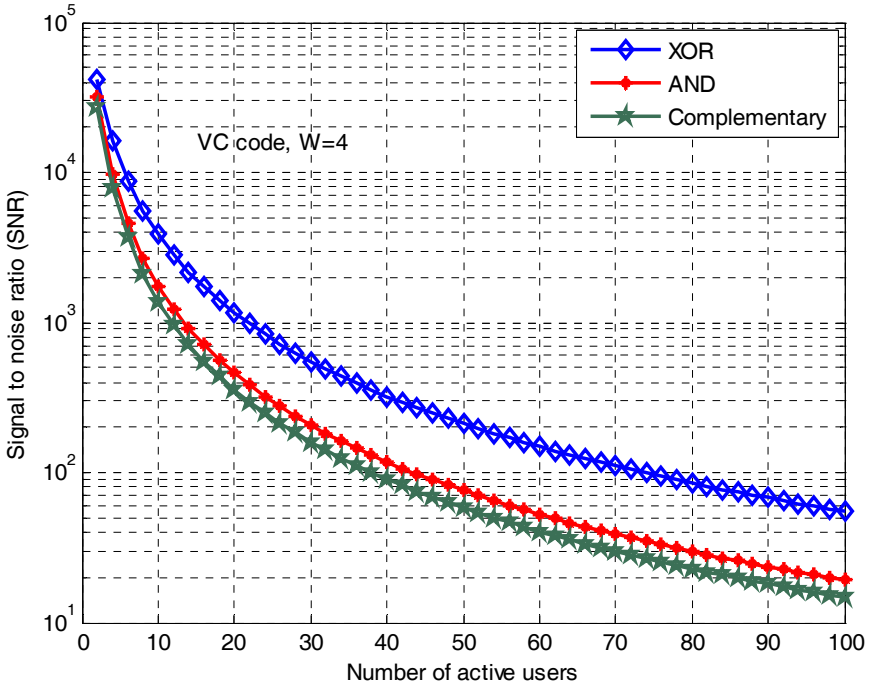

Figure 4.8: SNR versus number of active users when P_{sr} = -10dBm at 622Mb/s for different detection techniques.

Figure 4.9 shows the bit error rate (BER) versus the number of users for XOR, AND and Complementary subtraction techniques, based on equations (4.32) and (4.54). The system parameters used to obtain the numerical results are listed in Table 4.3.

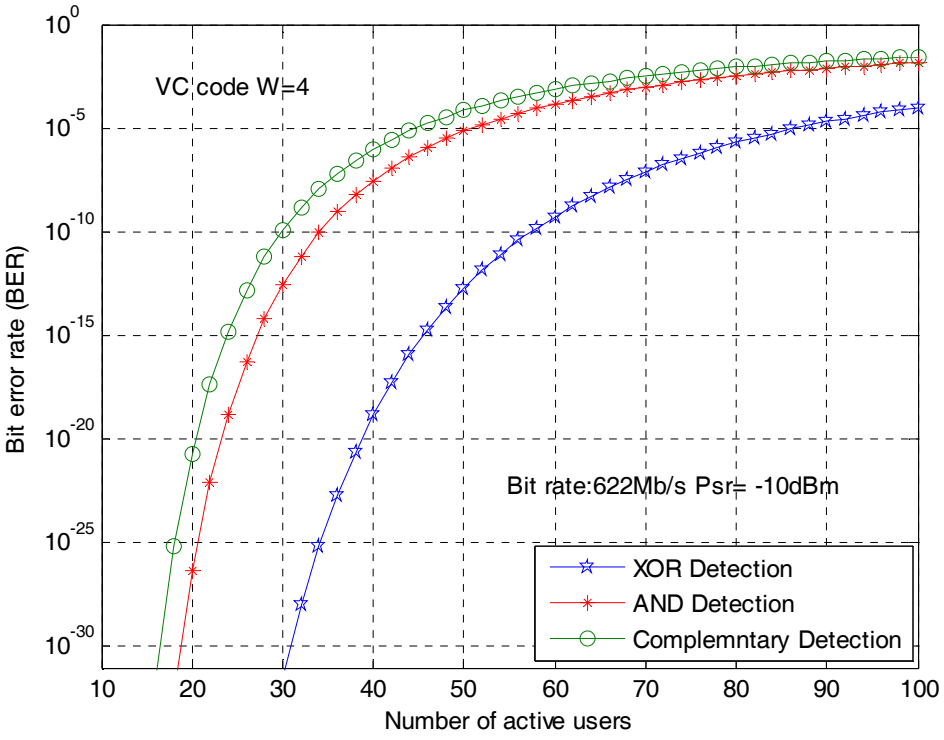

Figure 4.9: BER versus number of active users when P_{sr} = -10dBm at 622Mb/s for different detection techniques.

Figure 4.9 shows the bit error rate (BER) versus number of users for XOR, AND and complementary subtraction techniques using VC code. It shows that the OCDMA system using XOR technique performs better than the system using existing AND and complementary techniques. The figure clearly demonstrates that XOR technique supports more users (50 users at BER of 10^{-12}) compared to complementary and AND techniques (25 and 18 users at BER of 10^{-12} respectively). This is evident that with XOR technique, the MAI in the receiver side is eliminated by reducing the power of interfering from other users.

Figure 4.10 shows the bit error rate (BER) versus number of users for XOR and complementary subtraction techniques for VC, MQC and MFH codes respectively. The calculated BER for VC was achieved for W = 4 at data rate 2.5Gb/s. The calculated BER for MFH and MQC codes were achieved for W = 8, and W = 10, respectively at data rates 622Mb/s.

Figure 4.10 proves that the OCDMA system using XOR technique performs better than the system using existing complementary techniques. The figure clearly reveals that XOR technique supports more users (18 users at BER of 10^{-12}) compared to complementary technique (8 and 9 users, respectively at BER of 10^{-12}).

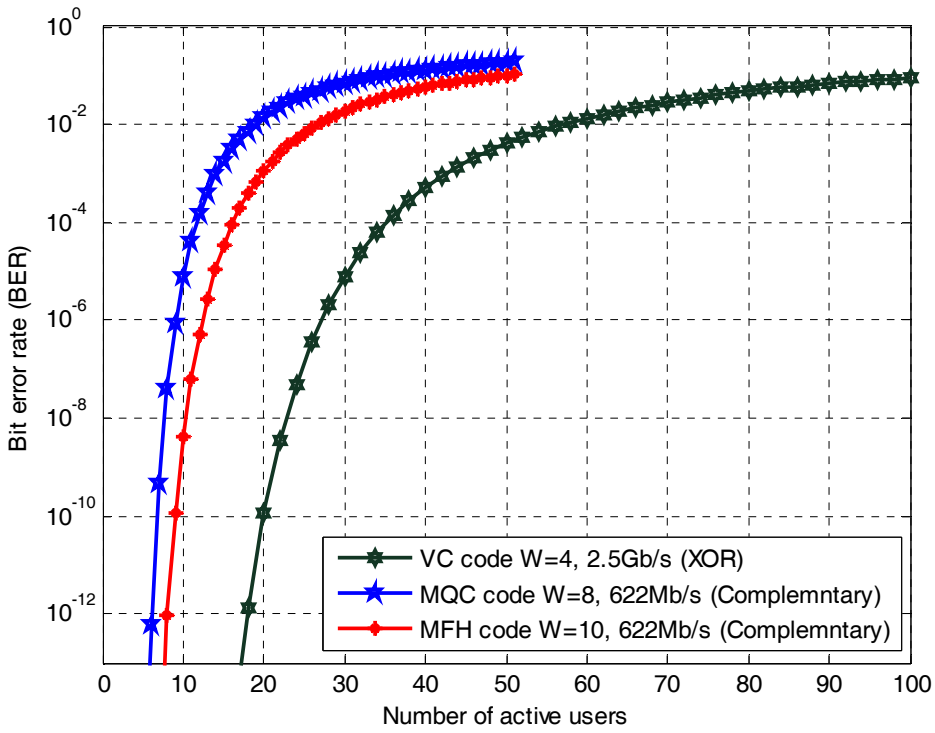

Figure 4.10: BER versus number of active users when P_{sr} = -10dBm at 2.5Gb/s, 622Mb/s for XOR and complementary detection techniques.

This further proves that using VC code with an XOR technique, the multiple access interference (MAI) in the receiver side is eliminated.

Note also that the calculated BER for VC code was achieved for W=4 while for MQC and MFH codes, the calculated BER were for W=8, and W=10 respectively.

4.7.2 Effect of Received Power P_{sr} on System Performance

Figure 4.11 shows the performance of the system using XOR, AND and complementary techniques at various values of received power P_{sr} using VC code. The number of active users in the system is fixed at 30 at data rate 622Mb/s. It is shown that XOR technique gives a much better performance when the effective received power Psr is large (when P_{sr} > -26 dBm). At the lower values of P_{sr} (when P_{sr} < -25 dBm), the performance of the system for the three techniques is almost the same.

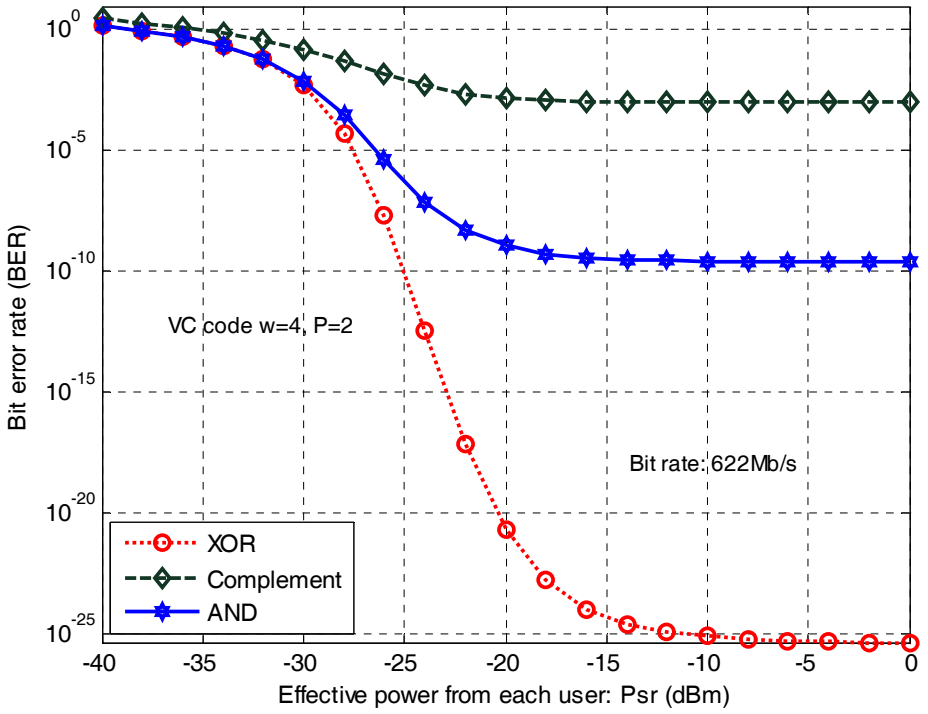

Figure 4.11: BER versus P_{sr} when number of active users is 30, taking into account intensity noise, thermal noise and shot noise at bit rate 622Mb/s.

It should be pointed out that fiber optic non-linear effects such as Four Wave Mixing (FWM), Self Phase Modulation (SPM) and Cross Phase Modulation (XPM), and also dispersions such as Chromatic Dispersion (CD) and Polarization Mode Dispersion (PMD) are not considered in this analysis. Nevertheless this will not affect the comparative analysis among the three detection techniques, as all of them are subjected to the same transmission conditions. Figure 4.12 shows the BER variations with P_{sr} when the number of active users is 30 while W=4, 8 and 10 at the data rate 622Mb/s by taking into account the effects of the intensity noise, thermal noise and shot noise for VC, MQC and MFH codes respectively. It has been shown that the VC using XOR detection technique has a lower BER than that of AND and complementary techniques; this is due to the elimination of MAI effects through XOR technique.

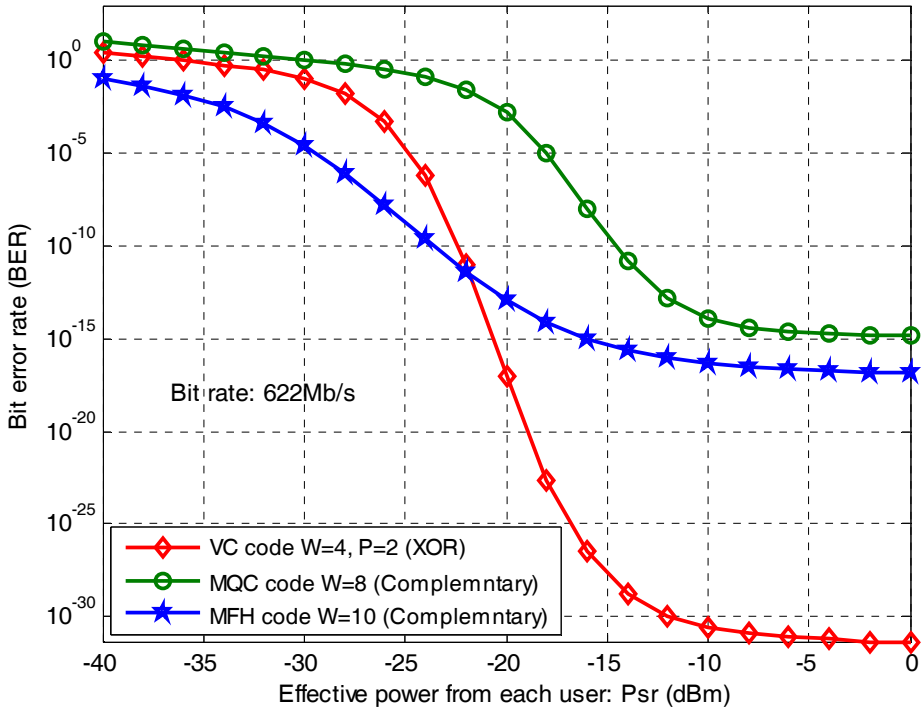

Figure 4.12: BER versus P_{sr} when number of active users is 30, taking into account intensity noise, thermal noise and shot noise at bit rate 622Mb/s for different OCDMA systems.

It has been shown that XOR technique gives a much better performance when the effective received power P_{sr} is large (when P_{sr} > -22 dBm). At the lower values of P_{sr}

(when P_{sr} < -22 dBm), the performance of MFH code using complementary technique will have a slightly better performance than the XOR due to high value of W.

4.8 Performance Comparison between the VC Code and Other Codes

Figure 4.13 shows the relation between the number of active users and SNR when the parameters used for the VC, MQC, MFH and Hadamard codes are W=6, 14, 17, 64 respectively while P=3, and R=1 for VC code. In this figure, the effective power from each user is -10dBm taking into account the effects of intensity noise, shot noise and thermal noise. It is shown that the VC code gives much higher SNR than MQC, MFH, and Hadamard. With large values of P and R, higher SNR can be obtained even for small weight while accommodating a high number of active users.

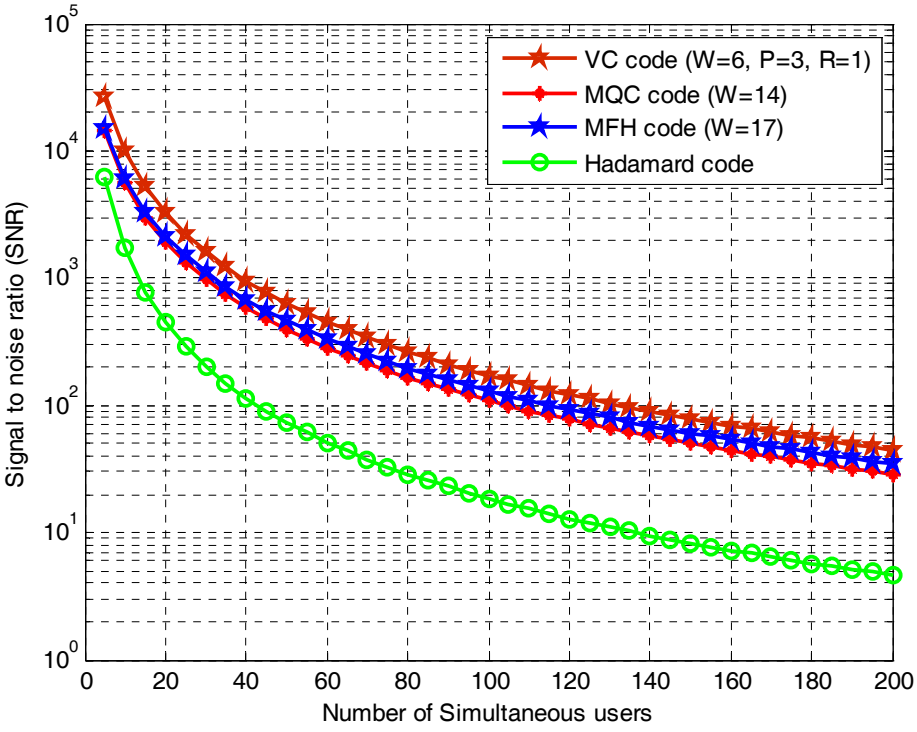

Figure 4.13: SNR versus number of active users when P_{sr} = -10dBm at 622Mb/s.

Figure 4.14 shows the BER variations with the effective power P_{sr} when the number of active users is 30 at a data rate of 2.5Gb/s for each user, taking into account the

effects of the intensity noise, thermal noise and shot noise. VC is adopted with the parameters W=6 and P=4, R=1, while for MQC and MFH the parameters are W=14, W=17, respectively. This figure shows that the efficient source power required for the VC is less (-22dBm) than that for the MQC and MFH codes when the number of active users is the same.

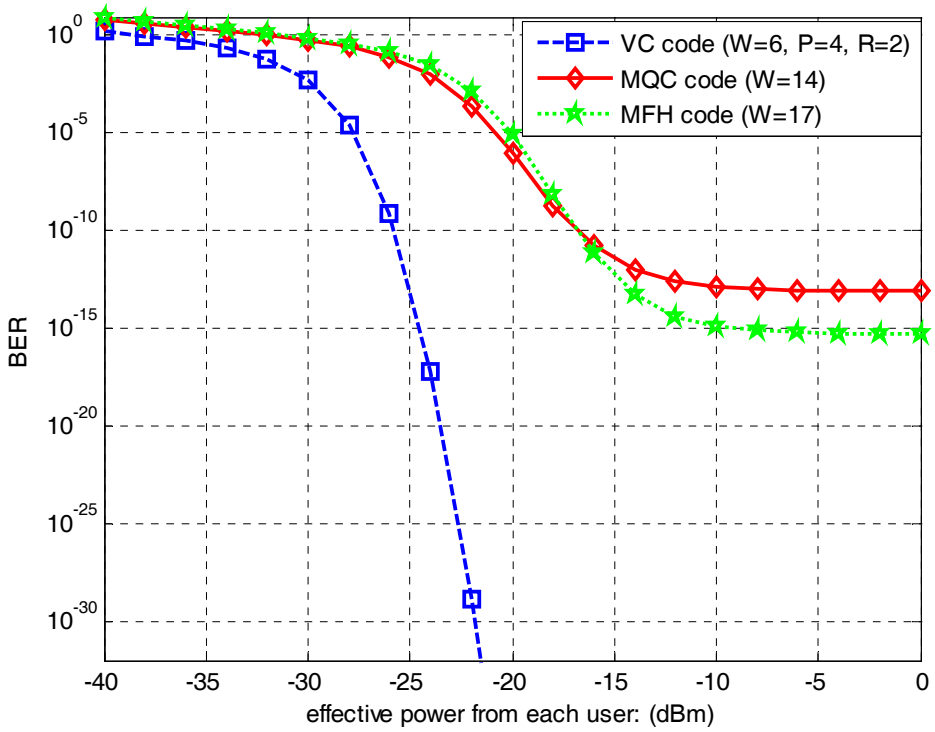

Figure 4.14: BERs versus effective source power P_{sr} when the number of active users is 30, taking into account the intensity noise, shot noise, and thermal noise at the data rate 2.5Gb/s.

4.8.1 Effect of Number of Users on System Performance Considering All Noise

In Figure 4.15, the bit error rate (BER) is plotted against the number of active users when P_{sr} = -10dBm at 622Mbit/s. From the figure, it is observed that the BER of VC code is lower compared to the MQC, MFH and Hadamard codes even though the weight is far less, which is 8 in this case. The maximum acceptable BER of 10^{-9} was

achieved by the VC code with 120 active users. This is better considering the small value of weight used. This is evident from the fact that VC code has an ideal in-phase cross correlation and good property that would eliminate the MAI effects through CC control by using mapping techniques while Hadamard code has increasing value of cross correlation as the number of users' increases. However, MQC and MFH used codes with a fixed in-phase cross correlation exactly equal to 1 for suppressing the effects of PIIN. Hence, this increases the probability of interfering which leads to performance degradation. The calculated BER for VC was achieved for $W = 8$ while for MFH, MQC and Hadamard codes were for $W = 10$, $W = 12$, and $W = 64$ respectively. With big values of P and R, VC code gives better result even for small value of W.

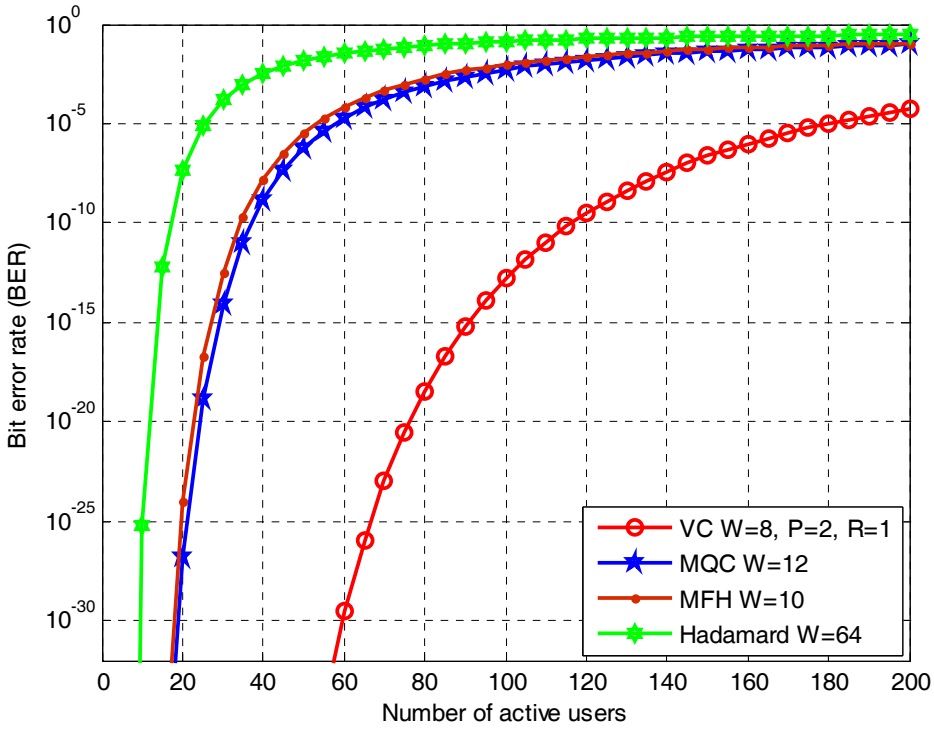

Figure 4.15: BER versus number of active users when P_{sr} = -10dBm at 622Mb/s.

4.8.2 Effect of Number of Users on System Performance considering different values of P_{sr}

Figure 4.16 shows the BER plotted against the number of active users with different effective power (-10, -20, -30 dBm) for VC code. It is shown that the performance improved significantly with large value of P_{sr}, for acceptable BER.

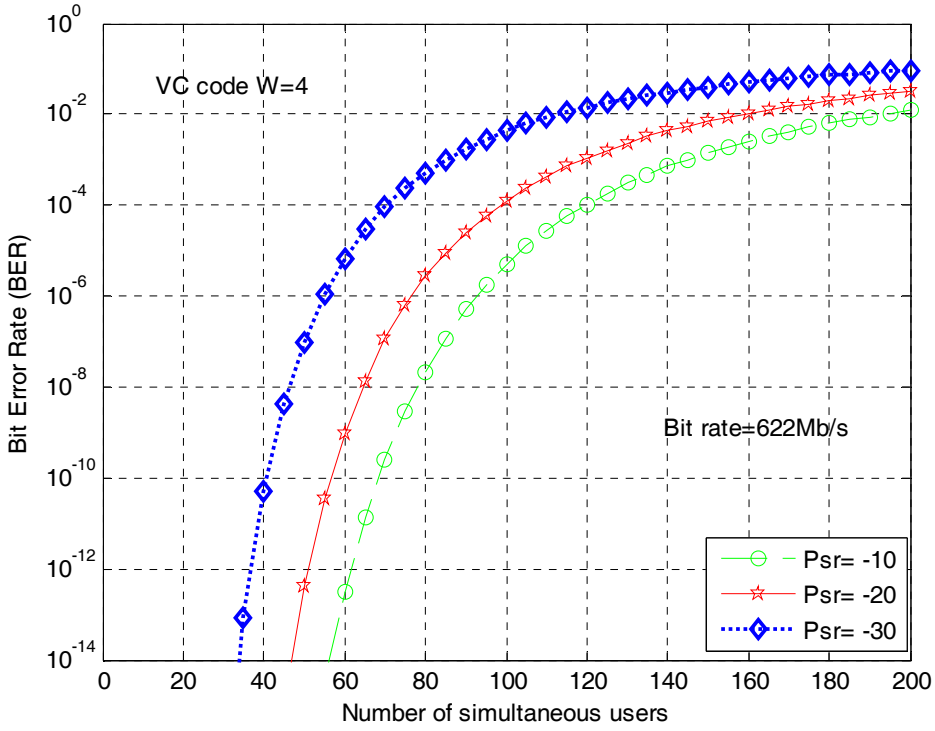

Figure 4.16: Bit error rate (BER) versus the number of active users under different power (-10, -20, -30 dBm) for VC code at 622Mb/s.

Figure 4.17 shows the BER plotted against the number of active users with different effective power (-10, -20, -30 dBm). It is shown that the performance with the VC is improved significantly with low power *Psr* while maintaing acceptable BER compared to the MQC code.

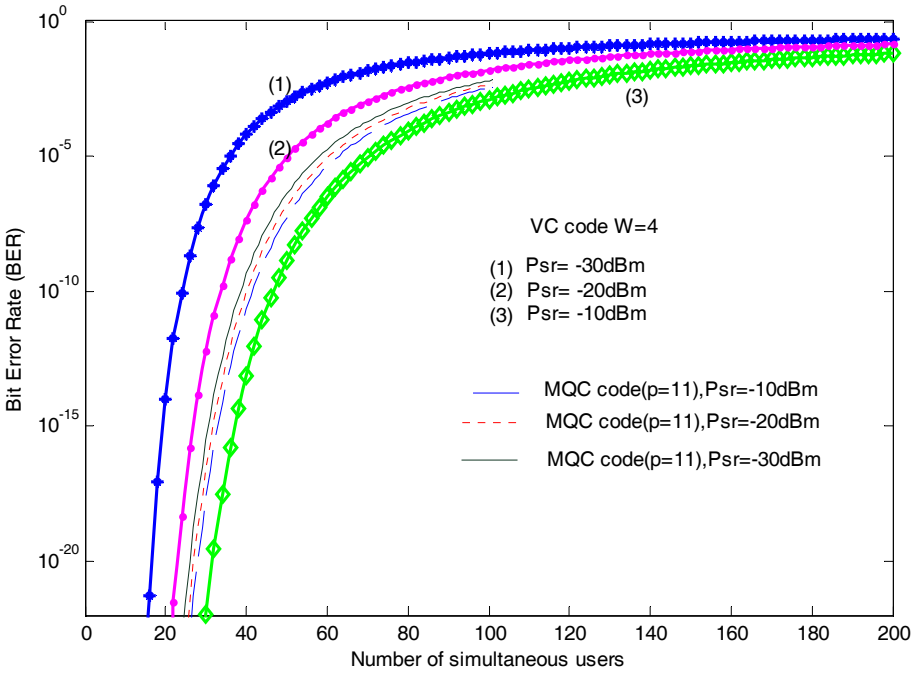

Figure 4.17: Bit error rate (BER) versus the number of active users under different power (-10, -20, -30 dBm) for VC and MQC codes at 622Mb/s.

4.8.3 Effect of distance on System Performance considering different data rates

Figure 4.18 shows the BER plotted against distance when the VC is adopted with the parameters W=4, P=3, R=1 and the number of users is 14. From Figure 4.18 it can be observed that for a data rate 622Mb/s, the performance of a VCC (P=2, R=1) can work well (BER=10^{-20}) and support a distance up to 50 km. However, for data rates 2.5 Gb/s and 10 Gb/s the performances are degraded from 50km to 10km and 4km respectively for the same BER (10^{-20}). This is because, when the distance decreases, the data rate should increase to recover a similar degradation of the signal form; eventually the pulse width will decrease, making the signal subject to fiber dispersion.

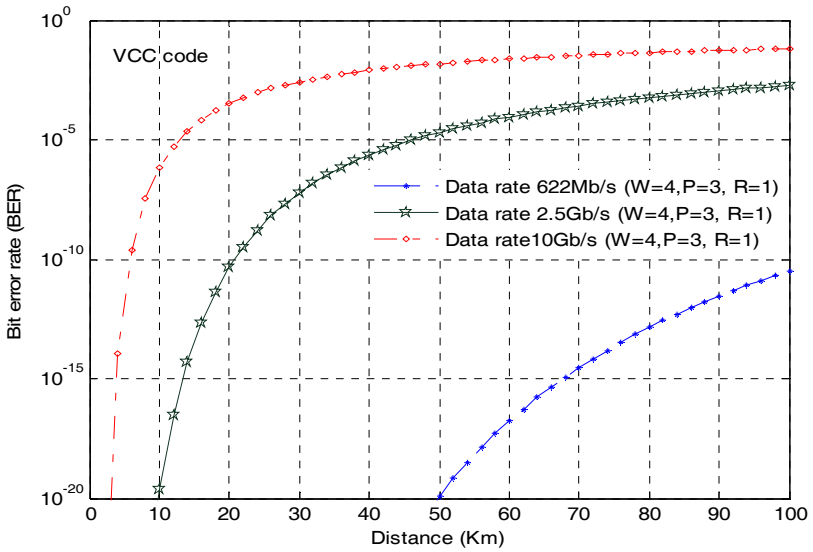

Figure 4.18: BER versus Distance for different data rates.

4.9 Code Evaluation and Comparison

Table 4.4: SAC-OCDMA Code Comparison

Code family	Existence	Weight	size	λ	Code length	SNR
MQC	Primes $p>2$	p+1	p^2	1	p^2+p	$\frac{\Delta v(p+1)}{BK[(K-1)/p+p+K]}$ [38]
MFH	All GF	q+1	q^2	1	q^2+q	$\frac{\Delta v(Q+1)}{BK[(K-1)/Q+Q+K]}$ [32]
MDW	Even integer n	N	w/2+1	1	3n+8/3[sin(Nπ/3)]^2	$\frac{2(\frac{W}{\lambda}-1)\Delta v}{BK[(\frac{K}{2}+\frac{W}{\lambda}-2]}$ [35, 60]
Hadamard	$m \geq 2$	2^{m-1}	2^m-1	2^{m-2}	2^m	$\frac{\Delta v}{BK(K+1)}$ [29]
RD	Integer n	n>3		2	$K+2W-3$	A/B+C+D [37]
IVC	$N=W+1$	Positive integer	W+1	1	$W \times N/2$	Refer to Eq (4.32)
NVC	$N<W+1$	Positive integer	W	1	$N(2W-N+1)/2$	Refer to Eq (C.23)
VC	$N>W+1$	Positive integer	$P(W+1)+R$	1	$(WN+R(W+1-R))/2$	Refer to Eq (4.58)

where

$$A=\frac{2\Re^2 P_{sr}^2 W^2}{N^2}$$

$$B=\frac{P_{sr} e B \Re W}{N}$$

$$C=\frac{P_{sr}^2 B \Re^2 N W}{2\Delta V N^2}\left[(K-1)+W\right]$$

$$D=\frac{4 K_b T_n B}{R_L}$$

The three VC code families have been compared with reported codes. The proposed IVC code always has the number of users equal W+1, which shorter length can be easily obtained. For the NVC code, it is important for the number of users to always equal W due to the fact that using a large weight provides a strong signal as required by the users. For the VC, the number of users always equals to P (W+1) +R. For comparison, the properties of Hadamard, MDW, MQC, MFH and VC families are listed in Table 4.4. It shows that the VC code exists for any number of users and weight, while the IVC and NVC exist for a restricted number of users. In addition, the VC code exists for any positive integer (regardless whether it is even, odd, prime, etc), while MDW exists for even n weight, Hadamard codes exists only when the weight is 2^{m-1} where $m\geq 2$, MQC and MFH exist for a prime number p and a prime power q given by $q= p^n$ where n is a positive integer respectively. The table also shows that the VC codes have an ideal cross correlation while Hadamard codes have increasing value of cross correlation as the number of user increases.

4.10 Summary

In this chapter, a detailed discussion of the influence of noise in OCDMA system, and the OCDMA detection schemes is provided. Noise is an unavoidable phenomenon that limits receiver performance. A mapping technique is applied to increase the number of users which changes the cross correlation of the code sequence to unfixed values; therefore Complementary detection is no longer sufficient. An XOR detection scheme is proposed to solve this problem. The performance of VC code families based on XOR detection in the presence of the phase induced intensity noise, the photodiode shot noise and the thermal noises are elaborated on this chapter.

The performance of the OCDMA system is degraded as the number of simultaneous users increase, especially when the number of users is large. This is attributed to the multiple access interference (MAI) which arises from the interference of the simultaneous users. MAI can be reduced by using subtraction techniques. It has been shown that using a newly proposed subtraction technique, XOR subtraction, the performance of the OCDMA system can be improved considerably. The overall system cost, the processing time and complexity of the system can be improved.

The results presented in this chapter have been based on theoretical calculations. Detailed discussions have been included on the effect of various noises such as thermal noise, shot noise, and phase induced intensity noise (PIIN) to the optical CDMA system using VC, MFH, MQC and Hadamard codes. VC code outperforms other optical CDMA codes because the total noise level is reduced. The VC code has excellent code properties that can reduce the PIIN noise and shot noise effects, and increase system performance. VC code can support more users as compared to the Hadamard and MFH codes, because the VC code has better BER than other codes.

A software simulation for all detection schemes using a commercial optical systems simulator, *Virtual Photonic Instrument* (VPI^{TM}), version 7.1 is discussed in the next chapter.

CHAPTER 5

RESULTS AND DISCUSSION

5.1 Introduction

This chapter discusses the results obtained for the ZVC code families with the direct recovery scheme (DRS) and VC code families with the Complementary, AND, and XOR subtraction techniques given in Chapter 4 based on the theoretical development, developed from theoretical analysis and more emphasis on simulation. Simulation tools can offer a powerful method to assist in analyzing the design of an optical component, circuit, or network before costly prototypes are built. VPItransmissionMaker^{TM} WDM, version 7.1 is used to accomplish this work [78-81]. The basic design issues such as design parameters, performance parameters, types of modulation and types of optical sources and receivers are addressed in this chapter.

5.2 Theoretical Performance Analysis

An adequate signal-to-noise ratio (SNR) is important because it gives the quality of the signal in the system. It is a ratio of the average signal power to total noise power. BER and SNR are interrelated; a better SNR yields a better BER. In Chapter 4 (see 4.34), the SNR for OCDMA system using VC code family is given by

$$SNR = \frac{\frac{\Re^2 P_{sr}^2 W^2}{L^2}}{\frac{P_{sr} eB\Re}{L}\left[(N-1)+W\right] + \frac{P_{sr}^2 B\Re^2 WN}{2\Delta VL^2}\left[(N-1)+W+(N-1)/P+R\right] + \frac{4K_b T_n B}{R_L}} \quad (5.1)$$

Based on the above formula, the effect of the various noises on the system performance is analyzed accordingly. In the denominator of equation (5.1), the first item results from the shot noise, the second item denotes the effect of PIIN and the third item represents the effect of thermal noise.

5.2.1 Relation between the Received Power and the PIIN Noise

Multiple Access Interference (MAI) that increases with the number of simultaneous users, severely limits the capacity of the system. MAI also leads to another type of noise, known as Phase Induced Intensity Noise (PIIN) that resulted from the phase incoherence of the overlapping signals on the same spectra causing fluctuations of the total signal intensity. Here, the relations between PIIN noise and received power will be analyzed. From Equation (5.1) PIIN can be written as:

$$PIIN = \frac{\frac{\Re^2 P_{sr}^2 W^2}{L^2}}{\frac{P_{sr}^2 B \Re^2 NW}{2\Delta V L^2}\left[(N-1) + W + (N-1)/P + R \right]} \qquad (5.2)$$

where W is the code weight, N is the number of active users, B is the noise equivalent electrical bandwidth of the receiver, ΔV is the optical source bandwidth, P_{sr} is the received power**,** L is the code length, $\Re$ is the responsivity of the photodetectors, P represents the number of mapping and R represents the remaining of N after modulo operation. In Figure 5.1, the values of B, K, and ΔV are fixed (ie. B = 311 MHz, N = 30 and ΔV = 3.75 THz) while P_{sr} varied from -40 dBm to 10 dBm.Figure 5.1 shows the PIIN plotted against the received power for the VC, MQC and MFH using the parameters: W=4, 14 and 17 for VC, MQC and MFH, respectively, at data rate 10Gb/s. From the figure, it can be observed that when the received power increases, the PIIN noise for all the codes increase linearly. The PIIN noise of VC code family is less compared to that of MQC and MFH codes.

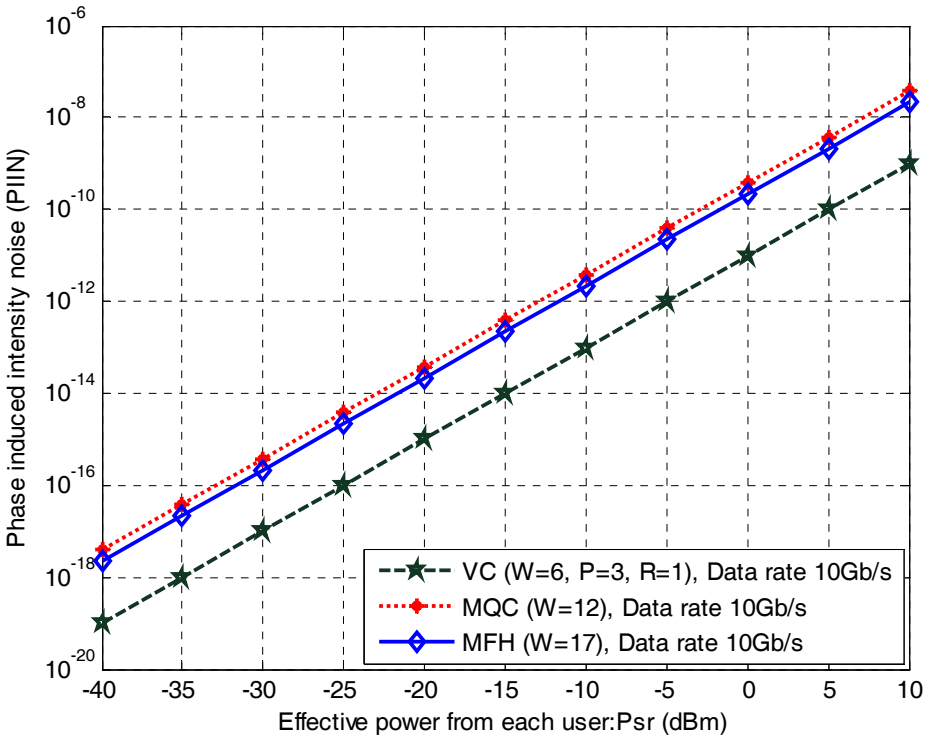

Figure 5.1: PIIN Noise versus received power for VC, MQC and MFH codes at data rate 10Gb/s when P_{sr} = -10dBm.

Moreover the PIIN noise can be effectively suppressed by using VC code family. This is because by using mapping techniques, the power of interference from other users is reduced with the increase of the code length, and eventually eliminates the MAI effects. Figure 5.1 also show that when the code weight is increased, the PIIN noise can further be suppressed.

5.2.2 Effect of Number of Users on System Performance by Considering PIIN Only

It has been shown in the above section that PIIN increases when the received power P_{sr} is increased. Here, the relation between PIIN noise and the number of users N will be investigated. Figure 5.2 shows the relation between number of active users and the PIIN noise for VC, MQC and MFH codes. In Figure 5.2, the parameters values are: W=8, 10, 4 and P=2 for MQC, MFH and VC respectively; the bit rate is 622Mb/s; P_{sr} =-10dBm but number of users N varies from 1 to 100.

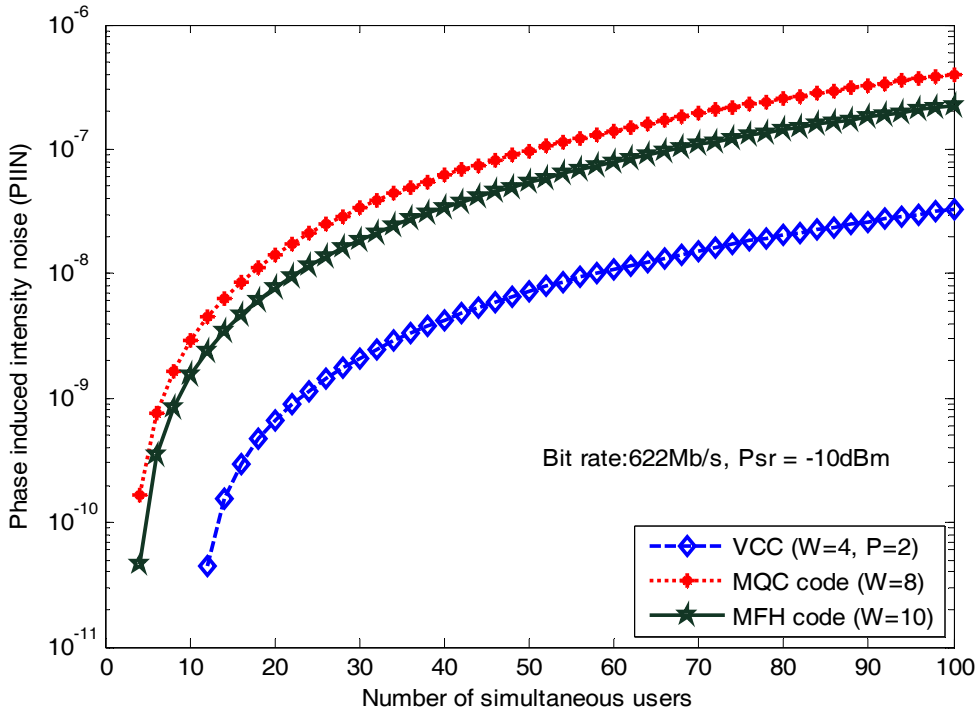

Figure 5.2: PIIN noise versus number of active users for VC, MQC and MFH codes at data rate 622Mb/s when P_{sr} = -10dBm**.**

The figure clearly shows that, for VC code family, the PIIN noise is maintained when the number of active user increases. This is due to the good properties of the code sequences and mapping technique. On the other hand, for MQC and MFH codes the PIIN noise increases when the number of active user increases.

5.2.3 Effect of Number of Users on System Performance by Considering PIIN Only

Figure 5.3 shows the relation between number of active user (N) and the system performance by considering only PIIN noise (where the effects of shot and thermal noise are neglected). It clearly shows that VC code has better BER than Hadamard, MQC and MFH codes.

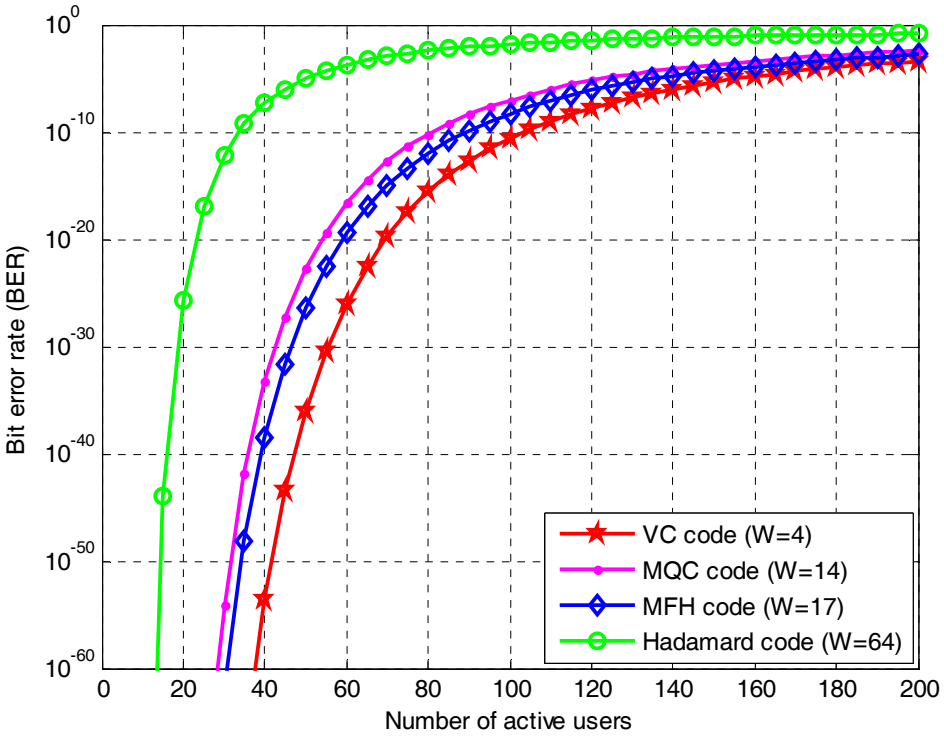

Figure 5.3: BER versus Number of Active User by Considering PIIN Noise Only.

It shows that the Bit Error Rate (BER) increases as the number of active user increases. If only the PIIN noise is considered, the SNR is given as:

$$\text{SNR} = \frac{2\,\Delta V\,W}{BN\left[\left(\frac{2(N-1)}{P+R}\right)+W\right]} \tag{5.3}$$

and

$$\text{BER} = \frac{1}{2}erfc\left(\sqrt{\frac{SNR}{8}}\right) \tag{5.4}$$

In Equation (5.3), SNR depends on code weight W, number of user N, ΔV, and B. However, in Figure 5.4, the values of B, and ΔV are fixed (ie. B = 311 MHz and ΔV = 3.75 THz) but N varies from 1 to 200 user. In Figure 5.3, it is shown that the system using VC code can support a much larger number of users for acceptable BER than Hadamard, MQC and MFH codes. When the code weight is increased, the performance of all the codes improved. The calculated BER for VC was achieved for

$W = 4$ while for MFH, MQC and Hadamard codes were for $W = 17$, $W = 14$, and $W = 64$ respectively. Nevertheless, there are large improvements in the VC code family performance. This is because of the superior properties of VC and cross correlation control through mapping technique of code family that can suppress the PIIN noise.

5.2.4 Relation between Received Power and Shot Noise

Figure 5.4 shows the relation between shot noise and effective power, P_{sr} at the receiver. From Equation (5.1), shot noise is given by:

$$\text{Shot Noise} = \frac{P_{sr} e W^2 \Re}{BL\phi[(N-1)+W]} \tag{5.5}$$

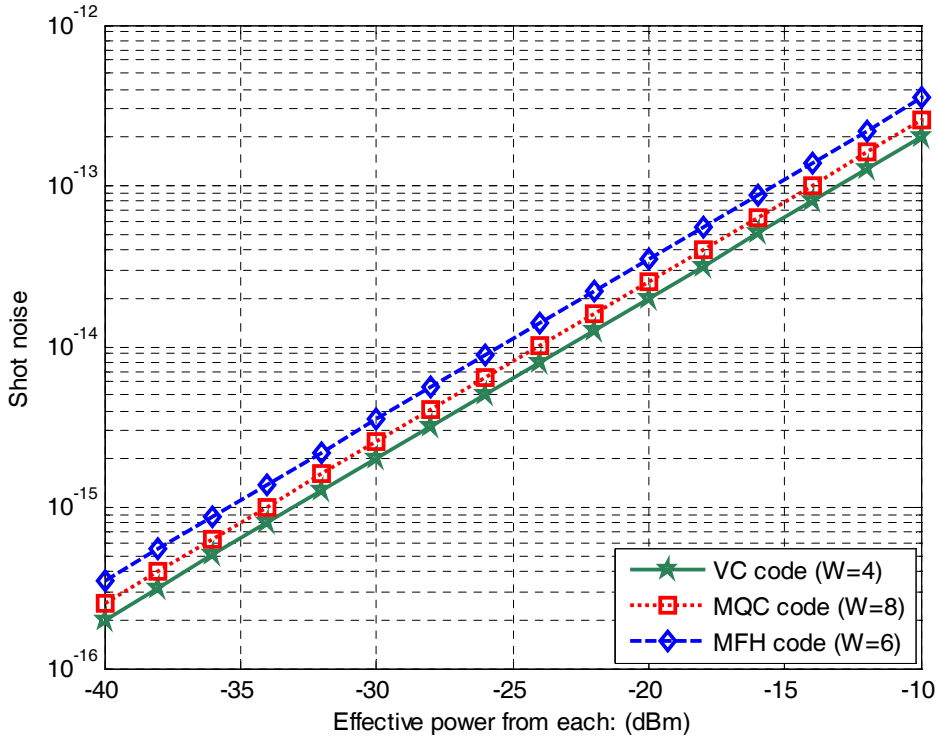

Figure 5.4: Shot noise versus effective power P_{sr} for VC code family when number of active users is 30.

Figure 5.4 shows the relation between P_{sr} and system performance (BER) by considering only the shot noise (where the effects of PIIN and thermal noise are neglected) for MQC, MFH, and VC when the number of users N equals to 30. From

the figure we can observe that the influence of P_{sr} is not significantly limited by the shot noise, as P_{sr} increases, the amount of signal power increases more than that of the shot noise.

5.2.5 Effect of P_{sr} on System Performance by Considering Only Shot Noise

Figure 5.5 shows the BER variations with P_{sr} when the number of active users is 30 and the system performance by considering only shot noise (where the effects of PIIN and thermal noise are neglected). It clearly shows that VC code has better BER than Hadamard, MQC and MFH codes.

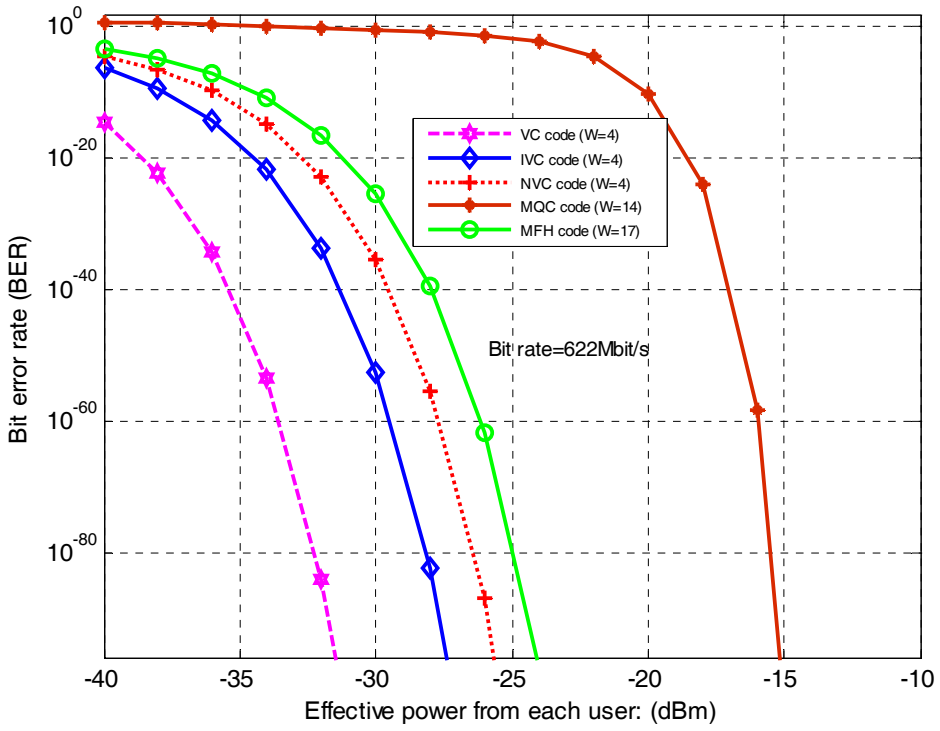

Figure 5.5: BER versus P_{sr} by considering only shot noise when number of active users is 30.

5.2.6 Effect of P_{sr} on Performance Considering All Noise

Figure 5.6 shows the BER variations with P_{sr} when the number of active users is 30, W=4 and the data rate is 622Mbit/s by taking into account the effects of the intensity noise, thermal noise and shot noise. It is shown that, when P_{sr} is less than -22 dBm, VC has lower BER than IVC and NVC codes, this due to the elimination of MAI effects through CC control by using mapping techniques.

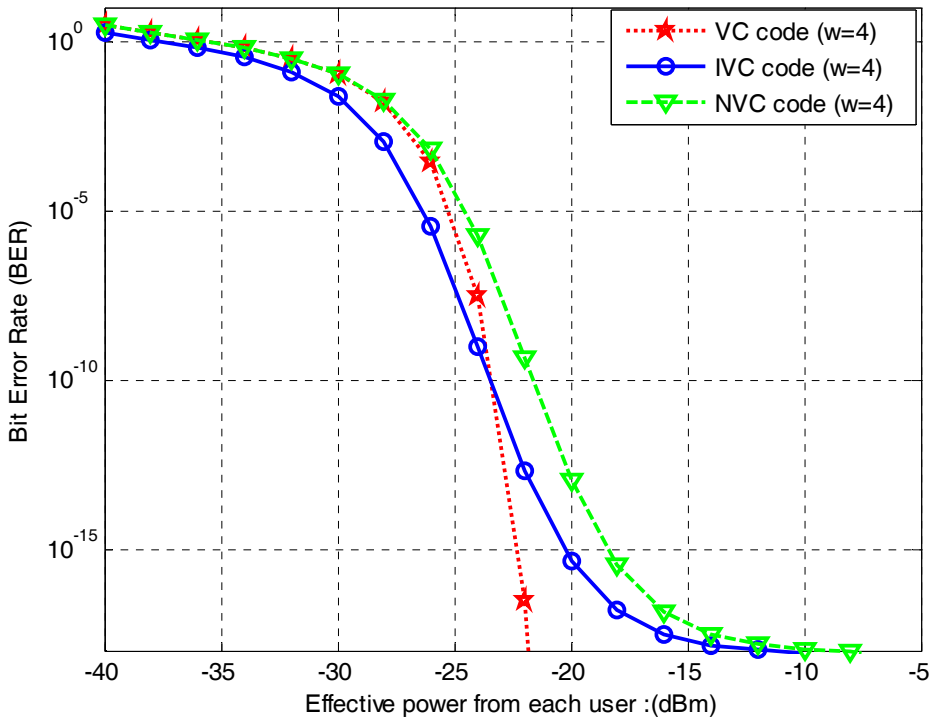

Figure 5.6: BER versus effective power P_{sr} for VC code families when number of active users is 30, taking into account the intensity noise, shot noise and thermal noise.

Figure 5.7 shows the BER plotted against P_{sr} when the number of active users is 69, W=4 and the data rate is 622Mbit/s. The green solid line with square represents the NVC when intensity noise and thermal noise are considered, while the red dotted line with star represents the IVC when intensity noise and shot noise are taken into account. The blue dashed line with circle represents the VC performance when effects of all noises are considered. It is shown that, when P_{sr} is less than -36 dBm, VC has

lower BER than IVC and NVC codes although all noises are considered, compared to intensity and thermal noises for NVC (less -22dBm), and intensity and shot noises for IVC (less -24dBm). This due to the elimination of MAI effects through CC control by using mapping techniques and good arrangement of VC construction.

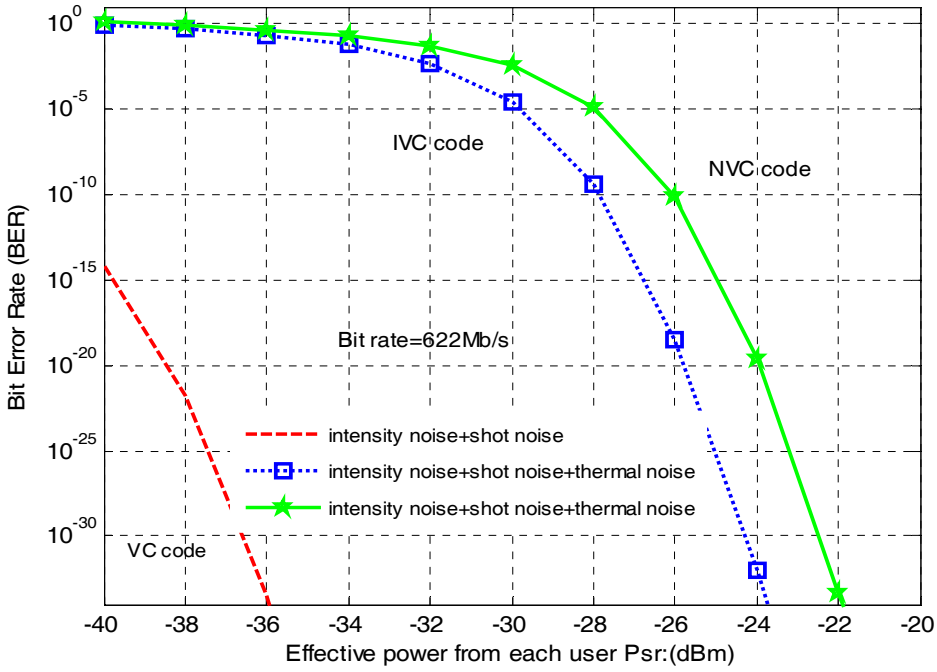

Figure 5.7: BER versus effective power P_{sr} for VC code families when number of active users is 69.

Figure 5.8 shows the BER plotted against the P_{sr} when the number of active users is 30, W=4 and the data rate is 622Mbit/s. The brown dashed line with point (MQC) represents the BERs, taking into account the effects of the intensity noise, and thermal noise. The green solid line with cross represents the NVC when intensity noise and thermal noise are considered while the red dotted line with star represents the IVC when intensity noise and shot noise are taken into account. The blue dashed line with circle represents the VC performance when effects of all noise sources are considered. It is shown that, when P_{sr} is large, both the shot and thermal noises are negligibly small compared to intensity noise, which becomes the main limitation factor of the

system performance. However, when P_{sr} is low, the effect of intensity noise becomes minimal, and, thus, the thermal source becomes the main factor that limits the system performance. From the figure, it can be observed that thermal noise is much more influential than shot noise on system performance.

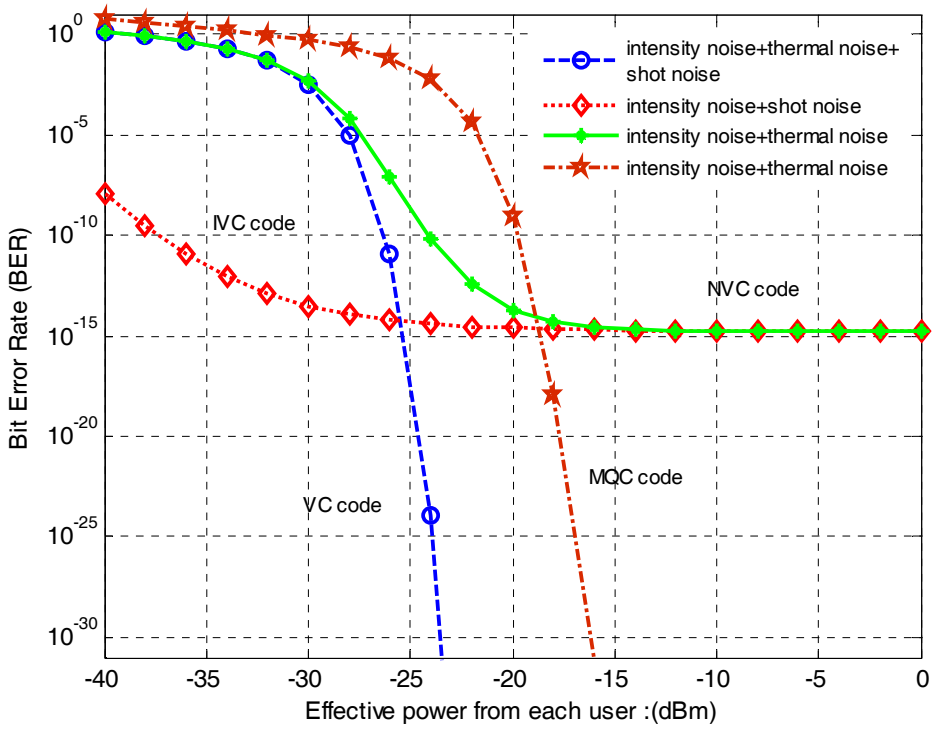

Figure 5.8: BER versus effective power P_{sr} for VC code families and MQC code.

Figure 5.9 shows the BER plotted against P_{sr} when the number of active users is 30, W=4 and the data rate is 622Mbit/s. The brown dashed line with point (MQC) represents the BERs, taking into account the effects of the intensity noise, thermal noise and shot noise. The green dashed with cross, and solid red with star lines represent the VC when intensity noise and thermal noise, and all noises are considered respectively. From this figure, it is observed that, VC outperforms the MQC code when all noises are considered; this is because VC code has the ability to suppress the contribution from MAI in contrast to MQC which MAI increases when a high number of users is involved.

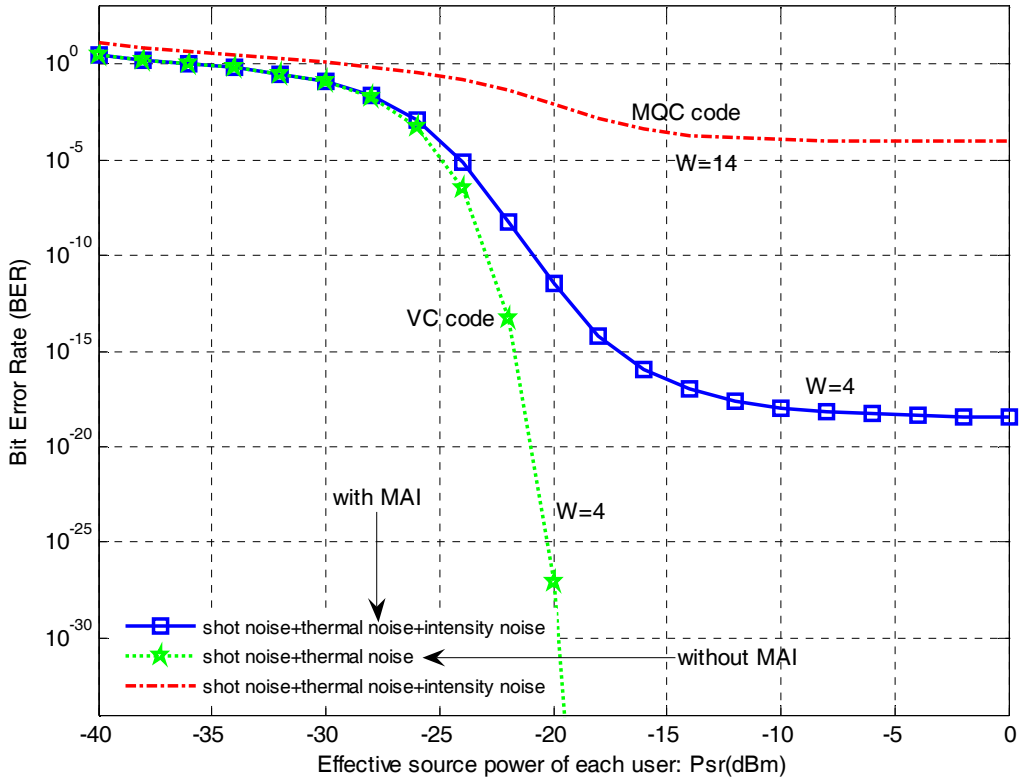

Figure 5.9: BER versus effective power P_{sr} for VC and MQC codes when number of active users is 30.

5.2.7 Effect of Distance on System Performance for Different data rates

Figure 5.10 shows the relationship between distance and BER for VC code when different data rates were used. It is shown that VC code can perform well up to 5 and 2 km only at 2.5Gbit/s and 10Gbit/s respectively, as compared to data rate 155Mbit/s which gives excellent performance up to a distance of 50 km, after which it starts to experience some interference but still performing much better than 10Gbit/s. It should be point out that, data rates 155Mb/s and 622Mb/s using for ATM system, 1.25Gb/s and 2.5Gb/s for Gigabit Ethernet while 10Gb/s for long haul system.

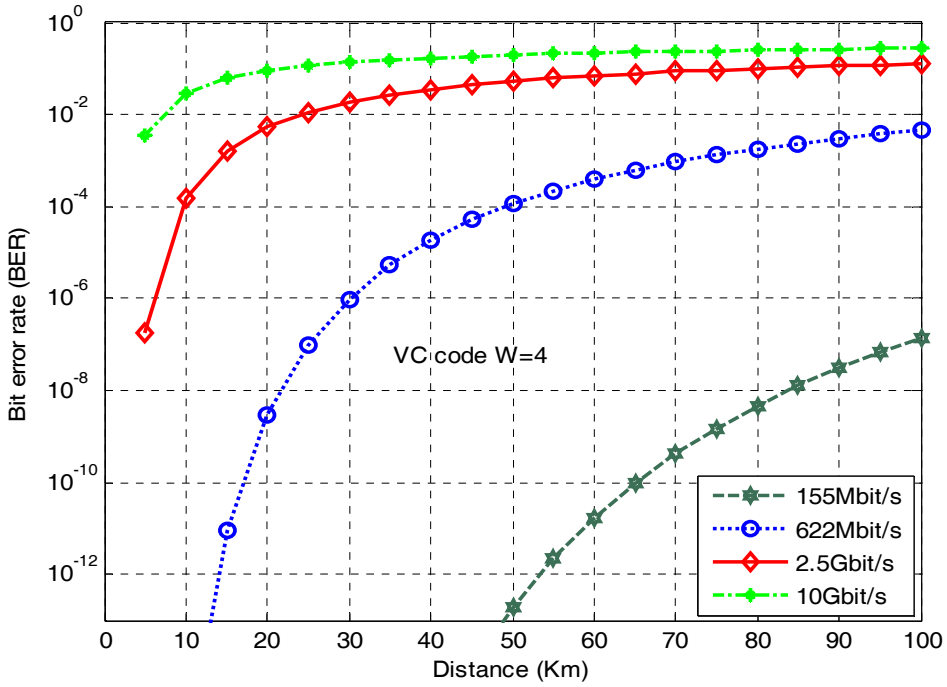

Figure 5.10: BER versus distance for the VC-OCDMA system at different transmission rates.

5.3 Simulation Result

Simulation tools can offer a powerful method to assist in analyzing the design of an optical system before costly prototypes are built. The analysis was carried out for various systems under study based on the model in Figure 1.2 (see Chapter 1). Two sorts of parameters were considered, design parameters and system parameters. The performance of each system is characterized by three main parameters, namely, the BER, output power and noise power.

5.3.1 Design Parameter

The design parameters are the system parameters that a designer can vary or change in order to study their effect on the system's performance. The designer must carefully choose the components to ensure that the desired performance level can be maintained over the expected system lifetime without over specifying the component characteristics. The design parameters used are distance, bit rate,

transmit power and chip spacing or width. Each of the design parameters is explained in Appendix C.

5.3.2 System Configuration

A simple schematic block diagram consisting of different users is illustrated in Figures 5.11, 5.12 and 5.13 as a descriptive example (the study was carried out for different users). The tests were carried out by using the simulation software, *Virtual Photonic Instrument* (VPI^{TM}) version 7.1. Each chip has a spectral width of 0.8 nm (100GHz). The tests were carried out at the rate of 2.5Gbit/s and 10Gbit/s for various distances with the ITU-T G.652 Non Dispersion Shifted Fiber (NDSF) single mode fiber (SMF) standard. At 1550 nm wavelength, the attenuation coefficient was 0.25 dB/km, and the chromatic dispersion coefficient was 18ps/nm-km and the polarization mode dispersion (PMD) coefficient was 5 ps/√km. Nonlinear effects such as four-wave mixing (FWM), the self phase modulation (SPM), and the group delay were activated and specified according to the typical industry values to simulate the real environment as close as possible.

A pseudo random bit sequence (PRBS) generator was used at the transmitter side as the input data of each user followed by a coder jitter to generate an NRZ sample ended by a rise time to adjust the rise time of the pulse. After that a Mach-Zehnder modulator was used to modulate the laser output. As shown in Figures 5.11-5.13, a filter optics spectral phase decoder that operates to decode the coded sequence was used after the transmission. A clock recovery ideal was used to synchronize the incoming optical signal with original transmitted signal. An additional clock recovery was used before the photo detectors to synchronize incoming optical signal from desired user and its complementary. The decoded signal was decoded by a photo detector (PD) followed by a 0.7 GHz low pass filter (LPF) and error detector, respectively.

The transmitted power used was -10 dBm out of the broadband source. The noise generated at the receiver was set to be random and totally uncorrelated. The dark current value was 5 nA and the thermal noise coefficient was $2.5\times e^{-23}$ W/Hz for each of the photo detectors. The performance of the system was evaluated by referring to the bit error rate, received power, output power and the eye pattern.

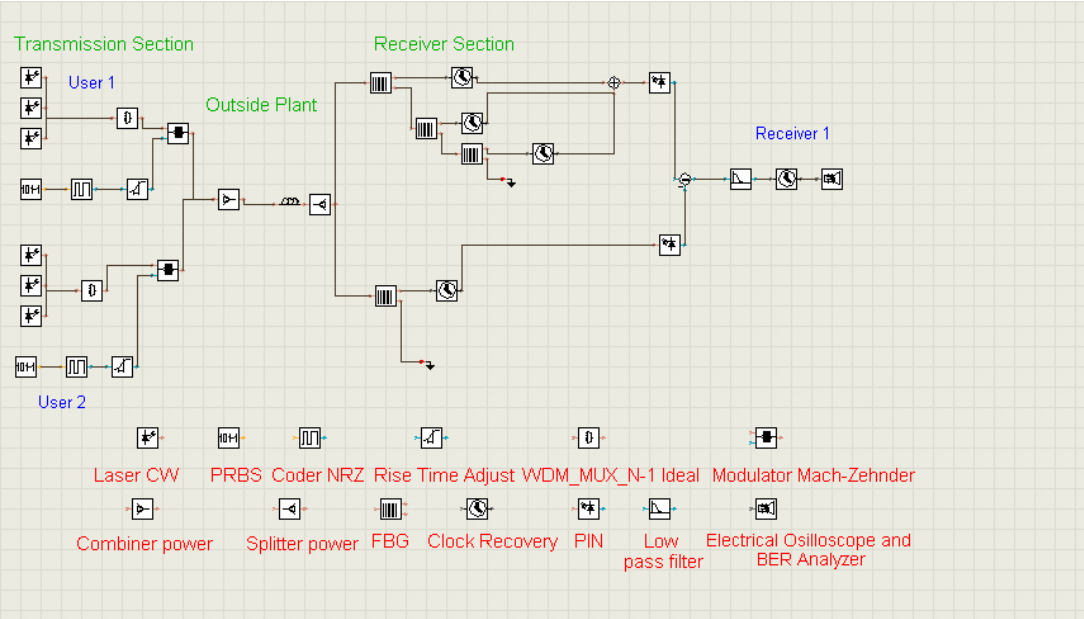

Figure 5.11: Simulation setup for the OCDMA system with Complementary technique.

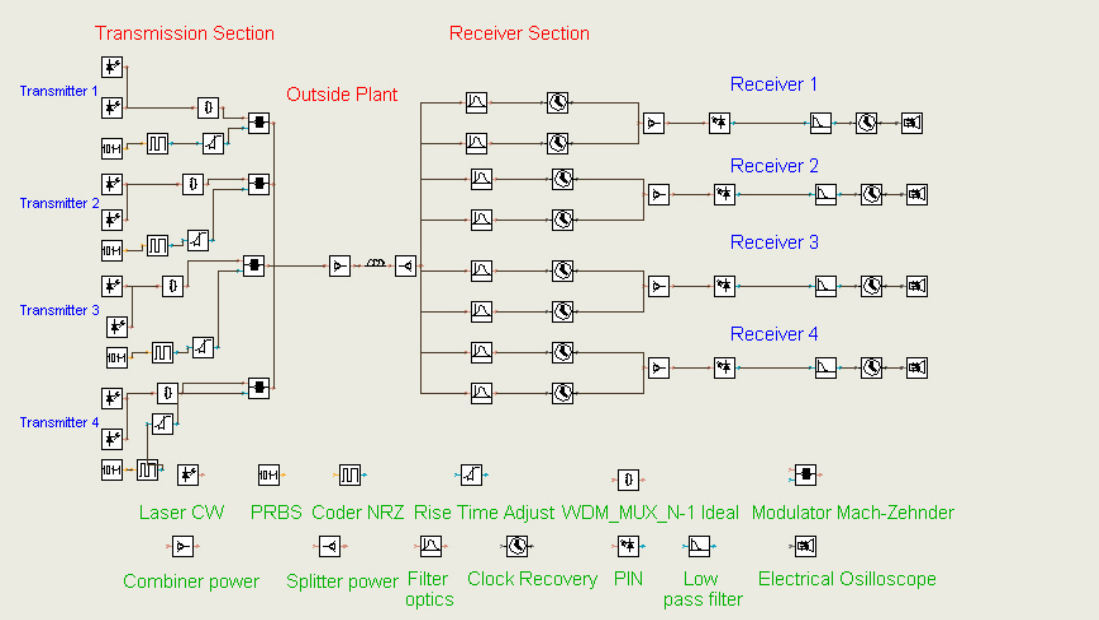

Figure 5.12: Simulation setup for the OCDMA system with direct recovery scheme.

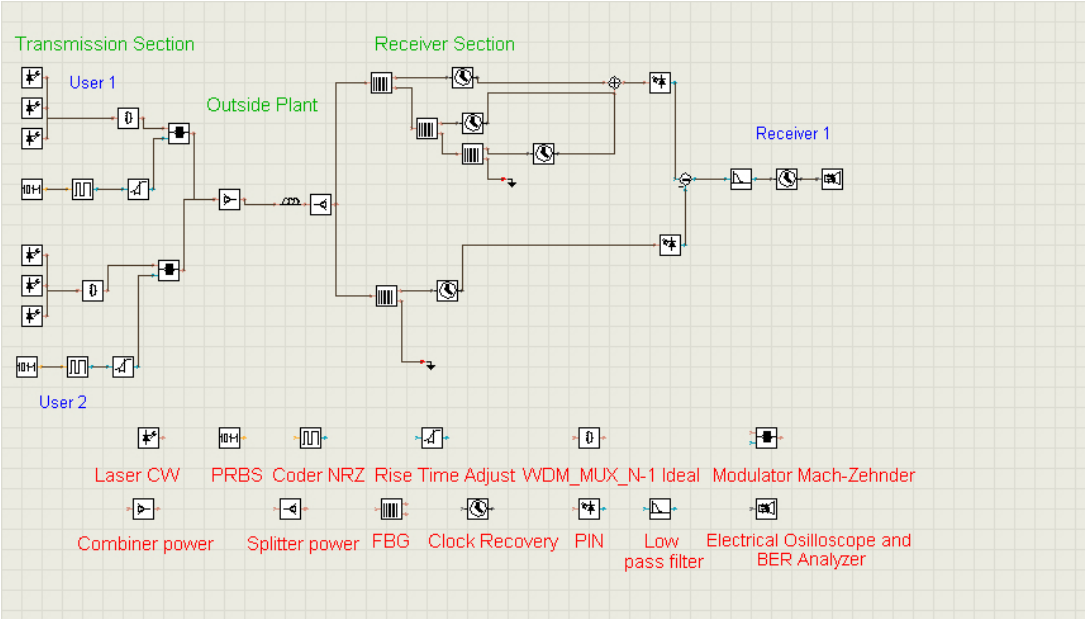

Figure 5.13: Simulation setup for the OCDMA system with XOR technique.

5.3.3 Performance analysis of ZVC code system

In this section, the proposed system based on direct recovery scheme will be analyzed using ZVC code. One of the important properties of this code is that the maximum cross correlation (CC) is always zero, which means that multiple user interference (MAI) and phase induced intensity noise (PIIN) are reduced. As stated previously, the main difference of direct recovery scheme compared to complementary subtraction is at the decoder. With direct recovery scheme, no subtractors are needed at the receivers, thus the number of filters is considerably reduced. This technique will improve the system performance such as higher signal-to-noise ratio and reduced probability of error as illustrated in Figure 5.12 for four users.

5.3.3.1 Eye Diagram

The Eye diagrams for the direct recovery scheme for weight four (W=4) for both 2.5Gbit/s and 10Gbit/s and various distances are investigated.

Figures 5.14 and 5.15 show the eye diagrams for the direct recovery scheme at 2.5Gbit/s for 10km and 30 km, respectively. The eye diagram for the direct recovery

scheme at 10Gbit/s for 10 km and 30 km are shown in Figures 5.16 and 5.17, respectively.

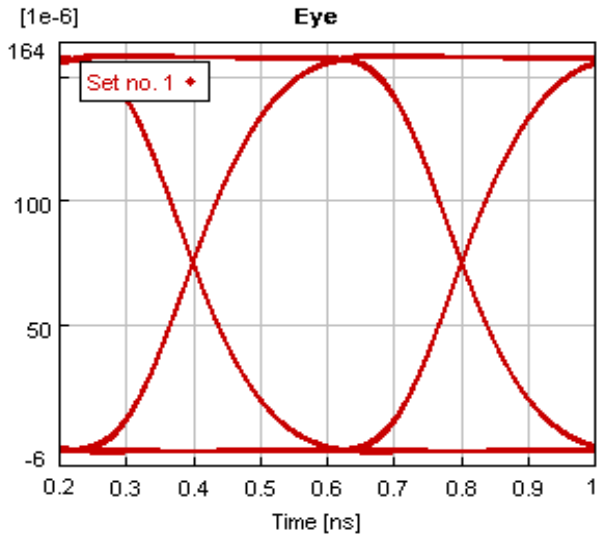

Figure 5.14: Eye diagram for ZVC code with direct recovery scheme at 2.5Gbit/s for 10 km.

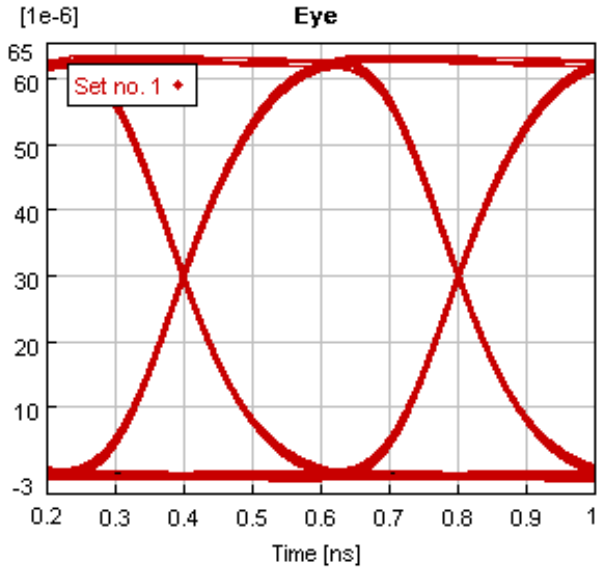

Figure 5.15: Eye diagram for ZVC code with direct recovery scheme at 2.5Gbit/s for 30 km.

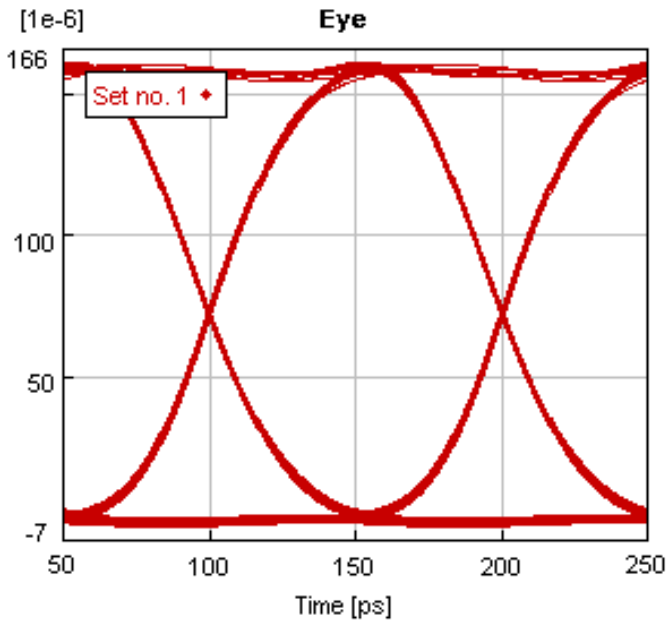

Figure 5.16: Eye diagram for ZVC code with direct recovery scheme at 10Gbit/s for 10 km.

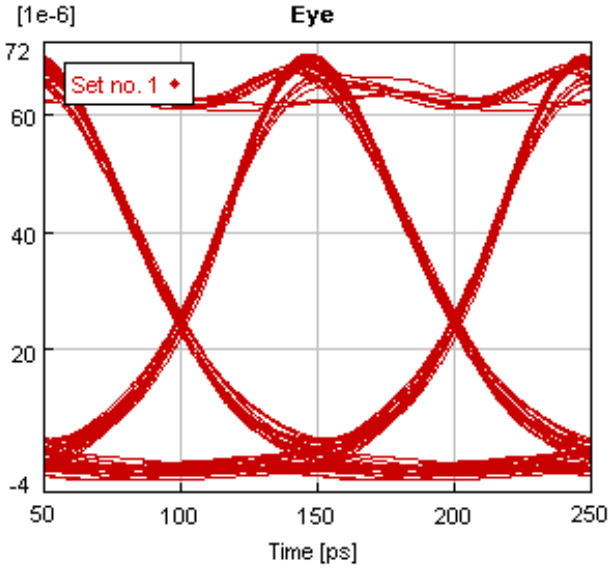

Figure 5.17: Eye diagram for ZVC code with direct recovery scheme at 10Gbit/s for 30 km.

The direct recovery scheme for a 2.5Gbit/s and 10Gbit/s have a clear eye opening as can be observed in Figures 5.14-5.17, and it can detect the intended signal with high precision even for long distance (30km) because the cross correlation is always zero. The figures also prove that even at high data rates, direct recovery scheme can recover

desired signals with minor distortion due to unavoidable effects of the fibers nonlinearities at high data rates.

Figure 5.18 shows the relationship between the number of users and the SNR, for ZVC, MQC, MDW, and Hadamard codes, where they have been plotted for different values of N (number of users) when P_{sr} = -10dBm at a data rate of 622Mb/s. This figure clearly depicts that ZVC code results in much better performance, i.e. (Higher SNR) than MQC, MDW and Hadamard codes. This is evident from the fact that by minimizing the cross correlation, the power of interference from other users is reduced, while the Hadamard code has an increasing value of cross correlation as the number of users increases. Note also that the calculated SNR for ZVC code was achieved for W=4 while for MQC, MDW and Hadamard codes, the calculated SNR were for W=12, W=6 and W=64, respectively. As can been seen in Figure 5.18, the eye diagram for ZVC code is wide open, suggesting that the minimum cross correlation values operates at a very high SNR compared to that of MQC code. The calculated BER for this figure is 10^{-12}.

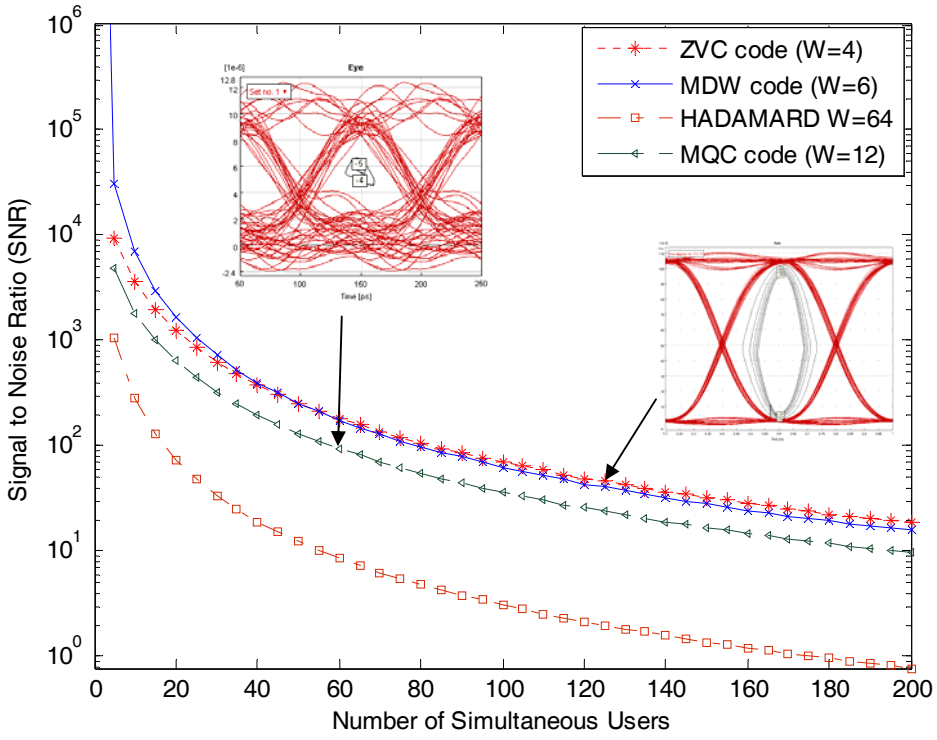

Figure 5.18: SNRs versus number of active users when P_{sr} = -10dBm at data rate 622Mb/s.

5.3.4 Performance analysis of VC code system

As mentioned in Chapter 4, the complementary and AND subtraction techniques can successfully recover desired signal only for codes having fixed cross correlation, besides AND filters out the half signal. In our proposed XOR detection technique, balanced detection can be achieved even if the cross correlation is not fixed, while a strong signal can still be maintained. In this section, a comparison between these three detection techniques will be addressed.

5.3.4.1 Eye Diagram

The Eye diagrams for Complementary detection technique, AND detection technique and XOR detection scheme for weight four (W=4) for both 2.5Gbit/s and 10Gbit/s and various distances are investigated. Figure 5.19 shows the eye diagram for the Complementary detection scheme at 2.5Gbit/s for 10km for four users. From the eye diagrams shown in Figures 5.19-5.20, it is found that the received pulses are severely distorted for Complementary and AND detection techniques due to fact that the desired signal cannot be retrieved. This is because the cross correlation between all the users is not fixed.

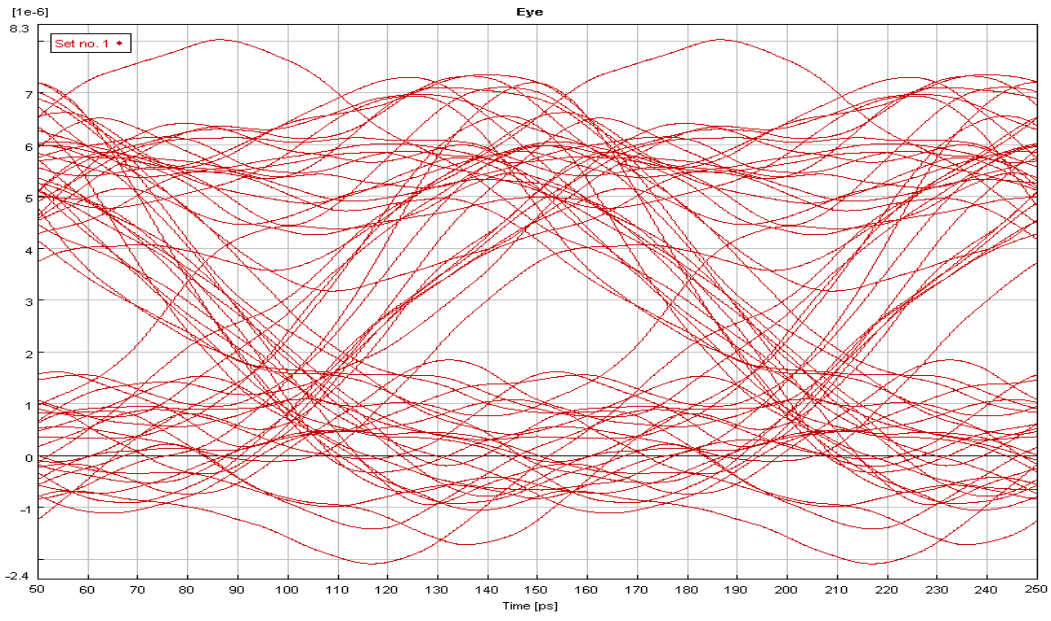

Figure 5.19: Eye diagram for VC code with Complementary SAC at 2.5Gbit/s for 10 km.

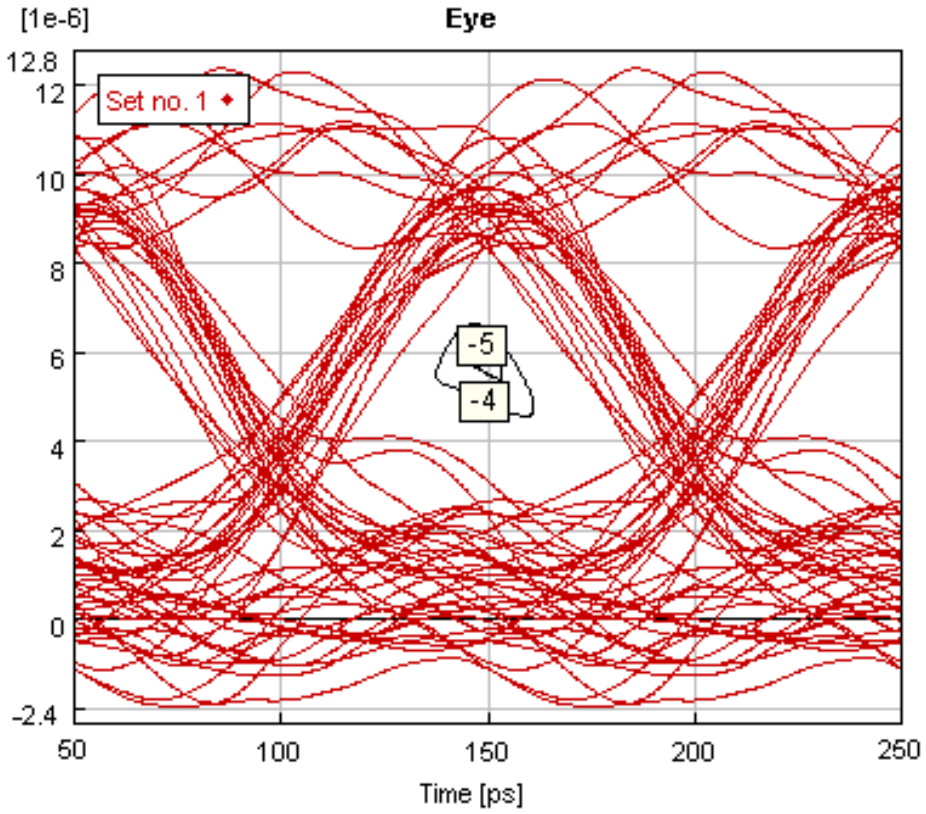

Figure 5.20: Eye diagram for VC code with AND SAC at 2.5Gbit/s for 10 km.

Using the parameters W=4, average power -10dBm, data rate 10Gb/s for 10 km, the eye diagram shown in Figure 5.21 clearly illustrates that the VC code system gives a better performance with XOR scheme, having a large eye opening and able to detect the intended signal with high precision for a practical BER equal to 10^{-29}. This is because the XOR detection scheme supports unfixed cross correlation codes.

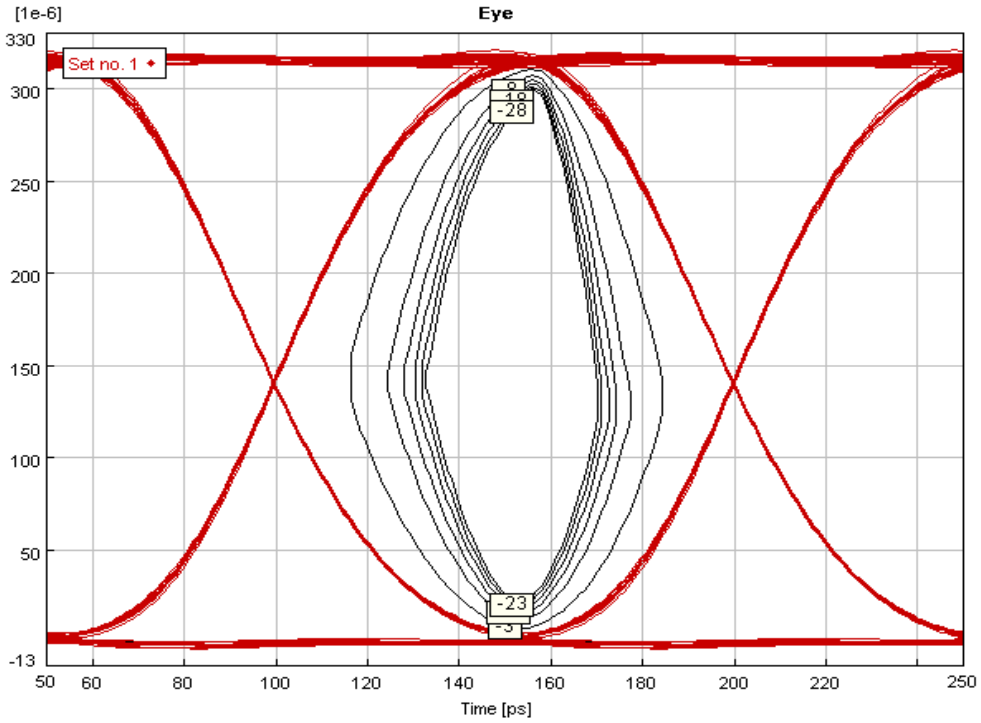

Figure 5.21: Eye diagram for VC code with XOR scheme at 2.5Gbit/s for 10 km.

The eye diagram for Complementary SAC at 10 Gbit/s for 30 km is shown in Figure 5.22. Figures 5.22-5.23 illustrate the same results for Complementary and AND detection techniques at higher data rate for 30km, where the eye opening cannot be seen and intended signal cannot be recovered. The deterioration is caused by the higher optical attenuation in the longer fiber span. It becomes more difficult to distinguish between ones and zeros in the signal as the eye closes more. The height of the eye opening at the specified sampling time shows the noise margin or immunity to noise.

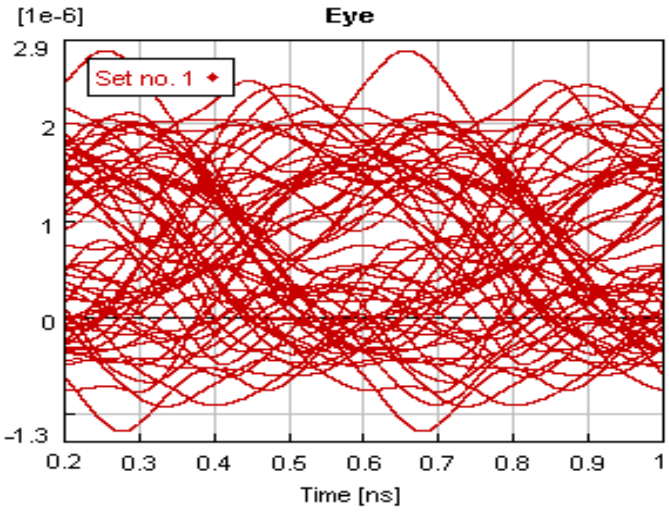

Figure 5.22: Eye diagram for VC code with Complementary SAC at 10Gbit/s after 30km.

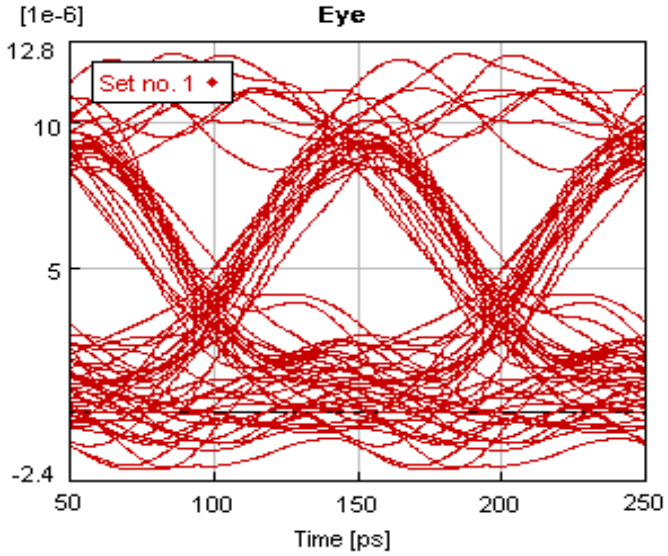

Figure 5.23: Eye diagram for VC code with AND SAC at 10Gbit/s after 30km.

The eye diagram in Figure 5.24 shows that even at high data rate, the XOR detection scheme is able to detect desired signals with minor distortion due to the fiber nonlinearities parameters. The XOR scheme at high data rates shows considerable improvement because the PIIN has been reduced at the second photodetector.

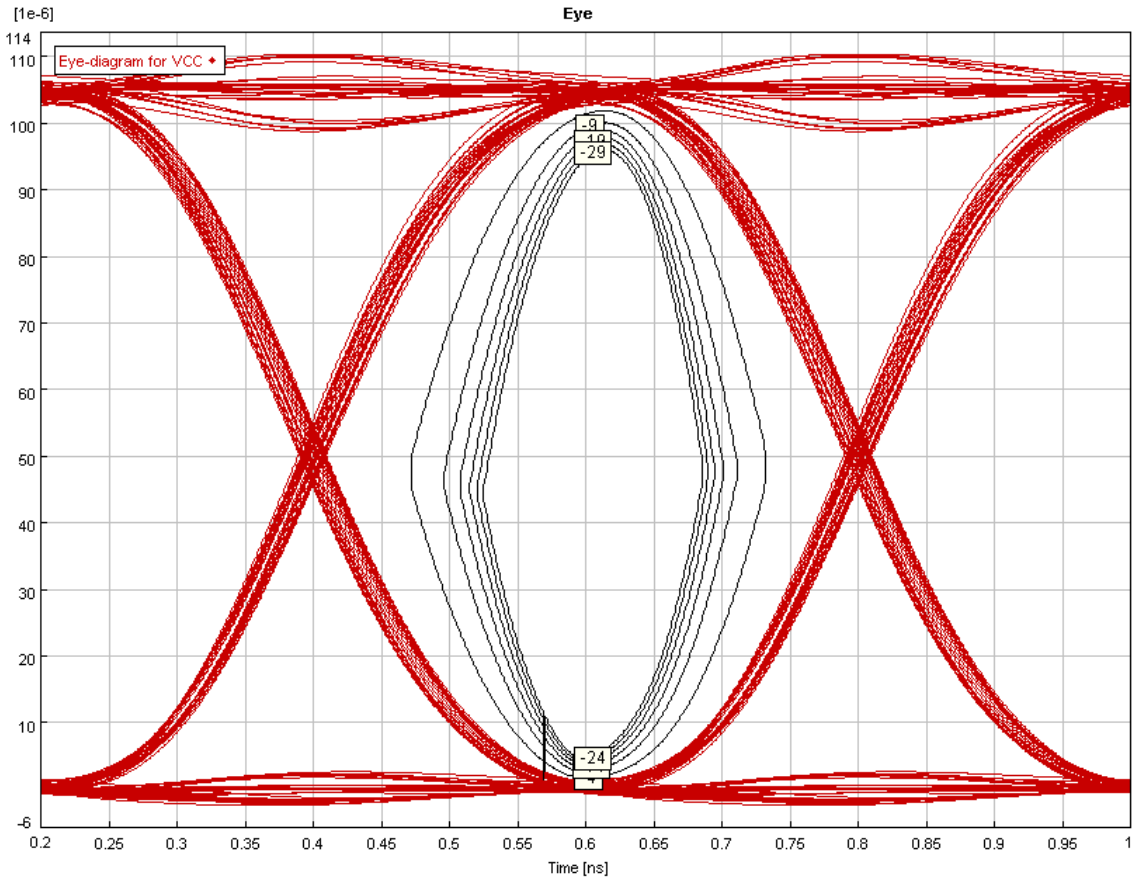

Figure 5.24: Eye diagram for VC code with XOR detection scheme at 10Gbit/s after 30 km.

Propagating data at high bit rates will enhance the disturbing effect of dispersion. With increased fiber distance, it will be the limiting transmission factor, but can be mitigated by the implementation of dispersion compensation techniques. Figures 5.25-5.26 show the BER versus laser power for compensated and uncompensated systems, respectively. For the uncompensated case, the system performance is limited by receiver noise at small values of laser power and by fiber dispersion at large values of laser power.

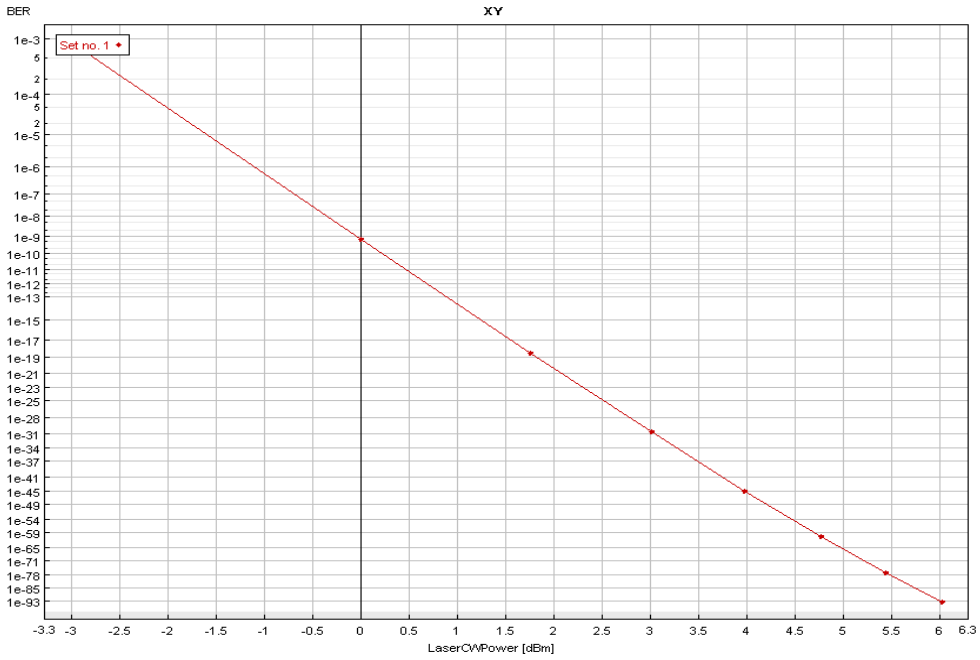

Figure 5.25: BER vs. laser power with dispersion compensation fiber (DCF) using VC code with two channels at 10Gbit/s.

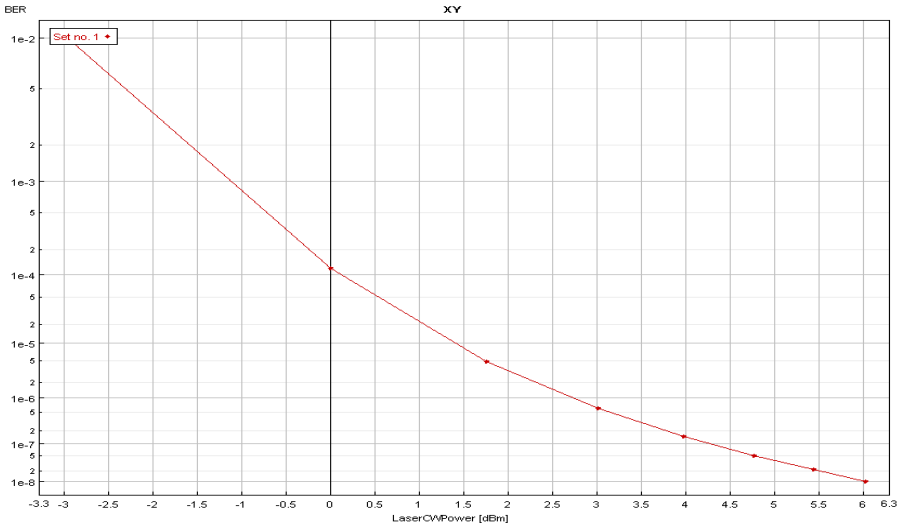

Figure 5.26: BER vs. laser power without dispersion compensation fiber (DCF) using VC code with two channels at 10Gbit/s.

Figure 5.27 shows BER versus laser power for VC code with two channels at 10Gbit/s using XOR detection scheme with dispersion compensation fiber (DCF) and without DCF. In order to transmit data at high bit rates over dispersive fiber, a dispersion compensation technique must be used. In Figure 5.27 the corresponding eye diagram appears to demonstrate the function of DCF.

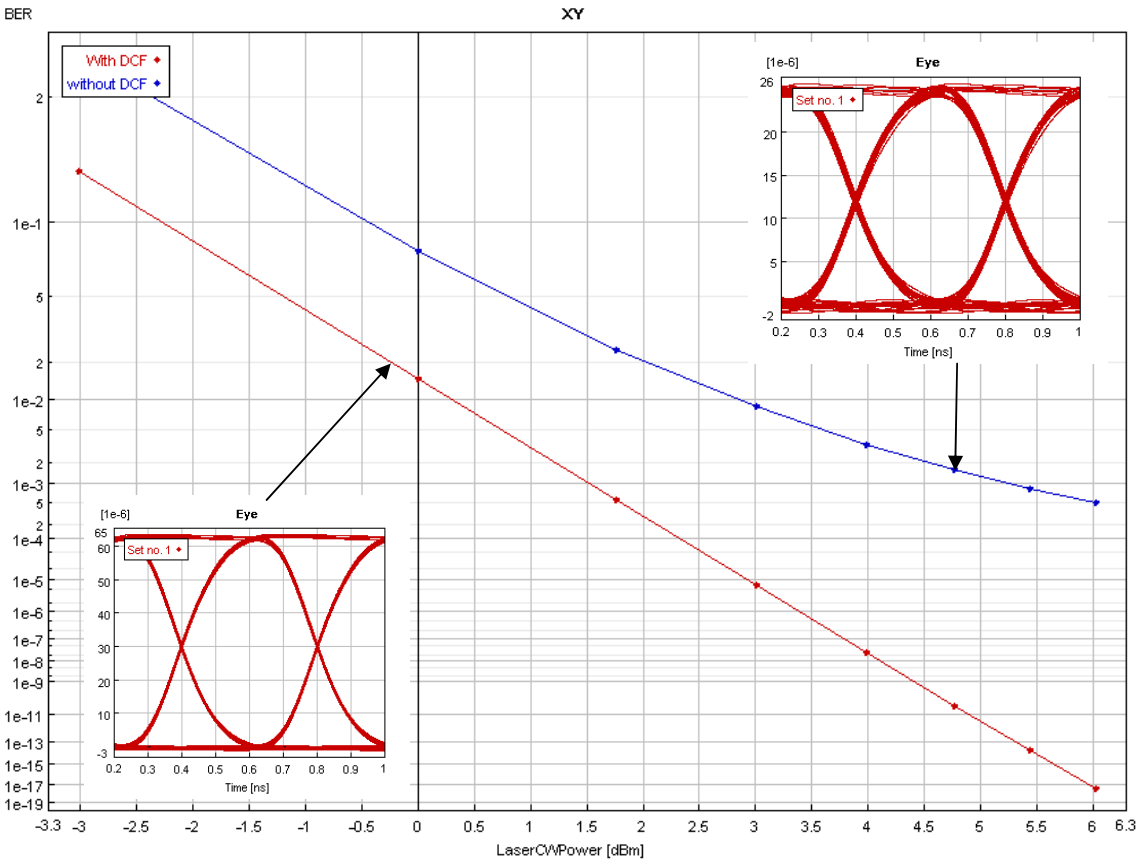

Figure 5.27: BER vs. laser power for two channels of VC code with and without DCF at10Gbit/s.

5.4 OCDMA Transmission Design Issues

The advantages of the proposed codes are numerous, including large flexibility in choosing the number of users, good property of cross correlation control, higher SNR, and easy implementation of the encoder/decoder structure using fiber Bragg gratings (FBGs). These properties make our proposed code an exceptional candidate for the future of optical communication systems. The basic design issues such as types of modulation technique, the format of the transmitted optical signal (non-return-to-zero (NRZ) and return-to-zero (RZ)), and types of optical source will be addressed in this section.

5.4.1 Modulation Technique

The process of imposing information on a light stream is called modulation. This can be realized either by directly varying the laser drive current with the information stream to produce a varying optical output power, or by using an external modulator to modify a steady optical power level emitted by the laser. External modulation is needed for high speed systems (>2.5Gbit/s) to minimize undesirable nonlinear effect such as chirping, which causes dispersion problem. This problem can be solved by using external modulation, which allows the laser to be turned on continuously, where the modulation is accomplished outside of the laser cavity. The purpose of this study is to analyze the behavior of the OCDMA systems using different modulation techniques. A simple schematic block diagram consists of two users using externally modulated technique is shown in Figure 5.28, while that uses directly modulated technique is illustrated in Figure 5.29. The tests were carried out for both the systems at the rate of 2.5Gbit/s and 10Gbit/s for varying fiber distance. The performances of the system were characterized by referring to the bit error rate (BER).

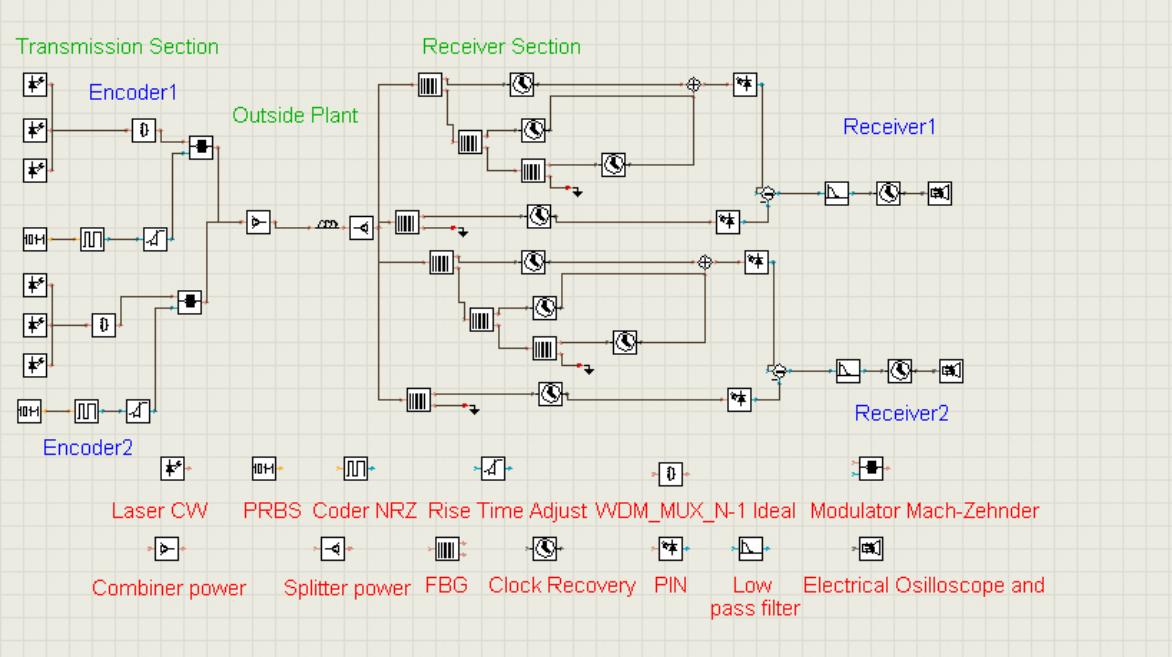

Figure 5.28: OCDMA System Using Externally Modulated Technique.

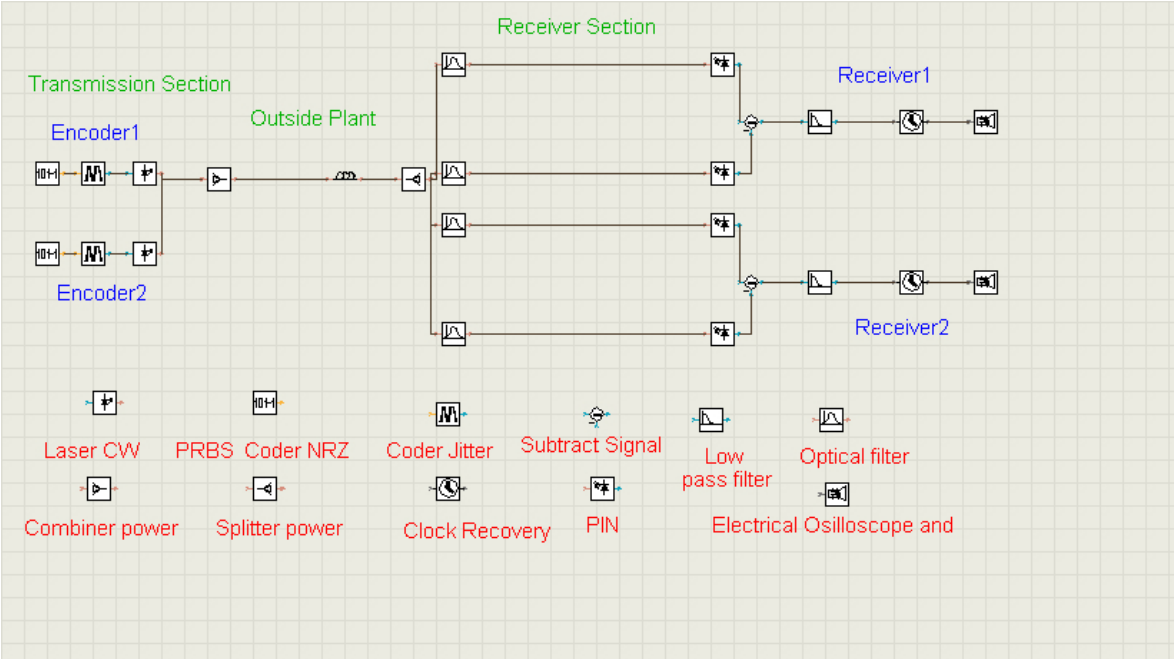

Figure 5.29: OCDMA System Using Directly Modulated Technique.

5.4.1.1 Effect of Distance on System Performance for Different Modulation Techniques

The study of system performance against transmission distance was carried out for the direct and external modulation techniques. Figure 5.30 shows BER versus distance for and corresponding eye diagrams. As shown in Figure 5.30, BER for the system using externally modulated technique gave a better performance than the system using directly modulated technique at the various bit rates. However, in terms of cost, the systems using externally modulated technique are more expensive because of the high cost of the external modulators. Thus, the system using external modulator is more suitable for high data rate environment and longer distances. For shorter distances, the directly modulated system is more suitable.

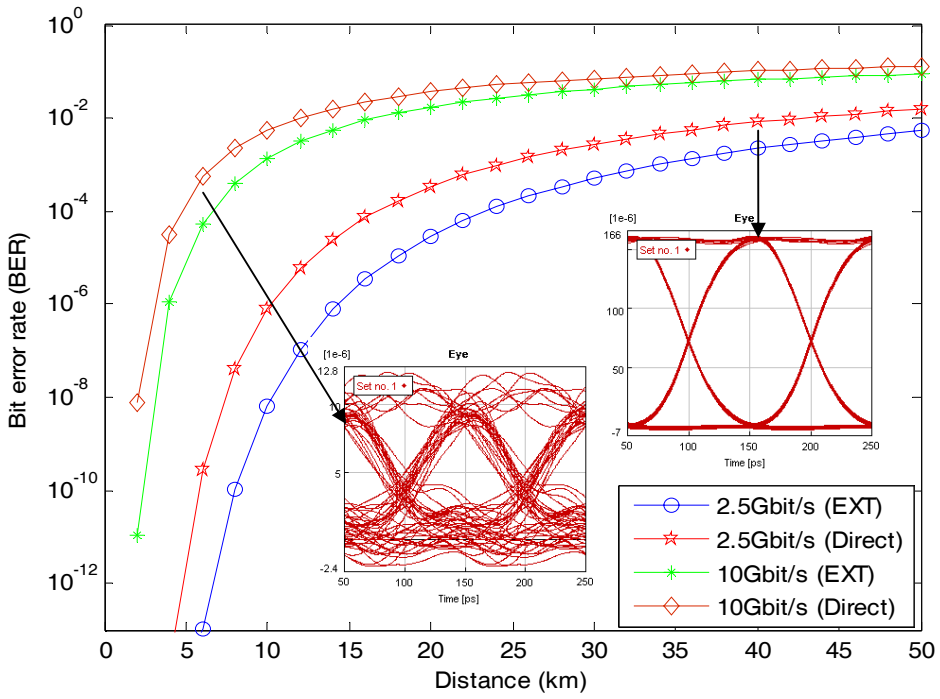

Figure 5.30: BER versus distance for different modulation techniques at various bit rates.

Figure 5.31(a, b) show eye diagrams for a different line code, return-to-zero (RZ) and non-return-to-zero (NRZ). Since an RZ pulse has a wider optical bandwidth than an NRZ pulse, it is more affected by dispersion, as can be seen from the eye diagrams in Figure 5.31. For comparison purposes, the performance of both line codes (NRZ, RZ) was varied depending on the type of application. Many factors have to be considered when making comparison such as bit rate, span link, channel spacing and polarization mode dispersion (PMD). For instance, higher bit rate systems are limited by dispersion. The RZ format would be beneficial for systems with few channels but would require NRZ as the number of channels increase.

5.4.1.2 Effect of line code (NRZ and RZ) on System Performance

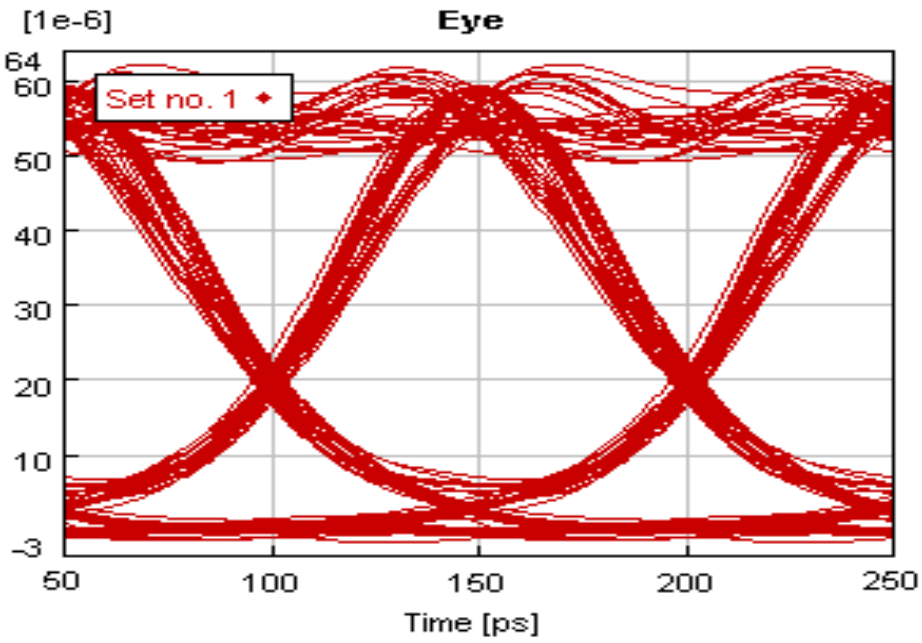

(a)

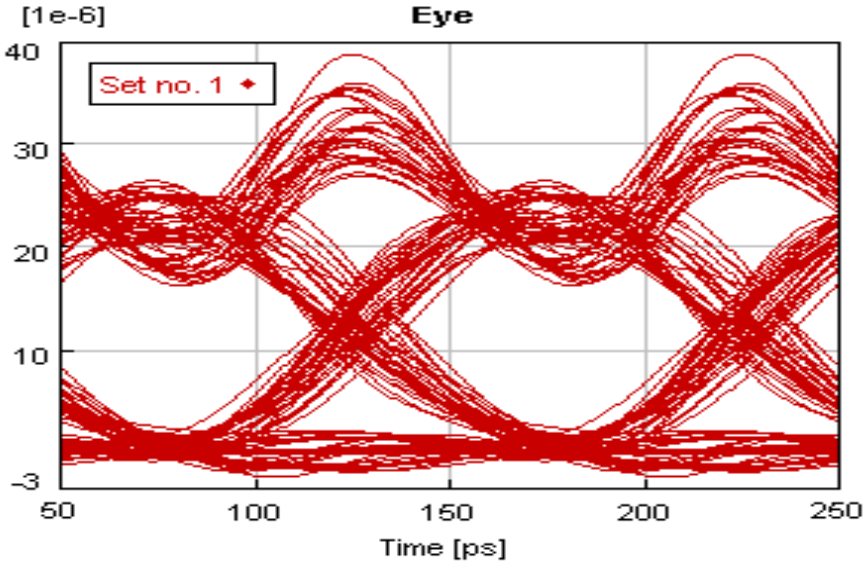

(b)

Figure 5.31: Eye diagram for VC code at 10Gbit/s for 50 km (a) NRZ format (b) RZ format.

5.4.1.3 Effect of APD and PIN on System Performance

Figures 5.32 (a, b) show the simulation results for VC code using avalanche photodiodes (APD) and PIN photodiodes. From the figure, it can be observed that an ADP outperforms PIN; this is because APD internally multiply the primary signal photocurrent before it enters the input circuitry. As shown in Figure 5.32, the advantage of APD receiver is that it can provide a higher signal-to-noise ratio (SNR) for the same incident optical power; this improvement is due to the internal gain that exhibits internal amplification of photocurrent through avalanche multiplication of carriers in junction region.

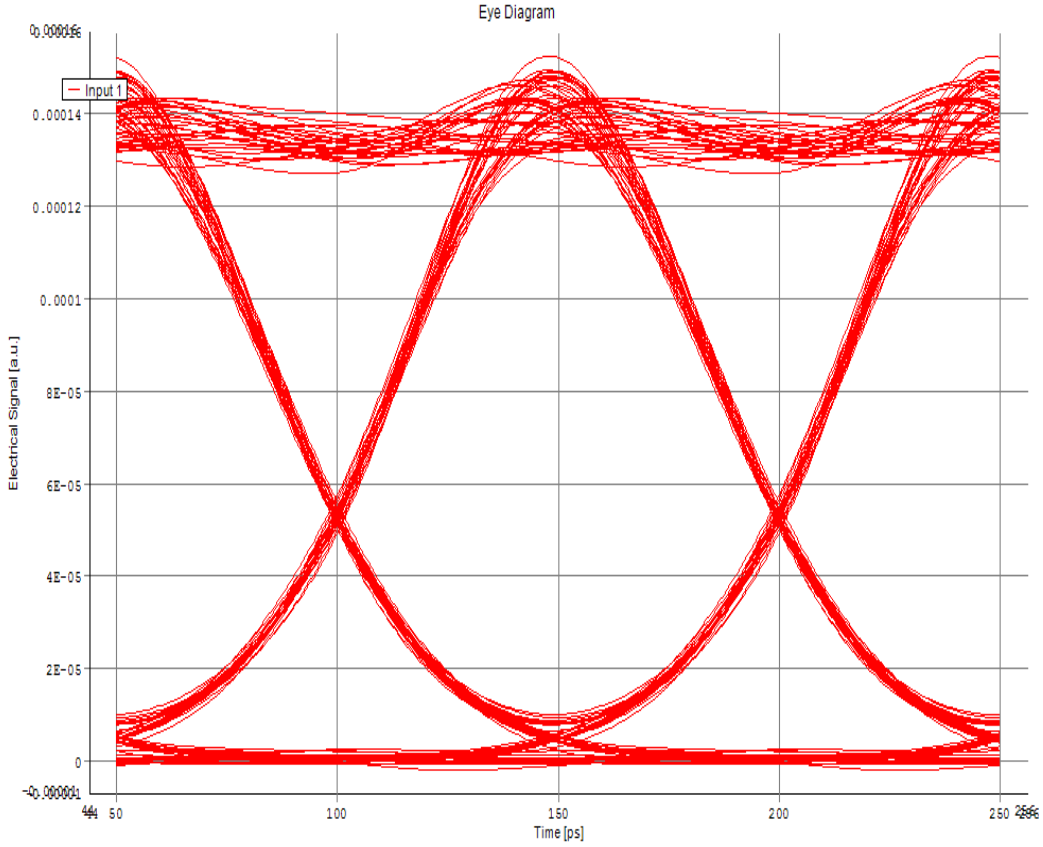

(a)

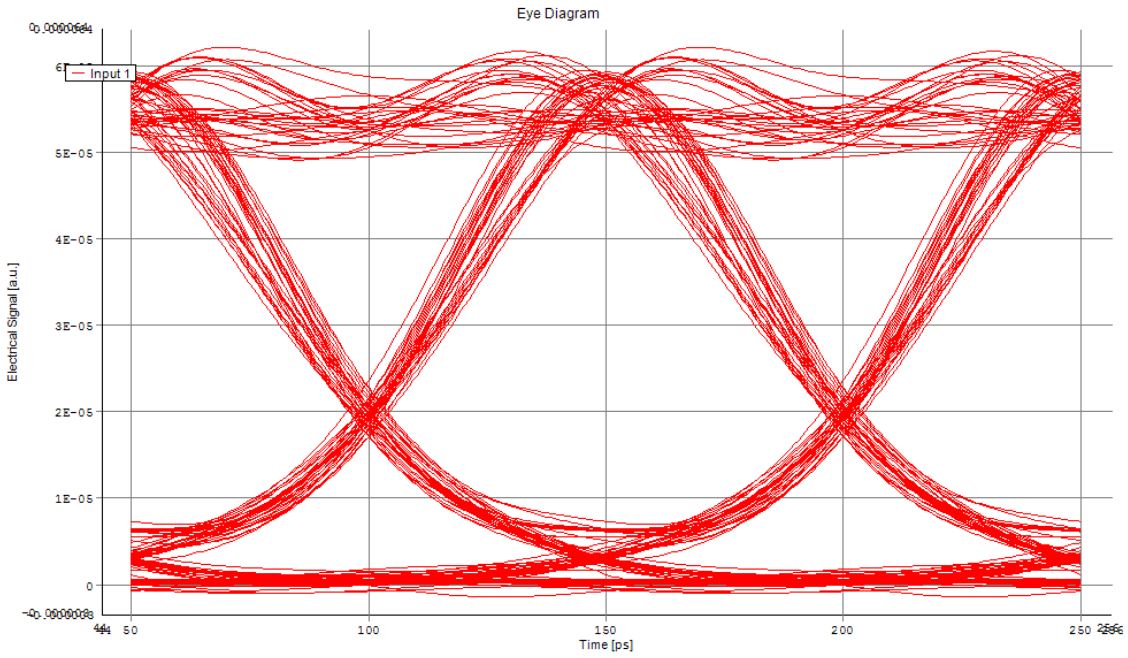

(b)

Figure 5.32: Eye diagram for VC code at 30 km using (a) APD photodiode and (b) PIN photodiodes.

5.5 Conclusion

The performance of ZVC and VC codes has been analyzed in this chapter. The obtained results were based on theoretical calculation and simulation work. A detailed discussion and analysis of the effect of various noises such as PIIN, shot noise, and thermal noise to the OCDMA system using MDW, MQC, MFH, Hadamard, ZVC and VC codes are included. The VC code families have been found to show better performance compared to reported OCDMA codes. Different detection techniques have been used throughout this chapter aimed at lowering the effect of MAI while accommodating large number of users. The analyses have shown that the VC code families have excellent code properties that can reduce the PIIN noise and shot noise effects. In other words, this study has shown that, the VC with XOR is able to improve the performance of OCDMA system for any number of users and weight which could not be done before.

The performance of the VC code families based on various transmission design issues have also been discussed in this chapter. The basic design issues have also been considered, such as types of modulation, types of optical receiver, and line code whether the NRZ or RZ have also been addressed carefully. The simulation results show that the complementary method cannot retrieve desired signals for unfixed cross correlation. The results also reveal that the proposed XOR detection gives a better performance than the AND and Complementary detections, for long transmission spans.

The next chapter will discuss the use of the OCDMA system using VC codes families in the local area application.

CHAPTER 6
APPLICATION OF VC CODE IN LOCAL AREAL NETWORK (LAN)

6.1 Introduction

The purpose of this chapter is to present the implementation of the newly proposed codes in local area network environment. The results obtained from the simulation works and experiments will be presented. In the simulation analysis, the study will be focused on the point-to-point network using VC code. The results are taken from the studies on the effect of distance, bit rate, input power, Q-factor and chip spacing. The key element of studying and investigating the light sources is to provide an adequate power for optical CDMA applications; therefore, an experiment to study and characterize the input and output powers of the LEDs as optical sources for OCDMA systems for the proposed code was conducted. In the simulation section, the results will be focused on the LAN network using the VC code. An experimental test bed for VC code is also proposed.

6.2 Optical Code Division Multiplexing (OCDM) for Local Area Network

This section reviews the architecture and deployment environment for optical CDMA in star LAN environment. Within the context of LAN applications, optical CDMA is treated as a multiple access network where the bandwidth of the optical medium is physically shared among many users with network addresses assigned to unique codes in the optical CDMA code space.

It is important to have reliable and flexible networks of the future applications. Optical CDMA provides a more flexible and robust bandwidth sharing technique for adaptable network interfaces. For comparison purpose between TDMA, WDMA and

OCDMA, the cost and complexity of each optical CDMA node can be designed for the data rate and service desired at a given node in contrast to optical LANs using OTDMA and WDMA. Additionally when users do not require the maximum data rate or the highest QoS, these codes can be assigned to other users to free available bandwidth for high priority applications. Optical Code Division Multiple Access (OCDMA) [8-11] offers an attractive alternative for local area networks where the traffic tends to be bursty. OCDMA offers several advantages in local area networks. First of all, OCDMA allows simultaneous users to send their data asynchronously and with no waiting time through the assignment of unique signature sequence. It also offers strong security in the physical layer. As a result, OCDMA receives substantial attention for the use in LAN. This chapter presents the transmission of carriers encoded with the newly proposed code structure, VC code.

6.3 SIMULATION MODEL FOR THE POINT-TO-POINT NETWORKS

The setup model for the point-to-point is shown in Figure 6.1. The transmitter section consists of five components: a pseudo random bit sequence (PRBS) generator, a non-return-zero (NRZ) pulse generator, a CW laser, rise time adjust and an external modulator.

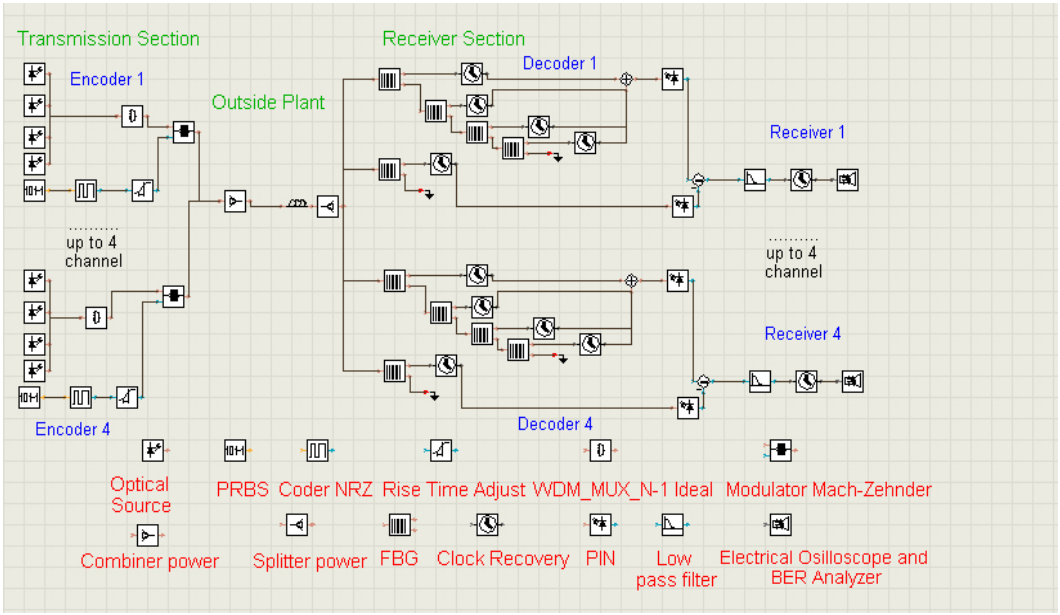

Figure 6.1: Point-to-Point System Simulation Layout.

The CW laser launched an optical power at 0 dBm with a linewidth of 10 MHz; the function of the encoder is to amplitude spectrally and encodes the source according to the specific code used. One unique encoded spectrum represents one channel. The external modulators are the Mach-Zehnder modulators, which are intensity modulators based on an interferometeric principle. The signals that are in the form of a transmitter are combined by the multiplexer and launched into a single fiber.

The outside plant section includes the fiber cables used for transmission. The fiber used in this system was of the Non Dispersion Fiber (NDF) standard. The fiber span was varied and all the fiber parameters such as attenuation, group delay, group velocity dispersion, dispersion slope and effective index of refraction, were wavelength dependent. The nonlinear effects such as four-wave mixing (FWM), cross-phase modulation (XPM) and Self Phase Modulation (SPM) were also activated. At 1550nm wavelength, the attenuation coefficient was 0.25 dB/km, the chromatic dispersion coefficient was 18ps/nm-km and the polarization mode dispersion coefficient was 0.07ps/√km.

At the receiver side, the incoming signal was split into two, one to the decoder that has an identical filter structure with the encoder, and the other to the decoder that has the XOR filter structure. The noise generated at the receivers was set to be random and totally uncorrelated. The dark current value was set at 5nA and the thermal noise coefficient was 2.5×10^{-14} A/Hz^ (1/2) for each of the photo detectors. An electrical subtractor was used to subtract the overlapping data from the wanted one. The performance of the system was characterized by referring to the bit error rate, the noise power and the output power.

6.4 Simulation Results for the Point-To-Point Network

The results obtained from the simulation for a point-to-point network are specified in this section. The results are taken from the studies on the effect of a set of design parameters. The distance, the bit rate, the input power and the channel spacing between the two carriers were the primary design parameters under study. The results display the performance of the VC code in the local access network by implementing the OCDMA multiple access schemes.

6.4.1 Effect of Distance in Point-to-Point Network

In general, a longer fiber will provide great dispersion and attenuation, thus increasing the bit error rate. For OCDM system using VC code, as a result of the subtraction process, the systems will considerably compensate the dispersion effect and therefore the performances are limited by the fiber losses.

Figure 6.2 shows the bit error rate (BER) versus the transmission distance for two rates. It clearly shows that the BER increases exponentially with the transmission distance. A longer fiber provides a larger dispersion and attenuation, and thus, increasing the error rate. The OCDMA system using the VC code could perform sufficiently. For example, using the VC code at data rate of 2.5 Gbit/s and 10 G/bit/s with fiber length 80 km and 59 km respectively, a BER of 10^{-9} was obtained without amplification. The results in Figure 6.2 reveal that the OCDMA system using the VC code is suitable for multiple access and multiplexing environments.

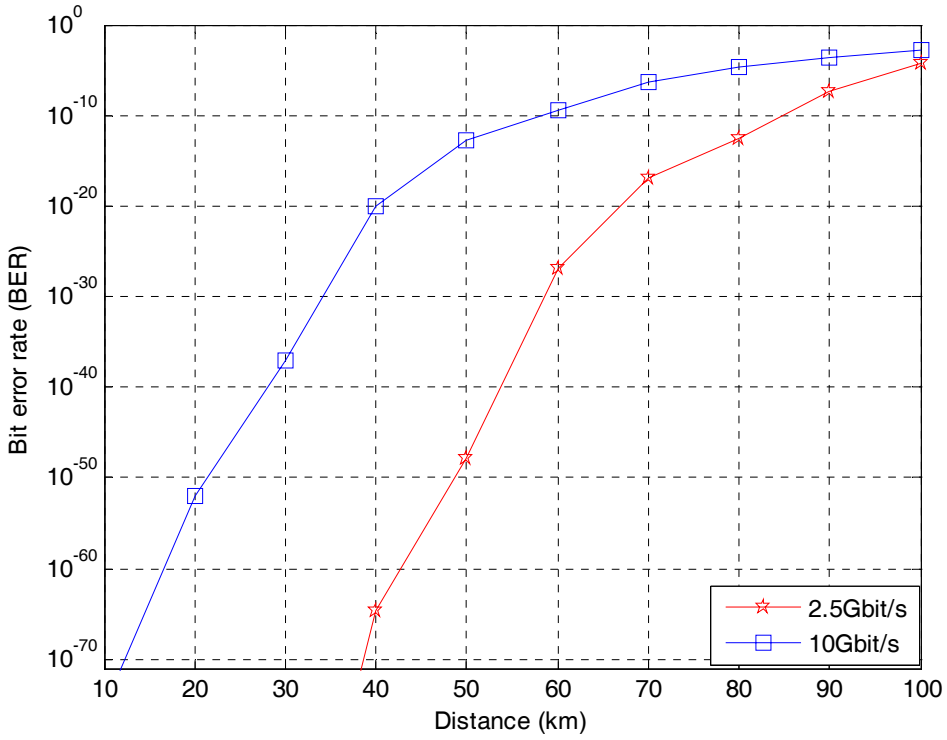

Figure 6.2: BER versus distance for two bit rates when P_{sr} = -10dBm.

6.4.2 The Effect of dispersion compensation in Point-to-Point Network

Figure 6.3 shows BER plotted against distance for compensated and uncompensated systems, dispersion compensate fiber (DCF) and single mode fiber (SMF). The advantage of dispersion compensation is to improve the system performance by providing a power in a sufficient manner; the compensated system includes an optical amplifier and a noise limiting optical filter. From the Figure, an obvious better BER can be recognized for compensated case compared to uncompensated case. The improvement can be attributed to a higher SNR for shorter distances.

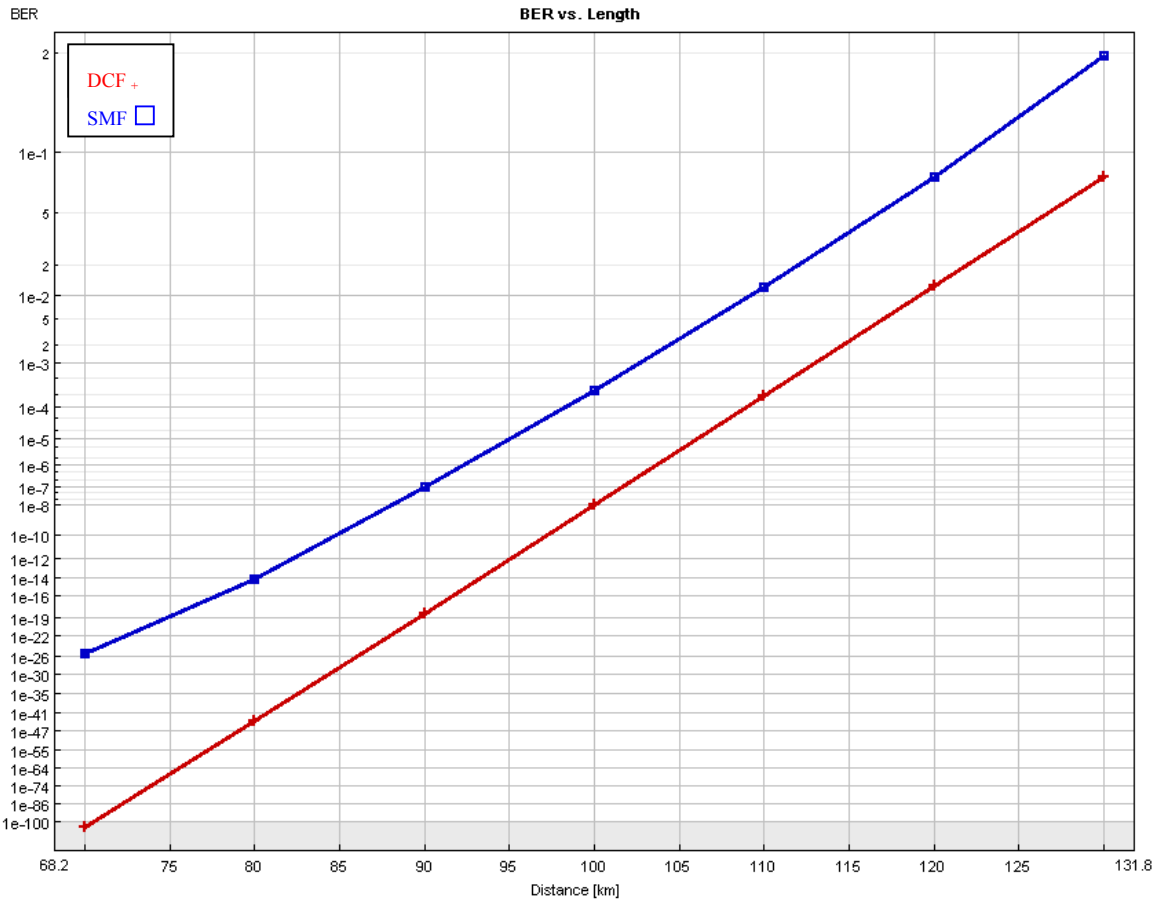

Figure 6.3: BER vs. distance for compensated and uncompensated system.

6.4.3 Effect of Input Power in Point-to-Point Network

Figure 6.4 shows that the BER is reduced exponentially when the input power increased, and by increasing the input power from -10 dBm to -6 dBm, there was a small improvement in system performance, while increasing the input power from -3 dBm to 2 dBm a considerable improvement in system performance can be observed. This shows that the performance of the OCDMA system using the VC code can be enhanced by increasing the input power.

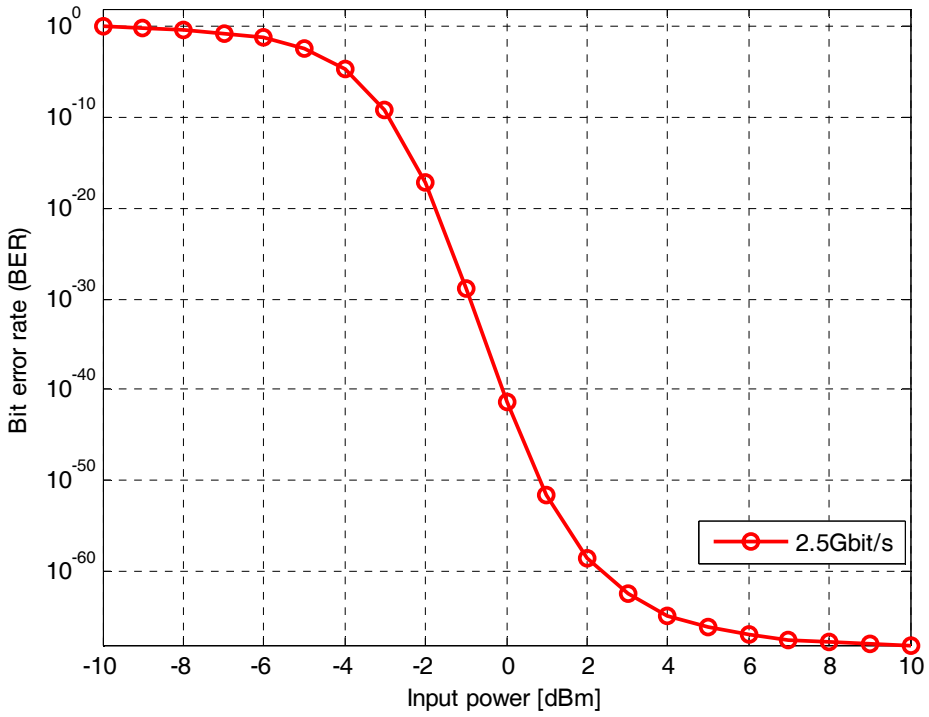

Figure 6.4: BER versus input power for OCDM system at bit rate 2.5 Gbit/s.

Figure 6.5 shows the plot of BER against laser power for a 15km. It is important to calculate the optical input power that is necessary to ensure a certain BER for a given link length which is 15km in this case. The determination of the launch power was done by creating a sweep with optical input powers ranging from 0.5 mW to 4 mW. When the simulation is running, the system performance is calculated for all parameter settings according to the sweep definition.

6.4.3.1 Determination of launch power in Point-to-Point Network

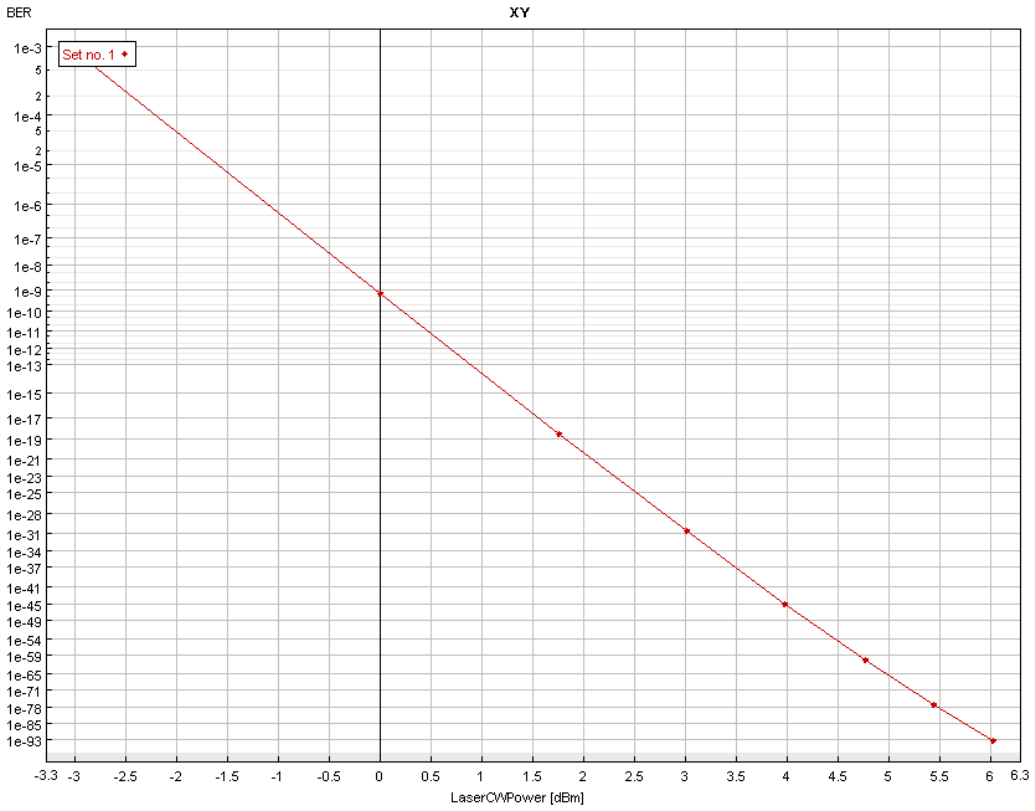

Figure 6.5: BER versus input power for OCDM system at bit rate 2.5 Gbit/s after 15km**.**

6.4.4 Effect of Chip Spacing in Point-to-Point Network

Chip spacing is an important design parameter in this study. Multiwavelength transmission using fiber is subjected to many effects. The nonlinear interactions, mixing, and wavelength dependent parameters in the fiber are the limiting factors in the system. Four-wave mixing, cross phase modulation, and group delay are the main nonlinear parameters considered in this study. In this thesis, the study on the effect of chip spacing on system performance was done by varying the spacing from 0.1 nm to 2 nm. Generally, with closer channel spacing, nonlinear effects such as four wave mixing (FWM) and cross phase modulation (XPM) become more critical.

6.4.4.1 Effect of Chip Spacing on System Performance at Bit Rate 10 Gbit/s

The effect of chip spacing is shown in Figure 6.6. As shown by the simulation results, the system gave the best performance (i.e lower BER) at the chip spacing of 0.6 nm to 1 nm. The reason for this is because when the spacing is less than 0.6 nm, the system became subjected to Four-Wave Mixing effect and hence the system performance is reduced. At larger spacing, the performance deteriorates again due to the effect of differential group delay between the spectral components of the chips. Each spectral component can be assumed to travel independently, it suffers from time delay or group delay as the signal propagates along the fiber. This caused more significant inter-symbol interference between adjacent data bits, which resulted in higher BER.

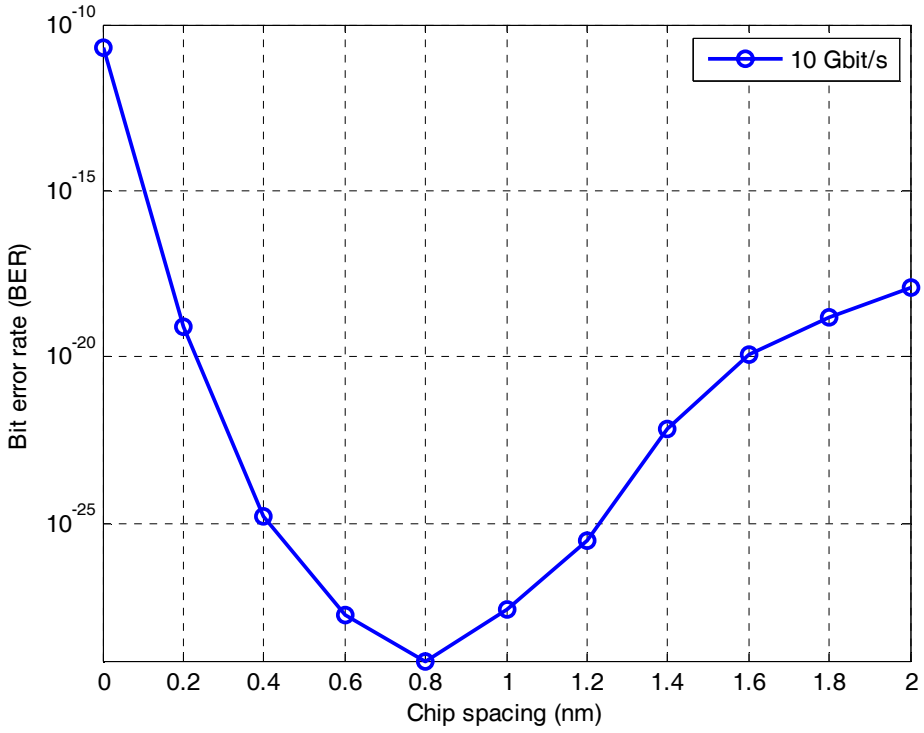

Figure 6.6: BER versus chip spacing at Bit Rate of 10 Gbit/s.

6.4.4.2 Effect of Chip Spacing on System Performance at different distances

The computed BER versus channel spacing width is shown in Figure 6.7 for different fiber lengths. The pulse duration was fixed to *Tc* = 1/(data rate × code length). Referring to Figure 6.7, it is observed that as the channel spacing width goes from very narrow to wider, the BER is minimum at 0.8 nm and begins to increase continuously beyond 0.8 nm. The optimum performance occurs at a spacing bandwidth between 0.8 (100 GHz) and 1 nm. This is because the system can work well for a practical BER (10^{-26}, 10^{-28}) up to 50km, and 40km, respectively. The reason for increasing BER after the minimum is due to the presence of MAI. Even though the SNR was improved as the result of using wider optical bandwidth, at the same time it was being counteracted by increasing crosstalk/overlapping between adjacent frequencies bins that yielded MAI.

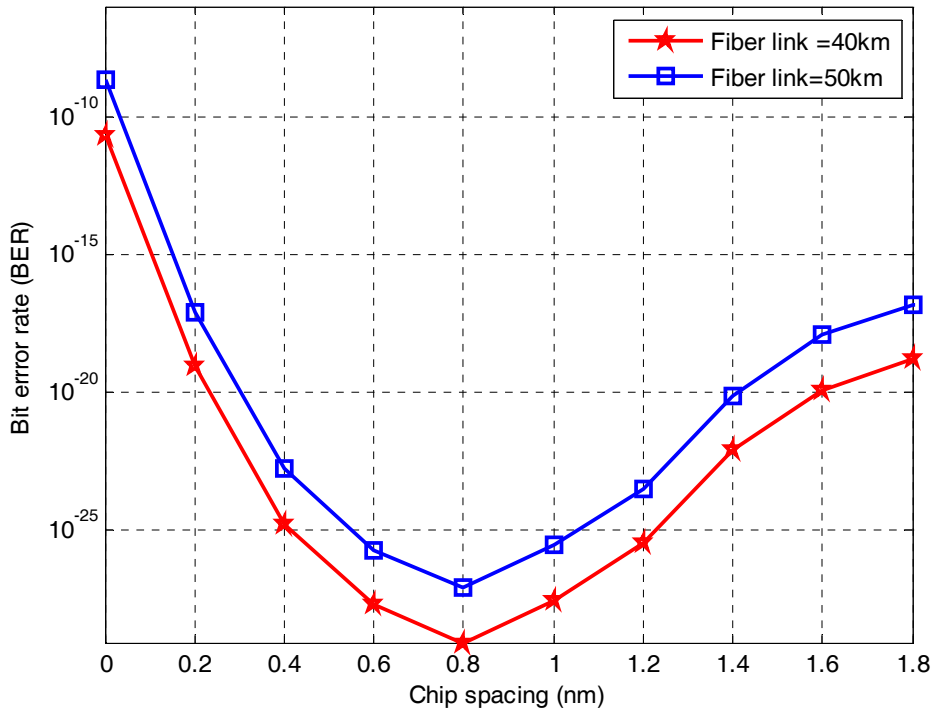

Figure 6.7: Variation of BER as a function of channel spacing width for VC code at different spans.

Note that the effect of four-wave mixing on optical transmission and in single fiber mode begin to appear as the channel spacing was decreased. This was noticeable in the degradation of optical SNR and the system BER performance.

6.4.5 Effect of Bit Rate in Point-to-Point Network

The data rate has a negative impact on system performance in terms of BER as shown in Figure 6.8. In the Figure, the error rate increases with bit rate. This is because increasing the bit rate will decrease the pulse width, thus making each bit more sensitive to dispersion effects.

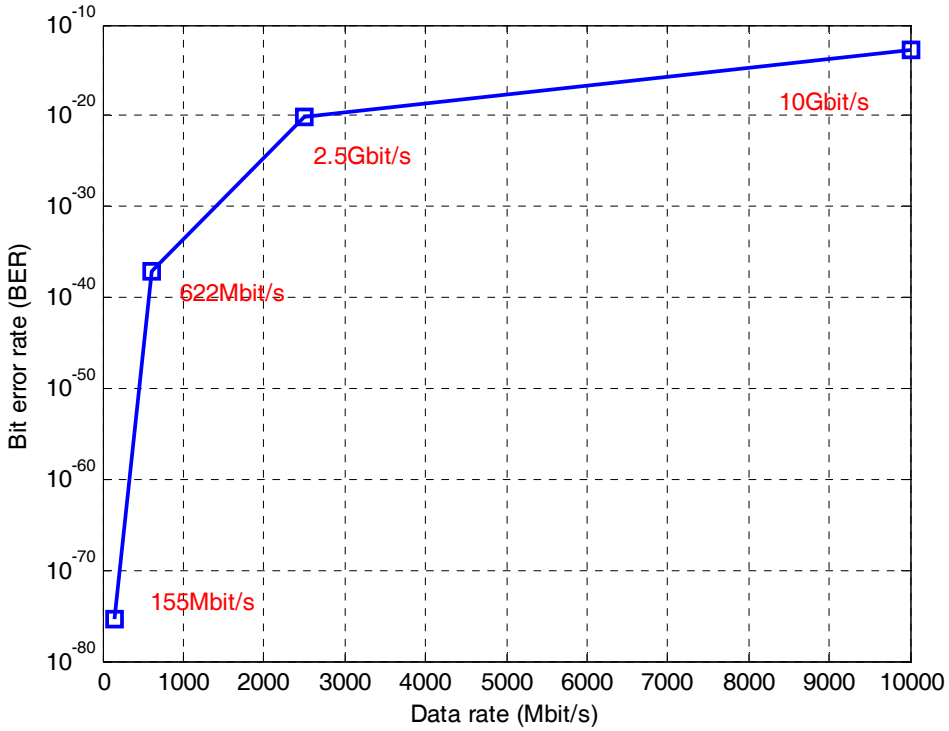

Figure 6.8: BER versus bit rate.

6.4.5.1 Performance analysis of multiple bit rate system in point-to-point network

Figure 6.9 shows a block diagram for point-to-point network to study the performance of the VC code for multi bit rate transmissions. Each chip has a spectral width of 0.8nm (100GHz). The tests were carried out at the rate of 2.5 Gbit/s and 10 Gbit/s for each codes. Channel 1 was running at 10 Gbit/s, while Channels 2 was at 2.5 Gbit/s. The performance of the system was characterized by referring to the bit error rate and the eye patterns.

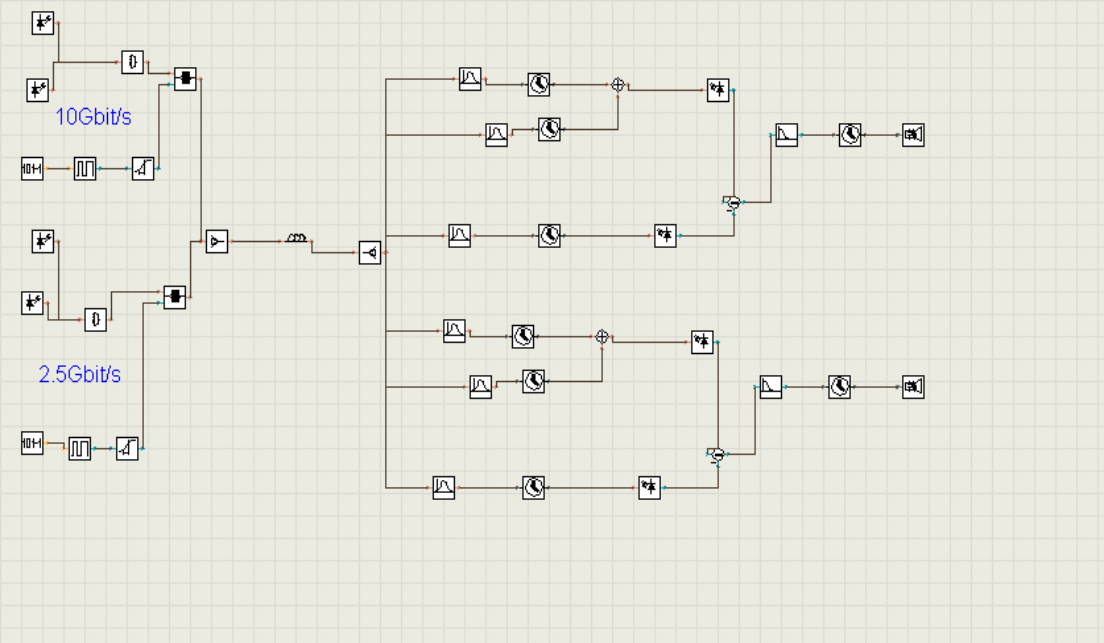

Figure 6.9: The multiple bit rate system in the point-to-point network.

The eye pattern diagrams for Channels 1 (10 Gbit/s) and 2 (2.5 Gbit/s) are shown in Figures 6.10 and 6.11, respectively for the VC code.

The width of the eye opening defines the time interval over which the received signal can be sampled without error from intersymbol interference. When the height of the eye opening is large, this represents the best time to sample the received signal. The eye diagram patterns shown in Figures 6.10 and 6.11 clearly shown that the VC code system gives a considerably performance and can support multiple bit rate system.

The eye pattern at 10 Gb/s shows that even the effects of nonlinearities at high date rates is unavoidable, still desired signal can be detected with minor distortion. Higher bit rate systems are limited by dispersion. As shown in Figure 6.11, for a 2.5Gb/s at 70km , the system still work well with slightly high precision than 10Gb/s.

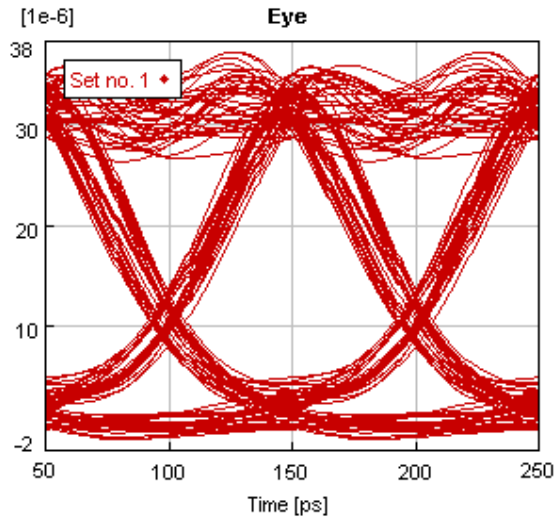

Figure 6.10: The eye diagram of the VC channel 1 at 10 Gbit/s with BER of 10^{-14} after 50km.

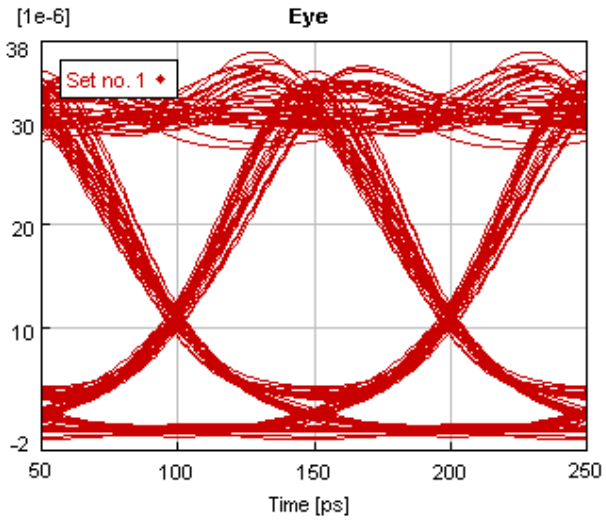

Figure 6.11: The eye diagram of the VC channel 2 at 2.5 Gbit/s with BER of 10^{-18} after 70km.

6.4.5.2 Performance analysis of Q-factor in point-to-point network

The Q-factor performance provides a qualitative description of the optical receiver performance, the performance of an optical receiver depends on the signal-to-noise ratio (SNR). The Q-factor suggests the minimum SNR required to obtain a specific BER for a given signal. The improvement can be attributed to a higher SNR for shorter spans. Figure 6.12 shows the Q-factor plotted against SMF and DCF span length. A considerable performance can be recognized for compensated case compared to uncompensated case for long span. For uncompensated case, the system performance is limited by receiver noise at small values of laser power and by fiber dispersion at large values of laser power.

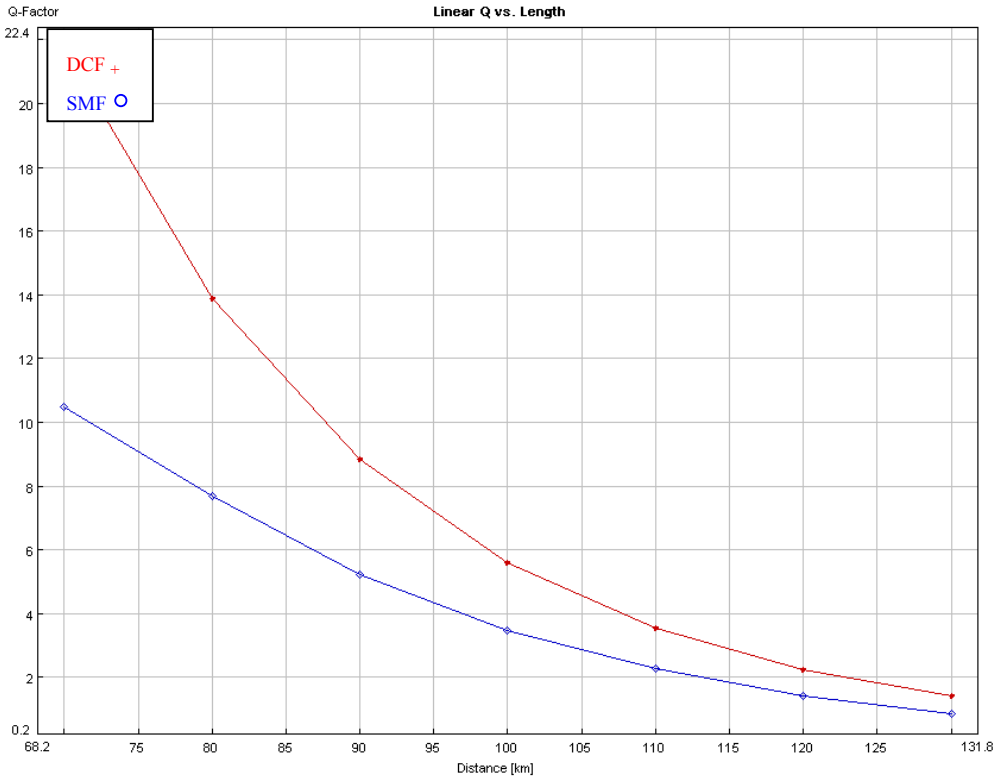

Figure 6.12: Q-factor vs. distance for SMF and DCF .

6.6.2 Proposal of VC code experimental test bed

The experimental setup for two channel OCDM system using VC code is as shown in Figure 6.19. In the transmitter section, each site consisted of six components: two Pseudo Random Bit Sequence (PRBS) generators, two non-return-zero (NRZ) pulse generators, two laser diodes, couplers, splitters and external modulators. The laser diode sources were -10 dBm with a linewidth of 10MHz. The two laser diodes have wavelengths of λ_1= 1548 nm, λ_2 = 1548.8 nm, λ_4= 1550.4 nm and λ_6= 1552 nm, which represented VC code sequences of 110 and 101 as Channel 1 and Channel 2 respectively.

At the receiver side, the incoming signal was split into two parts, one to the decoder with identical filtering structure as the encoder, and the other to the decoder that had the XOR filtering structure by using Fiber Bragg Grating (FBG). A subtractor was used to reduce multiple access interference.

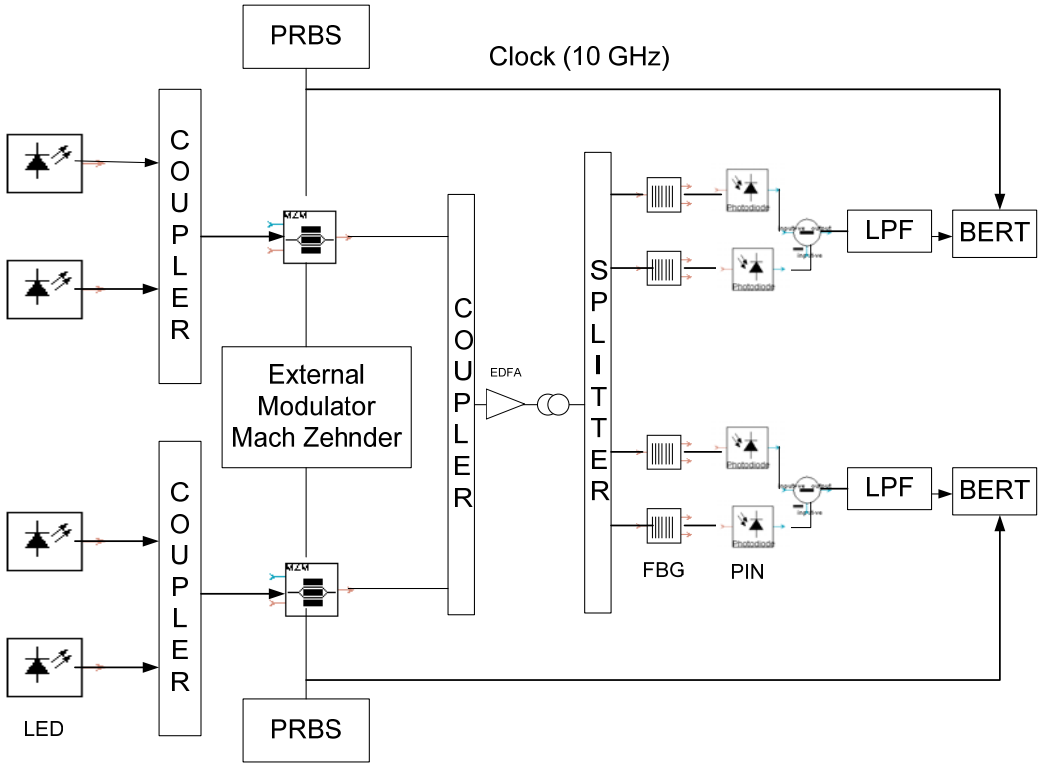

Figure 6.13: Experimental setup for OCDM System Using VC code.

6.4.6 Comparison between theoretical and simulation results

Figure 6.20 shows the BER versus the received power at the bit rate of 2.5 Gbit/s based on simulation and theoretical calculation. The figure reveals that BER decreases with an increasing received power. Figure 6.21 shows the relation between the number of active users and the BER based on simulation and calculated results. It is shown that the calculated performance is better than the simulation result. This is because, in the calculation, the effects of signals impairment were not considered.

Figures 6.20 and 6.21 reveal that the theoretical result outperforms the simulated result. This is because, in the calculation, the effects of attenuation, fiber nonlinearity, and insertion loss were not considered. The calculation was based on Equations (4.57) and (4.58), given earlier in chapter 4. On the other hand, those parameters not considered in the theoretical calculation such as fiber nonlinear effect, insertion loss and attenuation was taken into account in the simulation.

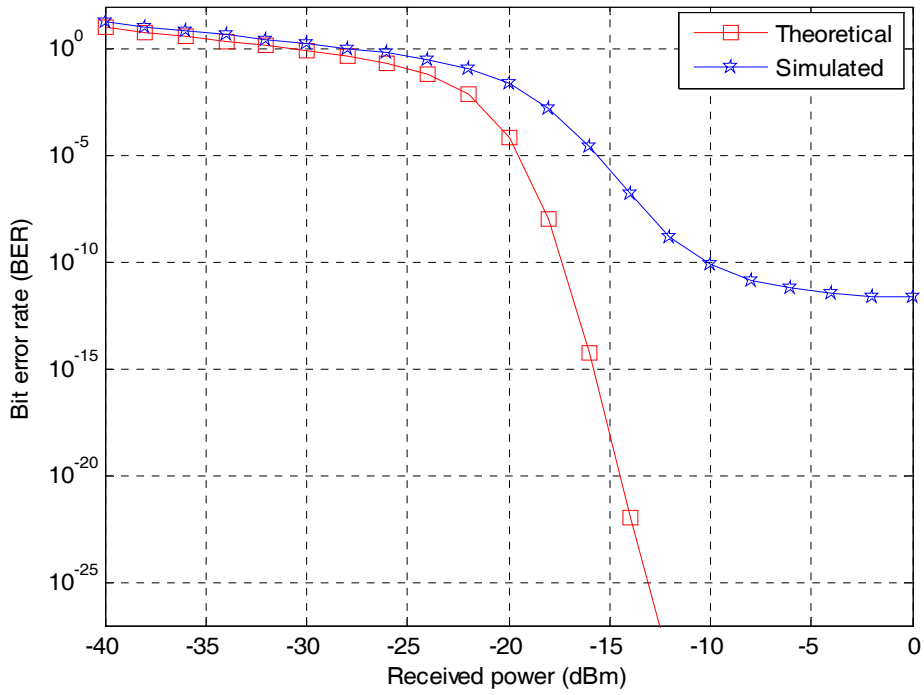

Figure 6.14: BER versus received power at bit rate of 2.5Gbit/s.

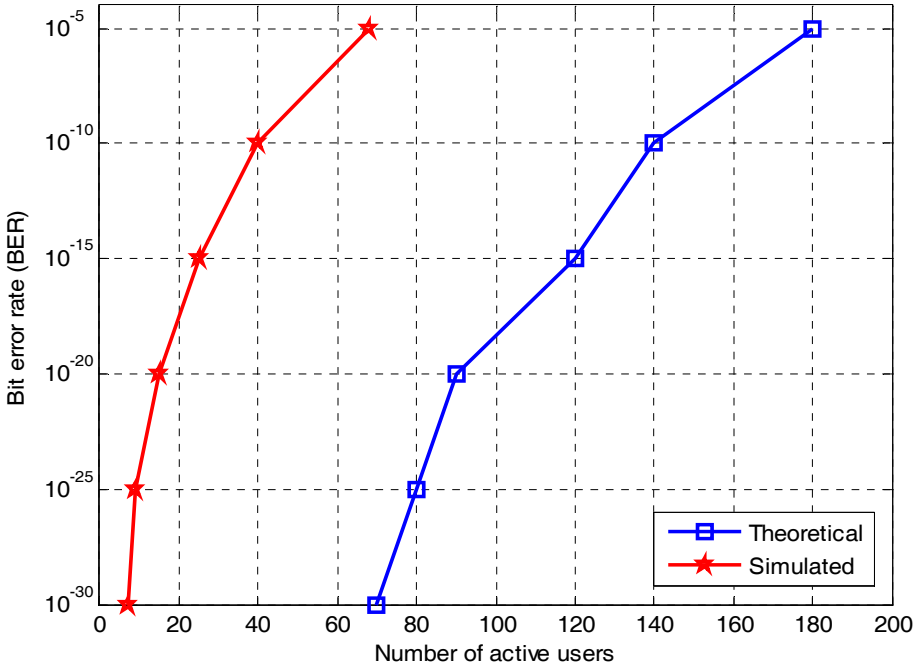

Figure 6.15: BER versus number of active users at bit rate of 2.5Gbit/s.

6.4.7 SUMMARY

In this chapter, the ability of the VC code to support simultaneous transmissions at different bit rates in a local area network environment has been discussed through extensive simulation. The results are focused on the point-to-point network using the vector combinatorial code. The effect of distance, input power, Q-factor, multibit rates, and dispersion fiber compensate system on the performance using VC code has been addressed in this chapter.

The simulation results indicate that VC code has a superior performance compared to other reported codes such as MQC, MFH and MDW.

CHAPTER 7
CONCLUSION AND RECOMMENDATIONS

7.1 Conclusion

The contributions and finding of this thesis, and possible future works are summarized in this chapter. In this thesis, a new variation of optical code structure for amplitude-spectral encoding optical code division multiple access (OCDMA) system, known as Vector Combinatorial (VC) code families have been developed, and proposed to overcome the problems of the existing codes which are complicated, support a few number of users and have high cross correlation. Two algorithms have been developed to construct several code families for OCDMA applications. The first algorithm is based on combinatorial theory, and the second is based on the distribution of ones in the code sequences based on the relationship between number of users and weight. For the first algorithm, the Zero Vector Combinatorial (ZVC) code families always have a zero maximum cross correlation. For the second algorithm the VC code families have the maximum cross correlation of one; a mapping technique is applied to increase the number of users which change the cross correlation of the code sequence to unfixed values. Simplicity of construction, larger code sequences families, existence for every positive integer, good cross correlation properties, higher SNR, and ease of implementation using fiber Bragg gratings (FBGs) are some of the properties that make the proposed VC families interesting candidates for future optical communication systems.

The study has been carried out through theoretical calculations and simulation results. There are two major problems that currently prevent the OCDMA system to become more practical, the beat noise and the speed of the receiver.

The performance of the OCDMA system is degraded as the number of simultaneous users increases, especially when the number of user is large. This is attributed to the multiple access interference (MAI) which arises from the interference of the simultaneous users. For example, the maximum acceptable BER of 10^{-9} was achieved by the VC and MQC codes with 120 and 40 active users, respectively. This is better considering the small value of weight used. This is evident from the fact that VC code has an ideal in-phase cross correlation and good property that would eliminate the MAI effects through CC control by using mapping techniques while Hadamard code has increasing value of cross correlation as the number of users' increases. However, MQC and MFH used codes with a fixed in-phase cross correlation exactly equal to 1 for suppressing the effects of PIIN. Hence, this increases the probability of interfering which leads to performance degradation. The calculated BER for VC was achieved for $W = 8$ while for MFH, MQC and Hadamard codes were for $W = 10$, $W = 12$, and $W = 64$ respectively. With big values of P and R, VC code gives better result even for small value of W.

MAI can be reduced by using subtraction techniques. A new subtraction technique has also been proposed to improve the OCDMA system performances and to reduce receiver complexity. The newly proposed technique, namely XOR subtraction, shows a better performance in comparison to the existing Complementary and AND techniques. It shows that the OCDMA system using XOR technique performs better than the system using existing AND and Complementary techniques. It demonstrates that XOR technique supports more users (50 users at BER of 10^{-12}) compared to Complementary and AND techniques (25 and 18 users at BER of 10^{-12} respectively).

A new transmitter-receiver structure based on fiber Bragg gratings (FBGs) for a Vector Combinatorial (VC) code is proposed. With a proper receiver design, a receiver can reduce the contribution of total noise power to total received power by rejecting overlapping spectra from other users.

The study on the effect of various noise source such as thermal noise, shot noise, and phase induced intensity noise (PIIN) to the OCDMA system using VC, MQC, MFH, and Hadamard codes show that the VC codes outperform the others. For performance analysis based on the theoretical calculation, the VC code surpasses other OCDMA

codes by reducing the total noise level. The VC code is found to have excellent code properties that can reduce the PIIN noise and MAI noise effects, and increase system performance. It is shown that XOR technique gives a much better performance when the effective received power P_{sr} is large (when P_{sr} > -26 dBm). At the lower values of P_{sr} (when P_{sr} < -25 dBm), the performance of the system for the three techniques is almost the same. This is evident that with XOR technique, the MAI in the receiver side is eliminated by reducing the power of interfering from other users.

It is shown that, when P_{sr} is large, both the shot and thermal noises are negligibly small compared to intensity noise, which becomes the main limitation factor of the system performance. However, when P_{sr} is low, the effect of intensity noise becomes minimal, and, thus, the thermal source becomes the main factor that limits the system performance. In order to reduce the effect of BER, extensive analysis and characterization of the data rate, fiber length, and channel spacing have been carried out. In fact, when the fiber length decreases, the data rate should increase to recover a similar degradation of the signal form. In terms of distance and data rates characterization, it is found that VC code can perform well up to 5 and 2 km only at 2.5Gbit/s and 10Gbit/s respectively, as compared to data rate 155Mbit/s which gives excellent performance up to a distance of 50 km, after which it starts to experience some interference but still performing much better than 10Gbit/s. It should be point out that, data rates 155Mb/s and 622Mb/s using for ATM system, 1.25Gb/s and 2.5Gb/s for Gigabit Ethernet while 10Gb/s for long haul system.

It is found that as the channel spacing width goes from very narrow to wide, the BER decreases and best performance occurs at a spacing bandwidth between 0.8 and 1 nm. One of the important properties of the VC code is free cardinality because compared to Hadamard, MQC, and MFH codes; the VC code has better BER than other codes.
Recent studies showed that, an OCDMA system cannot be designed only by considering the properties of the code. The detection technique plays an important role and should be addressed as well. In particular, various optical CDMA detection techniques have also been studied, such as the Complementary balance detection and AND detection techniques based on the VC code to improve the optical code division multiple access (OCDMA) system performance. It has been shown through

simulation that the OCDMA system using XOR technique has better BER at the same bit rate as compared to that of Complementary and AND subtraction techniques.

A software simulation with different SAC OCDMA families has been implemented using the Virtual Photonics Instrument (VPI), VPITransmissionMakerTMWDM, version 7.1. The optical nonlinearities, shot noise, thermal noise, insertion loss and dark current noise have been activated to keep the simulation environment as real as possible. The study was conducted using various design parameters such as bit rate, distance, and chip spacing. The effects of these parameters on the system were elaborated through the BER, Q-factor and eye diagrams patterns. The impact of the detection techniques and data rate effects on the multiple access interference (MAI) is reported using a VPI^{TM}. Simulation results showed that by using a point to point transmission with two encoded channels, VC has better BER performance than other codes. It is also found that for a transmitted power at 0 dBm, BER specified by eye diagrams patterns are 10^{-14} and 10^{-5} for VC and MQC codes respectively.
The results reveal that the proposed XOR detection technique is able to give better performance than the AND and Complementary, thus enabling long span of transmission. It is found that, in order to transmit data at high bit rate over dispersive fiber, a dispersion compensation technique has to be used.

7.2 Recommendations

Several key research areas to improve the VC-OCDMA systems are identified as follows:

- A full experimental test to study the practicability of VC code families in real environment.
- A more detailed study on the hybrid systems since the combinations of spectral amplitude coding with wavelength division multiplexing have a promising future for OCDMA systems.
- Security for optical CDMA system based on Vector Combinatorial (VC) code.
- Implementation issues of higher layers.

REFERENCES

[1] Gerard Keiser, *Optical Fiber communications*. New York: McGraw-Hill, 1991.

[2] Bahaa. E. A. Saleh, M. C, Terich., *Fundamentals of Photonics*. New York: John Wiley and sons, 1991.

[3] Smith. E. Miller, and Ivan.P.Kaminow, *Optical fiber telecommunications II*. los Angeles: Academic press, 1988.

[4] Paul. E. Green, Englewood Cliffs, *Fiber Optic Networks*. New Jersey: Prentice Hall, 1993.

[5] Harry. J. R. Dutton., *Understanding Optical Communication*. New Jersey: Prentice Hall, 1998.

[6] Joseph. C. Palais, *Fiber Optic Communication*. New Jersey: Pearson Prentice Hall, 2004.

[7] Guu-Chang Yang, Wing. C. Kwong, *Prime Codes with Application to CDMA Optical and Wireless Networks*. Boston: Artech House, 2002.

[8] Jawad. A. Salehi, "Code division multiple access techniques in optical fiber network-Par I: Fundamental principles," *IEEE Trans. Commun.,* vol. 37, no 8, pp. 824-833, Augst 1989.

[9] Jawad. A. Salehi, Charles. A. Brackett, "Code division multiple access techniques in optical fiber network-Part II: System performance analysis," *IEEE Trans. Commun.,* vol. 37, no. 8,pp. 834-842, Augst. 1989.

[10] Andrew Stok, Edward. H. Sargent, "Lighting the local network: Optical code division multiple access and quality of service provisioning," *IEEE Network,* vol. 14, no.9, pp. 42-46, November 2000.

[11] Paul R. Pruncnal, Mario A. Santro and Ting. R. Fan, "Spread-spectrum fiber-optic local area network using optical processing," *Journal of Lightwave Technology,* vol. LT-4, no. 5, pp. 547-554, May 1986.

[12] S. A. Aljunid, "Development and implementation of a novel optical code division multiplexing technique for MAN," PhD, School of Electronics and

Computer Science, Universiti Putra Malaysia (UPM), Kuala Lampuer, Feb 2005.

[13] Gerard Keiser, *FTTX concepts and applications*. New Jersey: John Wiley and sons, 2006.

[14] M. J. Parham, C. Smythe and B. L. Weiss, "Code division multiple access techniques for use in optical-fiber local-area networks," *Electronics and Communication Engineering Journal,* vol. 4, pp. 203-212, Augest 1992.

[15] K. L. Hall, "Progress in high-speed TDMA communications," *IEEE lasers and electro-optics Society,* vol. 2, pp. 389 - 390, May 1999.

[16] J. M. Senior, S. D. Cusworth and A. Ryley, "Wavelength division multiple access in fibre optic LAPIS," *IEE Coldoquium on fibre optic LANS and techniques for the local loop,* vol. 5, no. 3, pp. 1-5, June 1989.

[17] Edward. H. Sergant and Andrew Stock, "System performance comparison of optical CDMA and WDMA in a broadcast local area network," *IEEE Comm. Letter,* vol. 6, no. 3, pp. 409-411, Sept 2002.

[18] Andrew Stock and Edward. H. Sergant, "Comparison of Utilization in optical CDMA and WDMA broad cast local area networks with Physical Noise," presented at the IEEE International Conference on Communication (ICC), Apr 2003.

[19] R. Prased and T. Ojanpera, "An overview of CDMA evolution Towards Wideband CDMA," *IEEE Communication Surveys,* vol. 1, no. 1, pp. 2-29, Mar 1998.

[20] G. R. Cooper. and R. W. Nettleton, "A Spread Spectrum Technique for high-capacity Mobile Communication," *IEEE trans. Vehicular Tech,* vol. 27, 1978.

[21] P. Saghari, V. R. Arbab, N. M. Jayachandran, and A. E. Willner, " Variable Bit Rate Optical CDMA Networks Using Multiple Pulse Position Modulation," presented at the in Optical Fiber Communication Conference and Exposition and The National Fiber Optic Engineers Conference, Anaheim, California, 2007.

[22] E. Marom, O. G. Ramor "Encoding-decoding optical fiber network," *IEEE Electronic Letter,* vol. 14, no. 3, pp. 48-49, Feb 1979.

[23] M. E. Marhic, "Coherent optical CDMA networks," *Journal of Lightwave Technology,* vol. 11, no. 5, pp. 854-864, May 1993.

[24] Jawad. A. Salehi, "Emerging Optical Code division-multiple access Communication systems," *IEEE Network Magazine,* vol. 3, no. 8, pp. 31-39, March, 1989.

[25] Nikos Karafolas and Deepak. Uttamchandani, "Optical Fiber Code-Division Multiple Access Networks: A Review," *Optical Fiber Technology,* vol. 2, no. 2, pp. 149-168, Apr 1996.

[26] Fan. R. K. Chung, Jawad. A. Salehi, and Vector. K. Wei, "Optical orthogonal codes: Design, analysis, and applications," *IEEE Transaction Information Theory,* vol. 35, no. 3, pp. 595-604, May 1989.

[27] H. Fathallah L. A. Rusche and S. LaRochelle, "Passive optical fast frequency-hop CDMA communication system," *Journal Lightwave Technology,* vol. 17, no. 3, pp. 397-405, March. 1999.

[28] Guu-Chang Yang and Wing. C. Kwong, "Extended carrier-hopping prime codes for wavelength-time optical code-division multiple-access," *IEEE Transactions on Communications,* vol. 52, no. 7, pp. 1084-1091, July 2004.

[29] M. Kavehrad and D. Zaccarin, "Optical Code-Division-Multiplexed Systems Based on Spectral Encoding of Noncoherent Sources," *Journal of Lightwave Technology,* vol. 13, no. 3, pp. 534-545, March 1995.

[30] Ivan B. Djordjevic and Bane Vasic, "Unipolar codes for spectral-amplitude-coding optical CDMA systems based on projective geometries," *IEEE Photonics Technology Letters,* vol. 15, no. 9, pp. 1318 - 1320, Sept. 2003.

[31] Ivan B. Djordjevic and Bane Vasic "Novel combinatorial constructions of optical orthogonal codes for incoherent optical CDMA systems," *Journal of Lightwave Technology,* vol. 21, no. 9, pp. 1869 - 1875, Sept. 2003.

[32] Zou Wei and H. Ghafouri-Shiraz, "Proposal of a novel code for spectral amplitude-coding optical CDMA systems," *IEEE Photonics Technology Letters,* vol. 14, no. 3, pp. 414 - 416, March 2002.

[33] Zou Wei and H. Ghafouri-Shiraz, "Unipolar codes with ideal in-phase cross correlation for spectral amplitude-coding optical CDMA systems," *IEEE Transactions on Communications,* vol. 50, no. 8, pp. 1209 - 1212, Aug. 2002.

[34] Li Chuanqi, Sun Xiaohan, Zhang Mingde and Ding Dong, "Performance of OCDMA spectral-amplitude-coding with optical orthogonal

codes,"International Conference of Microwave and Millimeter Wave Technology (ICMMT 2002), Tornto, Aug. 2002.

[35] S. A. Aljunid, Ismail, M, Ramli A.R, Ali B.M, Abdullah, M.K, "A new family of optical code sequences for spectral-amplitude-coding optical CDMA systems," *IEEE Photonics Technology Letters,* vol. 16, no. 10, pp. 2383 - 2385, Oct. 2004.

[36] Feras. N. Hasoon. Mohamad Khazani Abdullah , S.A. Aljunid and Sahbudin Shaari, "Performance of OCDMA systems with new spectral direct detection (SDD)technique using enhanced double weight (EDW) code," *ScienceDirect, Optics Communications,* vol. 281, no. 8, pp. 4658-4662, Sept 2008.

[37] Hilal A. Fadhil. S. A. Aljunid and R.Badlishah Ahmed, "New code structure for spectral-amplitude coding OCDMA systems," *IEICE Electronics Express,* vol. 5, pp. 846-852, Oct 2008.

[38] Zou Wei. M. H. Shalaby and H. Ghafouri-Shiraz, "Modified Quadratic Congruence codes for Fiber Bragg-Grating-Based SAC-OCDMA," *Journal of Lightwave Technology,* vol. 19, no. 9, pp. 1274-1281, September. 2001.

[39] P. R. Prucnal, *Optical Code Division Multiple Access: Fundamentals and Applications*. New York: Taylor & Francis Group, 2006.

[40] N. W. Xu Wang, T. Miyazaki and K. Kitayama "Coherent OCDMA system using DPSK data format with balance detection," *IEEE Photonics Technology Letters,* vol. 18, no. 7, pp. 826 - 828 April 2006.

[41] Torn Banwell. S. Etemad, S. Galli, J. Jackel, R. Menendez, P. Toliver, J. Young, P. Delfyett, C. Price, and T. Turpin, "Optical-CDMA incorporating phase coding of coherent frequency bins: concept, simulation, experiment," in *in Optical Fiber Communication Conference*, Los Angeles, California, 2004, p. FG5.

[42] Xu Wang and K. Kitayama, "Analysis of beat noise in coherent and incoherent time spreading OCDMA," *Journal of Lightwave Technology,* vol. 22, no. 8, pp. 2226-2235, Oct 2004.

[43] Jawad A. Salehi, Andrew M. Weiner and Jonathan. P. Heritage, "Coherent Ultrashort light pulse CDMA communications systems," *IEEE Journal of Lightwave Technology,* vol. 8, no. 3, pp. 478-491, March 1990.

[44] R. Papannareddy and A. M. Weiner, "Performance comparison of coherent ultrashort light pulse and incoherent broad-band CDMA systems," *IEEE photonic Technology letters,* vol. 11, no.7, pp. 1683-1685, May 1999.

[45] Jamo Oksa "Multiuser Detection in CDMA Mobile Communications " presented at the FALL-97 optical CDMA system, Poland, 1997.

[46] S. A. Newton. K. P. Jackson, B. Moslehi, M. Tur, C. C. Cutler, J. W. Goodman, and H. J. Shaw, "Optical fiber delay-line signal processing," *IEEE Trans. Microwave Theory Tech,* vol. 33, no. 4, pp. 193-209, Aug1985.

[47] H. P. Sardasai, C.-C. Chang, and A. M. Weiner, "A Femtosecond code-Division Multiple-Access communication System Test Bed," *IEEE/OSA Journal of Lightwave Technology,* vol. 16, no. 11, pp. 1953-1964, Nov 1998.

[48] A. M. Weiner, J. P. Heritage, R. N. Thurston, "Synthesis of phase-coherent, picosecond optical square pulses," *IEEE Optics Letters,* vol. 11, no. 3, pp. 153-155, March 1986.

[49] A. M. Weiner, J. P. Heritage and Jawad A. Salehi, "Encoding and Decoding of femtosecond pulses," *Optics Letters,* vol. 16, no. 4, pp. 300-302, April 1988.

[50] Andonovic. T. Tanceviki, M. Shabeer and L. Bazgaloski, " Incoherent all-optical Code Recognition with Balance Detection," *Journal Lightwave Technology,* vol. 12, no. 6, pp. 1073-1080, June 1994.

[51] M. Kaverhad and D. Zaccarin, "Performance evaluation of optical CDMA systems using non-coherent detection and bipolar codes," *IEEE Journal of Lightwave Technology,* vol. 12, no. 3, pp. 96-105, Jan 1994.

[52] M. Keverhard and D. Zaccarin, "New architecture for incoherent optical CDMA to achieve bipolar capacity," *IEEE Electronic letters,* vol. 30, no. 3, pp. 258-259, Feb 1994.

[53] Cedric Fung Lam, "Multi-wavelength Optical Code-Division-Multiple-Access Communication Systems," Doctor of Philosophy, Electrical Engineering, University Of California Los Angeles, 1999.

[54] D. Zaccarin and M. Kavehrad, "An Optical CDMA System Based on Spectral Encoding of LED," *IEEE Photonics Technology Letters,* vol. 4, no. 4, pp. 479-482, April 1993.

[55] K. Invesen. and O. Ziemann, "An All-Optical CDMA Communication Network By Spectral Encoding of LED Using Acoustically Tunable Optical

Filters," in *Proc. Int. Symposium on Signals, Systems and Electronics (ISSSE'95)*, SanFrancisco, 1995, pp. 529-532.

[56] V. Hinkov, I. Hinkov, K. Iversen and O. Ziemann, "Feasibility of Optical CDMA Using Spectral Encoding by Acoustically Tunable Optical Filters," *IEEE Electronics Letters,* vol. 31, no. 5, pp. 384-386, March 1995.

[57] B. Aazhang, J. F. Yong, and L. Nguyen, "All-Optical CDMA with Bipolar Codes," *IEEE Electronics Letters,* vol. 31,no. 6, pp. 469-470, March 1995.

[58] T. Deneins, L. Nguyen, B. Aazhang and J.F. Young, "Experimental Demonstration of Bipolar Codes for Optical Spectral Amplitude CDMA Communication," *Journal of Lighwave Technology,* vol. 15, no. 9, pp. 1647-1653, Sept 1997.

[59] Syed Alwee Aljunid, Zhuradiah Zan, Siti Barirah Ahmad Anas and Mohd. Khazani Abdullah "A New Code for Optical Code Division Multiple Access Systems," *Malaysian Journal of Computer Science,* vol. 17, no. 2, pp. 30-39, December 2004.

[60] A. Shaar and P. Davies, "Prime sequences: Quasi-optimal sequences for or channel code division multiplexing"," *IEEE Electron. Lett,* vol. 19, no.21, pp. 888-890, Oct 1983.

[61] F. R. Chung, Jawad A. Salehi and V. K. Wei "Optical orthogonal codes: design, analysis and applications," *Information Theory, IEEE Transactions on Communications,* vol. 35, no.3, pp. 595 - 604, May 1989

[62] G.-C. Yang, "Some new families of optical orthogonal codes for code-division multiple-access fibre-optic networks," *IEEE Proc. Commun,* vol. 142, pp. 363-368, Dec 1995.

[63] J. L. Kelley, *General Topology*. New Jersey: Prentice-Hall, 1975.

[64] S. Anuar, S. A. Aljunid, N.M.Saad and S.M. Hamzah, "New design of Spectral-Amplitude Coding in Optical code Division Multiple Access (OCDMA) with Zero Cross-Correlation," *Optics Communication,* vol. 282, pp. 2659-2664 March 2009.

[65] R. J. B. Elwyn D. J. Smith, and Desmond P. Taylor, "Performance Enhancement of Spectral-Amplitude-Coding Optical CDMA using Pulse-Position-Modulation," *IEEE Transaction on Communications,* vol. 46, no. 9, pp. 1176 - 1185, Sept 1998.

[66] G. Lachs, *Fiber Optic Communication Systems, Analysis and Enhancement*. Boston: McGraw Hill, 1998.

[67] J. C. PALAIS, *Fiber Optic Communications*. New Jersey: Prentice Hall, 2004.

[68] E. H. Dinan, and B. Jabbari, "Spreading codes for direct sequence CDMA and wideband CDMA cellular networks," *IEEE Communications Magazine,* vol. 36, pp. 48-54, Sep 1994.

[69] J. J. Komo and C. C. Yuan, "Evaluation of code division multiple access systems," in *IEEE proceeding of Energy and Information Technologies in the Southeast*, Columbia, USA, April 1989, pp. 849-854.

[70] Zou Wei, H. Ghafouri.-Shiraz and H. M. Shalaby, "New Code Families for Fiber-Bragg-Grating-Based Spectral-Amplitude-Coding Optical CDMA Systems," *IEEE Photonics Technology Letters,* vol. 13, no.8, pp. 890-892, August 2001.

[71] Cheing-Hong Lin, Jingshown Wu and Chun-Liang Yang, "Noncoherent Spatial/Spectral Optical CDMA systems with Two-Dimensional Perfect Difference Codes," *IEEE Journal of Lightwave Technology,* vol. 23, no. 12, pp. 3966-3979, Dec 2005.

[72] J. W. Goodman, *statistical optics*. New York: Wiley, 1985.

[73] R. K. Z. Sahbudin, M. K. Abdulla, M. D. A Samad, M. A. Mahdi and M. Ismail, "Hybrid SCM SAC-OCDMA system employing new optical spectral amplitude direct decoding technique," *Journal of applied science,* vol. 7, no. 14, pp. 1942-1947, 2007.

[74] A. B. Mohammed, E.I. Elfadel, N. Saad, N.M. Anuar, M.S. Aljunid, S.A. Abdullah, M.K, "New Approach of Double Weight Code Family Detection Using Reduced Set of Fiber Bragg Gratings," presented at the IEEE, International Conference Wireless and Optical Communications Networks (WOCN '07), Singapore, 2007.

[75] M. K. Abdulla. R. K. Z. Sahbudin, S. Hitam, M. A. Mahdi, "Cost Comparison of the Detection Techniques for Optical Spectrum CDMA System," *IJCSNS International Journal of Computer Science and Network Security,* vol. 8, pp. 87-90, Aug 2008.

[76] Hilal Adnan Fadhil, S. A. Aljunid and R.B. Ahmad "Performance of random diagonal code for OCDMA systems using new spectral direct detection technique," *Optical Fiber Technology,* vol. 15, no. 4, pp. 283-289, June 2009.

[77] H. A. Fadhil, S. A. Aljunid and R.B. Ahmed "Design and demonstration of a novel Spectral Amplitude Coding OCDMA code for suppression Phase Intensity Induced Noise," *journal of communication,* vol. 4, no. 1 pp. 17-21, Feb 2009.

[78] A. Mohammed, Saad, N.M, E.I. Babikier, N. Elfadel, Anuar, M.S. Aljunid, S.A. Abdullah, M.K, "Modeling and Simulation of the Double Weight Code Family Detection Schemes," in International Conference on Intelligent and Advanced Systems 2007, Kula Lampur Jun 2007, pp. 348-351.

[79] L. P. A. Akhtar, and S. Kumar, "Impact of Walk-off on FWM in RZ-OOK Transmission," in National Fiber Optic Engineers Conference, OSA Technical Digest Series (CD)Torento, March 2007.

[80] K. J. Dexter, P.J. Maguirea, L.P. Barry, Chun Tian, Morten Ibsen, Periklis Petropoulos and David J. Richardson, "Multiple access interference rejection in OCDMA using a two-photon absorption based semiconductor device," Optics Communications,, vol. 282, pp. 1281-1286, April 2009.

[81] S. C. Chung, B. Kim and K. Kim, "Experimental demonstration of secuirty-improve OCDMA scheme based on incoherent broadband light source and bipolar coding," Optical Fiber Tecknology, vol. 14, no. 2, pp. 130-133, April 2008.

PUBLICATIONS

Journals:

Hassan Yousif Ahmed, Ibrahima Faye, N.M. Saad'' Vectors Combinatorial Code Family for Spectral Amplitude Coding (SAC-OCDMA)'' International Journal of Computer Science and Network Security (IJCSNS), Vol. 8 No. 3 pp. 20-26, 2008.

Hassan Yousif Ahmed, Ibrahima Faye, N.M. Saad "Spectral Amplitude Coding Optical CDMA: Performance Analysis of PIIN Reduction Using VC Code Family" International Journal of Electronics, Communications and Computer Engineering, Vol. 1, No 2, June 2009, pp. 72-78.

Hassan Yousif Ahmed, Ibrahima Faye, N.M. Saad "Effects of the Vector Combinatorial code connection parameters on the performance of an OCDMA system for high-speed networks" Journal of Computer Theory and Engineering (IJCTE), Vol. 1, No 5, Dec 2009, pp. 500-505.

Hassan Yousif Ahmed, Ibrahima Faye, N.M. Saad'' Spectral Amplitude Coding OCDMA: Performance Analysis on Detection Schemes using Vectors Combinatorial Code Families" Journal of Optical Communication, Vol. 5. No 4, 2009.

Hassan Yousif Ahmed, Ibrahima Faye, N.M. Saad "OCDMA System: New Detection Scheme and Encoder-Decoder Structure Based On Fiber Bragg Gratings (FBGs) for VCC Code", has been accepted for publication in the International Journal of Computers and Applications. ACTA Press / IASTED.

Hassan Yousif Ahmed, Ibrahima Faye, N.M. Saad "Optical CDMA Systems: A new Detection Scheme To minimize The MUI and PIIN for VCC Codes Families" International Association of Engineering, IAENG, accepted pending for publish.

Conferences:

Hassan Yousif Ahmed, Ibrahima Faye, N.M.Saad Vectors ‘’Combinatorial Code Family for Spectral Amplitude Coding Optical Code Division Multiple Access (SACOCDMA)’’ National Postgraduate Symposium-UTP-NPC 2008.

Hassan Yousif Ahmed, Ibrahima Faye, N.M.Saad ‘‘An efficient Method to construct Code Family for Spectral Amplitude Coding OCDMA’’ IEEE 2008 Regional Student Conference on Research and Development, 26-27 Nov. 2008, Johor, Malaysia.

Hassan Yousif Ahmed, Ibrahima Faye, N.M.Saad ‘‘Performance Analysis: Vectors Combinatorial Codes (VCC) Families for SAC-OCDMA” IEEE 2008 Regional Student Conference on Research and Development, 26-27 Nov. 2008, Johor, Malaysia.

Hassan Yousif Ahmed, Ibrahima Faye, N.M.Saad ‘‘A new transmitter-receiver structure based on fiber Bragg gratings (FBGs) for VCC code” IEEE 2008 Regional Student Conference on Research and Development, 26-27 Nov. 2008, Johor, Malaysia.

Hassan Yousif Ahmed, Ibrahima Faye, N.M. Saad’’ Effects of connection parameters on the performance of OCDMA system using Vector Combinatorial (VC) code ’’ The 14th International Conference on Optical Networking and Modeling, 1-3 Feb, 2010. Accepted.

N.Elfadel, HassanYousif Ahmed, Maisara A, E.I.Babekir, A.Mohammed, A.A.Aziz and N.M.Saad, “Performance study of Optical Parallel Interference Cancellation with Varying Threshold Values”, The six IASTED International Confernce of Communication, Internet, and Information Technology (CIIT 2007), 2nd-4th July 2007 , Bnaff, Alberta, Canada.

Elfadel, N. Aziz, A.A. HassanYousif Ahmed. Musa, M. Aziz, A. Idriss, E. Mohammed, A. Saad, “One stage Optical Parallel Interference Cancellation for the optical CDMA” IEEE International Conference on Intellegent & Advance systems (ICIAS 2007), 25th-28th November 2007, Kuala Lumpur- Malaysia.

Elfade, N. Aziz, A.A. HassanYousif Ahmed. Musa, M. Aziz, "Multi-user detection for the OCDMA: Optical Parallel Interference Cancellation with optical limiter" IEEE International Conference on Intellegent & Advance systems (ICIAS 2007), 25th-28th November 2007, Kuala Lumpur- Malaysia

APPENDIX A

Examples of OCDMA Code

1. In Table A.1, Example of Prime Code sequences for P=5.

Table A.1 Prime sequence S_x and prime sequence code C_x for GF(j)

	i						
x	01234	Sequence	Code Sequence				
0	00000	S_0	C_0=10000	10000	10000	10000	10000
1	01234	S_1	C_1=10000	01000	00100	00010	00001
2	02413	S_2	C_2=10000	00100	00001	01000	00010
3	03142	S_3	C_3=10000	00010	01000	00001	00100
4	04321	S_4	C_4=10000	00001	00010	00100	01000

2. In Table A.2, example of Required Codeword Length N for A Given Number of User |C| and Weight W for an OOC Code Construction.

Table A.2 OOC code for 7 users

User No	Chip 1	Chip 2	Chip 3
N1	0	1	19
N2	0	2	22
N3	0	3	15
N4	0	4	13
N5	0	5	16
N6	0	6	14
N7	0	7	17

3. In Table A.3, Example of Hadamard Code Sequences for 6 Users.

Table A.3 Hadamard code

Kth	C_8	C_7	C_6	C_5	C_4	C_3	C_2	C_1
1	1	0	1	0	1	0	1	0
2	1	1	0	0	1	1	0	0
3	1	0	0	1	1	0	0	1
4	1	1	1	1	0	0	0	0
5	1	0	1	0	0	1	0	1
6	1	1	0	0	0	0	1	1

4. In Table A.4, listed some code examples for different values of parameters α and b when q is equal to 2^2 (i.e $q = 4$). Here the selected primitive irreducible polynomial is written as $x^2 + x + 1$ and the primitive element β is (10) in binary form, which can be represented as '2' in decimal system.

Table A.4 MFH code example

	y(k)	s(i)
a=0, b=1	(0 3 2 1 0)	1000 0001 0010 0100 1000
a=1, b=0	(2 3 1 0 1)	0010 0001 0100 1000 0100
a=2, b=3	(0 2 1 3 2)	1000 0010 0100 0001 0010
a=0, b=3	(2 1 0 3 0)	0010 0100 1000 0001 1000
a=2, b=2	(1 3 0 2 2)	0100 0001 1000 0010 0010
b=2 for y'(k)	(2 2 2 2 3)	0010 0010 0010 0010 0001

Table A.5: Example of MDW ($W = 4$) Code Sequences

Kth	C_{18}	C_{17}	C_{16}	C_{15}	C_{14}	C_{13}	C_{12}	C_{11}	C_{10}	C_9	C_8	C_7	C_6	C_5	C_4	C_3	C_2	C_1
1	**0**	**0**	**0**	**0**	**0**	**0**	**0**	**0**	**0**	**0**	**0**	**0**	**0**	**1**	**1**	**0**	**1**	**1**
2	**0**	**0**	**0**	**0**	**0**	**0**	**0**	**0**	**0**	**0**	**1**	**1**	**0**	**0**	**0**	**1**	**1**	**0**
3	**0**	**0**	**0**	**0**	**0**	**0**	**0**	**0**	**0**	**1**	**1**	**0**	**1**	**1**	**0**	**0**	**0**	**0**
4	**0**	**0**	**0**	**0**	**1**	**1**	**0**	**1**	**1**	**0**	**0**	**0**	**0**	**0**	**0**	**0**	**0**	**0**
5	**0**	**1**	**1**	**0**	**0**	**0**	**1**	**1**	**0**	**0**	**0**	**0**	**0**	**0**	**0**	**0**	**0**	**0**
6	**1**	**1**	**0**	**1**	**1**	**0**	**0**	**0**	**0**	**0**	**0**	**0**	**0**	**0**	**0**	**0**	**0**	**0**

APPENDIX B

Derivation of SNR for NVC code family

4.6.1 Complementary Subtraction System

The setup of the proposed IVC system using complementary subtraction technique is shown in Figure B.1. In the performance analysis, we have considered incoherent intensity noise, as well as shot and thermal noises in both photodetectors. The effect of the receiver dark current is neglected because it's value is small compared with the shot and thermal noises [30-33, 35-38]. Gaussian approximation is used for the calculation of the BER (Bit Error Rate) as in [30-33, 73-76].

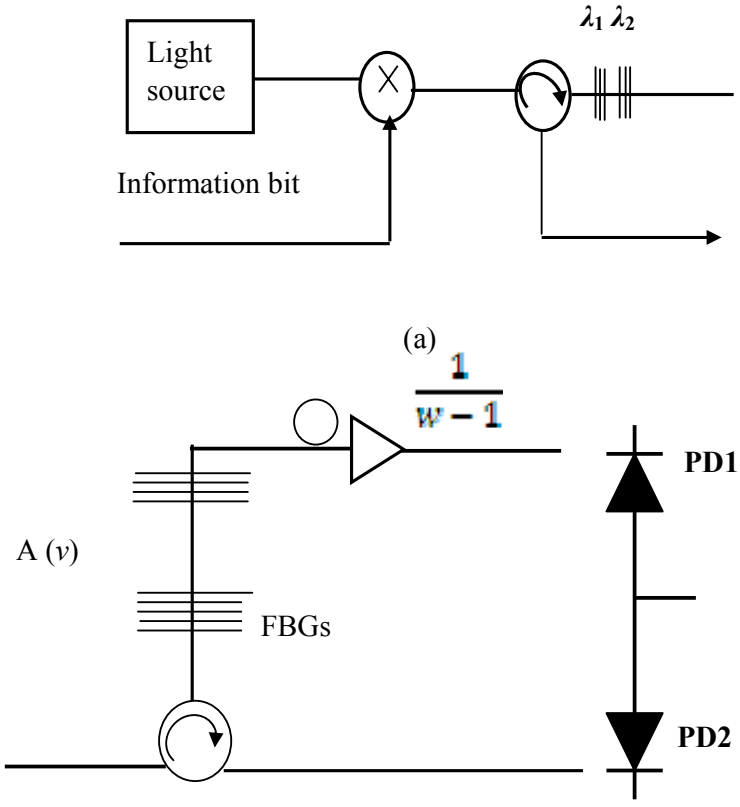

Figure B.1: Optical CDMA System Architecture using Complementary Subtraction Technique (a) Transmitter, (b) Receiver.

The variance of the photocurrent due to the detection of an ideally unpolarized thermal light, which can be generated by spontaneous emission [30-33, 35-38] can be expressed as

$$\langle i^2 \rangle = 2eIB + I^2 B\tau_c + \frac{4K_b T_n B}{R_L} \tag{B.1}$$

The parameters used in Equation (B.1) are as shown in TABLE B.1. In Equation (B.1), the first term results from the shot noise, the second term denotes the effect of Phase Induced Intensity Noise (PIIN) and the third term represents the effect of thermal noise.

When incoherent light fields are mixed and incident upon a photodetector, the phase noise of the fields causes an intensity noise term in the photodetector output. The coherent time of a thermal source τ_c is given by [38]

$$\tau_c = \frac{\int_0^\infty G^2(v)dv}{\left[\int_0^\infty G(v)dv\right]^2} \tag{B.2}$$

Where G(v) is the power spectral density (PSD) of the thermal noise source. In equation (C.2), the total effect of PIIN has negative binomial distribution [76]. While thermal noise has a Gaussian distribution, in general we used Gaussian Approximation for all of them

The total effect of PIIN and shot noise obeys negative binomial distribution [76]. To analyze the system with transmitter and receiver shown in Figure 4.5, we used the same assumptions that were used in [30-33, 35-38] and are important for mathematical simplicity. Without these assumptions, it is difficult to analyze the system. We assume the following:

1. Each light source is ideally unpolarized and its spectrum is flat over the bandwidth [$\boldsymbol{\nu}_o$-$\Delta\boldsymbol{\nu}$/2, $\boldsymbol{\nu}_o$+$\Delta\boldsymbol{\nu}$/2] where ν_o is the central optical frequency and $\Delta\boldsymbol{\nu}$ is the optical source bandwidth in Hertz.
2. Each power spectral component has identical spectral width.

3. Each user has equal power at the receiver.
4. Each bit stream from each user is synchronized.

Table B.1: Typical Parameters used in the calculation

No	Symbols	Parameters
1	e	Electron's charge
2	I	Average photocurrent
3	B	Noise–equivalent electrical Bandwidth of the receiver
4	τ_c	Coherence time of the source
5	K_b	Boltzmann Constant
6	T_n	Absolute receiver noise temperature
7	R_L	Receive load resistor

The above assumption is important for mathematical simplicity. Based on the above assumptions, we can easily analyze the system performance using Gaussian approximation. The power spectral density of the received optical signals can be written as [38]

$$r(v) = \frac{P_{sr}}{\Delta V} \sum_{N=1}^{N} d_N \sum_{i=1}^{L} c_N(i) \left\{ u\left[v - v_o - \frac{\Delta v}{2L}(-L + 2i - 2)\right] - u\left[v - v_o - \frac{\Delta v}{2L}(-L + 2i)\right] \right\} \quad \text{(B.3)}$$

where P_{sr} is the effective power of a broadband source at the receiver, N is the active users and L is the VC code length, d_N is the data bit of the Nth user that is "1" or "0", and $u(v)$ is the unit step function expressed as

$$u(v) = \begin{cases} 1, & v \geq 0 \\ 0, & v < 0 \end{cases} \quad \text{(B.4)}$$

In the following analysis we have considered the effects of both shot and thermal noises as well as the effect of PIIN.

Let $C_N(i)$ denote the *ith* element of *N*th NVC code sequence, the code properties can be written as

$$\sum_{i=1}^{L} C_N(i)C_m(i) = \begin{cases} W, & For \quad N = m \\ 1, & For \quad N \neq m \end{cases} \tag{B.5}$$

and

$$\sum_{i=1}^{L} C_N(i)\overline{C}_m(i) = \begin{cases} 0, & For \quad N = m \\ W-1, & For \quad N \neq m \end{cases} \tag{B.6}$$

From Equation (C.3), the power spectral density at photodetector 1 and photodectotor 2 as in Figure C.1 of the *m*th receiver during one bit period can be written as

$$G_1(V) = \frac{P_{sr}}{\Delta V}\sum_{N=1}^{N} d_N \sum_{i=1}^{L} C_N(i)\overline{C}m(i)\left\{ u\left[V - V_0 - \frac{\Delta V}{2L}(-L+2i-2)\right] - u\left[V - V_0 - \frac{\Delta V}{2L}(-L+2i)\right]\right\} \tag{B.7}$$

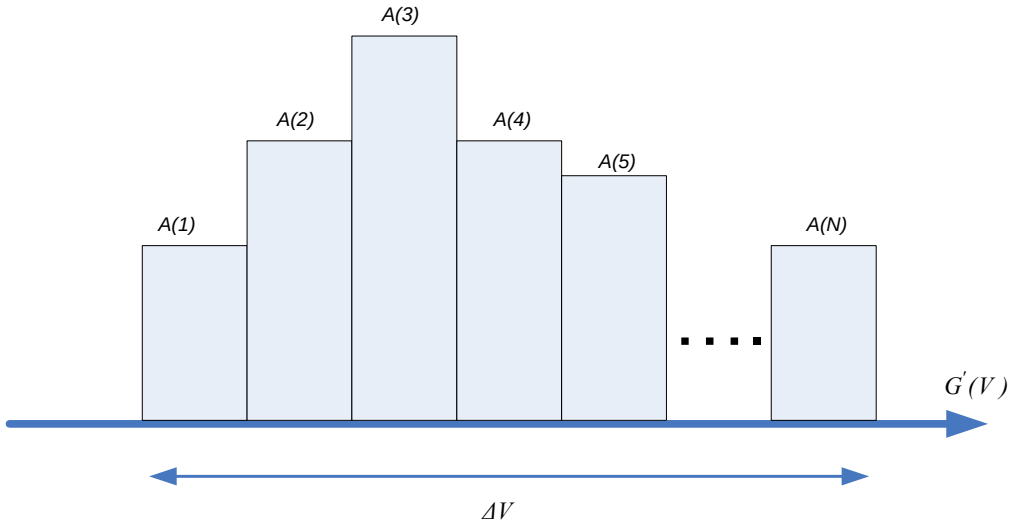

Figure B.2: The PSD of the Received Signal $r(v)$.

$$G2(V) = \frac{P_{sr}}{\Delta V}\sum_{N=1}^{N} d_N \sum_{i=1}^{L} C_N(i) Cm(i) \{ u\left[V - V_0 - \frac{\Delta V}{2L}(-L+2i-2)\right] - u\left[V - V_0 - \frac{\Delta V}{2L}(-L+2i)\right] \} \quad \text{(B.8)}$$

Then

$$\int_0^{\infty} G_1(V)dV = \frac{P_{sr}}{L}\sum_{N=1}^{N}\sum_{N\neq m} d_N \quad \text{(B.9)}$$

$$\int_0^{\infty} G_2(V)dV = \frac{P_{sr}W}{\Delta V} + \sum_{N=1}^{N}\sum_{N\neq m} d_N \quad \text{(B.10)}$$

To calculate the integral of $G_1^2(V)$ and $G_2^2(V)$, let us first consider an example of the PSD (denoted by $G'(V)$) of the received superimposed signal, which is shown, in Figure C.2, where $A(i)$ is the amplitude of the signal of the ***i***th spectral slot with width of $\frac{\Delta V}{N}$.

The integral of $G'^2(V)$ can be expressed as

$$\int_0^{\infty} G'^2(V)dv = \frac{\Delta V}{N}\sum_{i=1}^{N} A^2(i) \quad \text{(B.11)}$$

Therefore, using (4.18), (4.19) and (4.20) we have

$$\int_0^{\infty} G_1^2(V)dV = \frac{P_{sr}^2}{L\Delta V}\sum_{i=1}^{L}\left\{\overline{Cm}(i)\cdot\left[\sum_{N=1}^{N} d_N C_N(i)\right]\cdot\left[\sum_{q=1}^{N} d_q C_q(i)\right]\right\} \quad \text{(B.12)}$$

And

$$\int_0^{\infty} G_2^2(V)dV = \frac{P_{sr}^2}{L\Delta V}\sum_{i=1}^{L}\left\{C_m(i)\cdot\left[\sum_{N=1}^{N} d_N C_N(i)\right]\cdot\left[\sum_{q=1}^{N} d_q C_q(i)\right]\right\} \quad \text{(B.13)}$$

Based on above equations, d_N is the data bit of the *N*th user that carries the value of either "1" or "0". Consequently, the photocurrent **I** can be expressed as

$$I = I_2 - I_1 = \Re\int_0^{\infty} G_2(V)dv - \Re\int_0^{\infty} G_1(V)dv \quad \text{(B.14)}$$

Then

$$\mathrm{I}= \Re\left[\frac{P_{sr}}{L}\right].\left[W + \sum_{N=1}^{N}\sum_{N\neq m} d_N - \sum_{N=1}^{N}\sum_{N\neq l} d_N\right]$$

After integrating and subtraction processes, the photocurrent can be expressed as:

$$\mathrm{I} = \Re \frac{P_{sr}}{L} W \tag{B.15}$$

$$\Re = \frac{\eta e}{h V_c} \tag{B.16}$$

Here, η is the quantum efficiency, $\boldsymbol{e}$ is the electron's charge, h is the Planck's constant, and V_c is the central frequency of the original broad-band optical pulse. Since the noises in photodetector 1 and 2 are independent, the power of noise sources that exist in the photocurrent can be written as [38].

$$\langle I^2 \rangle = \langle I_1^2 \rangle + \langle I_2^2 \rangle + \langle I_{th}^2 \rangle \tag{B.17}$$

where,

I^2 = Total noise power;

I_1^2 = Shot noise;

I_2^2 = Phase Induced Intensity Noise (PIIN);

I_{th}^2 = Thermal noise.

from equation (.17)

$$\langle I^2 \rangle = 2eB(I_1+I_2)+BI_1^2\tau_{c1}+BI_2^2\tau_{c2}+\frac{4K_bT_nB}{R_L} \tag{B.18}$$

$$\langle I^2 \rangle = 2eB\Re\left[\int_0^\infty G_1(v)dv + \int_0^\infty G_2(v)dv\right]+B\Re^2\int_0^\infty G_1^2(v)dv + B\Re^2\int_0^\infty G_2^2(v)dv +\frac{4K_bT_nB}{R_L} \tag{B.19}$$

from equation (C.4), when all the users are transmitting bit ''1'' using the average value as $\sum_{N=1}^{N} c_N \approx \frac{NW}{L}$ and the noise power can be written as

$$\langle I^2 \rangle = 2eB\Re \left[\frac{P_{sr}}{L}((N-1) + W + (N-1)\right] + B\Re^2\left[\frac{P_{sr}^2}{\Delta V L}\cdot\left[\frac{NW}{L}\right].[(N-1) + W + (N-1)]\right] + \frac{4K_bT_nB}{R_L} \quad \text{(B.20)}$$

Noting that the probability of sending bit '1' at any time for each user is $\frac{1}{2}$ [38], and then the above equation becomes

$$\langle I^2 \rangle = \frac{P_{sr}\, e\, B\, \Re}{L}\left[(2N-2) + W\right] + \frac{P_{sr}^2 B \Re^2 N W}{2\Delta V L^2}\left[(2N-2) + W\right] + \frac{4K_bT_nB}{R_L} \quad \text{(B.21)}$$

From (B.15) and (B.21), we can get the average of SNR as in (B.22) and (B.23)

$$SNR = \frac{(I_2 - I_1)^2}{\langle I^2 \rangle} \quad \text{(B.22)}$$

$$SNR = \frac{\frac{\Re^2 P_{sr}^2 W^2}{L^2}}{\frac{P_{sr}\, e\, B\, \Re}{L}\left[(2N-2) + W\right] + \frac{P_{sr}^2 B \Re^2 N W}{2\Delta V L^2}\left[(2N-2) + W\right] + \frac{4K_bT_nB}{R_L}} \quad \text{(B.23)}$$

Where $\Re$ is the photodiode responsivity, P_{sr} is the effective power of a broad-band source at the receiver, e is the electronic charge, B is the electrical equivalent noise band-width of the receiver, K_B is the Boltzmann's constant, Tn the absolute receiver noise temperature, R_L is the receiver load resistor, ΔV is the optical source bandwidth, W, N, L are the code weight, the number of users, the code length respectively as being the parameters of NVC code itself. The Bit Error Rate (BER) is computed from the SNR using Gaussian approximation as [38]

$$\text{BER} = P_e = \frac{1}{2}\, erfc\left(\sqrt{\frac{SNR}{8}}\right) \quad \text{(B.24)}$$

APPENDIX C

Design parameters

1. Distance

The transmission distance is one of the most important elements in an optical CDMA system. The distance of the fiber is characterized by the light propagation time, line attenuation, and dispersion. Attenuation of a light signal as it propagates along a fiber is an important consideration in the design of an optical communication system, since it plays a major role in determining the maximum transmission distance between a transmission and a receiver. The basic attenuation mechanisms in a fiber are absorption, scattering and radiative losses of the optical energy. As light travels along a fiber, its power decreases exponentially with distance. This phenomenon is known as attenuation and it is related to the reduction of the pulse amplitude. The variation of the fiber length can be characterized by the amount of dispersion. Dispersion is a pulse spreading as a function of wavelength and is measured in picoseconds per kilometer per nanometer $[p_s/(km \times nm)]$. The effect of the length increment is explained by the amount of dispersion and loss that the signal experiences. Throughout the study, the type of fiber used is of the G.652 Non-Dispersion Shifted Fiber (NDSF) standard with the characteristics listed in Table C.1.

Table C.1 Parameters for Nonlinear Dispersion Shifted Fiber G.652.

No	Parameter	Unit
1	Attenuation constant	0.25 dB/km
2	Chromatic dispersion	18 ps/nm/km
3	All non-linear effects	On
4	Group delay	Wavelength Dependent
5	Polarization mode dispersion coefficient	0.07 ps/√km

2. Bit rate

Bit rate is the number of bits (0, 1) that can be transmitted per second over a channel. It is the direct measure of information carrying capacity of a digital communications link or network. The system bandwidth that is required to carry a signal may be more than or equal to the bit rate, depending on the coding scheme (NRZ line code is used in this study). As the data rate increases, the detection and regeneration circuit becomes more complex because of the high speed requirements. In this study, four main bit rates STM-1 (155 Mb/s), STM-4 (622 Mb/s), STM-16 (2.5 Gb/s), STM-64 (10 Gb/s) are used, according to the Synchronous Digital Hierarchy (SDH) standard.

3. Transmit power

Transmit power is measured in dBm. The need for adequate light to overcome all the optical transmission losses and to obtain desired BER is related to power. It must be considered in a way to allow for system aging, fluctuation, and repairs and not to overload the receiver. The coupling of the optical power from a source into a fiber needs the consideration of the numerical aperture, core size, refractive index profile, and core-cladding index difference of the fiber, plus the size, radiance, and angular power distribution of the optical source. All these parameters are chosen based on the standard fibers (G.652) used.

4. Chip Spacing

Chip spacing is the spacing between two weights or non-zero spectrum that are being transmitted in an OCDMA code. Up till now, there is no standard spacing for OCDMA systems. In this research, the spacing has been varied to study the effect of it on system's performance. Usually, with the closer channel spacing, nonlinear effects such as four wave mixing (FWM) and cross phase modulation (XPM) become more critical.

Performance Parameter

In this thesis, we consider three performance parameters to evaluate the system under study. The main parameter is bit error rate (BER). The BER of 10^{-12} was used as the threshold as proposed by G.983 standard. The other performance parameters that used

in this study are the received power or the output power and the noise power. The signal's OSNR and eye pattern are also used sparingly.

1. Bit Error Rate (BER)

BER is the probability of errors in number of bits of data over the total transmitted bits at a certain time interval. The minimum error rate is 10^{-12}, which means that, on the average, one error occurs for every billion pulses sent. Typically, error rate for optical communication system ranges from 10^{-9} to 10^{-12} depending on the service types.

2. Received Power (Output Power)

Received power or output power is the power that is measured at the receiver and given in dBm. Note that it is the averaged total power which is considered, not the peak power. The receiver must first detect weak, distorted signals and then make decisions on what type of data was sent back based on an amplified version of this distorted signal. In the experiment, the averaged total power is measured by using a power meter while an Optical Spectrum Analyzer (OSA) is used for peak power.

3. Noise Power

Receiver noise is defined here as any signal present in the receiver other than the desired signal. This includes any unwanted disturbances that mask, corrupt, reduce the information content of, or interfere with the desired signal. In the simulation of the proposed system, we have considered shot noise, incoherent intensity noise, as well as thermal noise and dark current in all photodetectors.

4. Eye Opening

Eye opening is a simple but powerful measurement to access performance of optical communication systems. A pattern is displayed when an oscilloscope is driven by a receiver output and triggered by the signal source that drove the transmitter. Eye pattern visualizing is made in time and allows the effect of waveform distortion to be shown immediately.

Eye opening is the difference between minimum value of sample with related to a logical 1 and the maximum value of samples related to a logical 0. It is measured at

the sampling instant. The more open the eye, the better the transmission quality and the more uniform the signal received.

APPENDIX D

Simulation Parameters

Amplitude Analysis

Metric	Value
MeanOfOnes	3.41E-05
StdDevOnes	4.77E-07
StdDevOnesRelative	0.013993073
MaxValueOnes	3.52E-05
MinValueOnes	3.30E-05
PeakToPeakOnes	2.23E-06
OvershootOnes	3.38923173
NumberSamplesOnes	59
MeanOfZeros	1.84E-07
StdDevZeros	2.30E-07
StdDevZerosRelative	1.250294508
MaxValueZeros	9.79E-07
MinValueZeros	-2.90E-07
PeakToPeakZeros	1.27E-06
UndershootZeros	1.401280317
NumberSamplesZeros	69

Eye setting

Metric	Value
AverageLevel	1.58E-05
ThresholdUsed	1.12E-05
EyeAmplitude	3.39E-05
EyeHeight	3.17E-05
EyeHeight_dB	-0.280769591
EyeOpeningFactor	0.97913196
EyeClosure	3.20E-05
EyeClosureGauss	3.17E-05

BER Analysis

Metric	Value
Q	47.92016967
Q_dB	33.61036694
Qeff	-1
Qeff_dB	NaN
BER	0
BERISI	0
ExtRatio	184.8972563
ExtRatio_dB	22.66930467
InvExtRatio_percent	0.540840908
BitPeriod	4.00E-10
MeanTime	2.00E-10
JitterRMS	7.66E-12
JitterRMSRising	6.80E-12
JitterRMSFalling	7.66E-12
JitterUI	0.019143887
JitterPeakToPeak	2.94E-11
JitterPeakToPeakRising	2.29E-11
JitterPeakToPeakFalling	2.94E-11
EyeWidth	6.99E-10
EyeWidthRatio	1.748612979
RiseTime20_80	1.50E-10
FallTime80_20	1.53E-10
RiseTime10_90	2.23E-10
FallTime90_10	2.28E-10
DutyCycleDistortion	3.43E-10
DutyCycleDistortion_percent	85.70316151
PulseWidth	7.43E-10
DutyCycle	185.7031615
ContrastRatio	0.991683574

CrossingLevel_percent	32.58877898

APPENDIX E

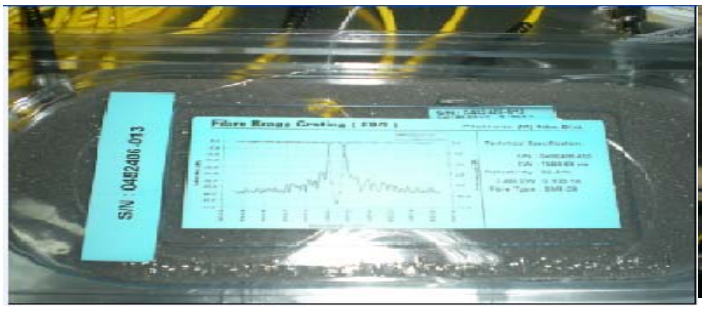

FBG

OSA

Fiber optic cables

AWG

Tunable Laser Source+ 10dBm